www.cardiol.br

www.dicsbc.org

ABC Imagem Cardiovascular

Sociedade Brasileira de Cardiologia • ISSN 2675-312X • Volume 33, Nº 4, October/November/December 2020

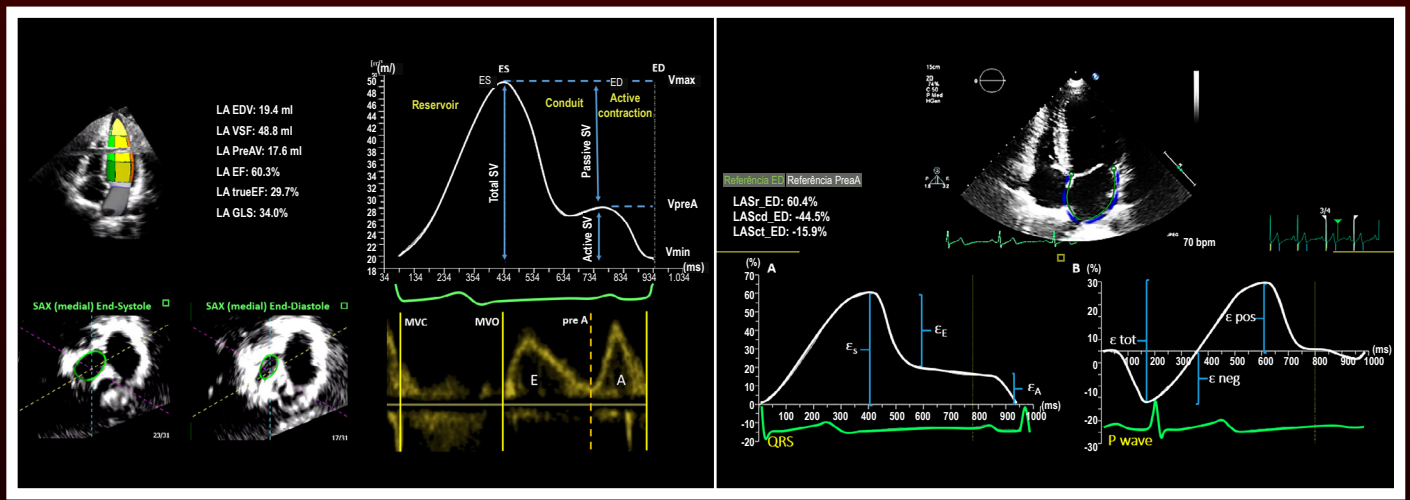

Figure 4 – *Function of the left atrium and its relationship with the cardiac cycle. When the mitral valve closes (MVC), at LV end-diastole (at the beginning of QRS), the LA is in its minimum volume (V min). In this phase (reservoir) the LA stores venous flow from the pulmonary veins and starts to increase in size until it reaches its maximum volume (V max), just before mitral valve opening (MVO) at the LV end-systole (at the end of the T wave). Thereafter, the conduit phase occurs wherein the LA passively transfers blood to the LV and the LA volume slightly decreases until it reaches the pre-contraction volume (V pre-A) (before the P wave), just prior to atrial systole. From these volumes the total atrial stroke volume (total SV =Vmax – Vmin), passive atrial stroke volume (passive SV = Vmax – Vpre-A), and active atrial stroke volume (active SV = Vmax – V pre-A) can be calculated. The ejection fractions (or emptying) can also be calculated: LA total emptying fraction (LA EF: Vmax – Vmin/V max), LA true emptying fraction (LA trueEF = V pre-A – Vmin/V pre-A) and LA passive emptying fraction (LA passive EF = Vmax – V pre-A/ V pre-A).* **Figure 5 –** *Measurement of LA phasic function with 2D speckle tracking using the QRS as a timing reference (A) versus the P wave (B). When the QRS is used as the reference point, the phasic curve starts with the peak positive longitudinal atrial strain (εs) corresponding to the reservoir function (LASr_ED), followed by the early diastolic strain waves (εe) representing the conduit phase (LAScd_ED) and finally the late diastolic strain wave (εa) expressing the booster pump function (LASct_ED). In contrast, when using the P wave, the first negative peak strain (εneg) expresses the booster pump function, followed by the positive peak strain (εpos) and later the total longitudinal strain (εtot) representing the conduit and reservoir functions, respectively.*

www.cardiol.br
www.dicsbc.org

ABC Imagem Cardiovascular

Departamento de Imagem Cardiovascular

Diretoria SBC

Arquivos Brasileiros de Cardiologia - Imagem Cardiovascular

Volume 33, Nº 4, October/November/December 2020

Indexing source: LILACS - Literatura Latino-Americana e do Caribe em Ciências da Saúde - www.bireme.br, LATINDEX - Sistema Regional de Información en Línea para Revistas Científicas de América Latina, El Caribe, España y Portugal - www.latindex.unam.mx

Department of Cardiovascular Imaging/ Brazilian Society of Cardiology
Rua Barata Ribeiro nº 380 cj.54
01308-000 - São Paulo - SP - Brasil
Fone/Fax: +55 (11) 3259-2988
Fones: +55 (11) 3120-3363
+55 (11) 3259-2988 / +55 (11) 2589-4168

Editorial Coordination
Atha Comunicação e Editora
Rua Machado Bittencourt, 190 - conj. 410
São Paulo, SP, Brasil
Tel.: (11) 50879502

Editorial Support
revista@dicsbc.com

The journal Arquivos Brasileiros de Cardiologia — Imagem Cardiovascular is the official body of the Department of Cardiovascular Imaging of the Brazilian Society of Cardiology.

www.cardiol.br
www.dicsbc.org
ABC Imagem Cardiovascular

Contents - *Sumário*

Click on the title to read the article

Editorials - *Editoriais*

Original Article - *Artigo Original*

www.cardiol.br
www.dicsbc.org
ABC Imagem Cardiovascular

My Approach to Left Ventricular Strain Assessment

Como eu faço a Avaliação do Strain do Ventrículo Esquerdo

Cintia Galhardo Tressino[1,2], Renato de Aguiar Hortegal[2,3], Marcela Momesso[1,2,4], Rodrigo Bellio de Mattos Barretto[1,2], David Le Bihan[1,2,5]

[1]DASA Group, São Paulo, SP; [2]Dante Pazzanese Cardiology Institute, São Paulo, SP; [3]Beneficência Portuguesa Hospital of São Paulo, São Paulo, SP; [4]Sírio-Libanês Hospital, São Paulo, SP; [5]Kidney and Hypertension Hospital, Federal University of São Paulo, São Paulo, SP, Brazil

Introduction

Strain and strain rate are regional and global myocardial deformation indexes that provide data to enable the early detection of possible cardiac changes, thus improving therapeutic approaches. Strain corresponds to a myocardial deformation represented as the percentage of muscle shortening/stretching compared to the initial measurement, while strain rate indicates the rate of myocardial deformation or, in other words, the speed of this deformation. The three main patterns of heart deformation during systole include longitudinal shortening, circumferential shortening, and radial thickening. The latter occurs due to transverse fiber thickening due to its incompressibility (therefore, secondary to its shortening) and apposition (Figure 1). Ultimately, it accounts for a decreased ventricular cavity.[1,2]

The strain can be evaluated using the tissue Doppler technique based on mathematical calculations that convert speed to deformation. Although useful in some specific contexts, this technique has significant limitations, such as the following: a low signal-to-noise ratio, high intra- and inter-observer variability, and dependence on the angle of insonation, which greatly limits the assessment of radial and circumferential deformations.[3]

As a result, strain analysis with two-dimensional (2D) speckle tracking (ST) is the most widely validated technique used in clinical practice. This technique is based on the tracking (on all planes) of natural myocardial acoustic markers present in the 2D image in grayscale throughout the cardiac cycle based on the comparison of frame-by-frame patterns. Strain represents the relative mean myocardial fiber deformation between two adjacent points. When there is systolic fibrous shortening (longitudinal and circumferential directions), the strain has a negative value. Radial systolic thickening, on the other hand, gives the strain a positive value. The ST technique is less dependent on the angle of insonation, enabling deformation measurements in different directions: circumferential and radial in left ventricular (LV) short-axis cuts and longitudinal in the apical view.[1,2]

Each myocardial segment can be subjected to strain evaluation (regional strain), and the global strain reflects the relative contraction (in percentage) of the entire LV myocardium. Some authors believe that ST allows for the differentiation between active versus "passive" myocardial segment deformation, that is, the one occurring due to dragging (and not deformation) of the changed segment caused by the traction suffered by another adjacent segment with preserved contractility.[4] Load conditions are also known to affect myocardial deformation, with the strain being a more vulnerable parameter in this condition compared to the strain rate.[5]

The ventricular systolic function assessment is a fundamental part of echocardiography, being extremely important for the management and prognosis of patients with heart disease. In clinical practice, ejection fraction is routinely used to assess ventricular systolic function. However, over the past decade, myocardial strain has become an important predictor of morbidity and mortality in several heart diseases, providing additional prognostic information compared to ejection fraction alone.[6]

The objective of this study was to explore the main points of strain measurement variability using the ST technique in daily practice and discuss the methods that should be considered to increase parameter accuracy and reproducibility, particularly longitudinal global strain (LGS).

Left ventricle longitudinal strain measurement by speckle tracking

Subendocardial myocardial fibers are longitudinal (parallel to the wall), progressively changing their orientation to slowly become more perpendicular to the cavity so that the subepicardial fibers are in a circumferential direction (Figure 1). The structural arrangement of LV myocardial fibers, their shortening in the longitudinal and circumferential directions, and radial thickening result in the mechanical processes that compose the LV systolic function. All these movements act synergistically to culminate in volumetric variations of the ventricular cavity.[7]

Longitudinal strain evaluates deformation of the

Keywords

Echocardiography; Left Ventricular Dysfunction; Parameters.

Mailing Address: David Le Bihan •
Avenida Doutor Dante Pazzanese, 500 – Vila Mariana. CEP: 04012-909, São Paulo, SP, Brazil.
E-mail: davidbihan@uol.com.br
Manuscript received 7/12/2020; revised 7/15/2020; accepted 7/20/2020

DOI: 10.47593/2675-312X/20203304ecom15

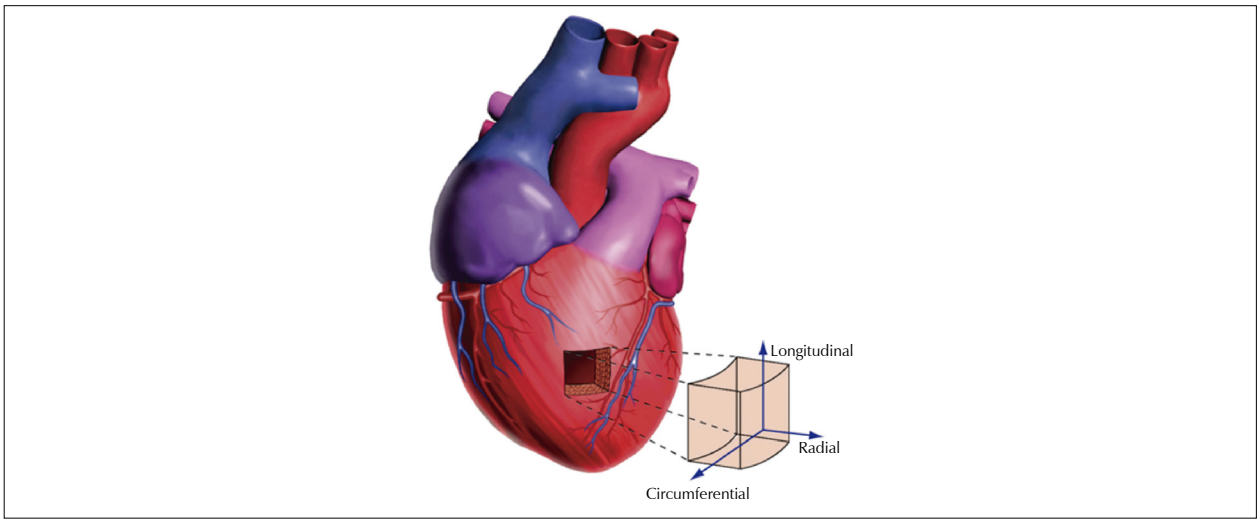

Figure 1 – *Different components of left ventricular deformation.*

subendocardial fibers, which tend to be involved in myocardial diseases. The circumferential strain measurement detects more significant myocardial lesions, as it measures the deformation produced by the subepicardial fibers affected by transmural lesions.[6] The study of circumferential and radial deformations is mostly intended for scientific research due to its low clinical applicability and reproducibility in echocardiography services.[4] Thus, this article focuses on LV LGS using the 2D ST technique, as it is the most widely studied and validated parameter as well as the most useful for prognostic stratification in several diseases and determining incipient myocardial involvement.

Images should be carefully acquired for LV LGS analysis using ST to obtain good technical quality for interpreting the results. The patient must be monitored and electrocardiogram tracing must be satisfactory. If possible, expiratory apnea should be attempted, avoiding the translation movements of the heart with respiratory incursions. Clips of four-, two-, and three-chamber apical acoustic windows must be acquired with at least three beats, excluding extrasystole. For device adjustments, the focus must be properly positioned and sector angle depth and width must be adjusted to include mainly the image of interest (i.e. LV). Likewise, the gain of the 2D image must be correctly adjusted, and the frame rate (FR) must be maintained at 40–80 frames/second in patients with a normal heart rate but may be higher in tachycardic patients or in those undergoing stress echocardiography (a low FR can result in loss of speckles, while a very high FR reduces spatial resolution, decreasing image quality).[4,8,9]

As the longitudinal strain presents higher values from the base to the apex, ventricular cavity shortening (foreshortening) should be avoided during image acquisition.[10] Artifacts, reverberations, and myocardial visualization limitations can result in the following of speckles outside the area of interest, leading to false results. Images must be acquired with a harmonic feature to obtain maximum quality.[9]

The LV segmentation model can have 16, 17, or 18 segments (the former being used in echocardiography and other diagnostic modalities) and reflects the myocardial perfusion territory used to analyze regional longitudinal strain values.[4,11,12]

The region of interest (ROI) must be adjusted to incorporate the entire analyzed wall thickness, leaving its shape and width as close as possible to the myocardial anatomy. Special care must be taken in segments with previous infarction or an asymmetric increased thickness. ROI angles and encompassing the pericardium and extracardiac spaces should be avoided, as these may erroneously reduce strain values.[9,12,13] Particularly in healthy people, the mitral ring presents a strong systolic movement toward the apex, sometimes leading to suboptimal ST in that region and impairing the basal segment strain analysis.[13]

Myocardial segment tracking is initially semi-automatically adjusted but then manually corrected according to the visual impression when necessary. Segments not properly read after an initial adjustment should be discarded. The greater the number of discarded segments, the lower the reliability of the LGS result.[2,8,12] Thus, when more than two myocardial segments are not clearly visible in a single window, use of the LGS calculation should be avoided.[14] A software was recently developed to automatically recognize echocardiographic windows, position the ROI, and provide strain results and curves with the ST technique using "just one button."

The ROI is outlined on the final diastole or systole (depending on the manufacturer), being divided into equidistant segments according to the segmentation model

used. The ROI can include the entire wall or be divided into endocardial, mesocardial, and epicardial layers, with each contour being automatically or manually defined. When no layer is selected, the results usually correspond to the results of all forces, representing the entire wall thickness. The measurements obtained in isolation are greater in the endocardial layer and smaller in the epicardial layer.[9,12]

The topographic definitions that form the ROI in the apical windows are the right and left bases at their endocardial borders immediately below the mitral valve, apex, and basal midpoint (midpoint between the right and left basal points).[12]

Event markers must be adjusted to define the beginning (final diastole) and the end (final systole) of the myocardial contraction in the cardiac cycle. Final diastole is the moment characterized by mitral valve closure. Other events related to this phase of the cycle are the beginning of the QRS complex (peak of the R wave) or the positive peak of the LGS curve. It should be considered that the mitral valve closure may dissociate from the electrocardiogram parameters in patients with conduction disorders or regional dysfunction. Thus, the software commonly uses the QRS complex peak to define the final diastole, marking it automatically without examiner interference.[12]

Closure of the aortic valve corresponds to the final systole and can be viewed in the apical three-chamber window (the reason why this window is the first to be analyzed by the software, followed by 4C and 2C windows) or detected by the end of the pulsed Doppler flow trace of the LV outflow tract. Substitute parameters can signal the end of the aortic flow by continuous Doppler, the nadir of the strain curve, or the volume curve. Most software asks the examiner for this mark, but it can be done automatically.[12]

The heart rate must be regular and without major variations for the software to allow the combination of strain values obtained in the three different apical windows (coincident curves) to obtain the LGS value and its representation in a polar map graph (better known as the bull's eye) (Figure 2)[9].

Strain analysis with the ST technique using the three-dimensional (3D) method is also possible, which has the relevant characteristic of acquiring the total heart volume in a single beat (full volume).[15] Comparison of the 3D- and 2D-methods showed no longitudinal displacement differences; however, the first method presented higher radial displacement values, indicating the limitation of the 2D method to track speckles coming out of the image plane. The 3D method allows area strain calculation (which integrates longitudinal and circumferential strain data) to reduce this tracking error.[16,17] The 3D strain technique requires image acquisition and analysis training as well as guidelines that incorporate their values into clinical practice. Thus, its applicability remains limited to research laboratories.

It is extremely important to know how to interpret the morphology and relevant values of the strain curves while considering amplitude and time in relation to the cardiac cycle in which they appear. The following parameters can be evaluated: positive systolic peak strain (occurs in final diastole with myocardial elongation or may represent relevant deformation in cases of regional dysfunction), systolic peak strain (the highest negative deformation value during systole), final systolic strain (deformation value coinciding with aortic valve closure), and post-systolic strain (maximum strain value that can appear after aortic valve closure).[12,13] The final systolic strain should be considered as a standard parameter to describe myocardial deformation (Figure 3).[12]

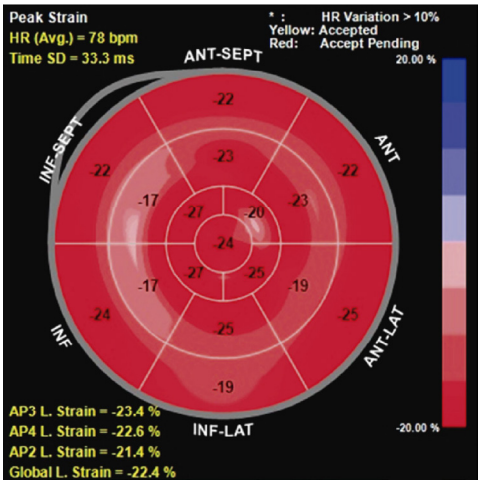

Figure 2 – *Graphical representation of longitudinal strain polar mapping in all segments as well as the global mean (longitudinal global strain) and means obtained in three-, four-, and two-chamber views.*

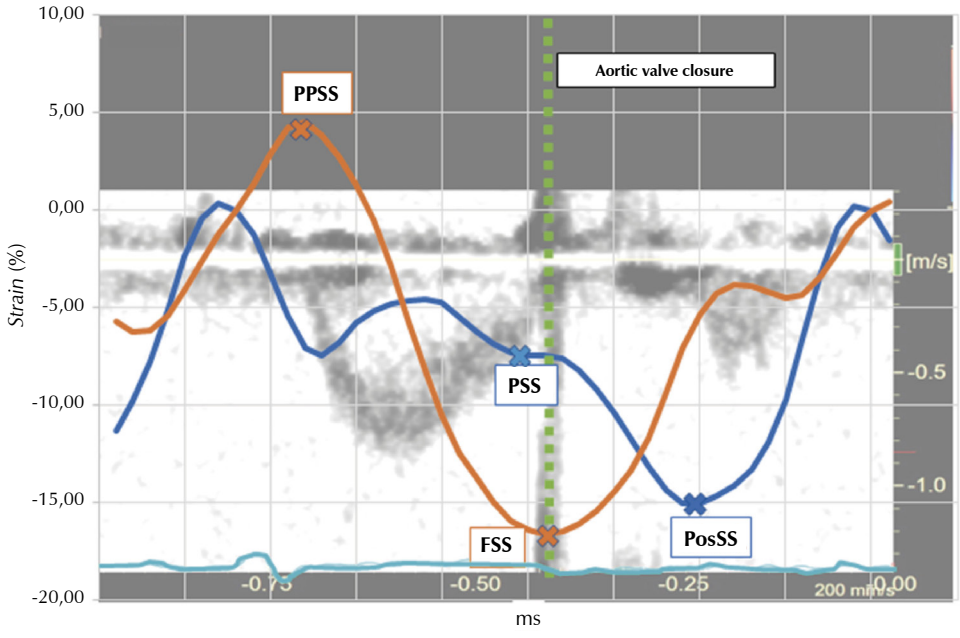

Figure 3 – *Strain curves and their relationship with the cardiac cycle.*

Post-systolic strain, which reflects the deformation of segments that contract after aortic valve closure and do not contribute to ventricular ejection, is a common finding in acute or chronic myocardial ischemia.[8,18] Some software has softening filters to reduce noise and improve curve interpretation. Excessive softening should be avoided when small time events are being investigated, such as segmental post-systolic shortening.[13]

Strain and strain rate can be assessed in each ventricular segment (regional strain), and the mean of these values now represents the global strain, which reflects global ventricular function.[19] An LGS is within the normal range when a module value is ≥20% (or ≤-20% when the strain is considered negative). Some authors currently prefer to use absolute values (in module) to avoid interpretation errors. There is evidence that women have slightly higher strain values than men and that strain values decrease with age.[12,14]

Farsalinos et al.[20] observed variability of LGS measurements obtained with seven different devices and software from different manufacturers. The largest absolute difference in LGS values between manufacturers was 3.7 percentage units of strain ($p < 0.001$, analysis of variance), with a significant and strong correlation between measures using different devices and with the mean measure of all manufacturers. There was slight variability between manufacturers in the mean LGS calculation or the 4C longitudinal strain, but the difference was statistically significant. These findings support the use of longitudinal strain in clinical practice, as long as the exams are repeated on machines produced by the same manufacturer.[20] A recent study suggested that software updates can also impact LGS calculations.[21] On the other hand, regarding the accuracy identify segmental abnormalities, manufacturers diverge significantly.[22]

Comparison of the different available software products revealed that LGS was a more robust and concordant parameter than the circumferential or radial global strain in the assessment of myocardial function.[23]

Despite these considerations, LGS was more reproducible than ejection fraction for assessing systolic function regardless of the echocardiographer's experience.[24] Another study also emphasized the intra- and inter-observer reproducibilities of the mean and 4C LGS as being superior to those of the LV ejection fraction measurement and other echocardiographic parameters.[20] These findings support the use of LGS in daily practice as an additional assessment tool in heart disease.[25]

Thus, inter-manufacturer biases must be considered when comparing LGS measurements acquired on different devices or analyzing them using different software. Thus, echocardiographic follow-up should ideally be performed using the same device under similar hemodynamic conditions, especially in situations in which LGS variation can have profound therapeutic implications, such as in the context of chemotherapy-induced cardiotoxicity assessments.

Step by step strain measurements for most manufacturers involve the following actions (Figure 4): perform cardiac monitoring; obtain three-, four-, and two-chamber acoustic windows with an FR of 40–80 QPS; mark the aortic valve closure; mark topographic definitions to define the ROI in three-, four-, and two-chamber windows; accept or

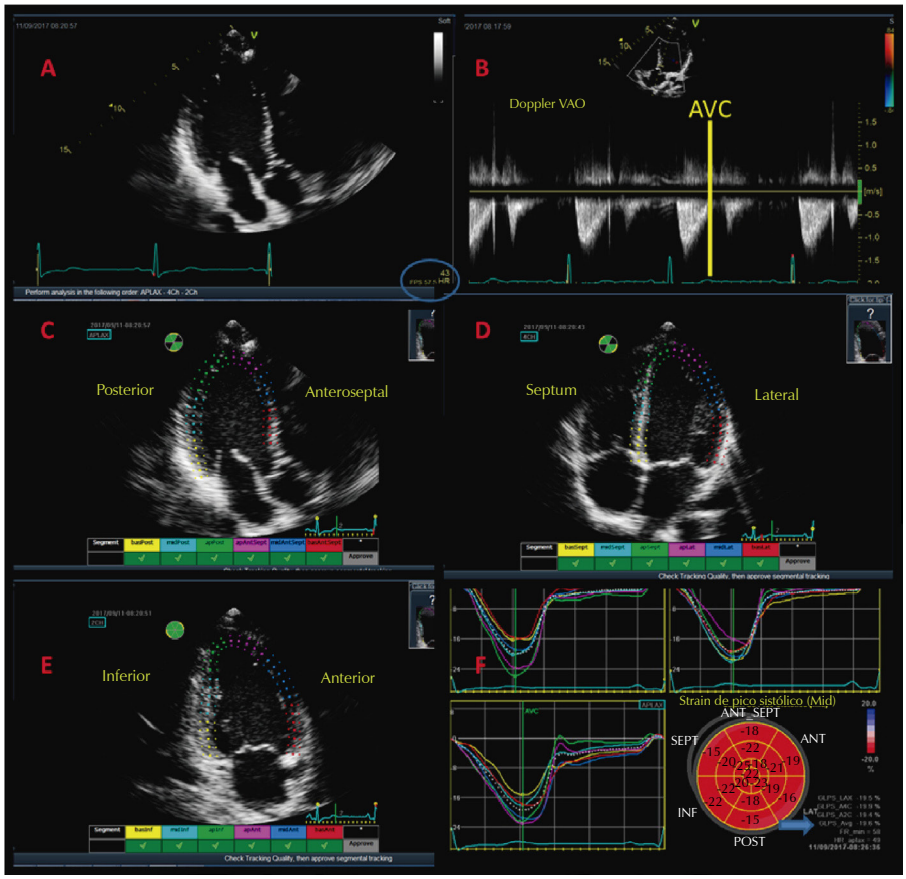

Figure 4 – *Sequence of steps followed to determine the longitudinal global strain (F, blue arrow). Initially, images are acquired in three-, four-, and two-chamber windows on a good-quality electrocardiogram with an adequate frame rate (40–80 frames/second) (A, blue ovoid). Aortic valve closure (AVC) was marked on a pulsed or continuous Doppler tracing (B). Then, three points are marked (two at the base, one at the apex) in the three acquired images and adequate monitoring by region of interest is ensured (C, D, and E). Finally, the curves, bull's eye, and global longitudinal strain values are observed (F).*

discard the myocardial segments tracked in each window and make adjustments as necessary; and evaluate the curves and interpret the results obtained on the polar map.

Authors' contributions

Manuscript writing: Peçanha MM, Tressino CG, Ortegal RA; critical review of the manuscript for important intellectual content: Barreto RBM, Bihan D.

Conflict of interest

The authors have declared that they have no conflict of interest.

References

1. Abduch MC, Alencar AM, Mathias W Jr, Vieira ML. [Cardiac mechanics evaluated by speckle tracking echocardiography]. Arq Bras Cardiol [Internet]. 2014 [citado 2020 Set 30];102(4):403-12. Disponível em: https://www.scielo.br/scielo.php?script=sci_arttext&pid=S0066-782X2014000400011. Portuguese.
2. Almeida AL, Gjesdal O, Newton N, Choi EY, Teixido G, Yoneyama K, et al. Speckle-tracking pela ecocardiografia bidimensional: aplicações clínicas. Rev Bras Ecocardiogr Imagem Cardiovasc [Internet]. 2013 [citado 2020 Set 30];26 (1):38-49. Disponível em: http://departamentos.cardiol.br/dic/publicacoes/revistadic/revista/2013/portugues/Revista01/09-revisao.pdf
3. Hoit BD. Strain and strain rate echocardiography and coronary artery disease. Circ Cardiovasc Imaging. 2011;4(2):179-90. doi: https://doi.org/10.1161/CIRCIMAGING.110.959817
4. Collier P, Phelan D, Klein A. A test in context: myocardial strain measured by speckle-tracking echocardiography. J Am Coll Cardiol. 2017;69(8):1043-56. doi: https://doi.org/10.1016/j.jacc.2016.12.012.
5. Weidemann F, Jamal F, Sutherland GR, Claus P, Kowalski M, Hatle L, et al. Myocardial function defined by strain and strain rate during alterations in inotropic states and heart rate. Am J Physiol Heart Circ Physiol. 2002;283(2):H792-9. doi: https://doi.org/10.1152/ajpheart.00025.2002
6. Luis SA, Chan J, Pellikka PA. Echocardiographic assessment of left ventricular systolic function: an overview of contemporary techniques, including speckle-tracking echocardiography. Mayo Clinic Proceedings. 2019;94(1):125-38. doi: https://doi.org/10.1016/j.mayocp.2018.07.017
7. Kocica MJ, Corno AF, Carreras-Costa F, Ballester-Rodes M, Moghbel MC, Cueva

CN, et al. The helical ventricular myocardial band: Global, three-dimensional, functional architecture of the ventricular myocardium. Eur J Cardiothorac Surg. 2006;29:S21-40. doi: https://doi.org/10.1016/j.ejcts.2006.03.011

8. Mor-Avi V, Lang RM, Badano LP, Belohlavek M, Cardim NM, Derumeaux G, et al. Current and evolving echocardiographic techniques for the quantitative evaluation of cardiac mechanics: ASE/EAE consensus statement on methodology and indications endorsed by the Japanese Society of Echocardiography. J Am Soc Echocardiogr. 2011;24(3):277-313. doi: https://doi.org/10.1016/j.echo.2011.01.015

9. Sade LE. Speckle tracking strain imaging: Practical approach for application. Turk Kardiyol Dern Ars. 2017;45(2):197-205. doi: 10.5543/tkda.2017.24358

10. Leitman M, Lysiansky M, Lysyansky P, Friedman Z, Tyomkin V, Fuchs T, et al. Circumferential and longitudinal strain in 3 myocardial layers in normal subjects and in patients with regional left ventricular dysfunction. J Am Soc Echocardiogr 2010;23(1):64-70. doi: https://doi.org/10.1016/j.echo.2009.10.004

11. Cerqueira MD, Weissman NJ, Dilsizian V, Jacobs AK, Kaul S, Laskey WK et al. Standardized myocardial segmentation and nomenclature for tomographic imaging of the heart. A statement for healthcare professionals from the Cardiac Imaging Committee of the Council on Clinical Cardiology of the American Heart Association. Circulation. 2002;105:539-42. doi: https://doi.org/10.1161/hc0402.102975

12. Voigt JU, Pedrizzetti G, Lysyansky P, Marwick TH, Houle H, Baumann R, et al. Definitions for a common standard for 2D speckle tracking echocardiography:consensus document of the EACVI/ASE/Industry Task Force to standardize deformation imaging. Eur Heart J Cardiovasc Imaging. 2015;16(1):1-11. doi: https://doi.org/10.1093/ehjci/jeu184

13. Mirea O, Corîci OM, Berceanu M, Donoiu I, Militaru C, Istratoaie O. Variability of longitudinal strain measurements: levelling the playing field. Acta Cardiologica. 2019;74(3). doi: https://doi.org/10.1080/00015385.2018.1480469

14. Lang RM, Badano LP, Mor-Avi V, Afilalo J, Armstrong A, Ernande L, et al. Recommendations for cardiac chamber quantification by echocardiography in adults: an update from the American Society of Echocardiography and the European Association of Cardiovascular Imaging. J Am Soc Echocardiogr. 2015;28(1):1-39.e14. doi: https://doi.org/10.1016/j.echo.2014.10.003

15. Chang SA, Lee SC, Kim EY, Hahm SH, Jang SY, Park SJ, et al. Feasibility of single-beat full-volume capture real-time three-dimensional echocardiography and auto-contouring algorithm for quantification of left ventricular volume: validation with cardiac magnetic resonance imaging. J Am Soc Echocardiogr. 2011;24(8):853-9. doi: https://doi.org/10.1016/j.echo.2011.04.015

16. Maffessanti F, Nesser HJ, Wienert L, Steringer-Mascherbauer R, Niel J, Gorissen W, et al. Quantitative evaluation of regional left ventricular function using three-dimensional speckle tracking echocardiography in patients with and without heart disease. Am J Cardiol. 2009;104(12):1755-62.

17. Saito K, Okura H, Watanabe N, Hayashida A, Obase K, Imai K, et al. Comprehensive evaluation of left ventricular strain using speckle tracking echocardiography in normal adults: comparison of three-dimensional and two-dimensional approaches. J Am Soc Echocardiogr. 2009;22(9):1025-30. doi: https://doi.org/10.1016/j.echo.2009.05.021

18. Kukulski T, Jamal F, Herbots L, D'hooge J, Bijnens B, Hatle L, et al. Identification of acutely ischemic myocardium using ultrasonic strain measurements. A clinical study in patients undergoing coronary angioplasty. J Am Coll Cardiol. 2003;41(5):810-9. doi: https://doi.org/10.1016/S0735-1097(02)02934-0

19. Reisner SA, Lysyansky P, Agmon Y, Mutlak D, Lessick J, Friedman Z. Global longitudinal strain: A novel index of left ventricular systolic function. J Am Soc Echocardiogr. 2004;17(6):630-3. doi: https://doi.org/10.1016/j.echo.2004.02.011

20. Farsalinos KE, Daraban AM, Ünlü S, Thomas JD, Badano LP, Voigt JU. Head-to-Head Comparison of Global Longitudinal Strain Measurements among Nine Different Vendors: The EACVI/ASE Inter-Vendor Comparison Study. J Am Soc Echocardiogr. 2015;28(10):1171-81. doi: https://doi.org/10.1016/j.echo.2015.06.011

21. Nagata Y, Takeuchi M, Mizukoshi K, et al. Intervendor variability of two-dimensional strain using vendor-specific and vendor-independent software. J Am Soc Echocardiogr. 2015;28(6):630-41. doi: doi: 10.1016/j.echo.2015.01.021

22. Mirea O, Pagourelias ED, Duchenne J, Bogaert J, Thomas JD, Badano LP, et al. EACVIASE- Industry Standardization Task Force. Variability and reproducibility of segmental longitudinal strain measurement: a report from the EACVI-ASE Strain Standardization Task Force. JACC Cardiovasc Imaging. 2018;11:15-24.

23. Manovel A, Dawson D, Smith B, Nihoyannopoulos P. Assessment of left ventricular function by different speckle-tracking software. Eur J Echocardiogr. 2010;11(5):417-21. doi: 10.1093/ejechocard/jep226

24. Karlsen S, Dahlslett T, Grenne B, Sjøli B, Smiseth O, Edvardsen T, et al. Global longitudinal strain is a more reproducible measure of left ventricular function than ejection fraction regardless of echocardiographic training. Cardiovasc Ultrasound. 2019;17:18. doi: 10.1186/s12947-019-0168-9

25. D'hooge J, Heimdal A, Jamal F, Kukulski T, Bijnens B, Rademakers F, et al. Regional strain and strain rate measurements by cardiac ultrasound: principles, implementation and limitations. Eur J Echocardiogr. 2000;1(3):154-70. doi: 10.1053/euje.2000.0031. Erratum in: Eur J Echocardiogr 2000;1(4):295-9.

My Approach to Assessing Right Ventricular Strain

Como Fazer a Avaliação do Strain do Ventrículo Direito

Marcela Momesso[1,2,3], Cintia Galhardo Tressino[1,2], Rodrigo Bellio de Mattos Barretto[1,2], David Le Bihan[1,2,4]

[1]DASA Group, São Paulo, SP; [2]Dante Pazzanese Cardiologic Institute, São Paulo, SP; [3]Sírio Libanês Hospital, São Paulo, SP; [4]Kidney and Hypertension Hospital, Federal University of São Paulo, São Paulo, SP, Brazil

Right ventricular (RV) systolic dysfunction is an independent predictor of morbidity and mortality in patients with pulmonary hypertension,[1] heart failure,[2] and coronary artery disease.[3] For this reason, RV function analyses are extremely important in clinical practice.

Echocardiography is an accessible, noninvasive, and fast method that enables accurate analyses of RV function. Despite the limitations related to the complex geometry of this cavity, new parameters have emerged in this context to improve the diagnostic accuracy.

Tricuspid annular plane systolic excursion and tricuspid lateral annular systolic excursion velocity are routinely used to evaluate RV systolic function due to their simplicity, reproducibility, and prognostic value in populations with heart failure and other cardiovascular diseases. However, these methods have limitations as they vary with pressure and volumetric load, can evaluate only a single RV segment (not consider regional function differences), and are angle-dependent.[4] Other analysis techniques, including fraction area shortening (FAS) and the Tei index, have prognostic value established in the literature. However, the FAS has low interobserver reproducibility, while the Tei index cannot be used in cases of increased right atrial pressure.[4]

RV strain overcomes some of these limitations. Two-dimensional systolic longitudinal deformation, calculated using speckle tracking echocardiography, has emerged as a viable and reproducible measure of RV systolic function. RV strain can be used to evaluate contractile function that corrects translation errors, being less dependent on the angle of the image plane.[5] Several studies in the literature have used it for determining both diagnosis and prognosis, especially in patients with heart failure,[6-8] pulmonary hypertension,[9-12] ischemic heart disease,[13] infiltrative heart diseases,[14,15] and heart valve diseases.[16,17]

Two-dimensional RV strain analysis requires an apical four-chamber window toward the RV that optimizes gain and depth with high frame rates (40–80 frames/s) and at least three heart beats. Patients should preferably be in apnea and have good electrocardiogram tracing.[18]

Keywords

Echocardiography; Strain; Ventricular Dysfunction, Right.

Correspondência: Mailing Address •
Avenida Doutor Dante Pazzanese, 500 – Vila Mariana – CEP: 04012-909 – São Paulo, SP, Brazil.
E-mail: davidbihan@uol.com.br
Manuscript received 7/12/2020; revised 7/15/2020; accepted 7/20/2020

DOI: 10.47593/2675-312X/20203304ecom14

The apical window toward the RV is obtained by lateral displacement of the transducer from the conventional apical position via transducer rotation (Figure 1A) to position the apex of the left ventricle (LV) in the center of the sector (avoiding its shortening) and simultaneously display the largest basal diameter, long axis, and entire RV free wall (Figure 1B).

Genovese et al. demonstrated that RV strain parameters determined in a directed apical four-chamber window were more reproducible than those identified in the conventional apical four-chamber window, reinforcing its use in clinical practice.[19]

The software used to measure the RV strain was originally created to evaluate the LV systolic function, being later adapted for the RV. Some companies are currently developing specific software for offline analysis on a workstation.

Similarly, to the LV, the RV region of interest (ROI) is defined by the endocardial borders (internal myocardial contour) and the epicardial borders (external myocardial contour) or, in the case of interventricular septum involvement, the left endocardial contour of the septum. The tracing must be started by marking the lateral tricuspid ring, medial ring, and apex. The ROI is generated automatically after these markings are made and can be adjusted by the examiner. The user must observe whether the ROI movement follows the wall movement. Inclusion of the pericardium and reference points below the tricuspid ring or inside the right atrium should be avoided because it will result in underestimation of the strain values.[5,20] Due to the thin wall of the RV, it is recommended that the ROI have a standard width of 5 mm.[20] In addition to observing the tracking of the points to verify their quality, the derived curves must be analyzed (Figure 2).

Most studies evaluating RV strain used longitudinal strain defined as strain in the direction tangential to the RV endocardial border in the apical window. The RV radial strain is inaccurate due to its thin wall, so its use is not recommended in the literature.[20]

RV strain calculation can analyze the six segments, including the interventricular septum, obtain the global longitudinal strain (GLS-RV) or an arithmetic mean of the strain values of the three segments of the free wall (basal, medium, and apical segments), and obtain the RV free wall longitudinal strain (FWLS-RV). The absolute GLS-RV values are lower than the FWS-RV values.[21,22] The interventricular septum is mainly composed of LV fibers, although it also improves RV systolic performance to a lesser extent.[21] In this sense, most studies showed a more robust FWS-RV prognostic value.[23,24] The literature recommends the use of this method to improve standardization, although the GLS may also be an option.[20] Because the two methods

Editorial

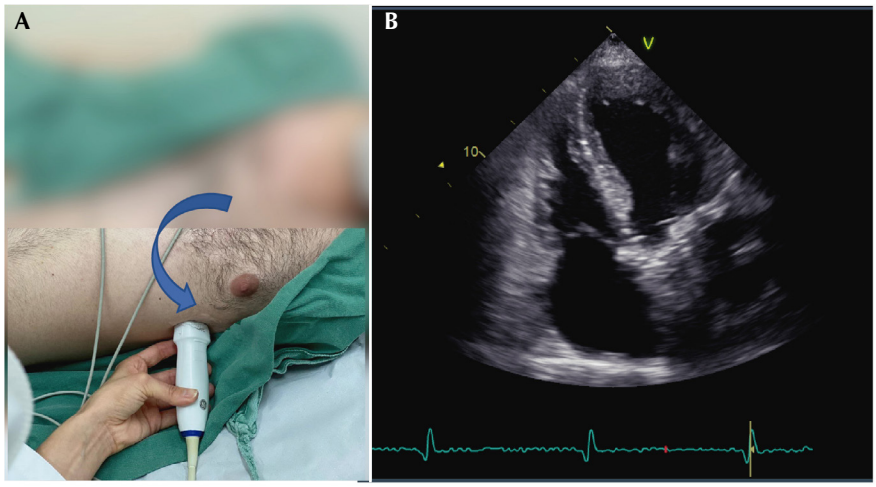

Figure 1 – *(A) Lateral displacement of the transducer from the conventional apical position. (B) Sample apical window image taken toward the right ventricle (including the largest basal diameter, long axis, and entire right ventricle free wall).*

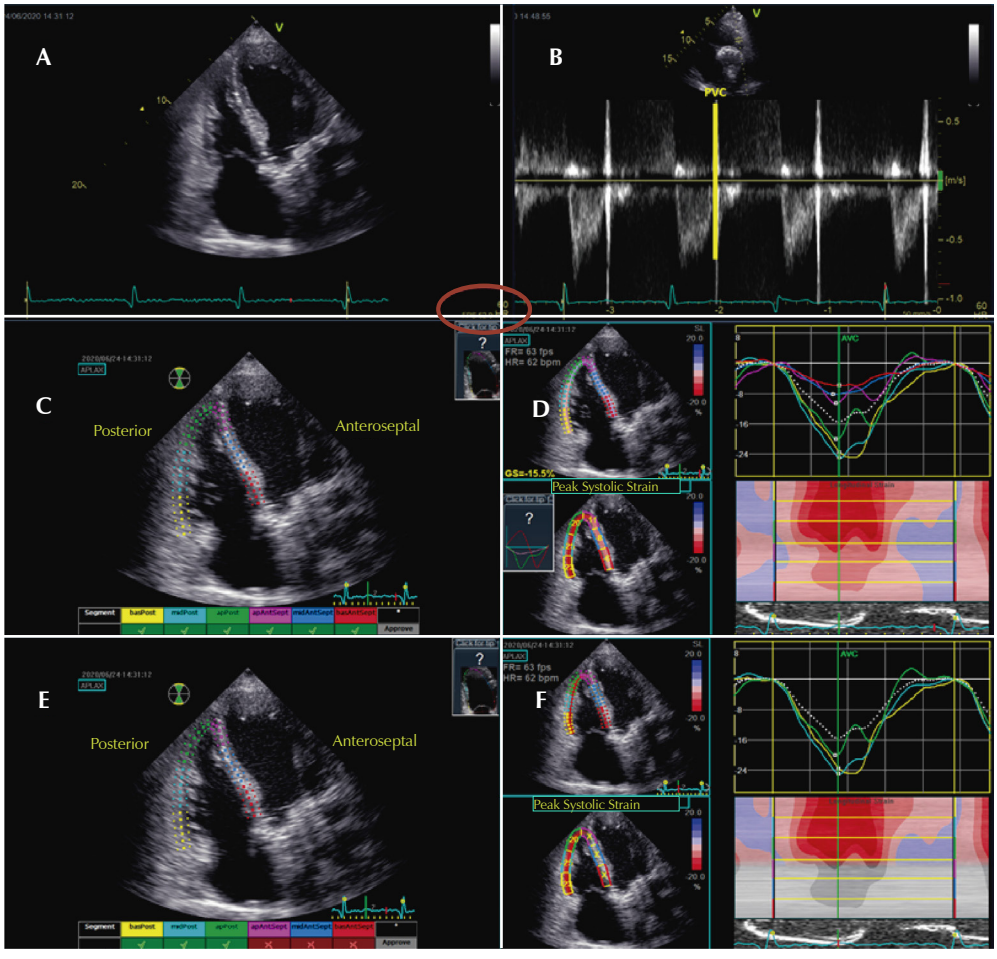

Figure 2 – *The first step in obtaining the right ventricular strain is acquiring a directed apical image (A) with an adequate frame rate (red ovoid) and marking the pulmonary valve closure time (B). Subsequently, points are marked on the septal and lateral tricuspid ring as well as on the right ventricle apex to observe the appropriate size of the region of interest and if the ventricular movement is being monitored, indicating adequate tracking (C, D). Finally, the septal curves are excluded to analyze only the global longitudinal strain of the free wall (E, F).*

achieve different results, it is necessary to specify the parameter used in the report. Even when the objective is to obtain only the FWS-RV, it is recommended that all six segments be initially tracked (free wall and interventricular septum) because the algorithms recognize the true RV apical segment better with this procedure.[5]

As with the calculation of LV strain, RV strain curves can generate four values, although only the peak systolic strain (that is, the highest deformation value during systole) has been studied and recommended. To adjust the cardiac cycle, it is assumed that the final diastole must be defined by tricuspid valve closure and the final systole by pulmonary valve closure, and both are obtained by Doppler tracing of these valves.[20]

Reference values vary among devices and software packages.[4] A systematic review published by Fine et al.[25] of healthy patients without cardiopulmonary disease reported normal FWS-RV values estimated at -27% ± 2% (95% confidence interval , 24–29%).[25] Muraru et al.[21] reported values of -29.3 ± 3.4% (lower limit of normal, -22.5%) for men and -31.6 ± 4.0% (lower limit of normal, -23.3%) for women. The same study reported GLS-RV values within the normal range as -24.7 ± 2.6% (lower limit of normal, -20.0%) for men and -26.7 ± 3.1% (lower limit of normal, -20.3%) for women.[21] The studies used devices created by the same manufacturer (General Electric). A recent study of 1,457 healthy volunteers analyzed 1,143 patients using EchoPAC software (GE) and reported FWS-RV values of -28.5 ± 4.8% (lower limit of normal, -20.2%) and GLS-RV values of -22.3 ± 2.4% (lower limit of normal, -17.4%). In contrast, 186 patients were evaluated using Syngo VVI software (Siemens), with FWS-RV values of -21.7 ± 4.2% (lower limit of normal, -13.4%) and GLS-RV values of -20.4 ± 3.2% (lower limit of normal, -14.1%).[26] The American Society of Echocardiography guideline for cardiac chamber quantification published in 2015 suggests that absolute FWS-RV values below 20% are probably abnormal. However, it also states that further large studies using equipment from various manufacturers are needed to obtain definitive reference values.[4]

Few studies in the literature have compared RV longitudinal strain values between manufactures, which could be a limitation. However, some studies[2,27] reported low inter- and intraobserver variation using equipment from the same manufacturer, which indicates good reliability.[28]

Park et al.[29] compared RV longitudinal strain analyzed by GE and Siemens software and reported lower intraobserver variability with the former and similar interobserver variation with both.[29]

Finally, it is worth mentioning that RV strain plays an important role in clinical practice. However, the method has some limitations requiring consideration because the software used was originally created to evaluate the LV and was later adapted for the RV. However, the RV has a more complex anatomy than the LV. RV-specific software has been developed and recently used to overcome this limitation.[28] Good image quality is essential to improving point tracking. Small random errors in point detection, as in limited acoustic windows, can lead to inaccurate results and greater inter- and intraobserver variability. Thus, this method may not be applicable in patients who are obese or have pulmonary disease.[30] An RV evaluation is performed in only one window (apical four-chamber), whereas an LV evaluation is performed through three windows (apical four-, two-, and three-chamber), a fact that limits the analysis of part of the RV walls and, therefore, of their systolic function. Unlike the LV, for which comparative studies have been performed of equipment created by different manufacturers,[31] RV strain requires additional studies on this subject to enable comparisons among brands. Due to technical difficulties correctly evaluating RV strain, its use should be restricted to trained and experienced echocardiographers unlike LV strain, which can be performed by less experienced professionals due to less interference in the result. Learning curve studies have reported that at least 100 FWS-RV analysis studies must be performed for a beginner to reach the skill level of a specialist.[26,32]

Perspectives include RV strain performed by the three-dimensional method, which can be an interesting tool that provides data on the longitudinal, circumferential, and radial functions of this cavity.[33] However, it also has its limitations. The strain technique is based on the point tracking analysis. Therefore, high temporal resolution, good image quality, and a regular heart rate are essential to its feasibility. However, one of the main limitations of the three-dimensional method is its relatively low temporal resolution. In addition, additional studies on protocols and reference values are needed to standardize this method.[28] Thus, such facts reduce its use in clinical practice today.

Authors' contributions

Manuscript writing: PMM and TCG; critical review of the manuscript for important intellectual content: BRBM and BD.

Conflict of interest

The authors have declared that they have no conflict of interest.

References

1. Motoji Y, Tanaka H, Fukuda Y, Ryo K, Emoto N, Kawai H, et al. Efficacy of right ventricular free-wall longitudinal speckle-tracking strain for predicting long-term outcome in patients with pulmonary hypertension. Circ J. 2013;77(3):756-63. doi: https://doi.org/10.1253/circj.cj-12-1083

2. Vizzardi E, Bonadei I, Sciatti E, Pezzali N, Farina D, D'Aloia A, et al. Quantitative analysis of right ventricular (RV) function with echocardiography in chronic heart failure with no or mild RV dysfunction: comparison with cardiac magnetic resonance imaging. J Ultrasound Med. 2015;34(2):24755. doi: https://doi.org/10.7863/ultra.34.2.247

3. Pfeffer MA, Braunwald E, Moye LA, Basta L, Brown EJ Jr., Cuddy TE, et al. Effect of captopril on mortality and morbidity in patients with left ventricular dysfunction after myocardial infarction. Results of the survival and ventricular enlargement trial. The SAVE Investigators. N Engl J Med. 1992;327(10):669-77. https://doi.org/10.1056/NEJM199209033271001

4. Lang RM, Badano LP, Mor-Avi V, Afilalo J, Armstrong A, Ernande L, et al. Recommendations for cardiac chamber quantification by echocardiography in adults: an update from the American Society of Echocardiography and the European Association of Cardiovascular Imaging. J Am Soc Echocardiogr. 2015;28(1):1-39. doi: https://doi.org/10.1016/j.echo.2014.10.003

5. Ayach B, Fine NM, Rudski L. Right Ventricular Strain: Measurement and Clinical Application. Curr Opin Cardiol. 2018;33(5):486-92. doi: https://doi.org/10.1097/HCO.0000000000000540

6. Motoki H, Borowski AG, Shrestha K, Hu B, Kusunose K, Troughton RW, et al. Right ventricular global longitudinal strain provides prognostic value incremental to left ventricular ejection fraction in patients with heart failure. J Am Soc Echocardiogr. 2014;27(7):726-32. doi: https://doi.org/10.1016/j.echo.2014.02.007

7. Sade LE, Özin B, Atar I, Demir Ö, Demirtaş S, Müderrisoğlu H. Right ventricular function is a determinant of long-term survival after cardiac resynchronization therapy. J Am Soc Echocardiogr. 2013;26(7):706-13. doi: https://doi.org/10.1016/j.echo.2013.03.013

8. Morris DA, Krisper M, Nakatani S, Köhncke C, Otsuji Y, Belyavskiy E, et al. Normal range and usefulness of right ventricular systolic strain to detect subtle right ventricular systolic abnormalities in patients with heart failure: a multicentre study. Eur Heart Cardiovasc Imaging. 2017;18(2):212-23. doi: https://doi.org/10.1093/ehjci/jew011

9. D'Andrea A, Stanziola A, D'Alto M, Di Palma E, Martino M, Scarafile R, et al. Right ventricular strain: an independent predictor of survival in idiopathic pulmonary fibrosis. Int J Cardiol. 2016;222:908-10. doi: https://doi.org/10.1016/j.ijcard.2016.07.288

10. Mukherjee M, Mercurio V, Tedford RJ, Shah AA, Hsu S, Mullin CJ, et al. Right ventricular longitudinal strain is diminished in systemic sclerosis compared with idiopathic pulmonary arterial hypertension. Eur Respir J. 2017;50(5):1701436. doi: https://doi.org/10.1183/13993003.01436-2017

11. Platz E, Hassanein AH, Shah A, Goldhaber SZ, Solomon SD. Regional right ventricular strain pattern in patients with acute pulmonary embolism. Echocardiography. 2012;29(4):464-70. doi: https://doi.org/10.1111/j.1540-8175.2011.01617.x

12. Fine NM, Chen L, Bastiansen PM, Frantz RP, Pellikka PA, Oh JK, et al. Outcome prediction by quantitative right ventricular function assessment in 575 subjects evaluated for pulmonary hypertension. Circ Cardiovasc Imaging. 2013;6(5):711-21. doi: https://doi.org/10.1161/CIRCIMAGING.113.000640

13. Chang WT, Liu YW, Liu PY, Chen JY, Lee CH, Li YH, et al. Association of decreased right ventricular strain with worse survival in non-acute coronary syndrome angina. J Am Soc Echocardiogr. 2016;29(4):350-358.e4. doi: https://doi.org/10.1016/j.echo.2015.11.015

14. Cappelli F, Porciani MC, Bergesio F, Perlini S, Attanà P, Moggi Pignone A, et al. Right ventricular function in AL amyloidosis: characteristics and prognostic implication. Eur Heart J Cardiovasc Imaging. 2012;13(5):416-22. doi: https://doi.org/10.1093/ejechocard/jer289

15. Joyce E, Kamperidis V, Ninaber MK, Katsanos S, Debonnaire P, Schalij MJ, et al. Prevalence and Correlates of Early Right Ventricular Dysfunction in Sarcoidosis and Its Association with Outcome. J Am Soc Echocardiogr. 2016;29(9):871-8. doi: https://doi.org/10.1016/j.echo.2016.06.001

16. Kusunose K, Popović ZB, Motoki H, Marwick TH. Prognostic significance of exercise-induced right ventricular dysfunction in asymptomatic degenerative mitral regurgitation. Circ Cardiovasc Imaging. 2013;6(2):167-76. doi: https://doi.org/10.1161/CIRCIMAGING.112.000162

17. Hyllén S, Nozohoor S, Ingvarsson A, Meurling C, Wierup P, Sjögren J. Right ventricular performance after valve repair for chronic degenerative mitral regurgitation. Ann Thorac Surg. 2014;98(6):2023-30. doi: https://doi.org/10.1016/j.athoracsur.2014.07.075

18. Rudski LG, Lai WW, Afilalo J, Hua L, Handschumacher MD, Chandrasekaran K, et al. Guidelines for the echocardiographic assessment of the right heart in adults: a report from the American Society of Echocardiography endorsed by the European Association of Echocardiography, a registered branch of the European Society of Cardiology, and the Canadian Society of Echocardiography. J Am Soc Echocardiogr. 2010;23(7):685-713; quiz 786-8. doi: https://doi.org/10.1016/j.echo.2010.05.010

19. Genovese D, Mor-Avi V, Palermo C, Muraru D, Volpato V, Kruse E, et al. Comparison Between Four-Chamber and Right Ventricular-Focused Views for the Quantitative Evaluation of Right Ventricular Size and Function. J Am Soc Echocardiogr. 2019;32(4):484-494. doi: https://doi.org/10.1016/j.echo.2018.11.014

20. Badano LP, Kolias TJ, Muraru D, Abraham TP, Aurigemma G, Edvardsen T, D'Hooge J, Donal E, Fraser AG, Marwick T, Mertens L, Popescu BA, Sengupta PP, Lancellotti P, Thomas JD, Voigt JU; Industry representatives; Reviewers: This document was reviewed by members of the 2016–2018 EACVI Scientific Documents Committee. Standardization of left atrial, right ventricular, and right atrial deformation imaging using two-dimensional speckle tracking echocardiography: a consensus document of the EACVI/ASE/Industry Task Force to standardize deformation imaging. Eur Heart J Cardiovasc Imaging. 2018;19(6):591-600. doi: https://doi.org/10.1093/ehjci/jey042. Erratum in: Eur Heart J Cardiovasc Imaging. 2018;19(7):830-833.

21. Muraru D, Onciul S, Peluso D, Soriani N, Cucchini U, Aruta P, et al. Sex- and method-specific reference values for right ventricular strain by 2-dimensional speckle-tracking echocardiography. Circ Cardiovasc Imaging. 2016;9(2):e003866. doi: https://doi.org/10.1161/CIRCIMAGING.115.003866

22. Sanz-de la Garza M, Giraldeau G, Marin J, Imre Sarvari S, Guasch E, Gabrielli L, et al. Should the Septum Be Included in the Assessment of Right Ventricular Longitudinal Strain? An Ultrasound Two-Dimensional Speckle-Tracking Stress Study. Int J Cardiovasc Imaging. 2019;35(10):1853-1860. doi: https://doi.org/10.1007/s10554-019-01633-6

23. Antoni ML, Scherptong RW, Atary JZ, Boersma E, Holman ER, Van der Wall EE, et al. Prognostic value of right ventricular function in patients after acute myocardial infarction treated with primary percutaneous coronary intervention. Circ Cardiovasc Imaging. 2010;3(3):264-71. doi: https://doi.org/10.1161/CIRCIMAGING.109.914366

24. Carluccio E, Biagioli P, Lauciello R, Zuchi C, Mengoni A, Bardelli G, et al. Superior prognostic value of right ventricular free wall compared to global longitudinal strain in patients with heart failure. J Am Soc Echocardiogr. 2019;32(7):836-844.e1. doi: https://doi.org/10.1016/j.echo.2019.02.011

25. Fine NM, Chen L, Bastiansen PM, Frantz RP, Pellikka PA, Oh JK, et al. Reference values for right ventricular strain in patients without cardiopulmonary disease: a prospective evaluation and meta-analysis. Echocardiography. 2015;32(5):787-96. doi: https://doi.org/10.1111/echo.12806

26. Badano LP, Muraru D, Parati G, Haugaa K, Voigt JU. How to do right ventricular strain. Eur Heart J Cardiovasc Imaging. 2020;21(8):825-7. doi: https://doi.org/10.1093/ehjci/jeaa126

27. Focardi M, Cameli M, Carbone SF, Massoni A, De Vito R, Lisi M, et al. Traditional and innovative echocardiographic parameters for the analysis of right ventricular performance in comparison with cardiac magnetic resonance. Eur Heart J Cardiovasc Imaging. 2015;16(1):47-52. doi: https://doi.org/10.1093/ehjci/jeu156

28. Longobardo L, Suma V, Jain R, Carerj S, Zito C, Zwicke DL, et al. Role of Two-Dimensional Speckle-Tracking Echocardiography Strain in the Assessment of Right Ventricular Systolic Function and Comparison with Conventional Parameters. J Am Soc Echocardiogr. 2017;30(10):937-946.e6. doi: https://doi.org/10.1016/j.echo.2017.06.016

29 Park JH, Kusunose K, Motoki H, Kwon DH, Grimm RA, Griffin BP, et al. Assessment of right ventricular longitudinal strain in patients with ischemic cardiomyopathy: head-to-head comparison between two-dimensional speckle-based strain and velocity vector imaging using volumetric assessment by cardiac magnetic resonance as a "gold standard". Echocardiography. 2015;32(6):956-65. doi: https://doi.org/10.1111/echo.12740

30. Voigt JU, Pedrizzetti G, Lysyansky P, Marwick TH, Houle H, Baumann R, et al. Definitions for a common standard for 2D speckle tracking echocardiography: consensus document of the EACVI/ASE/Industry Task Force to standardize deformation imaging. Eur Heart J Cardiovasc Imaging. 2015;16(1):1-11. doi: https://doi.org/10.1093/ehjci/jeu184

31. Yang H, Marwick TH, Fukuda N, Oe H, Saito M, Thomas JD, et al. Improvement in strain concordance between two major vendors after the strain standardization initiative. J Am Soc Echocardiogr. 2015;28(6):642-8. e7. doi: https://doi.org/10.1016/j.echo.2014.12.009

32. Chamberlain R, Scalia GM, Wee Y, Hlaing S, Lee A, Hotham I, et al. The Learning Curve for Competency in Right Ventricular Longitudinal Strain Analysis. J Am Soc Echocardiogr. 2020;33(4):512-514. doi: https://doi.org/10.1016/j.echo.2019.12.011

33. Smith BC, Dobson G, Dawson D, Charalampopoulos A, Grapsa J, Nihoyannopoulos P. Three-dimensional speckle tracking of the right ventricle: toward optimal quantification of right ventricular dysfunction in pulmonary hypertension. J Am Coll Cardiol. 2014;64(1):41-51. doi: https://doi.org/10.1016/j.jacc.2014.01.084.

Left Atrium: Novel Insights and Future Directions

Átrio esquerdo: Novas percepções e direcionamentos futuros

Cristiane de Carvalho Singulane,[1,2] Karima Addetia,[2] Roberto Miguel Lang[2]

[1]Post-Graduation Division, São José do Rio Preto Medical School, São José do Rio Preto, Brazil; [2]Noninvasive Cardiac Imaging Laboratories, Section of Cardiology, Heart & Vascular Center, University of Chicago Medicine, Chicago, USA.

Introduction

The left atrium (LA) is an intricate chamber with complex geometry and multiple functions, the most important of which is the modulation of LV filling.[1] Recent studies have highlighted our understanding of the contributions of left atrial function to overall cardiac performance in multiple disease states.[2] Both LA size and extent of remodeling are powerful predictors of adverse cardiovascular outcomes in multiple clinical settings, including development of atrial fibrillation, ischemic stroke and congestive heart failure.[3] Accordingly, it is crucial to strictly follow the guidelines[4] when performing measurements of LA dimension, volumes and function to enhance accuracy and reproducibility.

LA assessment on 2D Echocardiography

LA size is still frequently assessed using linear measurements of the anteroposterior diameter of the LA in the parasternal long-axis view perpendicular to the aortic root long axis, at the level of the aortic sinuses using M-mode and 2-dimensional echocardiography (2D).[4] Because this measurement is easy to obtain and highly reproducible, echocardiography laboratories continue to report it despite being strongly discouraged in the latest chamber quantification guidelines.[4,5] The main reason for this recommendation is that the LA is an asymmetrical cavity which does not dilate proportionally in all directions. In fact, it has been shown that the LA tends to enlarge more in the superior-inferior than the antero-posterior direction due to presence of the spine and sternum.[6,7] Consequently, these linear measurements tend to underestimate true left atrial size (Figure 1).

Left atrial volumes can be measured on 2D echocardiography using either the biplane method of discs or the area-length method. The method currently recommended by American Society of Echocardiography (ASE) is the biplane Simpson disk summation technique. While the area-length method is effective, the Simpson method is preferred because it relies on fewer geometrical assumptions. LA volumes should be measured in both the four and two-chamber apical LA focused views at end-ventricular systole. The endocardial contour should be traced up to the connecting juxtaposed points of the mitral annulus, taking care to exclude the tenting area under the mitral valve leaflets as well as the confluence of the left atrial appendage and pulmonary veins.[4]

A few remarks are worth making in reference to the acquisition of 2D LA volumes. First, a dedicated "focused-view" should always be attempted because it provides larger volumes compared with the standard LV chamber acquisition in which usually the LV is elongated but the LA is foreshortened.[8] (Figures 2 and 3). Secondly, it is strongly advised to measure LA volume in both apical two and four chamber views since biplane volume showed better agreement with 3D volume than single plane and also because single-plane method can result in misclassification of patients when the ASE cutoffs are applied.[9] If the acquisition of both the four and two-chamber LA focused views are adequate, the length of the LA long-axis (distance between the midpoint of the mitral annulus plane to the base of the atrium) should be nearly identical avoiding LA foreshorting.[4] Importantly, while LA size is gender-dependent, this inter-gender difference is no longer present after adjusting for body size.[10] Therefore, only the indexed values of LA volumes should be reported.[4] Finally, recent data suggests that the cutoff values used to partition LA volumes should be based on outcomes instead of standard deviation (SD).[3,4] For instance, LA volumes are normally larger in elite athletes and this needs to be accounted for in order to avoid an incorrect diagnosis of LA enlargement in these patients.[9]

LA Volume Assessment on 3D Echocardiography

Three-dimensional echocardiography (3DE) has been shown to have superior prognostic ability and measurement accuracy compared to the 2D biplane Simpson's method.[4,11] This volumetric method has better correlation with cardiac magnetic resonance, the current gold standard to assess LA volumes.[12] This methodology should become the method of choice because it is completely independent of geometric assumptions.[4] 3D LA volumes obtained using semi-automated methods have demonstrated a reduction in intra- and interobserver variability.[8,13] A full volume acquisition acquired from an focused LA apical four chamber view, can be analyzed offline in less than 2 min, avoiding foreshortening by allowing the operator to manually select non-forshortened orthogonal planes and correct minor mistakes on the LA endocardial tracing border made by the software.[5,14] The accurate analysis of a 3D dataset is highly dependent on image quality, more so than analysis of a 2D dataset. Accordingly, during data acquisition, it is encouraged to decrease imaging depth and narrow the sector size so that only the LA is in view. In this

Keywords

Atrial Function; Echocardiography, Left Atrium; Strains; Three-Dimensional.

Mailing Address: Cristiane de Carvalho Singulane •
The University of Chicago Medical Center, 5758 South Maryland Avenue, MC 9067, DCAM 5509, Chicago, IL 60637 EUA.
E-mail: csingulane@uchicago.edu
Manuscript received 0/0/0000; revised 0/0/0000; accepted 0/0/0000

DOI: 10.47593/2675-312X/20203304eabc157

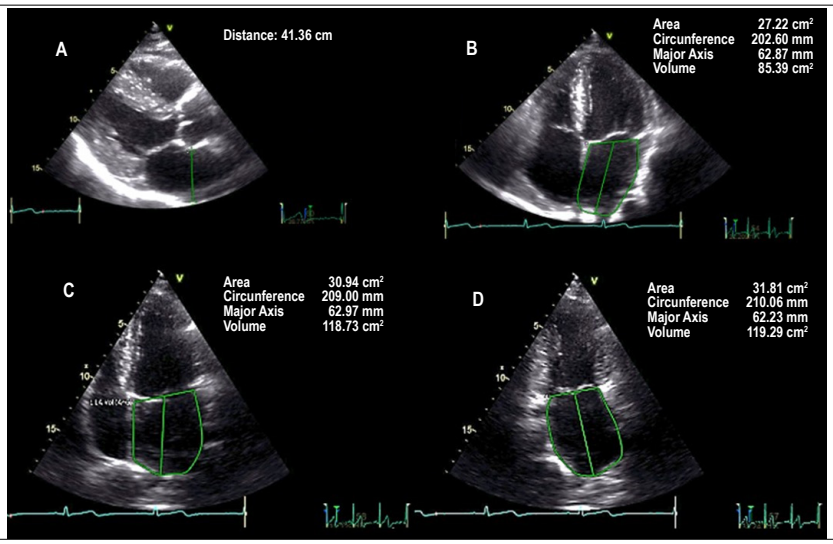

Figure 1 – *The left atrium is seen in the parasternal long-axis view (A), apical four chamber non-focused view (B) and LA focused four- (C) and two chamber views (D). When viewing the images side by side the underestimation of the antero-posterior diameter becomes apparent. The LA remodeling is constricted in the antero-posterior dimension because of the spine and sternum. The underestimation is greater when the LA is assessed in the LV focused view.*

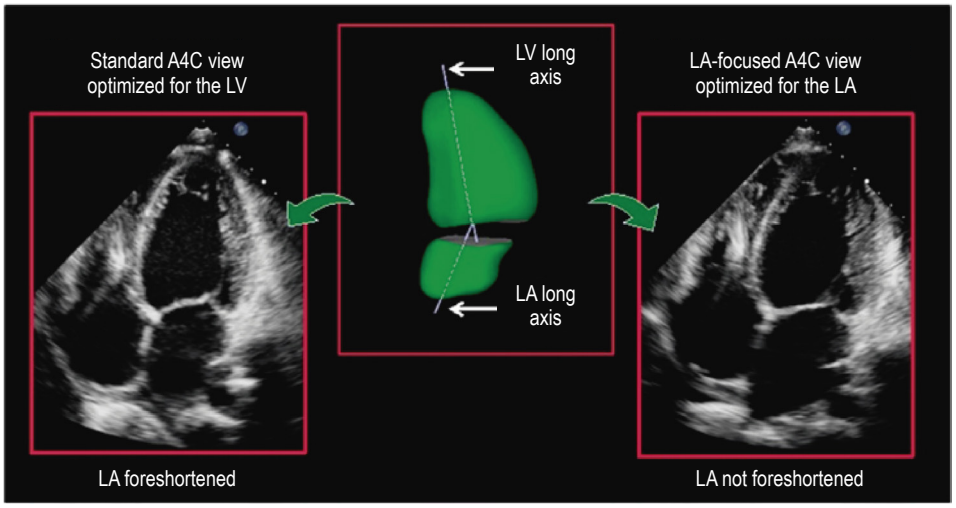

Figure 2 – *The left atrium must be acquired using dedicated focused two and four chamber views, instead of dedicated LV view, to avoid forshortening. The LA and LV longitudinal axis lie in different planes as is clearly illustrated in this image. In a focused view the base of LA should be at its largest dimension and the length maximized to ensure alignment along the true LA long axis.*

window part or most of the LV will also be visible. A multibeat (usually 4-beat) acquisition, will achieve better temporal resolution while maintaining high spatial resolution. This acquisition mode requires patient cooperation and breath-holding to avoid chest motion that can result in stitching artifacts with ultimately sub-volume misalignment. These may be avoided in part with ECG and respiratory gating.[4,14]

Previous studies have reported a variety of normal values for LA volumes often in-line with the population studied. The upper limit of 34ml/m² for 2D LA volume proposed by the 2015 ASE Chamber Quantification guidelines and used around the globe, was derived largely from white American and European subjects, despite the fact that it has been suggested that LA values are not universal and that population specific normal values should be used for different geographic groups.[4,5,15] For example, Badano et al[8] reported that in Italian subjects, 3D LA values greater than 43ml/m² should be considered abnormal. The NORRE study,[13] a multi-center study of predominantly white European subjects reported a similar value of 40ml/m². However, Wu et al.,[16] a Japanese cohort study, reported a much smaller value of 33ml/m². While, image optimization, such as the use of a dedicated LA focused view as opposed to the standard four-chamber view acquisition and the software package used

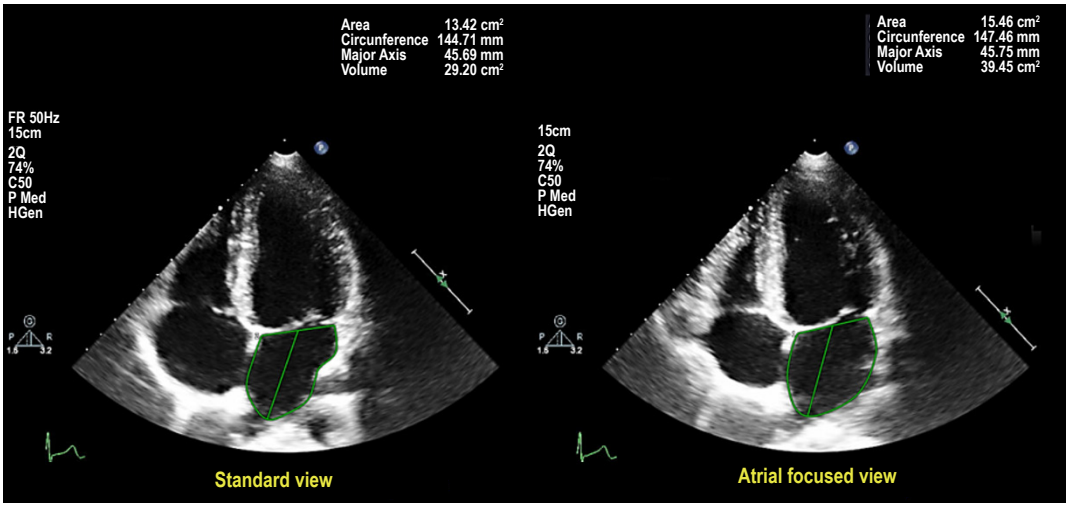

Figure 3 – *This image shows the discrepancy in LA volume measurements when using the standard view, optimized for the left ventricle and the dedicated atrial focused view. See text for additional explanation.*

(i.e. use of dedicated LV instead of LA-based software) can account for some of these differences, it is highly possible that the main reason for these discrepancies lies in differences that exist between ethnicities.[5] This hypothesis will soon be answered with the publication of the LA analysis by the World Alliance Societies of Echocardiography (WASE) Normal Values Study which includes approximately 2 000 subjects from 15 countries, including Brazil.

LA Phasic Function

Assessment of LA function provides valuable insight into the pathophysiology of numerous cardiovascular disorders. LA phasic function can be assessed using 2D echocardiography either using tissue Doppler velocities, or spectral Doppler combined with transmitral, pulmonary venous, and LA appendage flow. Lately, 2D deformation analysis of longitudinal LA strain and strain rate, using speckle-tracking (2D STE) has also been effectively used to determine LA phasic function.[1, 17, 18] Alternatively, LA phasic function may be derived from 3D LA volume vs. time curves, obtained from measurements of the largest (at LV end-systole, at the end of the T wave), minimal (at LV end-diastole, at the beginning of QRS) and pre-A (prior to atrial systole, before the P wave) volumes. These volumes will provide estimates of total (reservoir), passive (conduit) and active (booster) emptying LA volumes and fractions (Figure 4).[1, 14]

Of the two reference ECG landmarks (onset of QRS complex or P wave) that can be used for LA volume curves or deformation imaging, numerous authors recommend using the first because the majority of studies used to obtain normative values have used it.[18] In the case of deformation imaging, if the ventricular cycle is used, the zero reference will be LV end-diastole and the first phase of the curve will be represented by the peak positive longitudinal atrial strain corresponding to reservoir function, followed by the early diastolic strain wave representing the conduit phase and finally the late diastolic strain wave representing the booster pump function (Figure 5).[1, 17]

In addition to image quality, 2D STE is also dependent on a relatively high frame rate (50-70 frame/sec) for accurate tracking.[17] The far-field position of the LA in the acoustic window, mobility of the interatrial septum and thin LA walls constitute additional challenges for STE assessment.[19] Accordingly, at present this technique is challenging and heavily depends on the expertise of the operator.[1] The other key drawback rests in the lack of uniform normative values that currently appear to be dependent on the echocardiographic equipment used with their unique STE algorithms and software packages.[1, 13] The reproducibility are being address with efforts to reduce intervendor variability and standardize deformation imaging.[20] While there has been improvement between inter-vendor concordance of LV strain, less is known about atrial strain.[18, 20] Although a novelty today, 3D STE has a prospect of become a great asset in LA evaluation in the future (Figure 4).

Studies have shown that changes in LA phasic behavior occur early in disease processes and might provide early diagnostic clues compared to the assessment of LA size such as in diastolic dysfunction,[21] heart failure with preserved ejection fraction (HFpEF),[22] as well as new-onset of atrial fibrillation (AF),[23, 24] hypertension, diabetes,[25] amyloidosis and hypertrophic cardiomyopathy,[26] to cite a few. More importantly, it can predict outcome before or independently of volume augmentation in certain disorders, such as in acute myocardial infarction,[27] asymptomatic rheumatic mitral stenosis,[28] recurrence of AF after ablation and acute embolism in patients with paroxysmal or persistent AF.[23] Accordingly, question has been raised as to the helpfulness of LA functional assessment in guiding clinical decision-making in certain scenarios regarding rhythm vs rate control strategies, use of anticoagulation and others.[1]

Conclusion

In summary, echocardiography remains the imaging modality of choice for LA assessment due to its wide availability

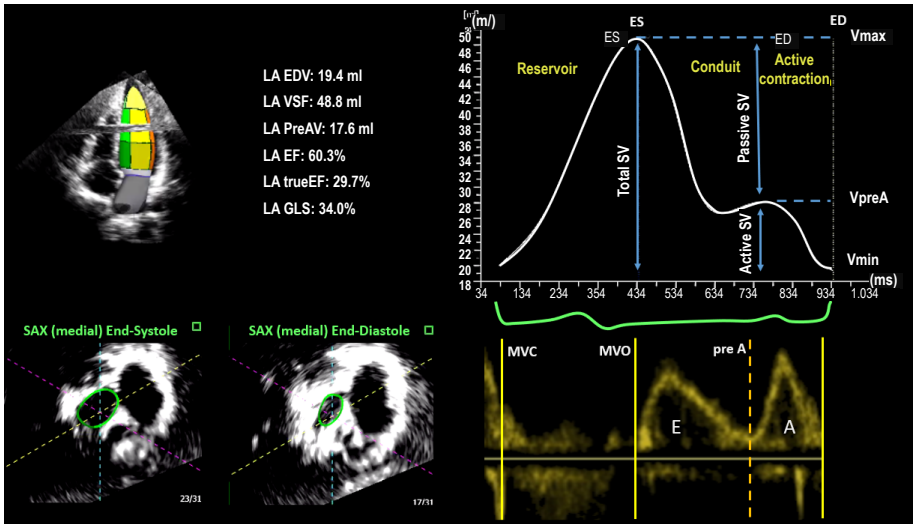

Figure 4 – *Function of the left atrium and its relationship with the cardiac cycle. When the mitral valve closes (MVC), at LV end-diastole (at the beginning of QRS), the LA is in its minimum volume (V min). In this phase (reservoir) the LA stores venous flow from the pulmonary veins and starts to increase in size until it reaches its maximum volume (V max), just before mitral valve opening (MVO) at the LV end-systole (at the end of the T wave). Thereafter, the conduit phase occurs wherein the LA passively transfers blood to the LV and the LA volume slightly decreases until it reaches the pre-contraction volume (V pre-A) (before the P wave), just prior to atrial systole. From these volumes the total atrial stroke volume (total SV =Vmax – Vmin), passive atrial stroke volume (passive SV = Vmax – Vpre-A), and active atrial stroke volume (active SV = Vmax – V pre-A) can be calculated. The ejection fractions (or emptying) can also be calculated: LA total emptying fraction (LA EF: Vmax – Vmin/V max), LA true emptying fraction (LA trueEF = V pre-A – Vmin/V pre-A) and LA passive emptying fraction (LA passive EF = Vmax – V pre-A/ V pre-A).*

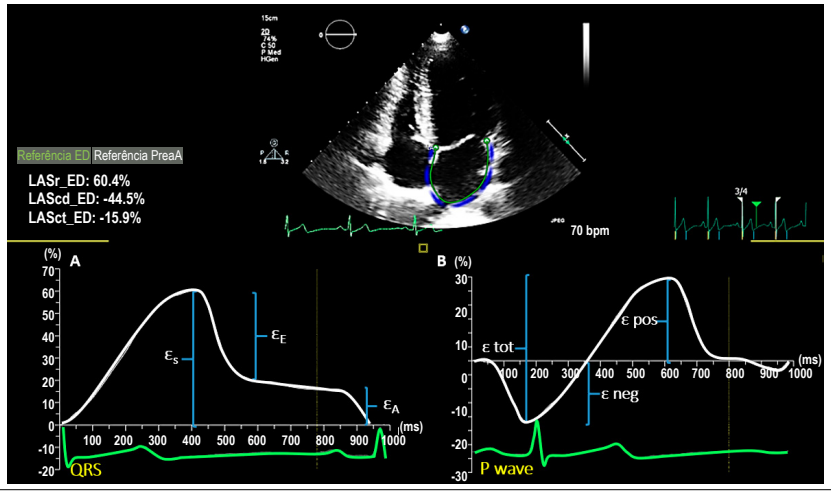

Figure 5 – *Measurement of LA phasic function with 2D speckle tracking using the QRS as a timing reference (A) versus the P wave (B). When the QRS is used as the reference point, the phasic curve starts with the peak positive longitudinal atrial strain (εs) corresponding to the reservoir function (LASr_ED), followed by the early diastolic strain waves (εe) representing the conduit phase (LAScd_ED) and finally the late diastolic strain wave (εa) expressing the booster pump function (LASct_ED). In contrast, when using the P wave, the first negative peak strain (εneg) expresses the booster pump function, followed by the positive peak strain (εpos) and later the total longitudinal strain (εtot) representing the conduit and reservoir functions, respectively.*

and cost-effectiveness. Although the biplane Simpson technique is currently recommended for the assessment of LA size, newer echocardiographic techniques such as 2D STE and 3DE volumes will soon assume a protagonist role in LA analysis due to their ability to measure LA size and phasic function more accurately and reproducibly providing risk stratification and evaluation of therapeutics.

Conflict of Interests

Dr Lang received a research grant from Phillips Healthcare (Phillips Imaging Systems) outside the submitted work.

Authors' contributions

CCS, KA, and RML drafted and revised the article.

References

1. Hoit BD. Assessment of Left Atrial Function by Echocardiography: Novel Insights. Current cardiology reports. 2018;20(10). doi: 10.1007/s11886-018-1044-1.
2. Thomas L, Marwick TH, Popescu BA, Donal E, Badano LP. Left Atrial Structure and Function, and Left Ventricular Diastolic Dysfunction: JACC State-of-the-Art Review. J Am Coll Cardiol. 2019;73(15):1961-1977. doi: 10.1016/j.jacc.2019.01.059.
3. Tsang TS, Abhayaratna WP, Barnes ME, Miyasaka Y, Gersh BJ, Bailey KR, et al. Prediction of cardiovascular outcomes with left atrial size: is volume superior to area or diameter? J Am Coll Cardiol. 2006;47(5):1018-23. doi: 10.1016/j.jacc.2005.08.077. Epub 2006 Feb 9. PMID: 16516087.
4. Lang RM, Badano LP, Mor-Avi V, Afilalo J, Armstrong A, Ernande L, et al. Recommendations for cardiac chamber quantification by echocardiography in adults: an update from the American Society of Echocardiography and the European Association of Cardiovascular Imaging. J Am Soc Echocardiogr. 2015;28(1):1-39.e14. doi: 10.1016/j.echo.2014.10.003..
5. Addetia K, Lang RM. Complexities of Left Atrial Analysis: More Than Meets the Eye? Circ Cardiovasc Imaging. 2016;9(7):e005196. doi: 10.1161/CIRCIMAGING.116.005196.
6. Lester SJ, Ryan EW, Schiller NB, Foster E. Best method in clinical practice and in research studies to determine left atrial size. Am J Cardiol. 1999;84(7):829-32. doi: 10.1016/s0002-9149(99)00446-4
7. Maddukuri PV, Vieira ML, DeCastro S, Maron MS, Kuvin JT, Patel AR, et al. What is the best approach for the assessment of left atrial size? Comparison of various unidimensional and two-dimensional parameters with three-dimensional echocardiographically determined left atrial volume. J Am Soc Echocardiogr. 2006 ;19(8):1026-32. doi: 10.1016/j.echo.2006.03.011.
8. Badano LP, Miglioranza MH, Mihăilă S, Peluso D, Xhaxho J, et al. Left Atrial Volumes and Function by Three-Dimensional Echocardiography: Reference Values, Accuracy, Reproducibility, and Comparison With Two-Dimensional Echocardiographic Measurements. Circ Cardiovasc Imaging. 2016;9(7):e004229. doi: 10.1161/CIRCIMAGING.115.004229.
9. Russo C, Hahn RT, Jin Z, Homma S, Sacco RL, Di Tullio MR. Comparison of echocardiographic single-plane versus biplane method in the assessment of left atrial volume and validation by real time three-dimensional echocardiography. J Am Soc Echocardiogr. 2010;23(9):954-60. doi: 10.1016/j.echo.2010.06.010. Epub 2010 Jul 21.
10. Kou S, Caballero L, Dulgheru R, Voilliot D, De Sousa C, Kacharava G, et al. Echocardiographic reference ranges for normal cardiac chamber size: results from the NORRE study. Eur Heart J Cardiovasc Imaging. 2014;15(6):680-90. doi: 10.1093/ehjci/jet284. Epub 2014 Jan 21. PMID: 24451180; PMCID: PMC4402333.
11. Caselli S, Canali E, Foschi ML, Santini D, Di Angelantonio E, Pandian NG, et al. Long-term prognostic significance of three-dimensional echocardiographic parameters of the left ventricle and left atrium. Eur J Echocardiogr. 2010;11(3):250-6. doi: 10.1093/ejechocard/jep198. Epub 2009 Dec 7.
12. Mor-Avi V, Yodwut C, Jenkins C, Kühl H, Nesser HJ, Marwick TH, et al. Real-time 3D echocardiographic quantification of left atrial volume: multicenter study for validation with CMR. JACC Cardiovascular imaging. 2012;5(8):769-77. doi: 10.1016/j.jcmg.2012.05.011.13. Sugimoto T, Robinet S , Dulgheru R, Bernard A, Ilardi F, Contu L, et al. Echocardiographic reference ranges for normal left atrial function parameters: results from the EACVI NORRE study. 2018;19(6):630-8. doi: 10.1093/ehjci/jey018..
14. Kebed KY, Addetia K, Lang RM. Importance of the Left Atrium: More Than a Bystander? Heart Fail Clin. 2019;15(2):191-204. doi: 10.1016/j.hfc.2018.12.001. Epub 2019 Feb 2.
15. Ethnic-Specific Normative Reference Values for Echocardiographic LA and LV Size, LV Mass, and Systolic Function: The EchoNoRMAL Study. JACC Cardiovascular Imaging. 2015 ;8(6):656-665. DOI: 10.1016/j.jcmg.2015.02.014..
16. Wu VCC, Takeuchi M, Kuwaki H, Iwataki M, Nagata Y, Otani K, et al. Prognostic value of LA volumes assessed by transthoracic 3D echocardiography: comparison with 2D echocardiography. JACC Cardiovascular imaging. 2013;6(10):1025-35. doi: 10.1016/j.jcmg.2013.08.002.
17. Badano LP, Kolias TJ, Muraru D, Abraham TP, Aurigemma G, Edvardsen T, et al. Standardization of Left Atrial, Right Ventricular, and Right Atrial Deformation Imaging Using Two-Dimensional Speckle Tracking Echocardiography: A Consensus Document of the EACVI/ASE/Industry Task Force to Standardize Deformation Imaging. Eur Heart J Cardiovasc Imaging. 2018;19(6):591-600. doi: 10.1093/ehjci/jey042. Erratum in: Eur Heart J Cardiovasc Imaging. 2018 Jul 1;19(7):830-833.
18. Pathan F, D'Elia N, Nolan MT, Marwick TH, Negishi K. Normal Ranges of Left Atrial Strain by Speckle-Tracking Echocardiography: A Systematic Review and Meta-Analysis. J Am Soc Echocardiogr. 2017;30(1):59-70.e8. doi: 10.1016/j.echo.2016.09.007.
19. Voigt JU, Măl ăescu GG, Haugaa K, Badano L. How to do LA strain. Eur Heart J Cardiovasc Imaging. 2020;21(7):715-717. doi: 10.1093/ehjci/jeaa091.
20. Thomas JD, Badano LP. EACVI-ASE-industry initiative to standardize deformation imaging: a brief update from the co-chairs. Eur Heart J Cardiovasc Imaging. 2013;14(11):1039-40. doi: 10.1093/ehjci/jet184.
21. Brecht A, Oertelt-Prigione S, Seeland U, Rücke M, Hättasch R, Wagelöhner T. Left Atrial Function in Preclinical Diastolic Dysfunction: Two-Dimensional Speckle-Tracking Echocardiography-Derived Results from the BEFRI Trial. J Am Soc Echocardiogr. 2016 ;29(8):750-758. doi: 10.1016/j.echo.2016.03.013.
22. Morris DA, Parwani A, Huemer M, Wutzler A, Bekfani T, Attanasio P, et al. Clinical significance of the assessment of the systolic and diastolic myocardial function of the left atrium in patients with paroxysmal atrial fibrillation and low CHADS(2) index treated with catheter ablation therapy. Am J Cardiol. 2013;111(7):1002-11. doi: 10.1016/j.amjcard.2012.12.021.
23. Yasuda R, Murata M, Roberts R, Tokuda H, Minakata Y, Keiko Suzuki K, et al. Left atrial strain is a powerful predictor of atrial fibrillation recurrence after catheter ablation: study of a heterogeneous population with sinus rhythm or atrial fibrillation. Eur Heart J Cardiovasc Imaging. 2015;16(9):1008-14. doi: 10.1093/ehjci/jev028. Epub 2015 Mar 6.
24. Cameli M, Mandoli GE, Loiacono F, Sparla S, Iardino E, Mondillo S. Left atrial strain: A useful index in atrial fibrillation. Int J Cardiol. 2016;220:208-13. doi: 10.1016/j.ijcard.2016.06.197. Epub 2016 Jun 28..
25. Mondillo S, Cameli M, Caputo ML, Lisi M, Palmerini E, Padeletti M, et al. Early detection of left atrial strain abnormalities by speckle-tracking in hypertensive and diabetic patients with normal left atrial size. J Am Soc Echocardiogr. 2011;24(8):898-908. doi: 10.1016/j.echo.2011.04.014. Epub 2011 Jun 12.
26. Gregorio Cd, Dattilo G, Casale M, Terrizzi A, Donato R, Bella G Di. Left Atrial Morphology, Size and Function in Patients With Transthyretin Cardiac Amyloidosis and Primary Hypertrophic Cardiomyopathy- Comparative Strain Imaging Study. Circ J. 2016;80(8):1830-7. doi: 10.1253/circj.CJ-16-0364. Epub 2016 Jun 28.
27. Modin D, Pedersen S, Fritz-Hansen T, Gislason G, Biering-Sørensen. Left Atrial Function Determined by Echocardiography Predicts Incident Heart Failure in Patients With STEMI treated by Primary Percutaneous Coronary Intervention. J Card Fail. 2020;26(1):35-42. doi: 10.1016/j.cardfail.2019.08.014. Epub 2019 Aug 24.
28. Caso P, Ancona R, Salvo G Di, Pinto SC, Macrino M, Palma V Di, et al. Atrial reservoir function by strain rate imaging in asymptomatic mitral stenosis: prognostic value at 3 year follow-up. Eur J Echocardiogr. 2009;10(6):753-9. doi: 10.1093/ejechocard/jep058. Epub 2009 May 13.

My approach to assess Kawasaki disease by echocardiogram

Como Eu Faço Diagnóstico e Avaliação Ecocardiográfica na Doença de Kawasaki

Evangelical Hospital of Cachoeiro de Itapemirim[1] – Cachoeiro de Itapemirim, ES, Brazil.

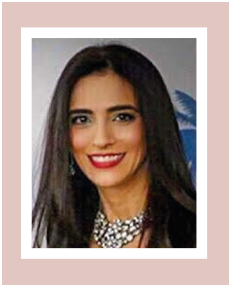

Andressa Mussi Soares[1]

Abstract

Kawasaki disease is the leading cause of acquired disease in children worldwide. The varied spectrum of this disease makes it both interesting and challenging to diagnose and follow up.

Kawasaki disease (KD) is an acute and self-limited disease of unknown etiology. A medium-sized artery vasculitis, it affects mainly the coronary arteries in approximately 25% of untreated patients and around 4–5% of those treated with intravenous immunoglobulin (IGVI) with the consequent formation of coronary artery aneurysms.[1,2] Other arteries can be affected, such as the subclavian, brachial, axillary, iliac, and femoral arteries, and occasionally the renal arteries and abdominal aorta.

The diagnosis of the disease remains eminently clinical and follows the classic criteria established by the American Heart Association,[3] according to which fever should persist for at least 5 days and be associated with four of the signs listed in Chart 1. Certainly, there are peculiar situations in which patients with fever for > 5 days and who demonstrate fewer than four other clinical signs already have coronary involvement on echocardiography, confirming the early KD diagnosis. More than the four main criteria may be evident before the fifth day of fever, leading to an early diagnosis of the disease and enabling earlier treatment.

KD mainly affects children up to 5 years of age, with a peak incidence between 9 and 11 months of age.[1] Although the disease is rare in babies up to 3 months of age, some cases have been reported.[4] Ischemic cardiac lesions, such as an undiagnosed KD sequela in childhood, correspond to 5% of acute coronary syndrome cases in adults aged < 40 years.[5] The varied spectrum of this disease makes it very interesting and challenging to diagnose and follow up.

Because specific diagnostic tests for KD are lacking, clinical recognition is of great importance for the therapeutic management of these patients, as a delayed or misdiagnosis can compromise the disease course and patient prognosis. Thus, echocardiography is extremely useful and valuable in cases of KD.

The echocardiographic study in KD focuses on the coronary arteries, which are affected by its major sequelae. Echocardiography is the imaging method of choice in cardiac evaluation due to its high specificity and sensitivity for detecting coronary artery abnormalities and noninvasive nature. It should be performed as soon as the diagnosis is suspected with the aim of visualizing all coronary segments. Echocardiography is a great tool even in cases of incomplete KD, which are characterized by the presence of fever for > 5 days but fewer than four of the associated clinical criteria listed in Table 1. In these cases, the finding of echocardiographic changes enables the diagnostic conclusion of the disease, greatly assisting with its clinical management (Table 2).[6]

The coronary artery should be measured between the internal extremities of the vessel on two-dimensional echocardiography in several planes, excluding the coronary ostia and branching points, in which the focal dilation is normal. In addition, perivascular brightness and echogenicity, which tend to increase in KD, and wall and flow irregularities on Doppler and color mapping should be observed.[7]

Several methods for analyzing coronary artery dimension have been reported. The dimension indexed by body surface

Keywords

Coronary Aneurysm; COVID-19; Echocardiography; Kawasaki disease.

Mailing Address: Andressa Mussi Soares •
Rua Papa João XXII, 1, apto. 1.202 – Gilberto Machado – CEP: 29303-297.
Cachoeiro de Itapemirim, ES, Brazil.
E-mail: amussisoares@gmail.com
Manuscript received 5/7/2020; revised 5/21/2020; accepted 5/27/2020

DOI: 10.47593/2675-312X/20203304eabc106

Table 1 - Diagnostic criteria for Kawasaki disease.

Fever for at least 5 days
Four of the following signs:
Bilateral conjunctival hyperemia
Changes in the oral mucosa:
Erythema or cleft lip
Diffuse or oropharyngeal erythema
Raspberry tongue
Extremity changes:
Hardened hand and foot edema
Palmoplantar erythema
Desquamation, usually periungual
Polymorphous rash
Cervical adenomegaly (>1.5 cm in diameter)

Note: Kawasaki disease can be diagnosed before the fifth day of disease in cases of fever and four of the other signs.

Editorial

(Z score) provides a more objective and accurate value, being the most valid score in the diagnostic and prognostic evaluation of these patients (Figure 1). Z score ≥ +2.5 is considered abnormal. Dallaire and Dahdah published the Z score calculation of the coronary arteries in all segments based on expected body surface values at all ages, increasing the importance of these echocardiographic measures.[8] The Z score can be quickly and effectively calculated at www.parameterz.com. Kobayashi et al. created a ready-to-use Z score calculator based on Microsoft Excel software to facilitate the specialists' routine (http://raise.umin.jp/zsp/calculator/). The calculator provides a median coronary artery diameter (Z score = 0) and the ratio, that is, the determined value divided by the median.[9]

Left coronary dilation usually does not involve the ostium and rarely occurs without ectasia of the anterior descendant and/or the circumflex arteries. Ectasia or coronary dilations are considered when the Z score is 2–2.5. At values > 2.5, they are already considered aneurysms. They are considered saccular when the axial and lateral diameters are approximately equal and fusiform if the dilation is symmetrical with proximal and distal thinning.[10] The number and location of aneurysms and the presence or absence of thrombi should also be investigated (Figure 2, Video 1). Table 3 clearly summarizes the classification of echocardiographic coronary changes according to the Z score, which must be followed by every echocardiographer.[10]

Table 2 - Conditions that confirm the suspected diagnosis of Kawasaki disease on echocardiography.

Z score of the right coronary or anterior descending artery internal diameter ≥ +2.5 or coronary aneurysm
OR at least three of the following findings:
Pericardial effusion
Mitral valve regurgitation
Left ventricular systolic dysfunction
+2 < coronary Z score < +2.5
↑ perivascular brightness and loss of usual coronary thinning

The aortic root should also be measured and compared with reference body surface values because there is evidence of mild aortic root dilation being common in patients with KD.[11] The pericardium and valves should always be evaluated with respective analysis of pericardial thickening and/or effusion and the presence and quantification of valve regurgitation as well as the anatomical characteristics of the valves, mainly the mitral and aortic.

Myocarditis in the acute phase is common in histological studies. Thus, the evaluation of left ventricular function is necessary in all patients with KD. Left ventricular performance can be evaluated using one-dimensional ejection fraction by calculating diastolic and systolic volumes from the left ventricle to two- and three-dimensional flows, dP/dT measured in a mitral regurgitation jet when present, and the myocardial performance index or Tei index.[10] The evaluation of myocardial deformation by strain using speckle tracking favors the direct analysis of the movement of myocardial fibers in different directions, making it a valuable tool for the early detection of systolic and diastolic dysfunction and segmental contractility changes and a promising technique for the diagnosis and follow-up of patients with KD[12] (Figure 3). It is worth mentioning that the American Heart Association has already incorporated the use of echocardiographic evidence of ventricular dysfunction as auxiliary criterion for incomplete Kawasaki diagnosis.[10] In the diagnostic phase it can be a more sensitive indicator of myocardial inflammation. McCandles et al.[13] demonstrated a reduction in LV GLS and strain rate to the initial echocardiogram of patients with KD who later came to develop coronary dilation, or although they showed resistance to the treatment with IGVI. The patients who did not develop coronary dilation and who responded promptly to treatment, had GLS LV and strain rate comparable to that of the healthy control group on the initial echocardiogram. These findings suggest that the strain LV should be used as a stratification tool for risk at Kawasaki disease.[13]

Follow-up echocardiography should be performed at the time of suspected diagnosis, 2 weeks thereafter, and between 6 to 8 weeks after disease onset in uncomplicated

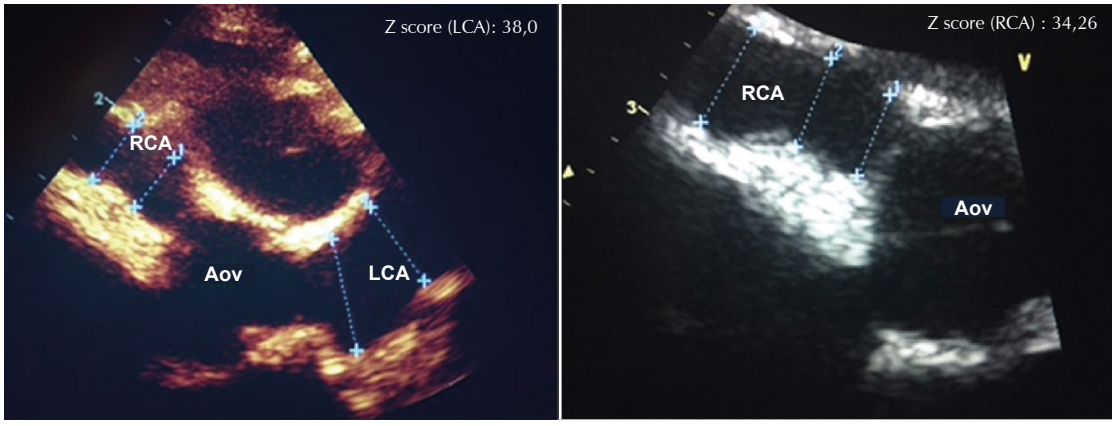

RCA, right coronary artery; Aov, aortic valve; LCA, left coronary artery.

Figure 1 – *Transthoracic echocardiogram taken in the transverse short-axis plane showing the giant right and left coronary aneurysms and the respective Z scores in an infant with Kawasaki disease diagnosed at six months of age.*

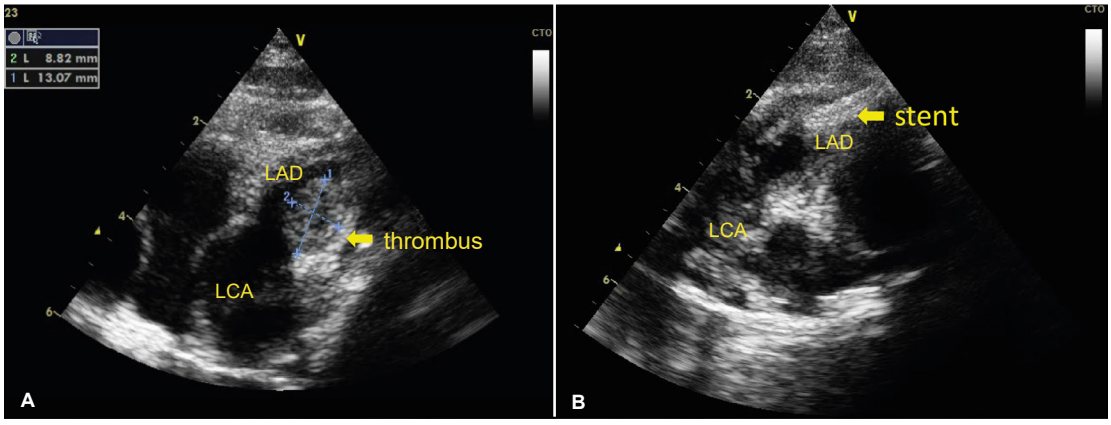

left anterior descending artery (LAD); left coronary artery (LCA).

Figure 2 – *Transthoracic echocardiogram showing the evolution of the infant in figure 1. (A) Eleven months after Kawasaki's disease, thrombus in the left coronary artery (LCA) and in the left anterior descending artery (LAD) in the short axis parasternal plane. (B) Two-dimensional echocardiogram shows stent implanted in LAD after acute myocardial infarction and cardiogenic shock.*

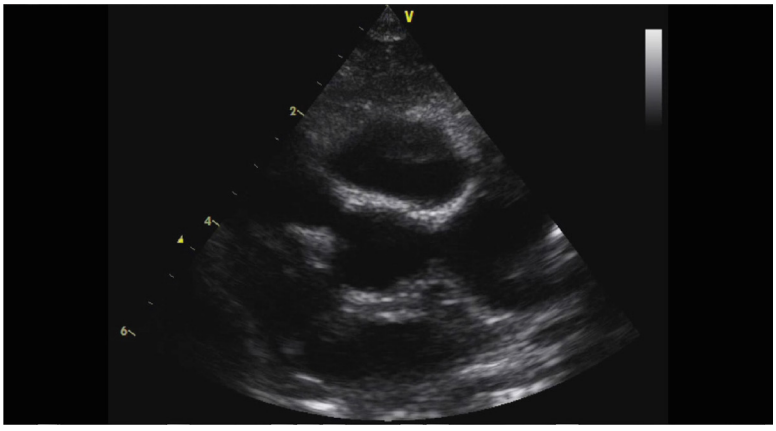

VIdeo 1 – *Infant with coronary aneurysms in the right, left and anterior descending coronary artery (LAD) evolved with thrombus, acute myocardial infarction and shock due to LAD obstruction. Stent was successfully implanted. The video shows the evolution of the case through echocardiographic study from the diagnosis of aneurysms, thrombus formation, obstruction of LAD on color mapping and post-stent evaluation.*

Table 3 - Classification of coronary changes on echocardiography by Z score.

No changes: Z score < 2
Dilatation only (ectasia): Z score of 2–2.5; or if initially <2 with an increase of ≥1 that occurs during follow-up
Small aneurysm: Z score ≥ 2.5 to <5
Medium aneurysm: Z score ≥ 5 to <10
Large or giant aneurysm: Z score ≥ 10 or absolute value ≥ 8 mm

cases. More frequent echocardiographic evaluations may be necessary in high-risk children with persistent fever, coronary abnormalities, ventricular dysfunction, pericardial effusion, or valve regurgitation. Additional echocardiographic studies after 8 weeks are not recommended in patients with previous normal findings due to the improbability of changes,[14] although this approach is not universally adopted due to interest in the long-term evaluation of the coronary flow reserve and dilation of the aortic root in previously normal patients. The need for longitudinal follow-up was reinforced by Crystal et al., whose study showed that > 50% of patients with a coronary artery Z score initially within the normal range showed a decrease in follow-up evaluations with greater detection of coronary abnormalities on subsequent echocardiograms.[15] Therefore, patients with slight or moderate coronary dilation should undergo an echocardiographic evaluation annually, while those with significant coronary dilation or obstruction should undergo the examination every 6 months (Tabela 4).[10]

The echocardiogram has some limitations, as in the evaluation of distal coronary segments and in the follow-up of patients with KD regarding adequate visualization of the coronary arteries, which can become progressively more difficult as children grow. Thus, the use of other diagnostic modalities may become

necessary, such as transesophageal echocardiography (Video 2), especially in rare cases of surgical myocardial revascularization and, more often, on coronary computed tomography angiography, when documenting improved detail of coronary lesions, aneurysms, stenoses, and thrombi becomes necessary.

The delayed or misdiagnosis of KD increases the likelihood of coronary artery lesions. Coronary aneurysms or moderate coronary dilation may persist or remodel.[16] Left ventricular systolic dysfunction tends to normalize during the subacute phase of the disease.

Stenotic coronary artery lesions are generally progressive due to myointimal proliferation and can lead to ischemia and death years after KD.[17] Patients with KD require monitoring and stratification by the relative risk of developing myocardial ischemia using functional tests,[18] which should be complemented by further tests depending on the magnitude of the identified coronary lesions (Table 4). Myocardial perfusion evaluation tests, such as stress echocardiography, myocardial scintigraphy, and magnetic resonance imaging with myocardial viability, must be critically performed in patients with coronary aneurysms. Angiography with intracoronary ultrasound, fractional flow reserve (FFR) and optical coherence tomography (OCT) are indicated in the most complex cases to evaluate therapeutic programming.[19]

Several studies suggested that genetic influences on the magnitude and nature of the immune response may determine KD susceptibility.[18] Conventional methods failed to discover the causative agent; without this information, specific

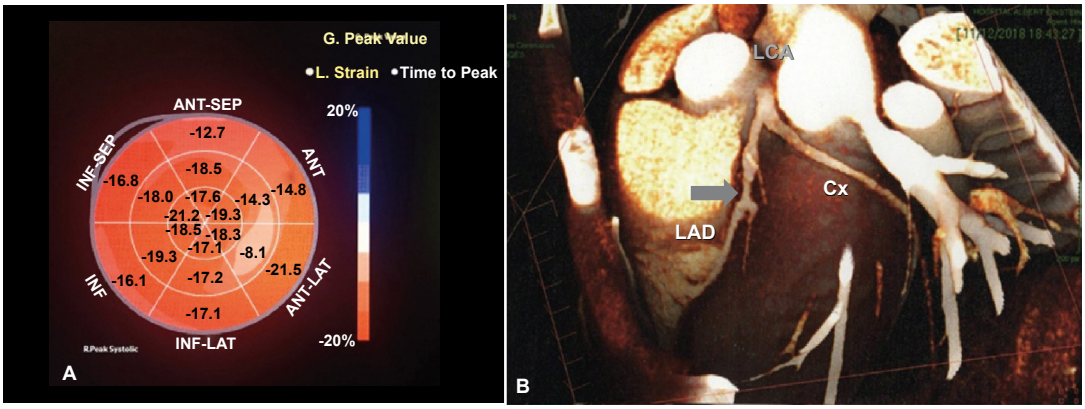

LAD, left anterior descending; LCA, left coronary artery; CX, circunflex.

Figure 3 – *Echocardiographic speckle tracking study in a 15-year-old adolescent who presented with Kawasaki disease at 2 years of age and had a 90% right coronary obstruction who successfully underwent drug-eluting stent placement. The evaluation of longitudinal deformation by strain performed 6 months after the hemodynamic procedure showed decreased values in the anterior wall. Computed tomography angiography performed later detected 50% obstruction of the left anterior descending artery.*

Table 4 - Guidance on sequential follow-up cardiovascular examinations in patients after Kawasaki disease by risk level.

Risk level	Follow-up and diagnostic examination	Invasive examination
I (without coronary artery changes at any disease stage)	Cardiovascular risk evaluation at 5-year intervals	Not recommended
II (transient coronary artery ectasia disappears within the first 6–8 weeks)	Cardiovascular risk evaluation at 3- to 5-year intervals	Not recommended
III (small to medium coronary artery/main coronary artery aneurysm)	*Annual cardiological follow-up with echocardiography + EKG combined with cardiovascular risk evaluation; biannual myocardial perfusion test/stress test*	Angiography if noninvasive test findings are suggestive of ischemia
IV (1 large or giant coronary artery aneurysm, or multiple or complex aneurysms in the same coronary artery without obstruction)	*Biannual cardiological follow-up with echocardiogram + EKG; annual myocardial perfusion test/stress test*	First angiography at ≤ 6–12 months if clinically indicated; repeated angiography if noninvasive test, clinical, or laboratory findings are suggestive of ischemia; repeated elective angiography in some circumstances
V (coronary artery obstruction)	*Biannual cardiological follow-up with echocardiogram + EKG; annual myocardial perfusion test/stress test*	Recommended angiography to approach therapeutic options

EKG, electrocardiography.

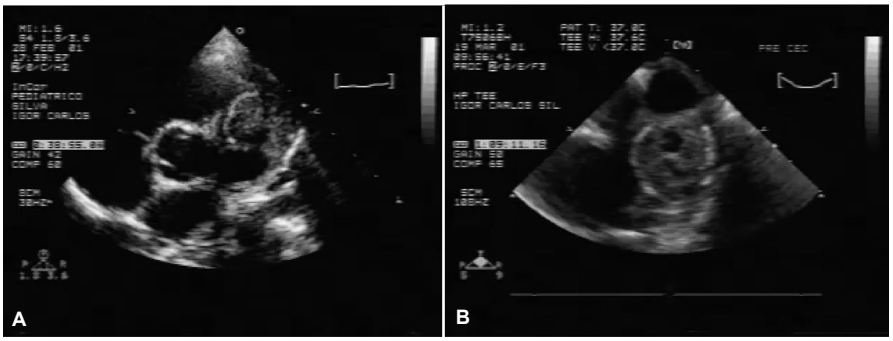

Video 2 – *(A) Transthoracic echocardiogram of a 7-year-old child with a history of Kawasaki disease progressing with chest pain showing a giant aneurysm and a thrombus occluding the left anterior descending artery. (B) Transesophageal echocardiogram taken during myocardial revascularization confirming the previous findings.*

diagnostic tests, preventive measures, and treatment for KD cannot be developed.

Many immunological changes occur in KD, such as cytokine cascade stimulation (interleukin 1, interleukin 6, tumor necrosis factor, and gamma interferon) and endothelial cell activation. Although the real mechanism that causes arteritis is not well understood, the activation of endothelial cells, CD68+ monocytes/macrophages, CD8+ lymphocytes, and oligoclonal immunoglobulin appear to be involved. The prominence of immunoglobulin A in the respiratory tract suggests the airway as a gateway for disease-triggering agents.

Recently, with the severe acute respiratory syndrome coronavirus 2 pandemic, many children and adolescents worldwide have presented a clinical status similar to that of KD and a multisystemic inflammatory syndrome characterized by a cytokine storm. It is speculated that this condition may be associated with a later immune reaction to the virus (by about 6 weeks). The cardiac involvement in these patients presents as pancarditis with possible myopericarditis, pericardial effusion, and mitral valve regurgitation. Echocardiography shows increased echogenicity of the interventricular septum, atrioventricular junction, and crux cordis in addition to coronary artery involvement with increased brightness and perivascular refringence and sometimes, dilations, and aneurysms. A peculiar aspect associated with patients with KD and coronavirus disease 2019 is that myocarditis with myocardial dysfunction seems to be even more severe and appear in older age groups, possibly affecting older children and adolescents.[20,21] Kawasaki-like usually presents greater hemodynamic instability and severity. The treatment also consists of IGIV and AAS, sometimes being necessary the use of corticosteroids, low molecular weight heparin and even immunomodulators such as interleukin-1 inhibitor (Anakinra) and interleukin-6 inhibitor (Tocilizumab), in refractory cases.[22,23] Institutions from around the world, including Brazil, are collaborating to study and advance the diagnostics, preventive approaches, and therapies for these diseases, and much work has yet to be done.

Conflict of interest

The author have declared that they have no conflict of interest.

References

1. Levin M, Tizzard EJ, Dillon MJ. Kawasaki disease: recent advances. Arch Dis Child. 1991;66(12):1369-74.
2. Soares AM, Foronda A, Baptista LP. DK e arterite de Takayasu. Cardiologia e cirurgia cardiovascular pediátrica. 2 ed. São Paulo: Roca; 2012. p. 887-906.
3. Newburger JW, Takahashi M, Gerber MA, Gewitz MH, Tani LY, Burns JC, et al.; Committee on Rheumatic Fever, Endocarditis and Kawasaki Disease; Council on Cardiovascular Disease in the Young; American Heart Association; American Academy of Pediatrics. Diagnosis, treatment, and long-term management of Kawasaki disease: a statement for health professionals from the Committee on Rheumatic Fever, Endocarditis and Kawasaki Disease, Council on Cardiovascular Disease in the Young, American Heart Association. Circulation. 2004;110(17):2747-71. doi: https://doi.org/10.1161/01.CIR.0000145143.19711.78
4. Soares AM, Soares PJ, Santos RA, et al. Doença de Kawasaki: importância da suspeita clínica, diagnóstico e tratamento precoces. Rev Soc Cardiol Estado de São Paulo. 2004;14(2; supl B):81.
5. Burns JC, Shike H, Gordon JB, Malhotra A, Schoenwetter M, Kawasaki T. Sequelae of Kawasaki disease in adolescents and young adults. J Am Coll Cardiol. 1996;28(1):253-7. doi: https://doi.org/10.1016/0735-1097(96)00099-x
6. Kurotobi S, Nagai T, Kawakami N, Sano T. Coronary diameter in normal infants, children and patients with Kawasaki disease. Pediatr Int. 2002;44(1):1-4. https://doi.org/10.1046/j.1442-200x.2002.01508.x
7. de Zorzi A, Colan SD, Gauvreau K, Baker AL, Sundel RP, Newburger JW. Coronary artery dimensions may be misclassified as normal in Kawasaki disease. J Pediatr. 1998;133(2):254-8. doi: https://doi.org/10.1016/s0022-3476(98)70229-x
8. Dallaire F, Dahdah N. New equations and a critical appraisal of coronary artery Z scores in healthy children. J Am Soc Echocardiogr. 2011;24(1):60-74. doi: https://doi.org/10.1016/j.echo.2010.10.004
9. T Kobayashi, N Sakamoto, and S Fuse on behalf of pediatric coronary artery diameter z score study group. Z score calculator of coronary arterial diameter. Acesso em 24/9/2020. Disponível em http://raise.umin.jp/zsp/calculator/
10. McCrindle BW, Rowley AH, Newburger JW, Burns JC, Bolger AF, Gewitz M, et al.; American Heart Association Rheumatic Fever, Endocarditis, and Kawasaki Disease Committee of the Council on Cardiovascular Disease in the Young; Council on Cardiovascular and Stroke Nursing; Council on Cardiovascular Surgery and Anesthesia; and Council on Epidemiology and

Prevention. Diagnosis, Treatment, and Long-Term Management of Kawasaki Disease: A Scientific Statement for Health Professionals From the American Heart Association. Circulation. 2017;135(17):e927-e999. doi: https://doi.org/10.1161/CIR.0000000000000484

11. Ravekes WJ, Colan SD, Gauvreau K, Baker AL, Sundel RP, van der Velde ME, et al. Aortic root dilation in Kawasaki disease. Am J Cardiol. 2001;87(7):919-22. doi: https://doi.org/10.1016/s0002-9149(00)01541-1

12. Xu QQ, Ding YY, Lv HT, Zhou WP, Sun L, Huang J, et al. Evaluation of left ventricular systolic strain in children with Kawasaki disease. Pediatr Cardiol. 2014;35(7):1191-7. doi: https://doi.org/10.1007/s00246-014-0915-5

13. McCandless RT, Minich LL, Wilkinson SE, McFadden ML, Tani LY, Menon SC. Myocardial strain and strain rate in Kawasaki disease. Eur Heart J Cardiovasc Imaging. 2013;14(11):1061-8. doi: https://doi.org/10.1093/ehjci/jet041

14. McMorrow Tuohy AM, Tani LY, Cetta F, Lewin MB, Eidem BW, Van Buren P, et al. How many echocardiograms are necessary for follow-up evaluation of patients with Kawasaki disease? Am J Cardiol. 2001;88(3):328-30. doi: https://doi.org/10.1016/s0002-9149(01)01655-1

15. Crystal MA, Manlhiot C, Yeung RS, Smallhorn JF, McCrindle BW. Coronary artery dilation after Kawasaki disease for children within the normal range. Int J Cardiol. 2009;136(1):27-32. doi: 10.1016/j.ijcard.2008.04.019

16. McCrindle BW, Harris KC. Coronary artery aneurysms after kawasaki disease: understanding the pathology. Can J Cardiol. 2018;34(9):1094-1097. doi: https://doi.org/10.1016/j.cjca.2018.07.412

17. Fernandez S, Trofimenko V, Fick DB Jr, Phan HA, Linz PE, Nayak K, et al. Prevalence of Kawasaki disease in young adults with suspected myocardial ischemia. Circulation. 2012;125(20):2447-53. doi: https://doi.org/10.1161/CIRCULATIONAHA.111.082107

18. Ben TS, Newburger JW, Burns JC, Takahashi M. Kawasaki Disease. Current understanding of mechanism and evidence – based treatment. Japan: Springer; 2017.

19. Harris KC, Manouzi A, Fung AY, De Souza A, Bezerra HG, Potts JE, et al. Feasibility of optical coherence tomography in children with Kawasaki disease and pediatric heart transplant recipients. Circ Cardiovasc Imaging. 2014;7(4):671-8. doi: https://doi.org/10.1161/CIRCIMAGING.113.001764

20. Riphagen S, Gomez X, Gonzalez-Martinez C, Wilkinson N, Theocharis P. Hyperinflammatory shock in children during COVID-19 pandemic. Lancet. 2020;395(10237):1607-1608. doi: https://doi.org/10.1016/S0140-6736(20)31094-1

21. Pain CE, Felsenstein S, Cleary G, Mayell S, Conrad K, Harave S, et al. Novel paediatric presentation of COVID-19 with ARDS and cytokine storm syndrome without respiratory symptoms. Lancet Rheumatol. 2020;2(7):e376-e379. doi: https://doi.org/10.1016/S2665-9913(20)30137-5.

22. L.R. Feldstein, E.B. Rose, S.M. Horwitz et al. Multisystem Inflammatory Syndrome in U.S. Children and Adolescents.N Engl J Med 2020;383:334-46. DOI: 10.1056/NEJMoa2021680.

23. Belhadjer Z, Méot M, Bajolle F, et al. Acute heart failure in multisystem inflammatory syndrome in children in the context of global SARS-CoV-2 pandemic. Circulation 2020; 142: 429–36.

Echocardiography and Analysis of Subclinical Cardiovascular Diseases in Indigenous People Living in Different Degrees of Urbanization: Project of Atherosclerosis Among Indigenous Populations (Pai)

Ecocardiografia e Análise de Doenças Cardiovasculares Subclínicas em Povos Indígenas que Vivem em Diferentes Graus de Urbanização: Projeto de Aterosclerose nas Populações Indígenas (Pai)

Pedro Vinícius Amorim de Medeiros Patriota[1]; Ana Marice T. Ladeia[2]; Juracy Marques[3]; Ricardo Khoury[4]; Aldina Barral[4]; Alvaro A. Cruz[5]; Luis Claudio L. Correia[2]; Manoel Barral-Netto[4]; Joao A. C. Lima[6]; Anderson C. Armstrong[1]

[1]Federal University of São Francisco Valley, Petrolina, Brazil; [2]Bahiana School of Medicine and Public Health, Salvador, Brazil; [3]Bahia State University, Juazeiro, Brazil; [4]Oswaldo Cruz Foundation, Salvador, Brazil; [5]ProAR - Federal University of Bahia, Salvador, Brazil; [6]Johns Hopkins Hospital, Baltimore, MD, USA.

Abstract

Background: The urbanization process impacts the burden of cardiovascular disease (CVD). Indigenous populations can undergo a devastating epidemiological transition.

Objective: The present study aimed to describe the Project of Atherosclerosis among Indigenous Populations (PAI) study protocol for assessing echocardiographic images and subclinical CVD in indigenous populations according to the degree of urbanization and report its preliminary results.

Methods: The PAI is a cross-sectional study that includes volunteers aged 30–70 years among Brazilian indigenous groups exposed to low and advanced stages of urbanization (Fulni-ô and Truká, respectively) and an urban control group. Individuals with known CVD or who were on hemodialysis were excluded. The pilot study began in Fulni-ô territory in September 2016. The participants underwent clinical and laboratory evaluations, electrocardiography, carotid artery ultrasound, and a comprehensive echocardiography protocol including global longitudinal strain (GLS) assessed by speckle tracking. The preliminary results are described by participant sex in univariate analysis.

Results: The pilot study evaluated the protocol used in 55 Fulni-ô individuals (mean age, 48.7 ± 12.0 years; 80% women). Traditional risk factors such as hypertension, diabetes, and dyslipidemia were found in 40%, 36%, and 54% of participants, respectively, without significant statistical differences between the sexes. Tobacco use was extremely prevalent, reported in 91% of participants. Most echocardiographic parameters were within the normal range; however, mean GLS was 17.3 ± 3.4% (p = 0.73 between sexes).

Conclusion: We described the PAI study protocol for assessing subclinical CVD and risk factors in indigenous populations by urbanization stage. Its preliminary results suggest a high prevalence of these factors in the indigenous population exposed to a lower degree of urbanization.

Keywords: Cardiovascular Disease; Indigenous Population; Urbanization.

Resumo

Fundamento: *O processo de urbanização tem impacto na carga de doenças cardiovasculares. As populações indígenas podem sofrer uma transição epidemiológica devastadora.*

Objetivos: *Descrever o protocolo de estudo do Projeto de Aterosclerose nas Populações Indígenas (PAI) para avaliar a análise ecocardiográfica e as doenças cardiovasculares (CV) subclínicas em populações indígenas de acordo com o grau de urbanização e mostrar resultados preliminares do estudo piloto.*

Métodos: *O PAI é um estudo transversal, com voluntários com idade entre 30 e 70 anos, em grupos indígenas brasileiros expostos a estágios baixos e avançados de urbanização (Fulni-ô e Truká, respectivamente) e um grupo controle urbano, excluindo indivíduos com doenças CV*

Mailing address: Anderson da Costa Armstrong •
Hospital Universitário/Universidade Federal do Vale do São Francisco/Comissão de Residência Médica. Avenida Jose de Sa Manicoba, s/n, Centro, Petrolina, Pernambuco, 56304-205
E-mail: anderson.armstrong@univasf.edu.br
Article received 12/10/2019; revised 12/12/2019; accepted 4/15/2020

DOI: 10.47593/2675-312X/20203304eabc78

conhecidas ou em hemodiálise. O estudo piloto começou no território de Fulni-ô em setembro de 2016. Os participantes foram submetidos a avaliação clínica e laboratorial, eletrocardiograma (ECG), ultrassonografia de carótidas e um protocolo ecocardiográfico abrangente, incluindo strain longitudinal global (SLG) avaliado por speckle tracking. Os resultados preliminares são descritos de acordo com o sexo em uma análise univariada.

Resultados: *O estudo piloto avaliou o protocolo descrito em 55 indivíduos do grupo indígena Fulni-ô (48,7 ± 12,0 anos, 80% mulheres). Foram encontrados fatores de risco tradicionais como hipertensão, diabetes e dislipidemia em 40%, 36% e 54%, respectivamente, sem diferenças estatísticas significativas entre os sexos. O uso de tabaco mostrou-se extremamente prevalente, referido em 91% dos participantes. Os parâmetros derivados da ecocardiografia estavam, em média, dentro da faixa normal. No entanto, a média do SLG foi de 17,3 ± 3,4% (p 0,73 por sexo).*

Conclusão: *Descrevemos o protocolo do estudo PAI para avaliar doenças cardiovasculares subclínicas e fatores de risco em populações indígenas de acordo com o estágio de urbanização. Resultados preliminares sugerem alta prevalência desses na população indígena em menor grau de urbanização.*

Palavras-chave: *Doença Cardiovascular; População Indígena; Urbanização.*

Introduction

Cardiovascular diseases (CVDs) play an important role in noncommunicable diseases, the most common causes of mortality worldwide.[1] In recent decades, the transition from a principally rural economy to a predominantly urban economy has led to a substantial change in the global environment, with a negative impact on population health mediated by multiple factors that vary according to the reality of each region.[2]

Urbanization, industrialization, and other signs of economic development and social organization are related to global environmental changes that generate an epidemiological transition in diverse areas of the world. Developing countries have changed their health profiles, decreasing mortality rates caused by infectious diseases and nutritional deficiencies while increasing mortality rates from CVDs.[3,4] However, different levels of epidemiological transitions can occur within a country,[4] with numerous behavioral and cultural particularities involved in different indigenous communities.

In fact, the burden of CVDs has proven to be more devastating in poor countries than in wealthy countries. In this regard, the lack of public resources and insufficient number of trained health professionals contribute to suboptimal assistance.[1,3] The nutritional particularities of each culture, as well as the lack of population-based health education in poor countries, also play a major role in CV morbidity and mortality. These aspects have an even stronger influence because of the late urbanization process that has recently affected indigenous populations.

Few data are available on CV risk factors in indigenous populations. In Brazil, a study of adult Xavante participants showed a significant association between anthropometric measures and socioeconomic indexes in a comparison of data from 1962 and 2006, demonstrating weight gain among young people and those with higher income status.[5] Individuals with a higher body mass index (BMI) and waist circumference also had higher blood pressure levels than their counterparts.

The vastness of Brazil's territory creates contrasts that are seen in urban areas and, importantly, can be identified among indigenous communities in different regions. Indigenous communities in Northeastern Brazil, where most of the European colonization efforts started in the 1500s, often experienced greater territorial losses and disadvantageous policies of their land rights.[6] Moreover, a more recent wave of urban development has generated large dams, canals, and hydroelectric power plants, greatly affecting not only the landscape but also the lifestyle of numerous native communities in the area.

Here, we aimed to describe the Project of Atherosclerosis among Indigenous Populations (PAI) study protocol for assessing echocardiographic images and subclinical CVD in indigenous populations according to the degree of urbanization. Furthermore, we showed the preliminary results of the pilot study of the least urbanized indigenous community in Northeast Brazil. This study only proposes a statistical analysis of participants in the pilot study, and much more testing of various test protocols will be required to obtain data for difficult-to-access populations. The authors did not intend to draw conclusions that will only be possible with the analysis of the study data with the entire sample already reached. These data will be sent for publication shortly.

Methods

Design and Eligibility

The PAI is an observational cross-sectional study that was designed to access volunteers of both sexes aged 30–70 years from three communities with different levels of urbanization. Patients with heart failure, a history of hospitalization for acute coronary syndrome or cerebrovascular disease, or a history of surgery for heart disease or peripheral arterial disease; who were undergoing hemodialysis; or who did not agree to participate in the study were excluded.

The PAI study was approved by institutional local and national ethics committees (CONEP number 1.488.268). It was also approved by the Brazilian agency that regulates indigenous affairs (Fundação Nacional do Índio, FUNAI; process number 08620.028965/2015-66). Finally, the study was approved by the tribal authorities of each indigenous group. All participants provided informed consent before taking part in the study.

Degree of Urbanization and Community Selection

The goal of recruitment was to obtain a representative sample of residents of the São Francisco Valley in Northeast Brazil who were exposed to different degrees of urbanization that contained indigenous and non-indigenous participants and aimed to distribute participants equally by age (30–50 years old vs. 51–70 years old) and sex (male vs. female). For this purpose, we included two indigenous groups and a non-indigenous group from a related urban area.

Establishing the degree of urbanization of a given community is challenging because of the lack of standardized criteria and the regional particularities that should be considered when defining urbanization. In fact, indigenous populations usually have cultural and religious aspects that are directly related to their idea of territory. Therefore, a concept of urbanization that considers only physical characteristics would be false and artificial for an indigenous group.[7] Thus, the PAI study aimed to integrate both cultural and physical parameters to establish a more accurate definition of urbanization throughout the study. We combined official urban density concepts with anthropological parameters related to the use of native language and adherence to a more traditional lifestyle.[8,9]

With the application of these criteria, three groups were selected for the PAI study: (1) the Fulni-ô people, considered the least urbanized group in Northeast Brazil, mostly because they practice periodic isolation from non-indigenous people and maintain daily use of native language in addition to inhabiting an area with a low density of urban constructions; (2) the Truká people, who are in a more advanced stage of urbanization, historically affected by territorial losses and environmental changes resulting from major national infrastructural constructions such as dams, canals, and power plants; and (3) an urban control population from the city of Juazeiro, Bahia, Brazil, also located on the São Francisco River. The latter was chosen by the authors according to to criteria established by IBGE - Brazilian Institute of Geography and Statistics - the city of Juazeiro is a densely urbanized territory.[8]

Data Collection

Recruitment began in September 2016, with the pilot study in the Fulni-ô territory designed to include at least 50 participants. The Fulni-ô were selected for the pilot assessment because they were located in the most remote area, thus comprising the most challenging part of the study. Volunteers underwent a screening interview to establish eligibility. As part of the main study protocol, the included participants underwent clinical assessments, laboratory tests, ECG, carotid duplex scans, ankle-brachial index assessment, and echocardiography.

Clinical Parameters

Comprehensive medical history was assessed and physical examinations were performed. Alcohol consumption and smoking were self-reported. In this study, we did not aim to assess alcohol consumption patterns; rather, we registered a positive alcohol intake if the participant reported any alcohol consumption. To assess the amount of tobacco from traditional use (with traditional pipes known as *chanduca*), the number of daily refills was used to calculate average consumption.

Weight was measured in kilograms using digital scales. Height was measured with validated equipment. BMI was calculated as weight/height^2 (kg/m^2). Overweight and obesity were classified as BMI $\geq$ 25 kg/m^2 and BMI $\geq$ 30 kg/m^2, respectively. Neck, hip, and waist circumferences were measured according to National Institutes of Health recommendations.[10]

Heart rate and oxygen saturation were recorded using automated equipment after at least a 5-minute rest with the participants seated. Three blood pressure measurements were performed (conventionally twice in the right arm and once in the left arm) using an Omron® BP785 IntelliSense® Automatic Blood Pressure Monitor in accordance with the recommendations of the Brazilian Society of Cardiology.[11] Hypertension was defined a systolic blood pressure $\geq$ 140 mmHg, diastolic blood pressure $\geq$ 90 mmHg, or use of medications for hypertension.

All clinical data were collected using RegaDB,[12] a database with software tools developed by the Rega Institute (Catholic University of Leuven; Leuven, Belgium) and MyBioData Biomedical (Leuven, Belgium). In this study, the software was further adapted as "RegaDB PAI" to store the clinical research data and configured to run simultaneously on all study computers using an intranet system.

Laboratory Testing

Approximately 10 mL of blood was drawn into adequate Vacutainer® tubes. The spun serum was aliquoted and shipped to a central laboratory (FIOCRUZ, Salvador, Brazil) for storage and subsequently tested for creatinine, HbA1c, total cholesterol, low-density lipoprotein cholesterol (LDL-C), high-density lipoprotein cholesterol (HDL-C), triglycerides, and ultra-sensitive C-reactive protein. Diabetes was identified if the participant was using any hypoglycemic medication or if HbA1c was $\geq$ 6.5%, while pre-diabetes was identified if the HbA1c was 5.7–6.4%. Dyslipidemia was established if the participant was using hypolipidemic medication or if at least one of the following criteria was met: reduced HDL-C, a level lower than 40 mg/dL in men or 50 mg/dL in women; hypertriglyceridemia, a triglyceride level > 150 mg/dL; and hypercholesterolemia, an LDL-C > 160 mg/dL. When the triglyceride level was $\geq$ 400 mg/dL, the calculation of LDL-C by the Friedewald formula was not adequate; thus, hyperlipidemia was identified if the total cholesterol level was $\geq$200 mg/dL.

Echocardiography Protocol

The echocardiography exam was conducted with a GE Vivid Q Portable Scanner (General Electric Medical Systems, Milwaukee, WI, USA) to obtain and store echocardiography-derived images in digital files. The images were acquired by echocardiography experts in accordance with a standardized protocol following the recommendations of the American Society of Echocardiography and the European Association of Cardiovascular Imaging.[13] Carotid duplex ultrasonography was used to assess cervical carotid artery disease, and intima-media thickness was computed following current recommendations.[14]

Transthoracic echocardiography was acquired from apical four-, three-, and two-chamber acoustic windows as well as from the parasternal longitudinal view and at the level of the papillary muscles in a short-axis view, including two-dimensional imaging, M-mode, tissue Doppler, and pulsed and continuous Doppler. An offline analysis was performed blindly following international recommendations.[13]

Left ventricular ejection fraction (LVEF) was calculated using the modified Simpson's rule. Left ventricular mass (LVM) was calculated with linear measurements and indexed by body surface area (BSA). Left ventricular hypertrophy was defined as LVM index > 115 g/m^2 in men or > 95 g/m^2 in women. Left atrial volume was acquired using the biplane area-length technique and then indexed by BSA. Transmitral Doppler–derived E and A waves and transaortic velocities were acquired. Tricuspid annular plane systolic excursion was assessed by M-mode in a four-chamber view. Tissue Doppler imaging computed velocities in the right ventricular free wall, interventricular septal wall, and left ventricular lateral wall in a four-chamber view. In the pilot study, echocardiographic parameters for the evaluation of diastolic function, such as E and e' velocities, were not obtained, but they will be presented and analyzed in future publications describing the other participants.

Speckle tracking echocardiography acquisition and interpretation techniques followed a standardized protocol similar to that of the CARDIA study.[15] In summary, left ventricular images were acquired in two-, three-, and four-chamber views, ensuring a frame rate of > 40 fps and documenting three consecutive cardiac cycles. Blind analysis was used to compute the global longitudinal strain (GLS) and the average of the longitudinal strain of the two-, three-, and four-chamber assessments.

Results of the carotid artery ultrasound analysis and the evaluation of the left ventricular diastolic function will be documented in another article to be submitted soon for publication. We believe that the analysis of clinical, laboratory, and CV images will be more succinct in this article since its main objective is to describe the PAI study methods.

Additional Assessments

Ankle-brachial index was obtained using portable Doppler ultrasound machine and manual sphygmomanometer following recommendations from the American College of Cardiology and American Heart Association.[16] The ankle-brachial index result was abnormal if <0.9 or >1.3. Twelve-lead electrocardiography (ECG) was recorded using portable digital equipment with the patient at rest in the dorsal decubitus position at a standard speed of 25 mm/s and amplitude of 10 mV. Each ECG was acquired and blindly analyzed according to the recommendations of the Brazilian Society of Cardiology.[17] To enhance sensitivity, we considered participants positive for chamber overload if the ECG showed at least one abnormal parameter: left atrial enlargement if the P wave duration in lead II was >120 ms, P wave notching in the interval duration between the atrial components was >40 ms (P mitrale), and/or the terminal negative component of a biphasic P wave in precordial lead V1 was >0.04 mm/s or area was >1 mm^2 (Morris index). Left ventricular overload was defined as the ECG criteria were expressed by sum of the S wave of the V1 derivation with the largest R wave of the V5 or V6 being ≥35 mm (Sokolow-Lyon index) and/or sum of the R wave in aVL and S wave in V3 derivation being ≥22 mm in women and >28 mm in men (Cornell index). Right ventricular overload was identified with the presence of axis deviation to the right and a sum of the S wave in V5 or V6 with the R wave in the V1 lead of >10.5 mm. Right atrial enlargement was defined as the presence of an amplitude > 2.5 mm in lead II.

Statistical Analysis

For the entire PAI study, we estimated a total sample of 957 participants (319 from each of the three groups) considering a statistical power of 90% and an alpha of 0.05 to detect statistically significant differences based on a previous World Health Organization report for the prevalence of hypertension according to urbanization.[18] In the current report, we present the preliminary results obtained after assessing a pilot study. The data are described for the population assessed in the pilot study according to participant sex. Categorical variables are presented as percentages at the 95% confidence interval, with p values for the intergroup comparisons calculated by Fisher's exact test. For continuous variables, normal distribution was assessed by comparing quantiles of variables against quantiles of normal distribution. According to the distribution, the data are summarized as mean and standard deviation or median and interquartile range (IQR), and differences were assessed by a t-test or 2-sample Wilcoxon rank-sum. STATA v. 14 was used for the statistical calculations and p values < 0.05 were considered statistically significant.

Results

For the PAI pilot study, a total of 55 participants were enrolled from the Fulni-ô territory. The majority of participants were middle-aged women (Table 1). The prevalence of hypertension was higher among women, although men showed a trend toward higher systolic and diastolic blood pressures (Table 1). Of those classified as having hypertension, 23.9% (n = 11) were using blood lowering medication. Of them, 45.4% (n = 5) showed uncontrolled systolic or diastolic blood pressure. All participants using blood pressure medication were women (29.7%).

Glucose serum levels as assessed by HbA1c were, on average, higher than normal (Table 1). Diabetes had a general prevalence of 36%, with no sex-related differences. Of those classified as having diabetes, 17% (n = 8) were using blood sugar lowering medication. Of those using medication, 87.5% (n = 7) had uncontrolled serum glucose levels defined as an HbA1c level ≥ 7.0%.

More than half of the participants were classified as having at least one type of dyslipidemia (Table 1), with lower serum triglyceride levels and higher LDL-C and HDL-C levels among women than among men.

Table 1 also shows that the majority of participants were active smokers and classified as overweight or obese with a similar prevalence between the sexes. The men had higher ankle-

Table 1. Description of clinical parameters of participants of the pilot study.

Parameter	Men (n = 11) Proportion (95% CI)	Women (n = 44) Proportion (95% CI)	All (n = 55) Proportion (95% CI)	P value (comparison of sexes)
Age, years	48.0 (10.2)	49.0 (12.6)	48.7 (12.0)	0.815
Hypertension	33% (8:74)	43% (27:60)	40% (27:56)	0.449
Diabetes	33% (8:74)	37% (22:55)	36% (23:52)	0.571
Pre-diabetes	55% (19:86)	60% (42:75)	59% (43:73)	
Dyslipidemia	44% (13:80)	57% (40:73)	54% (39:69)	0.430
Overweight	33% (8:74)	45% (29:63)	43% (29:58)	0.938
Obesity	22% (4:67)	20% (9:37)	20% (11:35)	
Tobacco use	100%	88% (72:95)	91% (77:96)	0.219
Alcohol consumption	22% (4:67)	8% (3:24)	11% (5:25)	0.440
	Média (DP)	Média (DP)	Média (DP)	
SBP, mmHg	141.9 (18.5)	128.3 (22.4)	131.2 (22.1)	0.085
DBP, mmHg	82.2 (9.9)	78.2 (10.8)	79 (10.6)	0.300
ABI	1.26 (0.12)	1.11 (0.18)	1.14 (0.18)	0.018
HbA1c*, %	6.26 (0.71)	6.32 (0.74)	6.31 (0.63)	0.78
Total cholesterol, mg/dL	192.9 (47.6)	217.3 (44.4)	212.1 (45.7)	0.136
LDL-C, mg/dL	92.2 (25.8)	123.9 (37.7)	118.3 (37.6)	0.041
HDL-C, mg/dL	35.6 (11.3)	50.8 (12.6)	47.5 (13.7)	0.001
Triglycerides, mg/dL	363.4 (296.1)	217.8 (139.4)	248.8 (189.7)	0.023
BMI, kg/m^2	26.3 (3.0)	27.1 (5.9)	26.9 (5.4)	0.938

*ABI, ankle-brachial index; BMI, body mass index; DBP, diastolic blood pressure; HbA1c, glycated hemoglobin; HDL-C, high-density lipoprotein cholesterol; LDL-C, low-density lipoprotein cholesterol; SBP, systolic blood pressure. P values were determined using a t-test except for HbA1c, which was determined using a two-sample Wilcoxon rank-sum test. *HbA1c is shown as median (IQR).*

Table 2. Description of electrocardiography-derived parameters by sex in the pilot study.

Parameter	Men (n = 9)	Women (n = 35)	All (N = 44)	P value (comparison of sexes)
Heart rate, beats per minute	68 (8)	75 (11)	73 (11)	0,06
Left atrial enlargement	55% (5)	34% (12)	38% (16)	0,25
Left ventricular overload	11% (1)	2.8% (1)	4.5% (2)	0,30

P values were determined using a t-test.

Table 3. Echocardiography-derived parameters of participants of the pilot study.

Parameter	Men (n = 10)	Women (n=32)	All (n = 42)	P value (comparison of sexes)
LV mass	166.3 (40)	121.6 (37.6)	132.3 (42.2)	0.002
LV mass index, g/m^2	91.5 (21.4)	70.5 (19.0)	75.5 (21.4)	0.005
Ao diameter, mm	30.0 (4.3)	28.5 (4.2)	28.8 (4.3)	0.35
LA volume, mL	51.3 (13.2)	42.9 (13.5)	44.8 (13.7)	0.09
LA volume index, mL/m^2	28.3 (7.6)	24.8 (6.3)	25.6 (6.7)	0.15
RA volume, mL	47.3 (15.7)	31.6 (9.7)	35.2 (12.9)	0.0004
RA volume index, mL/m^2	26.1 (8.7)	18.4 (4.8)	20.3 (6.7)	0.001
TAPSE, mm	22.4 (2.5)	22.3 (4.7)	22.3 (4.3)	0.96
LVEF, %	63.6 (7.8)	63.8 (10.6)	63.8 (9.9)	0.94
GLS, %	-17.6 (3.0)	-17.2 (3.6)	-17.3 (3.4)	0.73

Ao, aorta; GLS, global longitudinal strain; LA, left atrium; LV, left ventricle; LVEF, left ventricle ejection fraction; RA, right atrium; TAPSE, tricuspid annular plane systolic excursion. P values were determined using a t-test. Data are shown as mean (standard deviation).

brachial index levels than the women. Alcohol consumption tended to be more frequent among men than women.

ECG-derived variables were in generally within the normal range with no differences between sexes (Table 2). All participants had sinus rhythm with a mean heart rate of 73 beats per minute (SD, 11 bpm; range, 55–103 beats per minute). One woman had a complete left bundle branch block. Another woman presented with a first-degree atrioventricular block. No participants showed any signs of ischemia or abnormal Q waves, right atrial enlargement, right ventricular overload, or complex arrhythmias.

Table 3 summarizes the echocardiography-derived parameters and intima-media thicknesses of the carotid arteries. LVM and right atrial volumes were higher among men than among women. Other echocardiography-derived parameters and intima-media thicknesses did not differ between Fulni-ô men and women.

Discussion

The PAI study is an original study aiming to demonstrate the prevalence of CV risk factors and subclinical cardiac disease in indigenous people exposed to different levels of urbanization. This paper presents the PAI study protocol and shows preliminary data on CV risk factors and subclinical disease collected during the pilot study that assessed the Fulni-ô people, an indigenous community from Northeast Brazil with a low degree of urbanization. Although the initial project design is cross-sectional, we will secure funding to follow up all subjects longitudinally and explore the most common comorbidities observed, including chronic respiratory diseases.

The pilot study proved that use of the PAI protocol is feasible in remote indigenous territories. The researchers are responsible for proving the viability of their projects, particularly when assessing traditionally neglected communities such as Native American tribes. Additionally, the PAI pilot study provided early identification of the CV risk burden of the Fulni-ô people, who underwent a comprehensive survey in CV health for the first time. The originality and, in particular, importance of the high-risk profile found in this preliminary assessment underscores the need for further investigations.

In the PAI pilot study, we examined a middle-aged group of adults with a high prevalence of CV risk factors, particularly indigenous women. We also report a high prevalence of subclinical disease compared to what would be expected in a general population as evidenced by a mean GLS < -18%.[13] In fact, although the participants' average traditional echocardiography-derived parameters (including

LV ejection fraction) were within the normal range, the assessed Fulni-ô people showed signs of subclinical LV dysfunction (Figure 1).

Our group's previous epidemiological reviews showed increasing rates of CV mortality among indigenous people in the São Francisco Valley that appeared to be related to the degree of urbanization.[19] In fact, urbanization has been associated with an epidemiological transition in indigenous groups characterized by a reduction in death rates related to infections or nutritional deficiency disorders and an increase in mortality from CVDs.[4,20,21] In the consideration of traditional people in the process of environmental changes, CV mortality rates have been related to lifestyle changes impacting the CV risk burden. Importantly, CV deaths in traditional groups have been associated with low socioeconomic status, low access to health care, and a breakdown in social structure such as the loss of social support and cohesion.[4,20]

The pilot findings demonstrated a higher proportion of indigenous Fulni-ô people with hypertension than previous reports on indigenous groups at earlier stages of urbanization.[4,22,23] There is significant variation in the reported prevalence of hypertension among indigenous Brazilian groups. The rural Xukuru community had a prevalence of hypertension near 30%,[22] whereas the Suruí people from Amazonia, at the initial stages of urbanization, are currently dealing with their first cases of hypertension.[23] Conversely, our reported prevalence of hypertension was similar to that in urban areas in Brazil and other low-income countries.[24]

Our group of Fulni-ô women tended to have a higher prevalence of hypertension than the men. Interestingly, compared to men, hypertensive Fulni-ô women were more prompted to use medication and adequately control their blood pressure. This may explain our finding of a higher proportion of LV hypertrophy among Fulni-ô men than among women. LV hypertrophy is a well-known CV risk marker, particularly in hypertensive patients.[25,26]

We reported an alarming prevalence of diabetes and uncontrolled glucose levels among Fulni-ô men and women. Similarly, the Xavante people, an indigenous tribe from Central Brazil, have a reported diabetes prevalence of 28.2%.[25,26] In fact, other Native American groups have shown a high prevalence of diabetes.[27-29] To emphasize this diabetes burden in native groups, the ORBITA trial investigating urban European participants with known coronary artery disease reported a prevalence of diabetes at a magnitude of about half that of our findings in the Fulni-ô pilot group.[30] Genetic predisposing factors and lifestyle changes related to the urbanization process may play an important role in the prevalence of diabetes among American indigenous communities.

We also found a high prevalence of dyslipidemia and a prevalence of overweight/obesity of > 60% among the assessed Fulni-ô participants. These findings appear to be directly affected by a modern urban lifestyle and relate to the worldwide pandemic obesity burden.[10] Traditional indigenous groups may be following the Western tendency regarding the most current challenges in body weight control. In fact, the Embera-Chami indigenous people from Colombia, who resemble the Fulni-ô people in many aspects, reportedly had a similar unfavorable cardiometabolic profile.[31] Public social policies are necessary to minimize this growing health problem.

Tobacco smoking is an increasing social problem in many indigenous communities globally.[32] In the Fulni-ô people assessed in this pilot study, the prevalence of tobacco smoking is remarkably higher than that in other communities, indigenous or non-indigenous.[1,32] Smoking is highly prevalent in men and women, found in almost the entire observed population in the Fulni-ô pilot study. Worldwide data show that the prevalence of tobacco smoking is much higher in men (37%) than in women (7%), Europe being the region with the highest rate of smokers (30%).[1] In the general population of Brazil, the prevalence of smoking is declining rapidly.[33] Social unacceptability is an important factor observed in urban areas where tobacco smoking has been decreasing.[6] However, for most of the Fulni-ô people, smoking is seen as culturally essential, especially with traditional pipes (*chanduca*).

Similar to worldwide findings in indigenous and non-indigenous groups,[1,32] the Fulni-ô pilot study showed that more men reported alcohol consumption than women. Alcohol consumption appears to be an increasing social problem in many indigenous communities, but our study design may not allow for comparisons in alcohol consumption patterns to those of other reported studies.

As can be expected from a study designed for a group of generally healthy participants, we found a low prevalence of abnormal parameters strongly related to clinically manifested CVD, such as ECG measures, and traditional echocardiographic functional parameters, such as LV mass and LVEF. However, GLS tended to be reduced in the assessed Fulni-ô men and women. GLS predicts cardiac outcomes beyond the traditional LVEF,[33] even with a lack of other echocardiographic or clinical evidence of heart failure.[34] GLS can also identify early subclinical cardiac dysfunction.[35,36] This pilot study population, despite including only 55 participants, demonstrated a high prevalence of CV risk factors and a possible considerable number of subclinical CVDs, as suggested by reduced values of global strain. However, these are preliminary data from a much smaller sample with no objective of reaching conclusions that will be of greater statistical importance when the analysis of the entire sample is published.

Conclusions

Here we described the PAI study protocol for assessing subclinical CVD and CV risk factors in indigenous populations according to the degree of urbanization. The pilot study proved the feasibility of the PAI study protocol. We also showed the preliminary data of the Fulni-ô study population, the least urbanized indigenous group that features a high prevalence of important atherosclerosis risk factors and the presence of subclinical cardiac disease as assessed by LV longitudinal deformation.

Contribution of authors

Research design and design: Armstrong AC, Patriota

PVAM, Lima JAC. Obtaining data: Patriota PVAM, Ladeia AM, Marques J, Armstrong AC. Data analysis and interpretation: Armstrong AC, Patriota PVAM, Correia LCL. Statistical analysis: Armstrong AC, Patriota PVAM. Obtain financing: Armstrong AC. Writing of the manuscript: Armstrong AC, Patriota PVAM. Critical review of the manuscript for important intellectual content: Patriota PVAM, Ladeia AM, Marques J, Khoury R, Barral A, Cruz AA, Correia LCL, Barral-Netto M, Lima JAC, Armstrong AC.

Sources of funding

Conselho Nacional de Desenvolvimento Científico e Tecnológico (CNPq) - National Council for Scientific and Technological Development (CNPq)

Conflict of interest

The authors have declared that they have no conflict of interest.

References

1. Mendis S, Armstrong T, Bettcher D, Branca F, Lauer J, Mace C, Poznyak V, et al. Global Status Report: on noncommunicable diseases. WHO, 2014. Accessed: May 1, 2017. Available at: http://www.who.int/nmh/publications/ncd-status-report-2014/en/
2. Teo K, Chow CK, Vaz M, Rangarajan S, Yusuf S. The Prospective Urban Rural Epidemiology (PURE) study: examining the impact of societal influences on chronic noncommunicable diseases in low-, middle-, and high-income countries. Am Heart J [electronic article]. 2009;158(1):1–7.e1.
3. Deaton C, Froelicher ES, Wu LH, Ho C, Shishani K, Jaarsma T. The global burden of cardiovascular disease. J Cardiovasc Nurs. 2011;26(4 Suppl):S5-14.
4. Yusuf S, Reddy S, Ounpuu S, Anand S. Global burden of cardiovascular diseases: general considerations, the epidemiologic transition, risk factors, and impact of urbanization. Circulation. 2001 Nov 27;104(22):2746-53.5. Welch JR, Ferreira AA, Santos RV, Gugelmin SA, Werneck G, Coimbra CEA. Nutrition transition, socioeconomic differentiation and gender among adult Xavante Indians, Brazilian Amazon. Hum Ecol. 2009;37:13–26.
6. Coimbra CEA, Santos RV, Welch JR, Cardoso AM, de Souza MC, Garnelo L, et al. The first national survey of indigenous people's health and nutrition in Brazil: rationale, methodology, and overview of results. BMC Public Health. 2013;13:52.
7. Fany R. Terras indígenas & unidades de conservação da natureza: o desafio das sobreposições. São Paulo: Instituto Socioambiental, 2004. 37–41p. Accessed: August 3, 2017. Available at: https://www.socioambiental.org/banco_imagens/pdfs/10144.pdf.
8. IBGE. Áreas urbanizadas. (Electronic) Available at: http://www.ibge.gov.br/home/geociencias/geografia/geografia_urbana/areas_urbanizadas/default.shtm?c=8. Accessed: August 2, 2017.
9. Dos Santos J M. Cultura material e etnicidade dos povos indígenas do São Francisco afetados por barragens: um estudo de caso dos Tuxá de Rodelas, Bahia, Brasil. Salvador. 2008. Available at: https://repositorio.ufba.br/ri/bitstream/ri/10835/1/tese_Juracy Marques1.pdf. Accessed: April 7, 2017.
10. Becker DM, Bouchard C, Carleton RA, Colditz GA, Dietz WH, Foreyt JP, et al. Practical guide to the Identification, evaluation, and treatment of overweight and obesity in adults. NIH, 2000. Available at: https://www.nhlbi.nih.gov/files/docs/guidelines/prctgd_c.pdf. Accessed: August 1, 2017.
11. Malachias MV, de Souza W, Plavnik FL, Rodrigues C, Brandão AA, Neves M, et al. 7ª diretriz brasileira de hipertensão arterial. Arq Bras Cardiol. 2016;107(3).
12. Katholieke Universiteit te Leuven. RegaDB. (Electronic) Available at: https://rega.kuleuven.be/cev/regadb. Accessed: August 2, 2017
13. Lang RM, Badano LP, Mor-Avi V, Afilalo J, Armstrong A, Ernande L, et al. Recommendations for cardiac chamber quantification by echocardiography in adults: an update from the American Society of Echocardiography and the European Association of Cardiovascular Imaging. J Am Soc Echocardiogr. 2015;28:1-39.
14. Stein JH, Korcarz CE, Hurst RT, Lonn E, Kendall CB, Mohler ER, et al. American Society of Echocardiography Carotid Intima-Media Thickness Task Force. Use of carotid ultrasound to identify subclinical vascular disease and evaluate cardiovascular disease risk: a consensus statement from the American Society of Echocardiography Carotid Intima-Media Thickness Task Force. Endorsed by the Society for Vascular Medicine. J Am Soc Echocardiogr. 2008;21(2):93-111.
15. Armstrong AC, Ricketts EP, Cox C, Adler P, Arynchyn A, Liu K, et al. Quality control and reproducibility in M-mode, two-dimensional, and speckle tracking echocardiography analysis: the CARDIA Study, year 25 examination experience. Echocardiography. 2015;32(8):1233-40.
16. Hirsch AT, Haskal ZK, Hertzer NR, Bakal CW, Creager MA, Halperin JL, et al. ACC/AHA 2005 Practice guidelines for the management of patients with peripheral arterial disease. Circulation. 2006;113 (11):e463-654.
17. Pastore CA, Pinho JA, Pinho C, Samesima N, Pereira-Filho HG, Kruse JCL, et al. III Diretrizes da Sociedade Brasileira de Cardiologia sobre Análise e Emissão de Laudos Eletrocardiográficos. Arq Bras Cardiol. 2016; 106(4Supl.1):1-23.
18. World Health Organization. World Health Statistics 2012. Accessed: April 8, 2017.Available at: http://apps.who.int/iris/bitstream/handle/10665/44844/9789241564441_eng.pdf?sequence=1
19. Armstrong, AC, Ladeia, AMT, Marques J, Armstrong DMFO, Silva AMLD, Morais Junior JC, et al. Urbanization is Associated with Increased Trends in Cardiovascular Mortality Among Indigenous Populations: the PAI Study. Arq Bras Cardiol. 2018; 110(3):240-5.
20. Reddy KS, Yusuf S. Emerging Epidemic of Cardiovascular Disease in Developing Countries. Circulation. 1998;97(6):596–601.
21. Sanderson JE, Mayosi B, Yusuf S, Reddy S, Hu S, Chen Z, et al. Global burden of cardiovascular disease. Heart. 2007; 93(10):1175.
22. Barbosa JMVB. Prevalência e fatores associados à pressão arterial elevada no povo Indígena Xukuru do Ororubá, Pesqueira-PE, 2010. 2013. Dissertação (Mestrado em Saúde Publica) – Centro de Pesquisas Aggeu Magalhães, Fundação Oswaldo Cruz, Recife, 2013.
23. Tavares FG, Coimbra CEA, Cardoso AM. Níveis tensionais de adultos indígenas Suruí , Rondônia , Brasil Blood pressure levels of Suruí indigenous adults in Rondônia, Brazil. 2012:1399–1409. Available at: https://pdfs.semanticscholar.org/730d/772bc2db01acc6d94e3ba4f957935d820446.pdf. Accessed: August 7, 2017.
24. Chow CK, Teo KK, Rangarajan S, Islam S, Gupta R, Avezum A, et al. Prevalence, awareness, treatment, and control of hypertension in rural and urban communities in high-, middle-, and low-income countries. JAMA. 2013;310(9):959-68.
25. Armstrong AC, Gidding S, Colangelo LA, Lima J. Influence of early adult modifiable cardiovascular risk factors on left atrial index: the CARDIA study. In: American College of Cardiology Meeting, 2012. JACC, 2012. v. 59. p. A283.
26. Armstrong AC, Jacobs DR, Gidding SS, Colangelo LA, Gjesdal O, Lewis CE, et al. Framingham score and LV mass predict events in young adults: CARDIA study. Int J Cardiol. 2014;172(2):350-5.
27. United Nations Office of the Special Adviser on Gender Issues and Advancement of Women and the Secretariat of the United Nations Permanent Forum on Indigenous Issues. Gender and indigenous peoples. (Electronic) New York, February 2010. Available at: <http://www.un.org/esa/socdev/unpfii/documents/Briefing%20Notes%20Gender%20and%20Indigenous%20Women.pdf>. Accessed: 14 November 2017.

28. Epidemiologia e prevenção do diabetes mellitus. Available at: http://www.diabetes.org.br/profissionais/images/pdf/diabetes-tipo-2/001-Diretrizes-SBD-Epidemiologia-pg1.pdf. Accessed: August 11, 2017.

29 Knowler WC, Saad MF, Pettitt DJ, Nelson RG, Bennett PF. Determinants of diabetes mellitus in the Pima Indians. Diabetes Care. 1993;16(1):216-27.

30. Al-Lamee R, Thompson D, Dehbi H, Sen S, Tang K, Davies J, et al. Percutaneous coronary intervention in stable angina (ORBITA): a double-blind , randomised controlled trial. Lancet. 2018 Jan 6;391(10115):31-40.

31. Bedoya, JUC, Botero JD, González CAN, Molina DCR, Gracia JR, Pineda AFG, et al. Prevalencia de factores de riesgo cardiovascular en indígenas embera-chamí de Cristianía (Jardín), Antioquia. Iatreia. 2015;28(1):5–16.

32. United Nations. State of the world's indigenous peoples: indigenous Peoples' access to health services. 2016. Available at: http://www.who.int/hhr/activities/indigenous/en/. Accessed: August 8, 2017.

33. Malta DC, Stopa SR, Santos MAS, Andrade S, Oliveira TP, Cristo EB, Silva MM. Evolution of tobacco use indicators according to telephone surveys, 2006-2014. Cad Saude Publica. 2017;33Suppl 3(Suppl 3):e00134915

34. De Almeida ALC, Gjesdal O, Mewton N, Choi E, Teixido-Tura G, Yoneyama K, et al. Speckle-tracking pela ecocardiografia bidimensional: aplicações clínicas. Rev bras ecocardiogr imagem cardiovasc. 2013;26(1):38-49.

35. Pellicori P, Kallvikbacka-Bennett A, Khaleva O, Carubelli V, Costanzo P, Castiello T, et al. Global longitudinal strain in patients with suspected heart failure and a normal ejection fraction: does it improve diagnosis and risk stratification?; Int J Cardiovasc Imaging. 2014;30(1):69-79.

36. Gonçalves S, Cortez-Dias N, Nunes A, Belo A, Cabrita Z, Sousa C, et al. Disfunção sistólica ventricular esquerda detetada por speckle tracking em hipertensos com fração de ejeção preservada. Rev Port Cardiol. 2014; 33(1):27-37.

Value of Cardiac Magnetic Resonance in the Diagnosis and Prognosis of Patients with Acute Myocardial Infarction with Nonobstructive Coronary Artery Disease (MINOCA)

Valor da Ressonância Magnética Cardíaca no Diagnóstico e no Prognóstico de Pacientes com Infarto Agudo do Miocárdio sem Doença Arterial Coronariana Obstrutiva (MINOCA)

Márcio Vinícius Lins de Barros[1,2], Carlos Eduardo Ornelas[2], Maria Helena Albernaz Siqueira[2], Rochelle Coppo Militão[2], Marcus de Almeida Melo Júnior[1], Sérgio Marcos Ferreira Costa[1], Welber Azevedo Rabello[1], Henrique Patrus Mundim Pena[2]

[1]Health and Human Ecology College, Vespasiano, MG; [2]Mater Dei Health Network, Belo Horizonte, MG, Brazil.

Abstract

Background: Myocardial infarction is one of the major causes of morbidity and mortality worldwide and 13.2% of patients with acute coronary syndrome have normal or unobstructed coronary arteries, called MINOCA (Myocardial Infarction with Non-Obstructive Coronary Artery). Cardiac magnetic resonance (CMR) is the gold standard for investigating the etiology of acute coronary syndrome. Although MINOCA has a more benign evolution than myocardial infarction due to coronary obstruction, its prognostic factors are not completely elucidated.

Objective: To evaluate prognosis, predictive factors and describe the incidence of major adverse cardiovascular events in patients with MINOCA.

Methods: Prospective cohort through data collection of patients admitted to the emergency department of a tertiary hospital, diagnosed with MINOCA from 2012 to 2019. The mean follow-up was 45 months, the outcomes considered were: death, rehospitalization due to cardiac causes, recurrence of chest pain, myocardial revascularization (MACE).

Results: Of the 179 patients, 52% were male, with a mean standard deviation age of 57.3 ± 15.5 years. A MACE rate of 17.9% was observed during a mean follow-up of 45 ± 21 months. Mortality at the end of follow-up was 3.8%. In the multivariate analysis using the Cox regression model, patients with normal CMR was shown to be a predictor of good prognosis (HR 0.09; 95% CI 0.01 – 0.88; p = 0.04). The Kaplan-Meier curve showed a significant difference (Log Rank x2 = 9.83 p = 0.02) in the prediction of free MACE.

Conclusion: Normal CMR was an independent predictor of good prognosis in this sample and could be useful in the risk stratification of patients with MINOCA.

Keywords: Acute Coronary Syndrome; Magnetic Resonance Imaging; Prognosis.

Resumo

Fundamento: *O infarto do miocárdio é uma das principais causas de morbimortalidade no mundo, e 13,2% dos pacientes com síndrome coronariana aguda apresentam coronárias sem obstrução significativa, denominada MINOCA (do inglês Myocardial Infarction with Non-Obstructive Coronary Artery, Infarto do Miocárdio sem Doença Coronariana Obstrutiva). Apesar do MINOCA ter evolução mais favorável que o infarto do miocárdio por obstrução coronariana, seu prognóstico não é benigno. A ressonância magnética cardíaca é o exame que apresenta importância no diagnóstico das diversas causas de MINOCA, e seu valor prognóstico não está completamente elucidado.*

Objetivo*: Avaliar o valor prognóstico da ressonância magnética cardíaca na detecção de eventos adversos maiores em pacientes com MINOCA.*

Métodos: *Coorte prospectiva por meio de coleta de dados de pacientes admitidos na urgência de pacientes com hospital terciário, diagnosticados com MINOCA, no período de 2012 a 2019.*

Resultados: *Foram avaliados 179 pacientes com seguimento médio de 45 ± 21 meses, sendo 52% do sexo masculino, com idade média de*

Mailing Address: Márcio Vinicius Lins Barros •
Av. do Contorno, 9000 - Barro Preto, Belo Horizonte - MG, 30110-062
E-mail: marciovlbarros@gmail.com.br
Manuscript received 3/8/2020; revised 5/11/2020; accepted 05/27/2020

DOI: 10.47593/2675-312X/20203304eabc97

57,3 ± 15,5 anos. Observou-se incidência de eventos adversos maiores de 17,9%. A taxa de mortalidade ao final do acompanhamento foi de 3,8%. Na análise multivariada, apenas a ressonância magnética cardíaca com resultado normal se mostrou como preditor independente de bom prognóstico (hazard ratio: 0,09; intervalo de confiança de 95% 0,01-0,88; p = 0,04), com curva de Kaplan-Meier apresentando diferença significativa (log-rank x2 = 9,83; p = 0,02) na predição de eventos adversos maiores.

Conclusão: *A ressonância magnética cardíaca normal mostrou-se como variável independente de bom prognóstico nessa população, podendo ser útil na estratificação de risco de pacientes com MINOCA.*

Palavras-chave: *Síndrome Coronariana Aguda; Imagem por Ressonância Magnética; Prognóstico.*

Introduction

Acute myocardial infarction (AMI) is a main cause of morbidity and mortality worldwide.[1] Of the affected patients, about 5–15% present with clinical and laboratory findings suggestive of AMI (chest pain, changes in plasma troponin levels, and/or electrocardiographic abnormalities) without significant coronary obstruction on coronary angiography, which is known as myocardial infarction with nonobstructive coronary artery (MINOCA).[2,3]

The pathophysiological mechanisms involved in the diagnosis of MINOCA are complex and heterogeneous since it has several causes related or unrelated to coronary atherosclerosis, and the identification of the underlying etiology is important in its clinical management. Although the prognosis of patients with MINOCA is more favorable than that of patients with AMI associated with obstructive coronary artery disease (CAD), a recent study demonstrated an annual mortality rate of 3.5%.[4]

According to the 2017 European Society of Cardiology guidelines for the management of acute myocardial infarction, MINOCA is now recognized as an entity distinct from AMI that requires special attention. The therapeutic approach is identified through a safe and accurate differential diagnosis of AMI and its underlying causes.[3]

Cardiac magnetic resonance (CMR) represents a particularly useful tool in the identification of the causes of MINOCA, such as AMI with spontaneous recanalization/embolism, acute myocarditis, stress cardiomyopathy (Takotsubo), or other cardiomyopathies, and is useful for stratifying risk factors for these patients.[5-7]

This study aimed to evaluate the role of CMR in the diagnostic and prognostic evaluation of a cohort of MINOCA patients.

Methods

Patients diagnosed with MINOCA[2,3] were prospectively selected from January 2012 to July 2019. All patients were admitted with clinical AMI (chest pain and/or electrocardiographic changes suggestive of myocardial ischemia and elevated troponin T) and underwent urgent angiography, which showed coronary arteries without significant obstruction, and subsequently underwent CMR for diagnostic definition.

The study exclusion criteria were age <18 years; a previous history of obstructive CAD, AMI, or myocardial revascularization; or unwillingness to participate in the study for any reason or failed to leave any contact information in hospital records, preventing them from being found for follow-up.

Upon admission, each patient completed a standardized data collection form on the presence of cardiac risk factors. Systemic arterial hypertension was defined as a documented history of high blood pressure or treatment with antihypertensive drugs. The presence of diabetes mellitus was defined as a previous diagnosis of diabetes and/or the use of insulin or oral hypoglycemic agents. Dyslipidemia was defined as a previous history of dyslipidemia or current treatment with lipid-lowering drugs. Smoking was considered the current smoking habit or smoking cessation within three months of the exam.

Adverse clinical outcomes were obtained through telephone interviews and classified as the occurrence of death of cardiac origin; myocardial infarction; unstable angina associated with hospitalization and revascularization; or hospitalization for cardiac reasons.

CMR was performed using a 1.5-T device (MAGNETOM Avanto, Siemens Healthineers, Erlangen, Germany). A comprehensive protocol included the study of ventricular function and the evaluation of edema and myocardial fibrosis. The presence of myocardial edema was analyzed using T2-weighted short-axis images with a short tau inversion recovery (STIR) sequence. Myocardial edema was considered present when the ratio between the signal intensity of the myocardium and the mean signal intensity of the skeletal muscle was >2 in T2-STIR images. Short-axis cine-CMR (steady-state free precession) was used to measure the left ventricular (LV) ejection fraction. The most basal short-axis cut was positioned just after the atrioventricular ring, and all subsequent respiratory pauses at maximum expiration were acquired with 8-mm thickness and 2-mm spacing between the other cuts up to the LV apex. A long- and short-axis gradient-echo sequence with inversion recovery (delayed enhancement technique) was performed 10–20 minutes after a gadolinium injection of 0.1–0.2 mmol/kg (Dotarem®, Guerbet) to identify myocardial fibrosis. Myocardial segments were evaluated in 17 segments. LV measurement and calculations were performed on a dedicated CMR workstation using specific software.

The patients were grouped into four categories based on CMR characteristics: normal (Figure 1A), ischemic (infarction; Figure 1B), myocarditis (Figure 1C), and cardiomyopathy (Figure 1D). The normal study corresponded to a heart without the evidence of contractile changes (except

desynchrony secondary to the left bundle branch block) and no edema or myocardial fibrosis. Myocarditis was diagnosed based on T2-STIR sequence changes and the detection of myocardial edema and the late epicardial or medium-myocardial enhancement pattern, according to the Lake Louise criteria.[8] The ischemic pattern (infarction) was diagnosed based on the presence of the late enhancement of a subendocardial or transmural pattern in the coronary territory. Takotsubo cardiomyopathy was diagnosed based on T2-STIR images detecting myocardial edema and medium-apical contractile changes without the evidence of significant myocardial fibrosis due to late enhancement. Dilated, hypertrophic, and restrictive cardiopathies were detected based on the specific characteristics of each pathology and grouped under cardiomyopathy together with Takotsubo cardiomyopathy. The extent of delayed enhancement and myocardial edema was quantified by the calculation of the number of involved segments.

The data were encoded, entered into a Microsoft Excel™ database, and subsequently analyzed using the Statistical Package for Social Science software version 20.0 (SPSS Inc., Chicago, IL, USA), with values of $p < 0.05$ considered statistically significant.

The study groups were compared using bilateral hypothesis tests with a significance level of 5% ($\alpha = 0.05$).

The Cox proportional-hazards model was used to estimate the survival of MINOCA patients. The hazard ratio was calculated with a 95% confidence interval as an estimated risk associated with a selected variable. The multivariate analysis included all variables selected in the univariate analysis. The survival analysis is expressed using the Kaplan–Meier plot, and the p values of the curves were compared using the log-rank test.

This study was approved by the Ethics Committee of the Health and Human Ecology College (no. CAAE66664017.0.0000.5101).

Results

The present study selected 179 patients, of whom 93 (52%) were male, with a mean age of 57.3 ± 15.5 years. Table 1 summarizes the baseline characteristics of the study population. Systemic arterial hypertension was the most common comorbidity (44% of patients). The median follow-up was 45 ± 21 months, with 13% of patients lost to follow-up. During follow-up, 28 (17.9%) adverse events occurred

Table 1 - Baseline characteristics of the studied population with myocardial infarction with nonobstructive coronary artery.

Characteristics	
Male	93 (52)
Age, years	57.3 ± 15.5
Dyslipidemia	52 (28.6)
Smoking	19 (10.4)
Hypertension	80 (44)
Diabetes	22 (12.1)
LVEF	58.1 ± 14.1
SBP, mmHg	126.7 ± 28.3
HR, bpm	75.9 ± 19.3
Follow-up, months	45 ± 21
MACE	28 (17.9)
Final diagnosis	
Normal	62 (35)
Ischemic	61 (34)
Cardiomyopathy	27 (15)
Myocarditis	29 (16)

Values are expressed as n (%) or mean ± standard deviation. HR, heart rate; LVEF, left ventricular ejection fraction; MACE, major adverse cardiovascular events; SBP, systemic blood pressure.

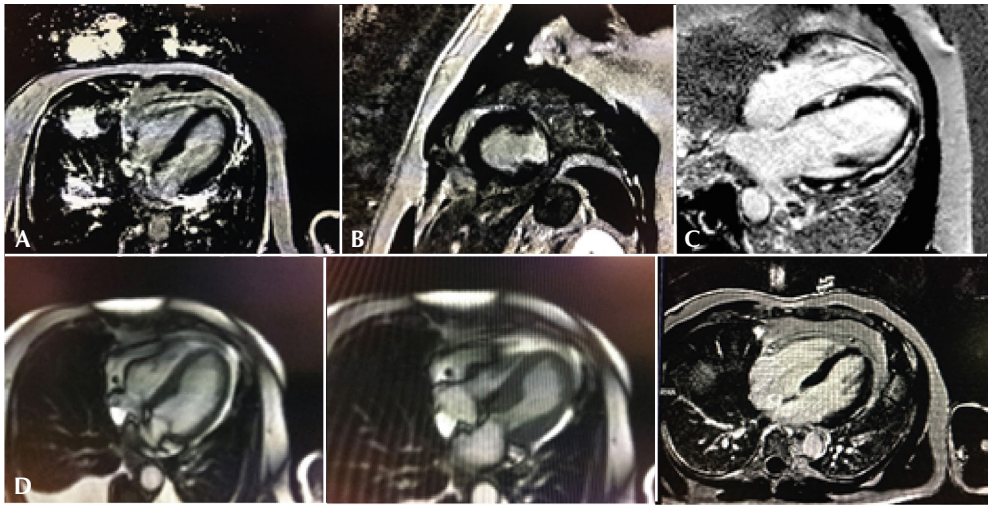

Figure1 – *Cardiac magnetic resonance images of patients with normal study findings using the delayed enhancement technique (1A); transmural infarction in the lateral wall (1B), myocarditis pattern (1C), and Takotsubo cardiomyopathy showing medium-apical contractile deficit and no changes using the delayed enhancement technique (1D).*

(selecting only adverse clinical outcomes occurring in the minimum follow-up period of three months), with 12 patients presenting with acute coronary syndrome (ACS), seven deaths, five with myocardial revascularization, and four owing to readmission for cardiac reasons. The mortality rate at the end of the follow-up period was 3.8%. Table 2 shows the univariate analysis of clinical characteristics and CMR to predict adverse events. Table 3 shows the independent predictors of adverse cardiac events, obtained by multivariate analysis using the Cox regression model. Statistical analyses considered normal CMR examination findings as an independent and significant predictor of a good prognosis.

Figure 2 illustrates the different patterns of CMR diagnosis in this cohort. The role of CMR in event-free survival was analyzed to compare normal examination results in relation to other diagnoses (Figure 3A: log-rank $\chi^2 = 9.83$; $p = 0.02$) and the normal and changed examination results (ischemic and nonischemic; Figure 3B: log-rank $x^2 = 6.83$; $p = 0.009$).

Discussion

The present study demonstrated important aspects in the evaluation of MINOCA patients, such as: CMR enabling a diagnosis in 65% of the evaluated cases; an adverse event rate of 17.9% and a mortality rate of 3.8% in a mean follow-up of 3.8 years; and the presence of normal CMR study findings demonstrated an excellent prognosis compared with other diagnoses on multivariate analysis.

The population group most affected by ACS with nonobstructive coronary arteries more commonly includes women and young people without dyslipidemia.[9] An observational study in Sweden using data from the Swedeheart registry showed a mean age of 69.1 years and that 59.1% of the patients were women.[10] A study conducted in China reported that patients diagnosed with MINOCA included a younger sample (aged 61.94 ± 13.07 years) and that 53% were male, 52% had arterial hypertension, 40% had a history of smoking, 20% had dyslipidemia, and 11% had diabetes mellitus.[11] Dastidar et al.[12] studied a sample of MINOCA patients, of whom 52% were male. The present study sample included 52% male patients, and the mean patient age was 57.3 ± 15.5 years, corroborating the findings of Dastidar et al.[12] and Abdu et al.[11] Regarding risk factors, this study relatively corroborates the frequency of arterial hypertension as a comorbidity reported by Abdu et al.[11]; however, the smoking rate was higher than that in the present study.

Although patients with MINOCA have a better prognosis than those with obstructive AMI[6], the prognosis is not benign. Recent studies indicated that up to 24% of MINOCA patients present adverse events within approximately four years.[13] A North American multicenter cohort study of data from the National Cardiovascular Data Registry® reported a 19% occurrence rate of adverse events beyond one year.[14] The

Table 3 - Multivariate analysis using the Cox regression model to predict outcomes.

Variable	HR	95% CI	p value
Normal CMR	0.09	0.01-0.88	0.04
Ischemia on CMR	1.04	0.25-3.96	0.99
Cardiomyopathy on CMR	1.07	0.49-2.29	0.86
Diabetes	1.22	0.28-5.34	0.79
Age	1.03	0.98-1.05	0.07
SBP	1.01	0.99-1.03	0.08
Heart rate	1.02	0.98-1.04	0.29
Creatinine	1.19	0.76-1.87	0.43
LVEF	0.98	0.96-1.01	0.37
Dyslipidemia	1.62	0.72-3.67	0.24

CI, confidence interval; CMR, cardiac magnetic resonance; HR, hazard ratio; LVEF, left ventricular ejection fraction; SBP, systemic blood pressure.

Table 2 - Univariate analysis of adverse event determinants in the population with myocardial infarction with nonobstructive coronary artery.

Variable	Patients with events (n = 28)	Without events (n = 128)	Hazard ratio (95% CI)	p value
Age	61.7 ± 10.4	55.2 ± 15.9	1.02 (0.99-1.05)	0.16
Male sex	13 (54)	53 (49)	0.86 (0.38-1.93)	0.71
Smoking	3 (15)	15 (16)	1.02 (0.59-1.94)	0.79
SAH	13 (65)	59 (48)	1.19 (0.81-2.19)	0.64
Diabetes mellitus	5 (25)	17 (14)	1.49 (0.92-6.10)	0.08
Dyslipidemia	09 (40)	60 (32)	1.44 (0.94-2.20)	0.09
SBP, mmHg	129.8 ± 42.3	125.8 ± 25.5	1.01 (0.99-1.01)	0.09
HR, bpm	71.9 ± 21.7	74.3 ± 14.7	1.01 (0.99-1.02)	0.07
Creatinine, mg/dL	0.92 ± 0.23	0.89 ± 0.27	5.12 (0.84-31.37)	0.28
LVEF, %	52.1 ± 16.2	60.0 ± 12.5	0.98 (0.95-1.001)	0.06
Normal CMR	1 (4)	47 (37)	0.11 (0.01-0.82)	0.03
Ischemia on CMR	17 (61)	39 (30)	1.80 (0.83-3.91)	0.14
Cardiomyopathy on CMR	7 (25)	18 (14)	2.26 (0.94-5.43)	0.08
Myocarditis on CMR	3 (11)	24 (19)	1.24 (0.68-2.29)	0.48
Late highlighting	1.5±2.4	1.1± 1.6	1.15 (0.90-1.51)	0.24

Values are shown as n (%), mean ± standard deviation, or median (95% CI). CI, confidence interval; CMR, cardiac magnetic resonance; HR, heart rate; LVEF, left ventricular ejection fraction; SAH, systemic arterial hypertension; SBP, systemic blood pressure.

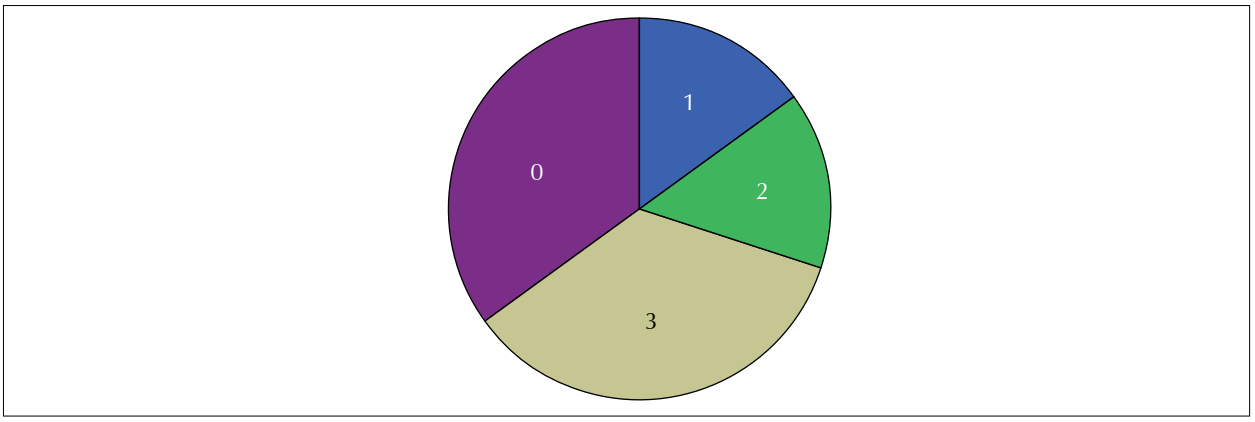

Figure 2 – *Frequency of cardiac magnetic resonance diagnoses. Normal diagnosis (0: 35%), myocarditis (1: 16%), cardiomyopathy (2: 15%), and ischemia (3: 34%).*

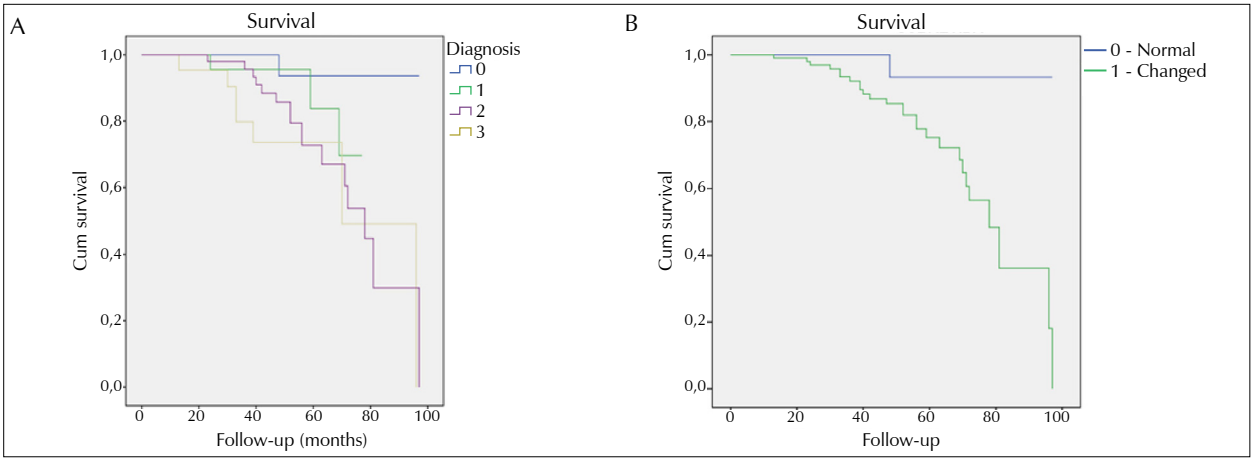

Figure 3 – *Event-free survival of patients with normal diagnosis (0), myocarditis (1), cardiomyopathy (2), and ischemia (3) on cardiac magnetic resonance (log-rank χ2 = 9.83, p = 0.02) (A) and between patients with normal (0) and a changed diagnosis (1: ischemic and nonischemic) (log-rank χ2 = 6.83, p = 0.009) (B).*

present study had a mean follow-up period of 3.8 years and a 17.9% occurrence rate of adverse events.

The present study had a mortality rate of 3.8% due to cardiovascular disease over a mean follow-up period of 3.8 years. A Canadian study conducted between 2002 and 2014 by Bainey et al.[5] showed a five-year mortality of 11% for MINOCA and 16% for obstructive AMI-CAD. Choo et al.[15] reported a 9.1% incidence of death in patients with MINOCA. Egger et al.[16] obtained a 7% general mortality rate from all causes over a follow-up of 3.8 years. According to Nordenskjöld et al.,[10] the mortality rate due to reinfarction in patients with MINOCA during a mean follow-up of 38 months was 13%. Dastidar et al.[12] reported a mortality rate of 5.7% in a mean follow-up of 3.5 years, with a worse prognosis in the group with cardiomyopathy. These data demonstrate that patients affected by MINOCA present greater morbidity and mortality rates than does the general population, showing the importance of a proper diagnosis, therapy, and follow-up.

The data from the present study showed that CMR provided the etiological diagnosis in two-thirds of patients. Dastidar et al.[12] identified the cause of MINOCA in 74% of patients (25% due to myocarditis, 25% due to AMI, and 25% due to cardiomyopathy), while the other 26% of patients had normal CMR findings. A study conducted in Stockholm by Collste et al.[17] revealed that 45% of patients had normal CMR findings, with 22% presenting with Takotsubo cardiomyopathy, 19% with myocardial infarction, 7% with evidence of myocarditis, and the remaining (7%) with hypertrophic cardiomyopathy or no classification. Gerbaud et al.[18] determined a diagnosis in 100 of 130 patients (76.9%) with MINOCA using CMR, with 23.1% presenting with normal study findings, 28.5% with AMI, 26.1% with myocarditis, 21.5% with Takotsubo cardiomyopathy, and 0.8% with hypertrophic cardiomyopathy. Pasupathy et al.[6] observed an infarction pattern in 24% of patients, myocarditis in 33%, Takotsubo cardiomyopathy in 18%, and normal examination findings in 26% in a meta-analysis of 26 studies using CMR.

Interstudy differences can be predominantly related to the sample characteristics such as age, number of cases, and time to perform CMR. However, all studies demonstrated the diagnostic capacity of the method and its importance in the management of these patients, with some showing that the

initial diagnosis and management can be modified in 65% and 32% of cases, respectively.[17-19] These findings reinforce the idea of using CMR as a standard propaedeutic in patients with MINOCA.

The limiting factors of the present study include its single-center design and small sample size. In addition, since it is a prospective study, the vulnerability of the methodology to follow-up bias should be considered. Obtaining information by telephone may also have influenced survival and adverse event data due to potential bias in the information provided by the patient or their relatives as well as the possibility of unknown deaths.

Conclusion

The present study demonstrated that patients with MINOCA can present with different diagnoses and have a heterogeneous but non-benign progression (adverse events and mortality) in a mean follow-up of four years, demonstrating the importance of the etiological definition in the management of these patients. Normal CMR imaging findings was a predictor of a good prognosis in this cohort, showing the value of this test in the diagnostic evaluation and risk stratification of patients with MINOCA.

Authors' contributions

Research conception and design: Barros MVL, Ornelas CE, Siqueira MHA, Melo Júnior MA, Costa SMF, Rabello WA, and Pena HPM; data collection: Barros MVL, Siqueira MHA, Militão RC, Melo Júnior MA, Costa SMF, and Rabello WA; data analysis and interpretation: Barros MVL; statistical analysis: Barros MVL; manuscript writing: Barros MVL; and critical review of the manuscript for important intellectual content: Barros MVL, Ornelas CE, Siqueira MHA, Militão RC, and Pena HPM.

Conflict of interest

The authors have declared that they have no conflict of interest.

References

1. Writing Group Member, Roger VL, Go AS, Lloyd-Jones DM, Benjamin EJ, Berry JD, Borden WB, et al. Heart disease and stroke statistics- update: a report from the American Heart Association. Circulation. 2012;125(1):e2-e220. doi: https://doi.org/10.1161/CIR.0b013e31823ac046

2. Agewall S, Beltrame JF, Reynolds HR, Niessner A, Rosano G, Caforio AL, De Caterina R, Zimarino M, Roffi M, Kjeldsen K, Atar D, Kaski JC, Sechtem U, Tornvall P; WG on Cardiovascular Pharmacotherapy. ESC working group position paper on myocardial infarction with non-obstructive coronary arteries. Eur Heart J. 2017;38(3):143-153. doi: 10.1093/eurheartj/ehw149

3. Ibanez B, James S, Agewall S, Antunes MJ, Bucciarelli-Ducci C, Bueno H, Caforio ALP, Crea F, Goudevenos JA, Halvorsen S, Hindricks G, Kastrati A, Lenzen MJ, Prescott E, Roffi M, Valgimigli M, Varenhorst C, Vranckx P, Widimský P; ESC Scientific Document Group. 2017 ESC Guidelines for the management of acute myocardial infarction in patients presenting with ST-segment elevation: The Task Force for the management of acute myocardial infarction in patients presenting with ST-segment elevation of the European Society of Cardiology (ESC). Eur Heart J. 2018;39(2):119-177. doi: 10.1093/eurheartj/ehx393

4. Tamis-Holland JE, Jneid H, Reynolds HR, Agewall S, Brilakis ES, Brown TM, Lerman A, Cushman M, Kumbhani DJ, Arslanian-Engoren C, Bolger AF, Beltrame JF; American Heart Association Interventional Cardiovascular Care Committee of the Council on Clinical Cardiology; Council on Cardiovascular and Stroke Nursing; Council on Epidemiology and Prevention; and Council on Quality of Care and Outcomes Research. Contemporary Diagnosis and Management of Patients With Myocardial Infarction in the Absence of Obstructive Coronary Artery Disease: A Scientific Statement From the American Heart Association. Circulation. 2019;139(18):e891-e908. doi: 10.1161/CIR.0000000000000670

5. Bainey KR, Welsh RC, Alemayehu W, Westerhout CM, Traboulsi D, Anderson T, Brass N, Armstrong PW, Kaul P. Population-level incidence and outcomes of myocardial infarction with non-obstructive coronary arteries (MINOCA): Insights from the Alberta contemporary acute coronary syndrome patients invasive treatment strategies (COAPT) study. Int J Cardiol. 2018;264:12-17. doi: 10.1016/j.ijcard.2018.04.004

6. Pasupathy S, Air T, Dreyer RP, Tavella R, Beltrame JF. Systematic review of patients presenting with suspected myocardial infarction and nonobstructive coronary arteries. Circulation. 2015;131(10):861-70. doi: 10.1161/CIRCULATIONAHA.114.011201. Erratum in: Circulation. 2015;131(19):e475.

7. Vignisson ST, Gudmundsdottir IJ, Gudnason T, Danielsen R, Gardarsdottir M, Andersen K. [MINOCA in Iceland. Acute coronary syndrome in patients with normal or nonobstructive coronary arteries]. Laeknabladid. 2018 Mai;104(5):237-242. doi: 10.17992/lbl.2018.05.185. Icelandic.

8. Friedrich MG, Sechtem U, Schulz-Menger J, Holmvang G, Alakija P, Cooper LT, White JA, Abdel-Aty H, Gutberlet M, Prasad S, Aletras A, Laissy JP, Paterson I, Filipchuk NG, Kumar A, Pauschinger M, Liu P; International Consensus Group on Cardiovascular Magnetic Resonance in Myocarditis. Cardiovascular magnetic resonance in myocarditis: A JACC White Paper. J Am Coll Cardiol. 2009;53(17):1475-87. doi: 10.1016/j.jacc.2009.02.007

9. Da Costa A, Isaaz K, Faure E, Mourot S, Cerisier A, Lamaud M. Clinical characteristics, aetiological factors and long-term prognosis of myocardial infarction with an absolutely normal coronary angiogram; a 3-year follow-up study of 91 patients. Eur Heart J. 2001;22(16):1459-65. doi: 10.1053/euhj.2000.2553

10. Nordenskjöld AM, Lagerqvist B, Baron T, Jernberg T, Hadziosmanovic N, Reynolds HR, et al. Reinfarction in Patients with Myocardial Infarction with Nonobstructive Coronary Arteries (MINOCA): Coronary Findings and Prognosis. Am J Med. 2019 Mar;132(3):335-346. doi: 10.1016/j.amjmed.2018.10.007

11. Abdu FA, Liu L, Mohammed AQ, Luo Y, Xu S, Auckle R, et al. Myocardial infarction with non-obstructive coronary arteries (MINOCA) in Chinese patients: Clinical features, treatment and 1 year follow-up. Int J Cardiol. 2019 Jul 15;287:27-31. doi: 10.1016/j.ijcard.2019.02.036

12. Dastidar AG, Baritussio A, De Garate E, Drobni Z, Biglino G, Singhal P, et al. Prognostic Role of CMR and Conventional Risk Factors in Myocardial Infarction With Nonobstructed Coronary Arteries. JACC Cardiovasc Imaging. 2019;12(10):1973-1982. doi: 10.1016/j.jcmg.2018.12.023

13. Nordenskjöld AM, Baron T, Eggers KM, Jernberg T, Lindahl B. Predictors of adverse outcome in patients with myocardial infarction with non-obstructive coronary artery (MINOCA) disease. Int J Cardiol. 2018;261:18-23. doi: 10.1016/j.ijcard.2018.03.056

14. Dreyer RP, Tavella R, Curtis JP, Wang Y, Pauspathy S, Messenger J, et al. Myocardial infarction with non-obstructive coronary arteries as compared with myocardial infarction and obstructive coronary disease: outcomes in a Medicare population. Eur Heart J. 2020;41(7):870-8. doi: 10.1093/eurheartj/ehz403

15. Choo EH, Chang K, Lee KY, Lee D, Kim JG, Ahn Y, Kim YJ, Chae SC, Cho

MC, Kim CJ, Kim HS, Jeong MH; KAMIR-NIH Investigators. Prognosis and Predictors of Mortality in Patients Suffering Myocardial Infarction With Non-Obstructive Coronary Arteries. J Am Heart Assoc. 2019;8(14):e011990. doi: 10.1161/JAHA.119.011990

16. Eggers KM, Hjort M, Baron T, Jernberg T, Nordenskjöld AM, Tornvall P, et al. Morbidity and cause-specific mortality in first-time myocardial infarction with nonobstructive coronary arteries. J Intern Med. 2019 Apr;285(4):419-428. doi: 10.1111/joim.12857

17. Collste O, Sörensson P, Frick M, Agewall S, Daniel M, Henareh L, et al. Myocardial infarction with normal coronary arteries is common and associated with normal findings on cardiovascular magnetic resonance imaging: results from the Stockholm Myocardial Infarction with Normal Coronaries study. J Intern Med. 2013 Feb;273(2):189-96. doi: 10.1111/j.1365-2796.2012.02567.x

18. Gerbaud E, Harcaut E, Coste P, Erickson M, Lederlin M, Labèque JN, et al. Cardiac magnetic resonance imaging for the diagnosis of patients presenting with chest pain, raised troponin, and unobstructed coronary arteries. Int J Cardiovasc Imaging. 2012;28(4):783-94. doi: 10.1007/s10554-011-9879-1.

19. Assomull RG, Lyne JC, Keenan N, Gulati A, Bunce NH, Davies SW, et al. The role of cardiovascular magnetic resonance in patients presenting with chest pain, raised troponin, and unobstructed coronary arteries. Eur Heart J. 2007;28(10):1242-9. doi: 10.1093/eurheartj/ehm113

Semiautomatic Quantification of Left Ventricular Ejection Fraction and Volumes by Two-Dimensional Echocardiography: Comparison with Automatic Three-Dimensional Echocardiography

Quantificação Semiautomática da Fração de Ejeção e Volumes do Ventrículo Esquerdo ao Ecocardiograma Bidimensional: Comparação com o Ecocardiograma Tridimensional Automático

Rafael Borsoi[1], Miguel Morita Fernandes da Silva[1], Silvio Henrique Barberato[1]
Quanta Diagnosis and Therapy – Curitiba, PR, Brazil.

Abstract

Background: Left ventricular ejection fraction is one of the most used echocardiographic parameters in clinical practice. Its estimation by two-dimensional manual method (Simpson method) has limited reproducibility and accuracy, and semi-automatic methods have been proposed. It becomes necessary to compare the semi-automatic two-dimensional method with more accurate methods of assessing left ventricular ejection fraction, such as measurement by automatic three-dimensional echocardiography.

Objective: To compare the left ventricular ejection fraction, and left ventricular end-diastolic and end-systolic volumes estimates by the semi-automatic two-dimensional method with those obtained using the automatic three-dimensional method.

Method: Observational cross-sectional study, including patients in sinus rhythm, left ventricular ejection fraction > 50% and without significant structural heart disease, submitted to transthoracic echocardiography. Student's t test, Pearson's coefficient and Bland-Altman analysis were used in the statistical analysis.

Results: Forty patients were included, 53% women, 35% with arterial hypertension, 25% with dyslipidemia, 10% diabetic, 10% smokers and 13% with previous angioplasty. The mean values of left ventricular ejection fraction by three-dimensional and two-dimensional were 62.1 ± 5.8% and 61.7 ± 5.9% (p = 0.50), respectively. There was a strong correlation between left ventricular ejection fraction determined by two-dimensional and three-dimensional (r = 0.75; p <0.001), as well as with left ventricular end-diastolic (r = 0.75; p <0.001) and end-systolic (r = 0.76; p < 0.001). There was good agreement between two-dimensional and three-dimensional left ventricular ejection fraction (mean difference: -0.39; 95% confidence interval -1.7-0.9).

Conclusion: Left ventricular ejection fraction estimated by the two-dimensional semi-automatic method showed good agreement with the automatic three-dimensional method. The findings suggest the two-dimensional semi-automatic method as a reliable alternative for assessing volumes and left ventricular ejection fraction.

Keywords: Echocardiography, Doppler; Echocardiography, Three-Dimensional; Stroke Volume; Ventricular Function, Left.

Resumo

Fundamento: *A fração de ejeção do ventrículo esquerdo é um dos parâmetros ecocardiográficos mais utilizados na prática clínica. Sua estimativa pelo método bidimensional manual (método de Simpson) tem reprodutibilidade e acurácia limitadas, e métodos semiautomáticos têm sido propostos. Torna-se necessário comparar o método bidimensional semiautomático com métodos mais acurados de avaliação da fração de ejeção do ventrículo esquerdo, como a medida pela ecocardiografia tridimensional automática.*

Objetivo: *Comparar as estimativas da fração de ejeção do ventrículo esquerdo e dos volumes diastólico final e sistólico final do ventrículo esquerdo pelo método bidimensional semiautomático com as obtidas pelo método tridimensional automático.*

Método: *Estudo observacional transversal, com pacientes em ritmo sinusal, fração de ejeção do ventrículo esquerdo >50% e sem cardiopatia estrutural significativa, submetidos ao ecocardiograma transtorácico. Teste* ***t*** *de* ***Student****, coeficiente de Pearson e análise de Bland-Altman foram usados na análise estatística.*

Resultados: *Foram incluídos 40 pacientes, sendo: 53% mulheres, 35% hipertensos, 25% dislipidêmicos, 10% diabéticos, 10% tabagistas e*

Mailing Address: Rafael Borsoi •
R. Alm. Tamandaré, 1000 - Alto da XV, Curitiba - PR, 80045-170
E-mail: rafaelborsoi@yahoo.com.br
Manuscript received 3/9/2020; revised 3/26/2020; accepted 4/17/2020

DOI: 10.47593/2675-312X/20203304eabc98

<< SUMÁRIO

13% com angioplastia prévia. Os valores médios da fração de ejeção do ventrículo esquerdo aos métodos tri e bidimensionais foram 62,1 ± 5,8% e 61,7 ± 5,9% (p = 0,50), respectivamente. Houve forte correlação da fração de ejeção do ventrículo esquerdo determinada melos métodos bi e tridimensional (r = 0,74; p<0,001), assim como com o volume diastólico final (r = 0,75; p<0,001) e o sistólico final (r = 0,76; p<0,001). Houve boa concordância entre a fração de ejeção do ventrículo esquerdo bi e tridimensional (diferença média: -0,39; intervalo de confiança 95% -1,7-0,9).

Conclusão: *A fração de ejeção do ventrículo esquerdo estimada pelo método bidimensional semiautomático mostrou boa concordância com o método tridimensional automático. Os achados sugerem que o método bidimensional semiautomático represente uma alternativa confiável para avaliação dos volumes e fração de ejeção do ventrículo esquerdo.*

Palavra-chave: Ecocardiografia Doppler; Ecocardiografia Tridimensional; Volume Sistólico; Função Ventricular Esquerda.

Introduction

The assessment of left ventricular ejection fraction (LVEF) and volumes is among the primary indications of transthoracic echocardiography; thus, it is essential that these measurements be accurately and reproducibly estimated.[1-3] Two-dimensional (2D) echocardiography, traditionally used for this purpose, has important limitations, such as broad intra- and interobserver variability and ventricular volume obtention through geometric presumptions.[4,5] Three-dimensional (3D) echocardiography allows for more reliable volumetric and functional left ventricular (LV) analyses and boasts greater reproducibility than manual 2D echocardiography (Simpson's method) and greater precision than cardiac magnetic resonance (CMR).[6-11] Three-dimensional echocardiography results are close to the volumes obtained by CMR, considered the gold standard, while 2D manual echocardiography significantly underestimates LV measurements.[7-9] In the first years using the method, image acquisition difficulties and delayed analysis limited the routine use of 3D echocardiography and decreased its spread.[12-14] Recent improvements in quantification methods made its use faster and simpler in daily practice.[15-18] The commercially available automatic 3D Philips HeartModel software can obtain cardiac chamber LVEF and volumes in approximately 30 seconds while requiring minimal operator training and maintaining a strong correlation with CMR results.[19-22] Similarly, 2D echocardiography quantification methods have also progressed by providing semiautomatic LVEF and volumes in addition to other relevant information for clinical practice, such as global longitudinal strain (GLS). However, no studies comparing semiautomatic LVEF 2D quantification software with the 3D echocardiographic method, which has proven greater accuracy, were found in the literature.

This study aimed to compare LVEF and end-diastolic LV (EDV) and end-systolic LV (ESV) estimates of the semiautomatic 2D and automatic 3D methods.

Methods

This observational cross-sectional study included an outpatient population referred for transthoracic echocardiography by their attending physician. The included patients had sinus rhythm and an LVEF > 50% without significant structural heart disease (moderate to severe aortic, mitral or tricuspid insufficiency; any degree of valve stenosis; congenital heart disease with any degree of hemodynamic repercussion; pericardial effusion; LV segment contractility; and moderate to severe myocardial hypertrophy) and with a high-quality acoustic window. After a complete standardized echocardiographic examination, 2D and 3D images were also acquired to analyze and compare LVEF, ESV, and EDV using the automatic 3D and semiautomatic 2D methods. The examinations were performed on an EPIQ 7 ultrasound machine (Philips) with an X5 transducer. The images for volume and LVEF assessment were obtained by the semiautomatic 2D method in four- and two-chamber apical windows. Additionally, the apical three-chamber view was obtained to calculate the GLS. Reference points were defined in the mitral annulus (septal and lateral, anterior and inferior) and in the apex at each of the windows. From these reference points, the semiautomated aCMQ software (Philips) detected the systolic and diastolic LV endocardial borders, providing LVEF, ESV, and EDV estimates (Figure 1). When necessary, manual adjustments were made to optimize identification of the cardiac borders.

Images were obtained by the automatic 3D method in the four-chamber apical window during controlled apnea to estimate LVEF and volumes. After acquisition, the images were analyzed by the HeartModel software, which uses an adaptive analytical algorithm to automatically detect the interface between the endocardial borders and the blood. At the touch of a single button on the HeartModel's screen, the software automatically calculated LVEF and volumes (Figure 2). If necessary, manual adjustments were made to optimize the identification of the endocardial borders.

The Statistical Package for Social Science software version 22.0.0.0 was used for the statistical analyses; values of $p < 0.05$ were considered statistically significant. The results are presented as mean and standard deviation. Student's t-test (numerical differences), Pearson's coefficient (correlation), and Bland-Altman analysis (concordance) were used in the statistical evaluation.[23]

Results

Of the 44 patients included in the study, four were excluded due to a lack of data or inadequate echocardiographic image quality, resulting in a final sample of 40 patients. The mean age was 58 ± 15 years and the body mass index was 26 ± 3; 52.5% (n = 21) of the patients were women, 35% (n = 14) were hypertensive, 25% (n = 10) had dyslipidemia, 10% (n = 4) were diabetic, 10% (n = 4) were smokers, and 12.5%

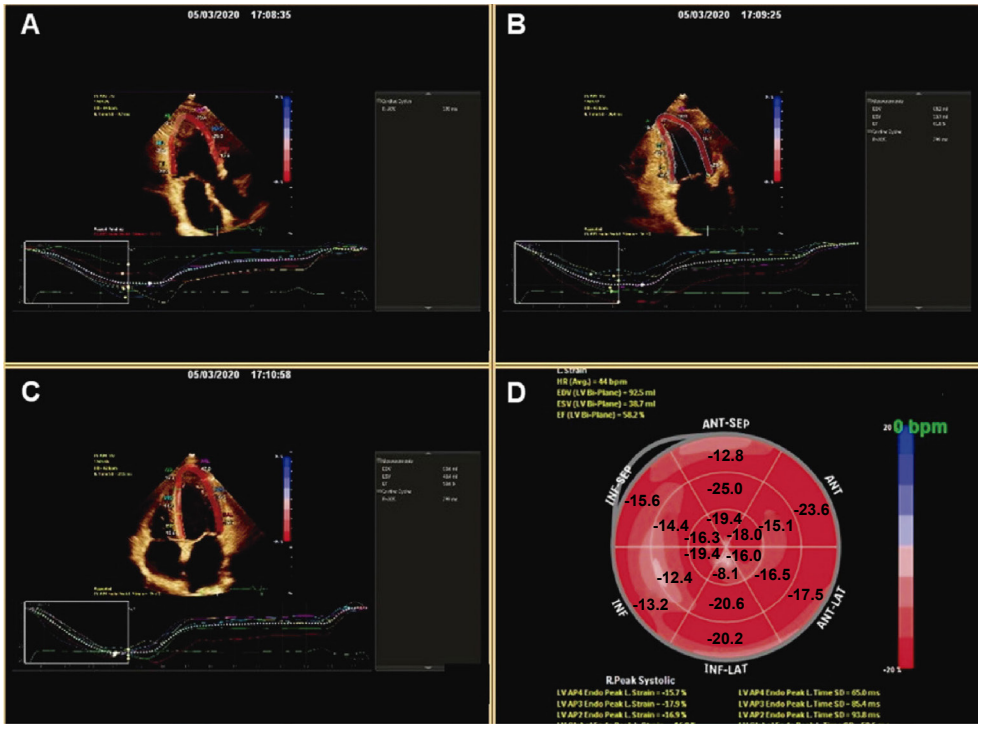

Figure 1 – *Left ventricular ejection fraction estimation by the aCMQ software from two- and four-chamber apical sections (B and C). The apical three-chamber view (A) and the bullseye graph with global longitudinal strain calculation (D) are shown.*

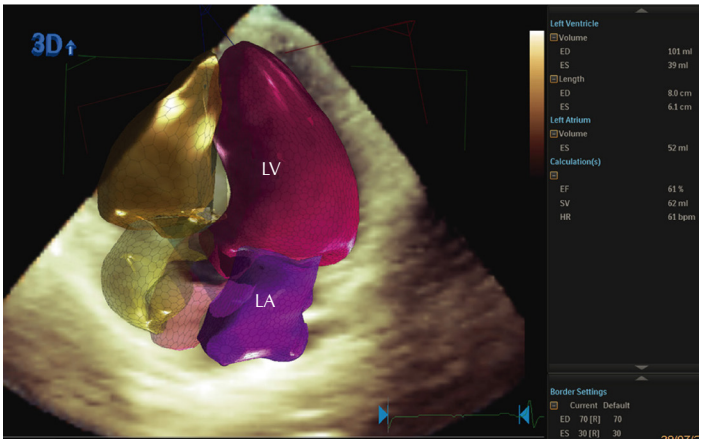

LV, left ventricle; LA, left atrium.

Figure 2 – *Sample three-dimensional reconstruction produced by the HeartModel software representing the left ventricle and other cardiac chambers. The software automatically calculates left ventricular ejection fraction and end-systolic and diastolic volumes.*

(n = 5) previously underwent coronary angioplasty. These and other clinical characteristics are shown in Table 1.

Regarding the echocardiographic parameters of the study population, 38% (n = 15) had grade I diastolic dysfunction (all others were normal), 18% (n = 7) had mild concentric LV hypertrophy, and 10% (n = 4) had a slightly increased LA. The mean GLS was 18.1 ± 2.7% (absolute value). The echocardiographic parameters are shown in Table 2.

The mean 3D and 2D FEVE values were 62.1 ± 5.8% and 61.7 ± 5.9% (p = 0.50), respectively. There was a strong correlation between 2D and 3D LVEF (r = 0.74; p < 0.001), EDV (r = 0.75; p < 0.001), and ESV (r = 0.76; p < 0.001) values. The Bland-Altman analysis (Figure 3) showed good concordance between 2D and 3D LVEF estimates (mean difference, -0.39; 95% confidence interval, -1.71 to -0.9; concordance, -8.67 to 7.89).

Table 1 - Demographic and clinical characteristics of the study population.

Characteristic	
Age, years	58 ± 15 (28-84)
Women	21 (52.5)
BMI	26 ± 3 (19-35)
Beta-blocker use	8 (20)
ACEI or ARB use	11 (27.5)
CCA	3 (7.5)
Diuretic	3 (7.5)
ASA use	8 (20)
Statin	7 (17.5)
SAH	14(35)
Dyslipidemia	10(25)
DM	4 (10)
Sedentary lifestyle	5 (12.5)
Smoking	4 (10)
Family history of CAD	3 (7.5)
CT or RxT	3 (7.5)
Prior CAD	6 (15)
Previous revascularization	5 (12)

Results expressed as mean ± standard deviation (range) or n (%). ACEI, angiotensin-converting enzyme inhibitor; ARB, angiotensin receptor blocker; ASA, acetylsalicylic acid; BMI, body mass index; CAD, coronary artery disease; CCA, calcium channel antagonist ; CT, chemotherapy; DM, diabetes mellitus; RxT, radiotherapy; SAH, systemic arterial hypertension.

Table 2 - Echocardiographic characteristics of the study population.

Characteristic	Value
LV mass, g/m²	87 ± 21
LA volume, mL/m²	26 ± 6
E/A ratio	1.1 ± 0.44
Septal e' wave, cm/s	7.2 ± 2.2
Lateral e' wave, cm/s	9.6 ± 2.9
Wave and 'mean, cm/s	8.4 ± 2.4
Septal E/e' ratio	10.9 ± 3.9
Lateral E/e' ratio	8.3 ± 2.9
Mean E/e' ratio	9.7 ± 3.8
GLS, %	18.1 ± 2.7

Values are shown as mean ± standard deviation. GLS, global longitudinal strain; LA, left atrium; LV, left ventricle.

Discussion

LV systolic function estimation by LVEF is a cornerstone of modern cardiology that has great use in clinical practice, with transthoracic echocardiography being the first-line examination for this purpose. Although 3D echocardiography enables a more reliable, accurate, and reproducible analysis, manual 2D echocardiography (Simpson's method) is still the most widely available and commonly used method for estimating LVEF. The evaluation of LV systolic performance using manual 2D echocardiography is based on endocardial border tracing, taking care to maximize the areas and avoid LV volume underestimation.[11,24] On the other hand, on 3D echocardiography, LV volume reduction is less relevant since the method is not based on geometric assumptions.[9-11] In cases of good image quality, the accuracy of the 3D method is comparable to that of CMR, with a tendency to obtain slightly smaller volumes.[6,7] In the present study, the good concordance between the results of the semiautomatic 2D and automatic 3D methods suggests that semiautomatic 2D echocardiography may be a reliable alternative for LVEF and volume evaluation. The calculated bias was low in the Bland-Altman analysis, i.e., the differences between methods seemed clinically acceptable. No previous study comparing the semiautomatic 2D and automatic 3D methods was found in a literature review.

Semiautomatic 2D echocardiography showed good practical applicability and processing time. The broad use of traditional 3D echocardiography was recently limited by image acquisition difficulties and delayed analysis[12-14] in addition to its limited availability. Although the present study did not specifically evaluate image acquisition and processing time, evaluations using the semiautomatic 2D method tended to be faster than those with the manual 2D and traditional 3D methods, enabling its inclusion in the standard echocardiography routine.[11,13]

Economically, the semiautomatic 2D echocardiography method is a more accessible option, considering that equipment using 3D technology has higher cost due to the greater complexity of its components (transducers and software). The disadvantages of using the semiautomatic 2D echocardiography method include an inadequate echocardiographic window or certain types of structural cardiac changes that can lead to incorrect recognition of the endocardial borders and atrioventricular junction. Manual adjustments can optimize the identification of the borders, but they require a longer analysis time. Likewise, arrhythmias or inappropriate electrocardiographic tracings can impair the identification of end-systolic and/or diastolic conditions, providing inaccurate or incorrect estimates. On the other hand, the same technical difficulties are observed in the automatic 3D echocardiography method, comprising common limitations to the two methods.[23] To minimize these difficulties, this study included only patients with an adequate thoracic acoustic window, a regular heart rhythm, and no significant structural heart changes. Prospects point to the development and optimization of software and automatic platforms for cardiac chamber volumetric and functional calculations. The progression of these platforms should enable more agile and precise measurements despite the current limitations.

The limitations of this study include its relatively small sample, absence of simultaneous measurement by traditional non-automatic methods (manual 2D and semiautomatic 3D), and lack of intra- and interobserver variability estimations. In addition, the findings cannot be extended to patients with arrhythmias, LV systolic dysfunction (LVEF < 50%), and/or moderate to severe structural heart disease.

Conclusion

This study is the first to demonstrate good concordance between LVEF and ventricular volumes estimated by the semiautomatic 2D and automatic 3D methods in patients without arrhythmias and/or significant structural heart disease.

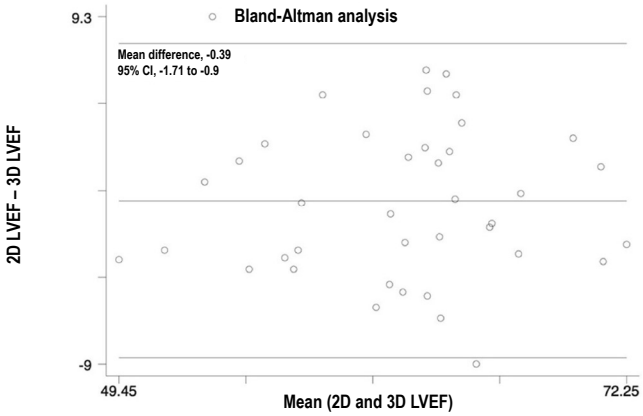

2D, two-dimensional; 3D, three-dimensional; 95% CI, 95% confidence interval; LVEF, left ventricular ejection fraction.

Figure 3 – *Bland-Altman analysis of two- and three-dimensional left ventricle ejection fraction.*

Thus, 2D transthoracic echocardiography with automatic quantification software was proven reliable for measuring LVEF and volumes in this group of participants.

Authors' contributions

Research creation and design: Borsoi R, Barberato SH; Data acquisition: Borsoi R, Barberato SH; Data analysis and interpretation: Borsoi R, Barberato SH, Silva MMF; Statistical analysis: Barberato SH, Silva MMF; Manuscript writing: Borsoi R, Barberato SH, Silva MMF; Critical revision of the manuscript for important intellectual content: Borsoi R, Barberato SH, Silva MMF.

Conflict of interest

The author have declared that they have no conflict of interest.

References

1. Wong M, Johnson G, Shabetai R, Hughes V, Bhat G, Lopez B, et al. Echocardiographic variables as prognostic indicators and therapeutic monitors in chronic congestive heart failure. Veterans Affairs cooperative studies V-HeFT I and II. V-HeFT VA Cooperative Studies Group. Circulation. 1993;87(6 Suppl):VI65-70. PMID: 8500242.

2. Kaufmann BA, Min SY, Goetschalckx K, Bernheim AM, Buser PT, Pfisterer ME, et al. How reliable are left ventricular ejection fraction cut offs assessed by echocardiography for clinical decision making in patients with heart failure? Int J Cardiovasc Imaging. 2013;29(3):581-8. doi: 10.1007/s10554-012-0122-5

3. Cameli M, Mondillo S, Solari M, Righini FM, Andrei V, Contaldi C, et al. Echocardiographic assessment of left ventricular systolic function: from ejection fraction to torsion. Heart Fail Rev. 2016;21(1):77-94. doi: 10.1007/s10741-015-9521-8

4. Jacobs LD, Salgo IS, Goonewardena S, Weinert L, Coon P, Bardo D, et al. Rapid online quantification of left ventricular volume from real-time threedimensional echocardiographic data. Eur Heart J. 2006;27(4):460-8. doi: 10.1093/eurheartj/ehi666

5. Hoffmann R, Barletta G, von Bardeleben S, Vanoverschelde JL, Kasprzak J, Greis C, et al. Analysis of left ventricular volumes and function: a multicenter comparison of cardiac magnetic resonance imaging, cine ventriculography, and unenhanced and contrast-enhanced two-dimensional and three-dimensional echocardiography. J Am Soc Echocardiogr. 2014;27(3):292-301. doi: 10.1016/j.echo.2013.12.005

6. Jenkins C, Bricknell K, Hanekom L, Marwick TH. Reproducibility and accuracy of echocardiographic measurements of left ventricular parameters using real-time three-dimensional echocardiography. J Am Coll Cardiol. 2004;44(4):878-86. doi: 10.1016/j.jacc.2004.05.050

7. Kühl HP, Schreckenberg M, Rulands D, Katoh M, Schafer W, Schummers G, et al. High-resolution transthoracic real-time three-dimensional echocardiography: quantitation of cardiac volumes and function using semi-automatic border detection and comparison with cardiac magnetic resonance imaging. J Am Coll Cardiol. 2004;43(11):2083-90. doi: 10.1016/j.jacc.2004.01.037

8. Caiani EG, Corsi C, Zamorano J, Sugeng L, MacEneaney P, Weinert L, et al. Improved semi-automated quantification of left ventricular volumes and ejection fraction using 3-dimensional echocardiography with a full matrix-array transducer: comparison with magnetic resonance imaging. J Am Soc Echocardiogr. 2005;18:779-88.

9. Mor-Avi V, Jenkins C, Kuhl HP, Nesser HJ, Marwick T, Franke A, et al. Real-time 3-dimensional echocardiographic quantification of left ventricular volumes: multicenter study for validation with magnetic resonance imaging and investigation of sources of error. JACC Cardiovasc Imaging. 2008;1(4):413-23. doi: 10.1016/j.jcmg.2008.02.009

10. Lang RM, Badano LP, Tsang W, Adams DH, Agricola E, Buck T, Faletra FF, Franke A, Hung J, de Isla LP, Kamp O, Kasprzak JD, Lancellotti P, Marwick TH, McCulloch ML, Monaghan MJ, Nihoyannopoulos P, Pandian NG, Pellikka PA, Pepi M, Roberson DA, Shernan SK, Shirali GS, Sugeng L, Ten Cate FJ, Vannan MA, Zamorano JL, Zoghbi WA; American Society of Echocardiography; European Association of Echocardiography. EAE/ASE recommendations for image acquisition and display using threedimensional echocardiography. J Am Soc Echocardiogr. 2012;25(1):3-46. doi: 10.1016/j.echo.2011.11.010

11. Lang RM, Badano LP, Mor-Avi V, Afilalo J, Armstrong A, Ernande L, et al. Recommendations for cardiac chamber quantification by echocardiography in adults: an update from the American Society of Echocardiography and the European Association of Cardiovascular

Imaging. J Am Soc Echocardiogr. 2015;28(1):1-39.e14. doi: 10.1016/j.echo.2014.10.003

12. Pepi M, Tamborini G, Pontone G, Andreini D, Berna G, De Vita S, et al. Initial experience with a new on-line transthoracic three-dimensional technique: assessment of feasibility and of diagnostic potential. Ital Heart J. 2003;4(8):544-50.

13. Soliman OI, Krenning BJ, Geleijnse ML, Nemes A, van Geuns RJ, Baks T, et al. A comparison between QLAB and TomTec full volume reconstruction for real time three-dimensional echocardiographic quantification of left ventricular volumes. Echocardiography. 2007;24(9):967-74.

14. Tsang W, Kenny C, Adhya S, Kapetanakis S, Weinert L, Lang RM, et al. Interinstitutional measurements of left ventricular volumes, speckle tracking strain, and dyssynchrony using three-dimensional echocardiography. J Am Soc Echocardiogr 2013;26(11):1253-7. doi: 10.1016/j.echo.2013.07.023

15. Muraru D, Badano LP, Piccoli G, Gianfagna P, Del Mestre L, Ermacora D, et al. Validation of a novel automated border-detection algorithm for rapid and accurate quantitation of left ventricular volumes based on threedimensional echocardiography. Eur J Echocardiogr. 2010;11(4):359-68. doi: 10.1093/ejechocard/jep217

16. Thavendiranathan P, Liu S, Verhaert D, Calleja A, Nitinunu A, Van Houten T, et al. Feasibility, accuracy, and reproducibility of real-time full-volume 3D transthoracic echocardiography to measure LV volumes and systolic function a fully automated endocardial contouring algorithm in sinus rhythm and atrial fibrillation. J Am Coll Cardiol Img. 2012;5(3):239-51. doi: 10.1016/j.jcmg.2011.12.012

17. Shibayama K, Watanabe H, Iguchi N, Sasaki S, Mahara K, Umemura J, et al. Evaluation of automated measurement of left ventricular volume by novel real-time 3-dimensional echocardiographic system: validation with cardiac magnetic resonance imaging and 2-dimensional echocardiography. J Cardiol. 2013;61(4):281-8. doi: 10.1016/j.jjcc.2012.11.005

18. Zhang QB, Sun JP, Gao RF, Lee AP, Feng YL, Liu XR, et al. Feasibility of single-beat full-volume capture real-time three-dimensional echocardiography for quantification of right ventricular volume: validation by cardiac magnetic resonance imaging. Int J Cardiol. 2013;168(4):3991-5. doi: 10.1016/j.ijcard.2013.06.088

19. Tsang W, Salgo IS, Medvedofsky D, Takeuchi M, Prater D, Weinert L, et al. Transthoracic 3D echocardiographic left heart chamber quantification using an automated adaptive analytics algorithm. J Am Coll Cardiol Img. 2016;9(7):769-82. doi: 10.1016/j.jcmg.2015.12.020

20. Otani K, Nakazono A, Salgo IS, Lang RM, Takeuchi M. Three-dimensional echocardiographic assessment of left heart chamber size and function with fully automated quantification software in patients with atrial fibrillation. J Am Soc Echocardiogr. 2016;29(10):955-65. doi: 10.1016/j.echo.2016.06.010

21. Medvedofsky D, Mor-Avi V, Amzulescu M, Fernández-Golfín C, Hinojar R, Monaghan MJ, et al. Three-dimensional echocardiographic quantification of the left-heart chambers using an automated adaptive analytics algorithm: multicentre validation study. Eur Heart J Cardiovasc Imaging. 2018;19(1):47-58. doi: 10.1093/ehjci/jew328

22. Tamborini G, Piazzese C, Lang RM, Muratori M, Chiorino E, Mapelli M. Feasibility and accuracy of automated software for transthoracic three-dimensional left ventricular volume and function analysis: comparisons with two-dimensional echocardiography, three-dimensional transthoracic manual method, and cardiac magnetic resonance imaging. J Am Soc Echocardiogr. 2017;30(11):1049-58. doi: 10.1016/j.echo.2017.06.026

23. Bland JM, Altman DG. Statistical method for assessing agreement between two methods of clinical measurement. Lancet. 1986;1(8476):307-10.

24. Knackstedt C, Bekkers SC, Schummers G, Schreckenberg M, Muraru D, Badano LP, et al. Fully automated versus standard tracking of left ventricular ejection fraction and longitudinal strain the FAST-EFs multicenter study. J Am Coll Cardiol. 2015 Sep 29;66(13):1456-66. doi: 10.1016/j.jacc.2015.07.052

Longitudinal Strain and Ischemic Stroke in the Absence of Known Heart Disease

Strain Longitudinal e Acidente Vascular Encefálico Isquêmico na Ausência de Cardiopatia Conhecida

Jeova Cordeiro de Morais Junior[1,2]; Nayane Carolina Pertile Salvioni[1], Dannyl Roosevelt de Vasconcelos Lima[1]; Crissvânia Firmino Confessor[1]; Alexsandro Paulo Costa Galdino Junior[1]; Lara Sodré Cardoso[1]; Antônio Marconi Leandro da Silva[1]; Joao Lima[4]; Anderson da Costa Armstrong[1]; Luis Claudio Lemos Correia[2,3]

[1]Federal University of São Francisco Valley, Petrolina, Pernambuco Brazil; [2]Bahian School of Medicine and Public Health, Salvador, Bahia, Brazil; [3]São Rafael Hospital, Salvador, Bahia, Brazil; [4]Johns Hopkins Hospital, Baltimore, MD, USA.

Abstract

Background: Stroke is prevalent worldwide, and early recognition of subclinical cardiovascular (CV) disease could predict a first ischemic stroke (IS) episode. Speckle-tracking echocardiography (STE) allows the detection of early subclinical myocardial dysfunction.

Aim: To examine the association between myocardial deformation, evaluated by STE, and first episode of IS in a sample of otherwise healthy patients.

Methods: We included individuals between 40–80 years old, with a first incidence of IS, with no known CV disease, matched to healthy controls by sex, age, and hypertension at a 1:2 ratio. STE was used to assess LV global longitudinal strain (GLS), and traditional echocardiography was performed. Univariate and multivariable analyses were performed to assess the relationship among stroke, CV risk factors, and echocardiography-derived parameters.

Results: A total of 29 cases and 62 controls were included. The mean age of the patients was 60 ± 12 y/o, and 54% were males. Smoking was more prevalent in cases compared to controls (34% vs. 9%; p = 0.001), and there were no significant differences in the other examined risk factors. Cases had less myocardial deformation compared to controls (GLS: -16.7% ± 3.4% vs. -19.2 ± 2.8%; p < 0.001), and there was no significant difference regarding traditional echocardiography parameters. After adjusting for smoking and hyperlipidemia, GLS maintained an independent association with stroke (OR = 1.3; 95% CI, 1.1–1.6; p = 0.005). The area under the ROC curve for stroke significantly increased after adding GLS to smoking (0.65 to 0.78, p = 0.009).

Conclusion: GLS has a consistent and independent association with a first IS episode in middle-aged adults with generally normal hearts. Therefore, GLS may be a useful risk marker in this population.

Keywords: Stroke; Cardiovascular Disease; Echocardiography.

Resumo

Fundamento: *O acidente vascular encefálico (AVE) é prevalente no mundo. Reconhecimento precoce da doença cardiovascular subclínica pode predizer um primeiro episódio de AVE isquêmico; o speckle tracking associado à ecocardiografia (STE) permite detecção precoce da disfunção miocárdica subclínica.*

Objetivo: *Provar a associação entre deformação miocárdica avaliada pelo STE e primeiro episódio de AVE em indivíduos saudáveis.*

Método: *Incluímos participantes entre 40-80 anos com primeiro episódio de AVE isquêmico sem cardiopatia conhecida, pareados por sexo, idade e hipertensão com grupo controle saudável na proporção 1:2. STE avaliou strain longitudinal (SL) do VE, e ecocardiografia tradicional foi realizada. Análises univariada e multivariada avaliaram as relações do AVE com fatores de risco cardiovasculares e parâmetros derivados da ecocardiografia.*

Resultado: *29 casos e 62 controles foram incluídos. Média etária foi 60 ± 12 anos; 54% eram homens. Tabagismo foi mais prevalente em casos do que em controles (34% vs. 9%; p=0.001). Nenhum outro fator de risco evidenciou diferença estatística. Casos tiveram menor deformação*

Mailing Address: Nayane Carolina Pertile Salvioni •
Rua Desembargador Eliseu Guilherme, 147, 3° subsolo, Paraíso. CEP: 04004-030, São Paulo, SP, Brazil.
E-mail: nayanepertile@gmail.com
Manuscript received 1/14/2020; revised 3/23/2020; accepted 7/9/2020

DOI: 10.47593/2675-312X/20203304eabc101

miocárdica comparados aos controles (SL -16.7 ± 3.4% vs. -19.2 ± 2.8%; p < 0.001). Não houve diferença em relação aos parâmetros ecocardiográficos tradicionais. Após ajuste para tabagismo e hiperlipidemia, SL manteve-se independentemente associado com AVE (OR=1.3; 95% CI, 1.1 – 1.6; p=0.005). A área abaixo à curva ROC para AVE aumentou significativamente após adicionar SL ao tabagismo (0.65 para 0.78, respectivamente; p=0.009).

Conclusão: *SL tem independente associação com o primeiro episódio de AVE isquêmico em adultos de média idade com corações geralmente normais. SL pode ser potencial marcador de risco nesta população.*

Palavras-chave: *Acidente Vascular Cerebral; Doenças Cardiovasculares; Ecocardiografia.*

Introduction

Stroke is the leading cause of disability worldwide,[1] affecting approximately 15 million people per year.[2] The impact of stroke-related disability is a major health concern, particularly in the aging population.[3,4] Although the risk for cerebrovascular disease is well established among the elderly, the increase in stroke incidence among younger adults is a growing concern.[5] In fact, it is unclear how to prevent a first stroke event in a previously healthy young adult population.

Therefore, early recognition of subclinical cardiovascular (CV) disease that could predict a first episode of ischemic stroke is of major clinical importance, especially in patients who appear to have no significant risk. Speckle tracking echocardiography (STE) allows for accurate detection of early subclinical myocardial dysfunction, beyond traditional echocardiography-derived parameters.[6] Indeed, STE has been validated in several clinical settings as a useful tool for assessing CV events.[7–9] However, how subclinical cardiac abnormalities might relate to incidents of cerebrovascular disease is less well understood.

In the current study, we explore the hypothesis that the reduction of the STE-derived LV global longitudinal strain (GLS) (as early subclinical cardiac dysfunction) is associated with the first episode of stroke in a sample of otherwise healthy patients. To this end, we utilized a comprehensive echocardiography protocol, and compared the sample population to healthy matched controls.

Material and methods

Study design and population

Men and women, 40 to 80 years old, with a first ischemic stroke and no prior known CV disease, were recruited from a single center from January 2015 to September 2016. Ischemic stroke was established following the validated National Institutes Health (NIH) Scale,[10] and confirmed by brain imaging. Individuals were excluded if they had a history of heart failure, coronary artery disease, atrial flutter or atrial fibrillation, abnormalities detected by electrocardiography that suggested structural cardiac change, or structural echocardiographic changes (left ventricular hypertrophy, increased chamber volumes, wall motion abnormality, or moderate/severe valvular dysfunction).

Control participants were healthy individuals, recruited in the proportion of 2:1, preferably relatives of included cases or recruits from the outpatient facility of the same institution. All controls were paired by sex, age, and previous diagnosis of hypertension. We chose to pair for hypertension to avoid confusion, as hypertension has been shown to reduce GLS[11] and is also a strong risk factor for cerebrovascular disease.[12]

Finally, cases and controls were excluded if they had poor quality images, when they or their caregivers refused to participate in the study, or when there was an absence of physical and mental conditions necessary to provide consent. Informed consent was obtained for all participants.

Clinical parameters

When self-reported, hypertension was defined if using anti-hypertensive medication, or following two blood pressure measurements of ≥ 140 (systolic blood pressure) or ≥ 90 mmHg (diastolic blood pressure). When self-reported, diabetes mellitus was defined if using hypoglycemic medication, or if two fasting blood glucose levels were ≥ 126 mg%, or if hemoglobin A1c (HbA1c) levels were > 6.5%. Dyslipidemia was defined when there was a self-reported history of hypercholesterolemia, use of lipid-lowering treatment, or total serum cholesterol > 200 mg/dL. Patients who had smoked cigarettes during the last 6 months were defined as current smokers. Body mass index (BMI) was calculated by dividing weight by the square of the height.

Traditional echocardiography protocol

Echocardiography images were acquired using a Vivid S6 scanner (General Electric Health; Jardim, São Paulo, Brazil), 2 to 14 days after the ischemic stroke event, in order to avoid the acute phase. A single reader then blindly analyzed the images.

Traditional echocardiography-derived parameters followed current American Society of Echocardiography (ASE) recommendations.[13,14] Left ventricular end-diastolic diameter, interventricular septum, posterior wall thickness, left atrial diameter, and aortic root diameter were measured from a parasternal long-axis view in two-dimensional images. The LV mass was then calculated and indexed by body surface area. The left ventricular ejection fraction (LVEF) was calculated using the biplane modified Simpson's rule. The left atrial volume (LAV) biplane was calculated with apical four- and two-chamber images, using the area-length method and indexing to the body surface area. The E/e' ratio was calculated from the peak early diastolic velocity of the E wave in the transmitral flow, evaluated by pulsed-wave Doppler imaging, divided by the average between the peak early diastolic velocity of the e' lateral and e' septal waves, and evaluated

by pulsed-wave tissue Doppler imaging. The tricuspid annular plane systolic excursion was obtained in M-mode at the level of the tricuspid annulus in the four-chamber image.

Speckle tracking echocardiography protocol

The STE protocol followed the previously published protocol used for the CARDIA study.[15] Images were acquired in two-dimension mode, in grayscale, in which at least three cycles were recorded at a frame rate of ≥ 50 fps. To analyze myocardial deformation (global longitudinal systolic strain, GLS), we calculated the average negative peak of the longitudinal strain from 12 ventricular segments assessed in the apical four- and two-chamber views. The number of segments excluded in the speckle tracking analysis was very low, with an average of below one segment per participant; significantly, more negative values indicate more myocardial deformation.

A sample of images from 30 participants (1:1 cases and controls) was randomly selected to be re-assessed by the same reader, and by a second reader to evaluate intra- and inter-reader reproducibility. The intra-class correlation coefficient (ICC) was 0.8 ($p < 0.001$) for both intra- and inter-reader assessment. Details of the reproducibility assessment are shown in Figure 1.

Statistical analysis

The clinical and echocardiography-derived parameters were compared for cases and controls using t-test or chi-squared test. All variables that had a p-value below 0.1 in the univariate analyses were included as covariates in the final multivariable logistic regression model (with stroke as a dependent variable). ROC curves of the final logistic regression models were also compared in order to evaluate the discrimination for stroke; initially, only including CV risk factors related to stroke in the univariate analysis, and then also including GLS.[16] Analyses were performed using STATA 14.2 and IBM SPSS Statistics version 18.1.

Results

Of the 330 recruited cases, 104 had previous ischemic stroke, 77 had heart disease, 71 had hemorrhage stroke at the moment of hospital admission, and 43 refused to participate in the study, or were unable to provide information. One case had wall motion abnormality and five had poor image quality. Of the 76 controls who were initially recruited, six refused to participate in the study, one had wall motion abnormality, one had left ventricular hypertrophy, and six had poor quality images. In total, 29 cases and 62 controls were included in the final analysis. Figure 2 details the recruiting process.

The clinical characteristics of the participants are shown in Table 1. Both cases and controls had similar mean ages and sex (predominantly male). There was no significant difference between cases and controls in univariate analysis regarding hypertension, diabetes mellitus, and BMI. Smoking was more prevalent in cases compared to controls (34% vs, 9%, $p = 0.001$), and dyslipidemia had a higher prevalence in cases compared to controls (54% vs. 37%, $p = 0.09$).

Individuals with a first ischemic stroke showed less myocardial deformation (less negative mean GLS) than healthy controls (mean GLS, -16.7% ± 3.4% vs. -19.2% ± 2.8%, respectively; $P < 0.002$), as shown in Figure 3. Cohen's d was used to evaluate the magnitude of the difference, and an index of 0.80 was obtained. However, there was no significant difference in the traditional echocardiography parameters between cases and controls (Table 2).

After adjustment for smoking and hyperlipidemia, GLS maintained an independent association with stroke (OR = 1.3; 95% CI, 1.1–1.6; $p = 0.005$) (Table 3 and Figure 4). There was a significant increase in the area under the ROC curve for stroke compared to the model that only included current smoking (a clinical variable that was associated with stroke) after adding GLS (0.65 vs. 0.78, $p = 0.009$).

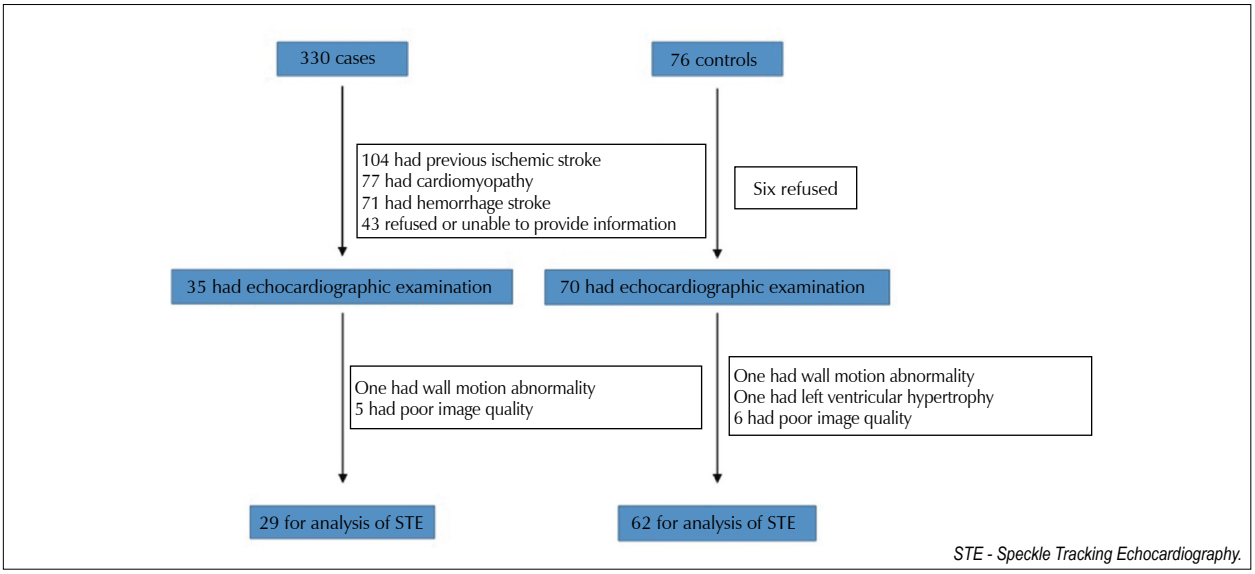

Figure 1 – *Recruitment of cases and controls.*

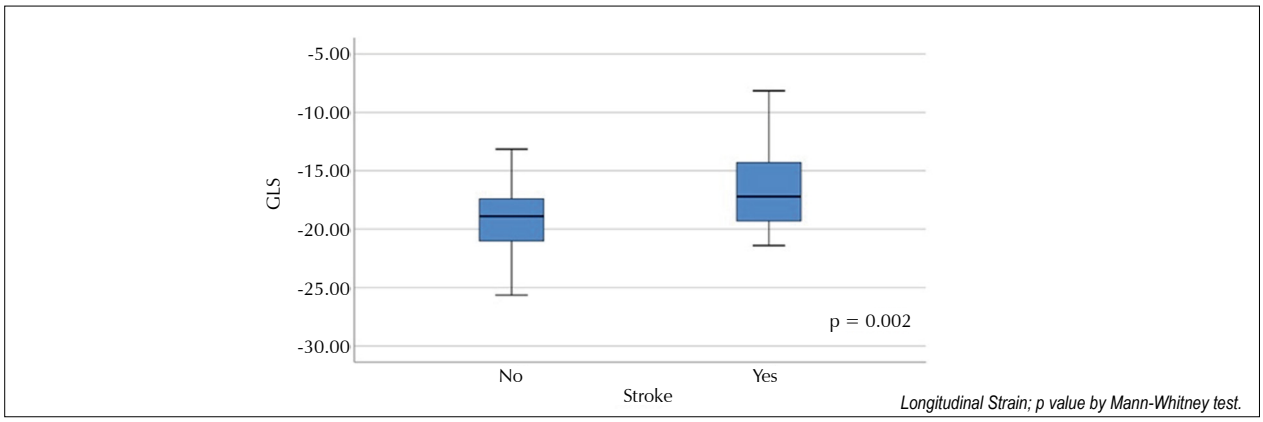

Figure 2 – *Distribuition of global longitudinal strain (GLS) between cases (n=29) and controls (n=62).*

Table 1 - Clinical characteristics for controls and cases.

Variables	Controls (68) Mean (±DP)	Cases (34) Mean (±DP)	P value
Age,years	59 (12)	60 (12)	0.85
Male sex, %	54	54	1.0
Hypertension, %	64	65	0.89
Diabetes Mellitus, %	16	20	0.58
Dyslipidemia, %	37	54	0.09
Current smoking, %	9	34	0.001
BMI, kg/m^2	26.3 (4)	27.2 (5)	0.32

BMI - body-mass index; SD - Standard Deviation.

Discussion

In the current study, we demonstrate that reduced longitudinal myocardial deformation is associated with a first ischemic stroke in individuals with a generally healthy heart, independent of known CV risk factors, and before identifiable changes in traditional echocardiography-derived parameters. For this purpose, we carefully excluded individuals with a history of known CV diseases, as well as those with electrocardiographic and echocardiographic abnormalities. Moreover, we paired the participants for sex, age, and hypertension, all of which may influence myocardial deformation. Our findings show that GLS is associated with a first episode of stroke, and that GLS could help to predict a first episode of ischemic stroke in a low risk population.

There is evidence of increasing stroke rates in young adults,[5] which frequently present as a first CV event. Importantly, stroke is related to high rates of death and disability,[1,2,17] and has a considerable impact on healthcare costs.[18] Therefore, the identification of an early marker for stroke is important, especially in apparently low-risk younger populations. Our population had a mean age of 60 ± 12 years, which was younger than that in other studies assessing stroke and subclinical CV disease. For instance, the Northern Manhattan Study (NOMAS), which demonstrated an association between GLS and silent cerebral ischemia, had an average age of 69 ± 10 years.[19]

The relationship between clinically evident heart failure and stroke is well established.[20,21] However, how subclinical cardiac changes relate to stroke is less clear. LVEF is an important marker in patients with known heart disease, but it was not associated with stroke in our study. In fact, the heart apparently has compensatory deformation mechanisms that allow for a stable LVEF in subclinical phases of cardiac dysfunction.[22,23] STE is more sensitive to early myocardial dysfunction because this new technique analyzes motion-tracking speckles in the ultrasonic image in two dimensions.[24]

We found that GLS could be used as a consistent risk marker for first ischemic stroke in a population free of known CVD. Russo C et al.[19] have shown that brain and cardiac subclinical abnormalities were simultaneously present in the participants of the abovementioned study, while Armstrong et al. demonstrated in the 25-year CARDIA study[25] that reduced GLS was associated with microscopic, macrostructural, and subclinical cerebral perfusion changes. These findings reinforce the hypothesis that brain and cardiac subclinical changes are present at the same time, before clinically manifested CV disease. In our study, the data collection for exposure (GLS) and outcome (stroke) was performed simultaneously. This leads us to the discussion of which comes first, because we know that cerebrovascular impairment may cause subclinical cardiac changes.[26] Therefore, the findings of the NOMAS and CARDIA studies reinforces the hypothesis that GLS is a good subclinical cardiac marker for ischemic stroke and not the cause of event. Some studies have demonstrated an association between abnormalities on electrocardiography with stroke and subclinical cerebrovascular changes.[27,28]

Although GLS showed an independent association with stroke, no association was found for LVEF and the first cerebrovascular event in this middle-aged adult population. In fact, it has been shown that GLS values relate to stroke after myocardial infarction.[29] In addition, GLS was superior to LVEF as a predictor of CV mortality (including stroke) in patients with advanced chronic kidney disease.[30] However, the relationship between myocardial deformation and stroke are still not entirely clear, particularly when considering stroke as the first manifestation of CV disease in generally healthy middle-aged adults.

Other traditional echocardiography-derived parameters

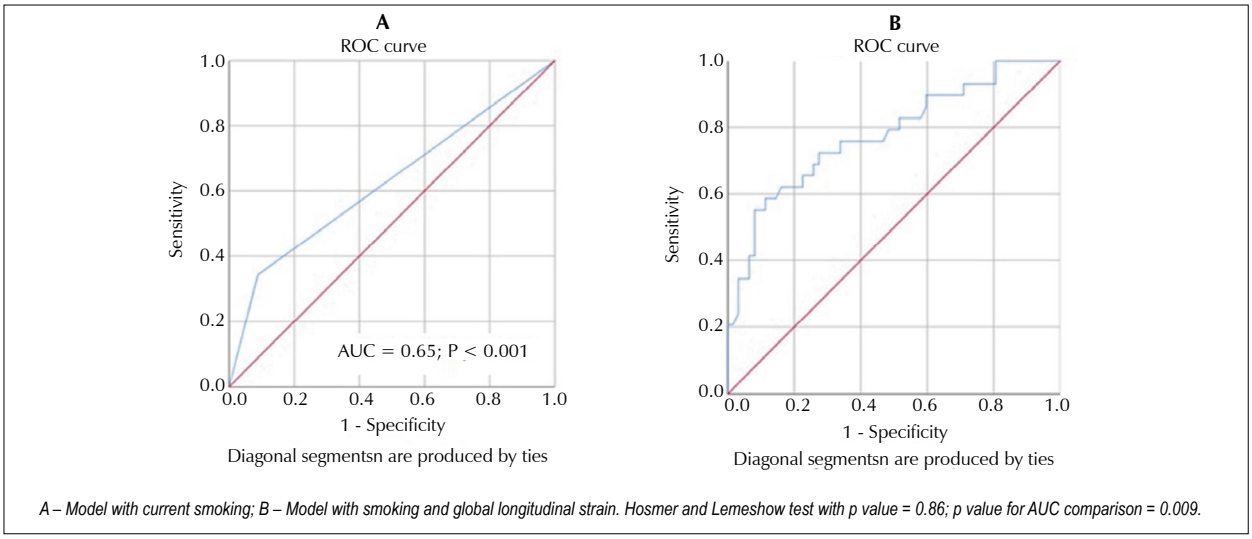

A – Model with current smoking; B – Model with smoking and global longitudinal strain. Hosmer and Lemeshow test with p value = 0.86; p value for AUC comparison = 0.009.

Figure 3 – *ROC curve of final logistic regression models (n=91).*

Table 2 - Description of the traditional echocardiography parameters in controls and cases.

Parameters	Controls (66) Mean (±DP)	Cases (32) Mean (±DP)	P value
LAV, ml/m²	30 (8)	28 (8)	0.21
LV mass, g/m²	78 (18)	84 (23)	0.11
E/e' ratio	7.1 (2.3)	6.7 (1.9)	0.37
LVEF, %	63 (6)	61 (7)	0.11
LVDD, mm	47 (4)	47 (4)	0.86
LAD, mm	34 (3)	34 (4)	0.41
Ao root, mm	33 (3)	33 (4)	0.82
TAPSE	34 (3)	34 (4)	0.11

LAV - left atrial volume indexed by BSA; LV mass - left ventricular mass indexed by BSA; E - Pulse-waved Doppler-derived peak diastolic velocity in transmitral inflow; é - tissue Doppler imaging-derived peak diastolic velocity (average for lateral and septal assessments); LVEF - left ventricular ejection fraction; LVDD - left ventricular diastolic diameter; LAD - left atrial diameter; Ao - aortic; TAPSE - tricuspid annular plane systolic excursion; BSA - body surface area.

Table 3 - Multivariable logistic regression models (n = 91).

Variables	Model 1 OR (CI 95%)	Model 2 OR (CI 95%)	P value
Age	1.0 (0.97 - 1.04)		
Male sex	1.0 (0.44 - 2.26)		
Hypertension	1.1 (0.48 - 2.62)		
Diabetes Mellitus	1.5 (0.50 - 4.21)		
Dyslipidemia	2.04 (0.98 - 4.67)	1.66 (0.58 - 4.64)	0.34
Current smoking	5.39 (1.81 - 16)	7.13 (1.88 - 26.9)	0.004
BMI	1.05 (0.96 - 1.16)		
GLS	1.35 (1.13 - 1.61)	1.31 (1.10 - 1.57)	0.005

BMI - body-mass index; GLS - global longitudinal strain; OR - Odds Ratio. Model 1 - univariate analysis; Model 2 - multivariate analysis.

had no significant association with stroke in our study. The relations between LV mass, LA size, and aortic root with CV risk factors and events among middle-aged adults is well known.[31, 32] In our study, we aimed to address the risk in otherwise healthy patients, therefore excluding participants with ECG and major echocardiography abnormalities. This strict patient selection, in addition to controls matched by hypertension, age, and sex, probably attenuated the relations between stroke and these traditional echocardiography-derived parameters. Based on our findings, GLS may have a higher magnitude impact when assessing risk for patients who would be classified as having a normal heart based on traditional echocardiography.

Smoking was also an independent predictor of stroke in our study, after controlling for age, sex, and hypertension. In fact, smoking is a known strong risk factor for stroke,[33, 34] and has also been shown to be associated with cryptogenic stroke in patients of similar ages.[35] However, we did not assess the predictive value of CV risk factors for stroke, as the controls were matched for hypertension, age, and sex. It is known that smoking relates to inflammatory and pro-thrombotic states,[36] which may present a higher impact in otherwise healthy younger patients.

This study has several limitations. First, self-referred information was used to address risk factors, which may have been subject to errors. Second, we followed the CARDIA speckle tracking protocol, which is a validated protocol tested in a substantial number of patients, but did not include three-chamber views for strain analysis. Third, and importantly, we did not include participants with known CV events, abnormal EKG findings, nor abnormal traditional echocardiography-derived parameters. Therefore, it is unlikely that the average GLS would suffer significant changes when adding three-chamber data in this sample of participants with generally normal hearts.

In patients without previous cardiac disease, we showed that myocardial dysfunction, as assessed by decreases in longitudinal deformation, is a promising marker of the first episode of stroke. However, longitudinal studies are needed

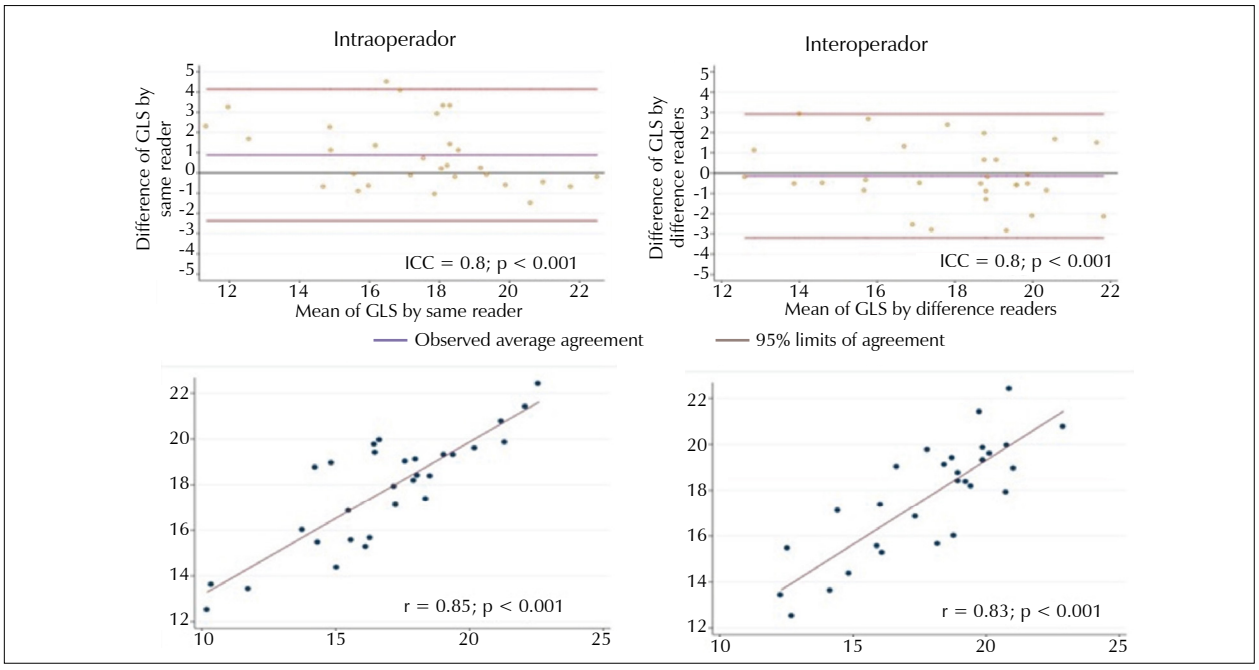

Figure 4 – *Intra and inter-reader evaluation of reproducibility.*

to further address this predictive potential. The ability to assess the early risk of stroke may aid policy planning to reduce the burden of this disease, particularly among younger patients.

Conclusion

GLS has a consistent and independent association with a first episode of ischemic stroke in middle-aged adults with generally normal hearts, after controlling for age, sex, and hypertension. Longitudinal deformation may be a potential risk marker in people without obvious cardiac structure or functional abnormalities.

Acknowledgments

Dr. Morais Jr. was funded by UNIVASF.

Authors' contributions

Research creation and design:: Armstrong AC; Morais Júnior JC; Data acquisition: Morais Júnior JC; Salvioni NCP; Cardoso LS; Confessor CF; Silva AML; Lima DRV; Galdino Júnior APC; Data analysis and interpretation: Morais Júnior JC; Salvioni NCP; Cardoso LS; Armstrong AC; Statistical analysis: Armstrong AC; Writing: Morais Júnior JC; Critical revision for important intellectual content: Lima DRV; Silva AML; Lima J; Armstrong AC; Correia LCL

Conflict of interest

The authors have declared that they have no conflict of interest.

References

1. Zhang Y, Chapman AM, Plested M, Jackson D, Purroy F. The Incidence, Prevalence, and Mortality of Stroke in France, Germany, Italy, Spain, the UK, and the US: A Literature Review. Stroke Res Treat.. 2012;2012:436125. doi: 10.1155/2012/436125.
2. Berzina G, Paanalahti M, Lundgren-Nilsson A, Sunnerhagen KS. Exploration of some personal factors with the International Classification of Functioning, Disability and Health core sets for stroke. J Rehabil Med. 2013 Jul;45(7):609-15. doi: 10.2340/16501977-1171..
3. Abete P, Della-Morte D, Gargiulo G, Basile C, Langellotto A, Galizia G, et al. Cognitive impairment and cardiovascular diseases in the elderly. A heart-brain continuum hypothesis. Ageing Res Rev. 2014 Nov;18:41-52. doi: 10.1016/j.arr.2014.07.003.
4. Lo Coco D, Lopez G, Corrao S. Cognitive impairment and stroke in elderly patients. Vasc Health Risk Manag. 2016;12:105-16. doi: 10.2147/VHRM.S75306.
5. Bejot Y, Bailly H, Durier J, Giroud M. Epidemiology of stroke in Europe and trends for the 21st century. Presse medicale. 2016;45(12 Pt 2):e391-e98. doi: 10.1016/j.lpm.2016.10.003.6. Geyer H, Caracciolo G, Abe H, Wilansky S, Carerj S, Gentile F, et al. Assessment of myocardial mechanics using speckle tracking echocardiography: fundamentals and clinical applications. J Am Soc Echocardiogr 2010;23(4):351-69; quiz 453-5. doi: 10.1016/j.echo.2010.02.015.
7. Joyce E, Hoogslag GE, Leong DP, Debonnaire P, Katsanos S, Boden H, et al. Association between left ventricular global longitudinal strain and adverse left ventricular dilatation after ST-segment-elevation myocardial infarction. Circulation Cardiovascular imaging. 2014;7(1):74-81. doi: 10.1161/CIRCIMAGING.113.000982.
8. Cong T, Sun Y, Shang Z, Wang K1, Su D1, Zhong L, et al. Prognostic Value of Speckle Tracking Echocardiography in Patients with ST-Elevation Myocardial Infarction Treated with Late Percutaneous Intervention. Echocardiography. 2015;32(9):1384-91. doi: 10.1111/echo.12864.
9. Lacalzada J, de la Rosa A, Izquierdo MM, Jiménez JJ, Iribarren JL, García-González MJ, et al. Left ventricular global longitudinal systolic strain predicts adverse remodeling and subsequent cardiac events in patients with acute myocardial infarction treated with primary percutaneous coronary intervention. The international journal of cardiovascular imaging 2015;31(3):575-84 Int J

Cardiovasc Imaging. 2015;31(3):575-84. doi: 10.1007/s10554-015-0593-2.

10. Meyer BC, Lyden PD. The modified National Institutes of Health Stroke Scale: its time has come. Int J Stroke. 2009 Aug;4(4):267-73. doi: 10.1111/j.1747-4949.2009.00294.x.

11. Galderisi M, Lomoriello VS, Santoro A, Esposito R, Olibet M, Raia R, et al. Differences of myocardial systolic deformation and correlates of diastolic function in competitive rowers and young hypertensives: a speckle-tracking echocardiography study. J Am Soc Echocardiogr. 2010 Nov;23(11):1190-8. doi: 10.1016/j.echo.2010.07.010..

12. Kjeldsen SE, Narkiewicz K, Burnier M, Oparil S. The INTERSTROKE Study: hypertension is by far the most important modifiable risk factor for stroke. Blood Press. 2017 Jun;26(3):131-2. doi: 10.1080/08037051.2017.1292456.

13. Lang RM, Badano LP, Mor-Avi V, Afilalo J, Armstrong A, Ernande L, et al. Recommendations for cardiac chamber quantification by echocardiography in adults: an update from the American Society of Echocardiography and the European Association of Cardiovascular Imaging. J Am Soc Echocardiogr. 2015;28(1):1-39.e14. doi: 10.1016/j.echo.2014.10.003.

14. Nagueh SF, Smiseth OA, Appleton CP, Byrd BF 3rd, Dokainish H, Edvardsen T, et al. Recommendations for the Evaluation of Left Ventricular Diastolic Function by Echocardiography: An Update from the American Society of Echocardiography and the European Association of Cardiovascular.Eur Heart J Cardiovasc Imaging. 2016 Dec;17(12):1321-1360. doi: 10.1093/ehjci/jew082.

15. Armstrong AC, Ricketts EP, Cox C, Adler P, Arynchyn A, Liu K, et al. Quality Control and Reproducibility in M-Mode, Two-Dimensional, and Speckle Tracking Echocardiography Acquisition and Analysis: The CARDIA Study, Year 25 Examination Experience. Echocardiography.2015;32(8):1233-40. doi: 10.1111/echo.12832.

16. Cleves MA. From the help desk : Comparing areas under receiver operating characteristic curves from two or more probit or logit models. The Stata Journal 2002;2(3):301-13.

17. Saposnik G, Del Brutto OH. Stroke in South America: a systematic review of incidence, prevalence, and stroke subtypes. Stroke. 2003;34(9):2103-7. doi: 10.1161/01.STR.0000088063.74250.DB.

18. Ovbiagele B, Goldstein LB, Higashida RT, Howard VJ, Johnston SC, Khavjou OA, et al. Forecasting the future of stroke in the United States: a policy statement from the American Heart Association and American Stroke Association. Stroke 2013;44(8):2361-75. doi: 10.1161/STR.0b013e31829734f2.

19. Russo C, Jin Z, Homma S, Elkind MS, Rundek T, Yoshita M, et al. Subclinical left ventricular dysfunction and silent cerebrovascular disease: the Cardiovascular Abnormalities and Brain Lesions (CABL) study. Circulation 2013;128(10):1105-11. doi: 10.1161/CIRCULATIONAHA.113.001984.

20. Alberts VP, Bos MJ, Koudstaal P, Hofman A, Witteman JC, Stricker B, et al. Heart failure and the risk of stroke: the Rotterdam Study. Eur J Epidemiol. 2010 Nov;25(11):807-12. doi: 10.1007/s10654-010-9520-y.

21. Cuadrado-Godia E, Ois A, Roquer J. Heart failure in acute ischemic stroke. Curr Cardiol Rev. 2010 Aug; 6(3): 202–213. doi: 0.2174/157340310791658776.

22. Kerkhof PL, Yasha Kresh J, Li JK, Heyndrickx GR. Left ventricular volume regulation in heart failure with preserved ejection fraction. Physiol Rep. 2013;1(2):e0007. doi: 10.1002/phy2.7..

23. Holst JM, Kilker BA, Wright S, Hoffmann B. Heart failure with preserved ejection fraction: echocardiographic VALVE protocol for emergency physicians. Eur J Emerg Med. 2014 Dec;21(6):394-402. doi: 10.1097/MEJ.0000000000000093.

24. Perk G, Tunick PA, Kronzon I. Non-Doppler two-dimensional strain imaging by echocardiography--from technical considerations to clinical applications. J Am Soc Echocardiogr. 2007 Mar;20(3):234-43. doi: 10.1016/j.echo.2006.08.023.

25. Armstrong AC, Muller M, Ambale-Ventakesh B, Halstead M, Kishi S, Bryan N, et al. Association of early left ventricular dysfunction with advanced magnetic resonance white matter and gray matter brain measures: The CARDIA study. Echocardiography. 2017. 34(11): 17–1622. doi: 10.1111/echo.13695

26. Cuisinier A, Maufrais C, Payen JF, nottin S, Walther G, Bouzat P. Myocardial function at the early phase of traumatic brain injury: a prospective controlled study. Scand J Trauma Resusc Emerg Med. 2016;24(1):129. doi. org/10.1186/s13049-016-0323-3

27. Kamel H, Soliman EZ, Heckbert SR, Kronmal RA, Longstreth WT Jr, Nazarian S, et al. P-wave morphology and the risk of incident ischemic stroke in the Multi-Ethnic Study of Atherosclerosis. Stroke. 2014;45(9):2786-8. doi: 10.1161/STROKEAHA.114.006364.

28. Kamel H, Bartz TM, Longstreth WT, Jr., Okin PM, Thacker EL, Patton KK, et al. Association between left atrial abnormality on ECG and vascular brain injury on MRI in the Cardiovascular Health Study. Stroke. 2015;46(3):711-6. doi: 10.1161/STROKEAHA.114.007762.29. Olsen FJ, Pedersen S, Jensen JS, Biering-Sørensen T. Global longitudinal strain predicts incident atrial fibrillation and stroke occurrence after acute myocardial infarction. Medicine (Baltimore). 2016 Nov;95(44):e5338. doi: 10.1097/MD.0000000000005338.30. Krishnasamy R, Isbel NM, Hawley CM, Pascoe EM, Burrage M, Leano R, et al. Left Ventricular Global Longitudinal Strain (GLS) Is a Superior Predictor of All-Cause and Cardiovascular Mortality When Compared to Ejection Fraction in Advanced Chronic Kidney Disease. PloS one 2015;10(5):e0127044. doi: 10.1371/journal.pone.0127044.

31. Armstrong AC, Jacobs DR, Jr., Gidding SS, Colangelo LA, Gjesdal O, Lewis CE, et al. Framingham score and LV mass predict events in young adults: CARDIA study. Int J Cardiol. 2014 Mar 15;172(2):350-5. doi: 10.1016/j.ijcard.2014.01.003.

32. Armstrong AC, Liu K, Lewis CE, Sidney S, Colangelo LA, Kishi S, et al. Left atrial dimension and traditional cardiovascular risk factors predict 20-year clinical cardiovascular events in young healthy adults: the CARDIA study. Eur Heart J Cardiovasc Imaging. 2014 Aug;15(8):893-9. doi: 10.1093/ehjci/jeu018.

33. O'Donnell MJ, Chin SL, Rangarajan S, Xavier D, Liu L, Zhang H, et al. Global and regional effects of potentially modifiable risk factors associated with acute stroke in 32 countries (INTERSTROKE): a case-control study. Lancet. 2016;388(10046):761-75. doi: 10.1016/S0140-6736(16)30506-2.

34. Wang W, Jiang B, Sun H, Ru X, Sun D, Wang L, et al. Prevalence, Incidence, and Mortality of Stroke in China: Results from a Nationwide Population-Based Survey of 480 687 Adults. Circulation. 2017;135(8):759-71. doi: 10.1161/CIRCULATIONAHA.116.025250.

35. Leong DP, Joyce E, Debonnaire P, Katsanos S, Holman ER, Schalij MJ, et al. Left Atrial Dysfunction in the Pathogenesis of Cryptogenic Stroke: Novel Insights from Speckle-Tracking Echocardiography. J Am Soc Echocardiogr. 2017 Jan;30(1):71-79.e1. doi: 10.1016/j.echo.2016.09.013.

36. Arboix A. Cardiovascular risk factors for acute stroke: Risk profiles in the different subtypes of ischemic stroke. World J Clin Cases. 2015 May 16;3(5):418-29. doi: 10.12998/wjcc.v3.i5.418.

Analysis of the Safety and Feasibility of Dobutamine Stress Echocardiography in Ten Thousand and Six Tests of a General Population

Análise da Segurança e Exequibilidade do Ecocardiograma sob Estresse com Dobutamina em Dez Mil e Seis Exames de uma População Geral

José Sebastião de Abreu[1,2], Tereza Cristina Diógenes Pinheiro[1,2], Marília Esther Benevides de Abreu[1,2], Ana Gardenia Liberato Ponte Farias[2,3], Marcia Maria Carneiro[2,3]

[1]Clinicárdio Diagnostic Methods, Fortaleza, CE; [2]Cardioexata of Fortaleza, CE; [3]Clinical Hospital, Federal University of Ceará, CE, Brazil.

Abstract

Background: Adverse effects and inconclusive results may occur on dobutamine stress echocardiography.

Objective: To assess the safety and feasibility of dobutamine stress echocardiography in a large general population.

Methods: A total of 10,006 dobutamine stress echocardiographies were performed between July 1996 and September 2007. Dobutamine was administered in four stages (10, 20, 30, and 40 μcg·kg^{-1}·min^{-1}) to research myocardial ischemia starting with 5 μcg·kg^{-1}·min^{-1} to analyze myocardial viability. Atropine was started according to the protocols used in the period. Clinical, hemodynamic, and adverse effect data associated with dobutamine stress echocardiography findings were verified.

Results: Typical angina (8.9%), hypertensive peak (1.7%), isolated ventricular ectopias (31%), supraventricular tachyarrhythmia (1.89%), atrial fibrillation (0.76%), and non-sustained ventricular tachycardia (0.6%) occurred during dobutamine stress echocardiography. The adverse effects occurred more frequently in patients with positive dobutamine stress echocardiography findings for ischemia than in those with negative findings. Paradoxical sinus deceleration (0.16%) did not occur in cases of positive dobutamine stress echocardiography findings. Three severe complications occurred in cases that tested positive for ischemia on dobutamine stress echocardiography: two (0.02%) of ventricular fibrillation and one of acute coronary syndrome (0.01%). There were no cases of sustained ventricular tachycardia, cardiac rupture, asystole, or death. Compared to those with complete tests, patients with inconclusive results used less atropine (81.5% versus 49.9%, $p < 0.001$) and more beta-blockers (4.7% versus 19%, $p < 0.001$) and more commonly presented with a hypertensive peak (1.1% versus 14.2%, $p = 0.0001$) or non-sustained ventricular tachycardia (0.5% versus 2.2%, $p < 0.001$).

Conclusion: When properly performed, dobutamine stress echocardiography is safe and has high feasibility.

Keywords: Dobutamine; Side Effects; Echocardiography, Stress.

Resumo

Fundamento: Durante o ecocardiograma sob estresse com dobutamina, podem ocorrer efeitos adversos e exames inconclusivos.

Objetivo: Avaliar em uma grande população geral a segurança e a exequibilidade do ecocardiograma sob estresse com dobutamina.

Métodos: Estudo de 10.006 ecocardiogramas sob estresse com dobutamina realizados no período de julho de 1996 a setembro de 2007. A dobutamina foi administrada em quatro estágios (10, 20, 30 e 40 μcg.kg^{-1}.min^{-1}) para pesquisa de isquemia miocárdica e iniciada com 5 μcg.kg^{-1}.min^{-1} apenas na análise de viabilidade miocárdica. A atropina foi iniciada conforme os protocolos vigentes. Foram verificados dados clínicos, hemodinâmicos e efeitos adversos associados ao ecocardiograma sob estresse com dobutamina.

Resultados: Durante os ecocardiogramas sob estresse com dobutamina, ocorreu angina típica (8,9%), pico hipertensivo (1,7%), ectopias ventriculares isoladas (31%), taquiarritmia supraventricular (1,89%), fibrilação atrial (0,76%) e taquicardia ventricular não sustentada (0,6%). Os efeitos adversos citados foram mais frequentes nos pacientes com ecocardiogramas sob estresse com dobutamina positivos para isquemia. A desaceleração sinusal paradoxal (0,16%) não ocorreu em ecocardiogramas sob estresse com dobutamina positivo. As três complicações graves ocorreram em ecocardiogramas sob estresse com dobutamina positivos para isquemia. Foram dois casos (0,02%) com FV e um caso de síndrome coronariana aguda (0,01%). Não houve caso de taquicardia ventricular sustentada, ruptura cardíaca, assistolia ou óbito. Comparados

Mailing Address: José Sebastião de Abreu •
Rua Dr. José Lourenço, 500, apto. 700 – Meireles – CEP: 60115-280 – Fortaleza, CE, Brazil.
E-mail: jsabreu@cardiol.br; jsabreu10@yahoo.com.br
Manuscript received 5/11/2020; revised 6/15/2020; accepted 6/22/2020

DOI: DOI: 10.47593/2675-312X/20203304eabc110

aos exames concluídos, nos inconclusivos, os pacientes usaram menos atropina (81,5% *versus* 49,9%; p< 0,001) e mais betabloqueador (4,7% *versus* 19%; p< 0,001), apresentando mais pico hipertensivo (1,1% *versus* 14,2%; p = 0,0001) e taquicardia ventricular não sustentada (0,5% *versus* 2,2%; p< 0,001).

Conclusão: O ecocardiograma sob estresse com dobutamina realizado de forma apropriada é seguro e apresenta elevada exequibilidade.

Palavras-chave: Efeitos Colaterais e Reações Adversas Relacionados a Medicamentos; Ecocardiografia sob Estresse; Dobutamina.

Introduction

Dobutamine stress echocardiography (DSE) is an accurate and well-established method of assessing coronary artery disease (CAD). Its wide use led to continuously improving safety of this important methodology in different sex and age groups. Thus, publications showing the adverse effects of DSE resulted in the development of more appropriate examination protocols and, consequently, provided strategies to reduce potential complications.[1-8]

Studies available in the literature describe the use of dobutamine as being more susceptible to being associated with adverse effects and severe complications than the use of exercise or vasodilators as stressors. Thus, the occurrence of death, ventricular rupture, acute myocardial infarction, complex ventricular and supraventricular arrhythmias, among other events, is verified under different expressions.[9-15] However, modifications in examination protocols and the accumulated experience avoid or reduce the occurrence of adverse effects, showing greater safety and feasibility of DSE over time, particularly by analyzing a large population.

Thus, this study aimed to assess DSE safety in a large general population, identify its adverse effects and complications, and verify conditions that affect its feasibility.

Methods

The present retrospective study included patients undergoing DSE whose data on clinical information, adverse effects, and severe complications were prospectively collected between July 1996 and September 2007. The patients were referred by their attending physicians with the diagnostic hypothesis of known or probable CAD. The examination was initiated only after the patients understood the information regarding the purpose of the DSE and its potential adverse effects and complications, and provided verbal consent. Regarding the use of atropine, it was mandatory that the ophthalmologist confirmed the absence of glaucoma contraindicating its use; in patients prone to urinary retention, this drug was avoided. The suspension of beta-blockers was requested within 48–72 hours prior to the examination except in cases in which the attending physician requested therapy maintenance. Following the service routine, all of the necessary conditions for effective cardiopulmonary resuscitation were checked and reviewed regularly.

An Apogee CX 200 and Vingmed System Five was used with a quadruple screen to enable the comparative analysis of the four stages of DSE and visualization of the heart in the parasternal (long- and short-axis) and apical (four- and two-chamber) views.

Blood pressure (BP) was measured at the beginning of each stage and at the end of the test. Electrocardiographic monitoring was continuous, and 12-lead electrocardiography was performed before and during the procedure.

Dobutamine was administered in a peripheral vein in four stages at increasing doses of 10, 20, 30, and 40 μcg·kg^{-1}·min^{-1} at three-minute intervals. The DSE was considered complete when at least 85% of the maximum heart rate (HR) was reached (220 minus age in years) and/or myocardial ischemia was determined through the occurrence of a contractile abnormality in a previously normal myocardium or the worsening of a pre-existing abnormality.

In cases referred for a myocardial viability assessment, only the presence of viable muscle was investigated as evidenced by increased or impaired contractility at rest. The initial dose of dobutamine was 5 μcg·kg^{-1}·min^{-1}, with increases at increments of 2.5 or 5 μcg·kg^{-1}·min^{-1}, and the final dose reaching up to 20 μcg·kg^{-1}·min^{-1}, if necessary, to complete the examination but without the use of atropine.

Following the initial and current DSE protocol, atropine was initiated at the end of the fourth stage, while the dobutamine infusion could be extended during the administration of atropine.[16,17] As the protocol progressed, atropine was administered during the fourth stage or after half of the third stage depending on the HR achieved or by the examiner's decision.[18,19] Atropine was administered in a bolus of 0.25/0.50 mg/min and reaching the maximum cumulative dose of 2 mg. An infrequent and important situation in which atropine would be administered earlier would be the need to interrupt sinus deceleration in some specific cases.

At the end of the test, 5 to 10 mg of intravenous metoprolol could be administered to control the ischemia and/or HR reduction.[1,3,5,9,16,18-23] As a routine service, after the DSE, the patient waited in the attached room for at least 20 minutes regardless of the test results.

Adverse effects and complications

Chest pain, when present, was defined as typical or atypical angina. The hypertensive peak was identified when the BP reached or exceeded 230/120 mmHg, while hypotension was identified when the systolic BP decreased to less than 100 mmHg. Arrhythmias were classified as supraventricular tachyarrhythmia (SVTA), atrial fibrillation (AF), sustained ventricular tachycardia (SVT) lasting > 30 seconds, non-sustained ventricular tachycardia (NSVT), and ventricular fibrillation (VF). The possible occurrence of paradoxical sinus deceleration, acute coronary syndrome, acute myocardial infarction, ventricular rupture, asystole, or death was also investigated. Even if not complete, DSE was stopped in cases of adverse effects that identified intolerance to the examination or were life-threatening.

Statistical analysis

Continuous variables are expressed as mean ± standard deviation, while categorical variables are expressed as absolute frequency and percentage. The descriptive analysis of data by group was performed using contingency and descriptive measure tables. The association between groups and categorized variables was analyzed using Fisher's exact test. The normality of the distribution of quantitative variables by group was evaluated using the Shapiro-Wilk test. Levene's test was used to analyze group homogeneity in relation to variance. Student's *t*-test was used to analyze group homogeneity in relation to the normal distribution of quantitative variables, while the non-parametric Mann-Whitney *U* test was used for non-normally distributed variables. The analyses were performed using Statistical Package for Social Science software version 20.0 (SPSS Inc., Chicago, IL, USA). Values of $p < 0.05$ were considered statistically significant in all analyses.

Results

A total of 10,006 DSE procedures performed between July 1996 and September 2007 were analyzed, including negative tests for myocardial ischemia (79.68%), positive tests for myocardial ischemia (14.41%), myocardial viability tests (1.19%), and inconclusive tests (4.78%). However, of the 478 inconclusive DSE procedures, 27 were excluded from the statistical analysis due to inadequate image quality during the test without any adverse effects.

Table 1 presents the clinical data, which showed a predominance of female patients (56.7%), a 52.4% incidence of hypertension, a 43% incidence of dyslipidemia, a 16% incidence of diabetes, and a 18.9% incidence of known CAD. Of the 2,153 patients using beta-blockers, 25% did not follow the recommendation to discontinue the drug.

The fourth stage of the DSE protocol was reached in 86% of the tests, with the use of atropine in 80% and the registration of the maximum HR for age in 38.3% of the cases. The adverse effects occurring during DSE included chest pain including typical angina (8.9%), hypertensive peak (1.7%), paradoxical sinus deceleration (0.16%), isolated ventricular ectopias (31%), SVTA (1.89%), AF (0.76%), NSVT (0.6%), acute coronary syndrome (0.01%), and VF (0.02%). There were no cases of SVT, Takotsubo cardiomyopathy, ventricular rupture, asystole, or death.

Analysis of the association between clinical variables at rest and the test results (positive or negative) revealed a greater association with male, older, hypertensive, and diabetic patients with known CAD in whom beta-blockers were used or suspended and who had a positive DSE result for myocardial ischemia (Table 2).

Table 2 - Analysis of the association between variables and positive or negative stress echocardiography results for myocardial ischemia.

Variable	Positive n (%)	Negative n (%)	P value
Sex			
Male	803 (55.7)	3,234 (40.6)	< 0.001
Female	638 (44.3)	4,734 (59.4)	< 0.001
Age, years			
≤ 65	860 (59.7)	5,112 (64.2)	0.001
> 65	581 (40.3)	2,856 (35.8)	0.001
Arterial hypertension	842 (58.4)	4,129 (51.8)	< 0.001
Dyslipidemia	710 (49.3)	3,400 (42.7)	< 0.001
Diabetes mellitus	349 (24.2)	1,183 (14.8)	< 0.001
Coronary artery disease	580 (40.2)	1,177 (14.8)	< 0.001
Beta-blocker			
Used	105 (7.3)	333 (4.2)	< 0.001
Suspended	306 (21.2)	1,234 (15.5)	< 0.001
Reached DSE stage 4	1,269 (88.1)	6,871 (86.2)	0.065
Used atropine	1,138 (79.0)	6,626 (83.2)	< 0.001
Reached HRmax during DSE	591 (41.0)	3,242 (40.7)	0.816
Typical angina	543 (37.7)	330 (4.1)	< 0.001
Hypertensive peak	36 (2.5)	67 (0.8)	< 0.001
Paradoxical sinus deceleration	0	14 (0.2)	0.148
Isolated ventricular ectopias	495 (34.4)	2,478 (31.1)	0.016
Supraventricular tachyarrhythmia	38 (2.6)	144 (1.8)	0.047
Atrial fibrillation	18 (1.2)	58 (0.7)	0.048
Non-sustained ventricular tachycardia	27 (1.9)	23 (0.3)	< 0.001

DSE, dobutamine stress echocardiography; HR, heart rate; HRmax, maximum HR.

Table 1 - Descriptive analysis of clinical data from stress echocardiography.

Variable	Negative for ischemia n (%)	Positive for ischemia n (%)	Myocardial viability n (%)	Inconclusive n (%)
Sex				
Male	3,234 (40.6)	803 (55.7)	82 (68.9)	216 (45.2)
Female	4,734 (59.4)	638 (44.3)	37 (31.1)	262 (54.8)
Arterial hypertension	4,129 (51.8)	842 (58.4)	29 (24.4)	242 (50.6)
Dyslipidemia	3,400 (42.7)	710 (49.3)	21 (17.6)	177 (37.0)
Diabetes mellitus	1,183 (14.8)	349 (24.2)	10 (8.4)	65 (13.6)
Smoking	539 (6.8)	105 (7.3)	3 (2.5)	33 (6.9)
Coronary artery disease	1,177 (14.8)	580 (40.2)	46 (38.7)	84 (17.6)
Beta-blocker				
Used	333 (4.2)	105 (7.3)	8 (6.7)	87 (18.2)
Suspended	1,234 (15.5)	306 (21.2)	5 (4.2)	75 (15.7)
Unused	6,401 (80.3)	1,030 (71.5)	106 (89.1)	316 (66.1)

The analysis of the association between variables occurring during stress and test results (positive or negative) also showed no intergroup difference in reaching the fourth stage of the protocol (reached in more than 86% of cases) or in maximum or submaximal HR during DSE. A positive DSE result for ischemia showed a stronger association with the occurrence of typical angina, hypertensive peak, SVTA, AF, and NSVT. Paradoxical sinus deceleration occurred only in patients with negative DSE findings, although atropine was more commonly used in this group (Table 2).

The comparative evaluation of DSE results in terms of clinical and hemodynamic variables showed that the patients who tested positive for ischemia were older, used less atropine, and had higher systolic BP at rest and under stress. On the other hand, patients with negative results for ischemia showed higher HR both at rest and under stress (Table 3). There was no intergroup difference in diastolic BP at rest or under stress.

The DSE stratification by results considering the comparison between the sexes and the distribution of the variables showed that women were older than men, used less atropine, and had a higher HR at rest despite positive or negative DSE results for ischemia. Women had a higher systolic BP, but only in negative tests for ischemia and at rest.

During stress, HR and diastolic BP were higher in male patients, but only in those who tested negative DSE for ischemia. However, systolic BP during stress was higher in male patients despite positive or negative DSE results. The other hemodynamic comparisons did not differ between the sexes despite positive or negative DSE results for ischemia (Table 4).

The comparison between complete and incomplete DSE results showed no intergroup differences in mean age (61 ± 11.7 versus 60 ± 11.9 years, p = 0.23). Inconclusive tests presented a lower occurrence of patients reporting chest pain, reaching the fourth stage, or using atropine in addition to having a lower incidence of isolated ventricular ectopias. However, inconclusive tests showed a higher percentage of patients using beta-blockers, with hypertensive peaks, and with NSVT (Table 5).

Table 3 - Comparison of stress echocardiogram negative or positive results for ischemia depending on the distribution of clinical and hemodynamic variables.

Variable	n	Mean	SD	Median	P value
Age, years					
Negative	7,968	60.603	11.874	61.0	< 0.001
Positive	1,441	62.353	10.767	63.0	
Atropine dose, mg					
Negative	6,502	O.67	0.34	0.5	0.003
Positive	1,097	0.63	0.25	0.50	
HR at rest, bpm					
Negative	7,968	76.591	13.415	75.0	< 0.001
Positive	1,441	74.056	12.907	72.0	
HR during DSE, bpm					
Negative	7,968	150.335	13.234	151.0	< 0.001
Positive	1,441	145.175	18.281	148.0	
SBP at rest, mmHg					
Negative	7,968	134.687	18.842	140.0	<0.001
Positive	1,441	136.998	20.223	140.0	
SBP during DSE, mmHg					
Negative	7,968	150.249	24.321	150.0	< 0.0001
Positive	1,441	153.380	26.942	150.0	

DSE, dobutamine stress echocardiography; HR, heart rate; SBP, systolic blood pressure; SD, standard deviation.

Table 4 - Stratification of stress echocardiography negative or positive results for ischemia: Comparison of sexes by distribution of variables.

Variable	Sex	n	Mean	SD	Median	P value
Age, years						
Positive	Male	803	61.740	10.866	62.0	0.017
	Female	638	63.125	10.598	63.0	
Negative	Male	3,234	59.235	12.506	59.0	< 0.001
	Female	4,734	61.538	11.328	61.0	
Atropine dose, mg						
Positive	Male	617	0.68	0.38	0.50	< 0.001
	Female	480	0.57	0.31	0.50	
Negative	Male	2,777	0.79	0.42	0.75	< 0.001
	Female	3,725	0.59	0.33	0.50	
HR at rest, bpm						
Positive	Male	803	73.269	12.705	72.0	0.012
	Female	638	75.045	13.100	74.0	
Negative	Male	3,234	74.401	12.674	73.0	< 0.001
	Female	4,734	78.087	13.700	77.0	
HR during DSE, bpm						
Negative	Male	3,234	151.711	13.256	153.0	< 0.001
	Female	4,734	149.395	13.138	150.0	
SBP at rest, mmHg						
Negative	Male	3,234	133.578	17.857	130.0	< 0.001
	Female	4,734	135.445	19.452	140.0	
SBP during DSE, mmHg						
Positive	Male	803	155.181	28.206	160.0	0.020
	Female	638	151.113	25.100	150.0	
Negative	Male	3,234	153.789	25.286	150.0	< 0.001
	Female	4,734	147.830	23.336	140.0	
SBP during DSE, mmHg						
Negative	Male	3,234	76.670	11.786	80.0	< 0.001
	Female	4,734	75.514	10.598	80.0	

DBP, diastolic blood pressure; DSE, dobutamine stress echocardiography; HR, heart rate; SBP, systolic blood pressure.

Table 5 - Comparison of complete and inconclusive stress echocardiography results.

Variable	Complete n (%)	Inconclusive n (%)	P value
Total	9,550 (100)	451 (100)	-
Dyslipidemia	4,135 (43.3)	165 (36.6)	0.005
Beta-blocker usage	446 (4.7)	86 (19.1)	< 0.001
Reached the fourth stage of DSE	8,189 (85.7)	356 (78.9)	< 0.001
Used atropine	7,785 (81.5)	225 (49.9)	< 0.001
Hypertensive peak	104 (1.1)	64 (14.2)	0.0001
Absent chest pain	7,838 (82.1)	423 (93.8)	< 0.001
Isolated ventricular ectopias	3,002 (31.4)	119 (26.4)	0.026
Non-sustained ventricular tachycardia	51 (0.5)	10 (2.2)	< 0.001

*DSE, dobutamine stress echocardiography; *No difference in mean age (61 ± 11.7 versus 60 ± 11.9 years, p = 0.23).*

Discussion

This study included a general population of 10,006 individuals who were subjected to DSE procedures, and analyzed several aspects related to clinical data resulting from dobutamine and atropine action. The adequacy of the different protocols used according to observations reported in the literature resulted in excellent feasibility to conclude the tests in this study associated with the use of atropine in 80% of the DSE procedures since some studies reported a variation of 32–41%, with inconclusive results occurring in 9–17% of procedures.[1,3,9,17]

The occurrence of conclusive DSE has varied over the years among the studied populations, examination protocols, and technological development of echocardiography equipment with the second harmonic multifrequency transducers and the use of microbubble contrast, among other factors, that may influence their accuracy and feasibility. The 27 cases with an inadequate echocardiography window for analysis in this study could probably have been better visualized.[24,25]

In this study, the association between positive DSE findings for myocardial ischemia and male sex, CAD risk factors, and a history of CAD was quite evident and within expectations. There was no difference between positive and negative results for ischemia in the proportion of cases in which the fourth stage of the test or target HR (maximum or submaximal) was reached; however, the patients with ischemia required less atropine, which could be compatible with the fact that the objective of the test had already been fulfilled.

Considering the diagnosis of myocardial ischemia using the contractile abnormality criterion, 14.41% of cases had positive DSE findings. This percentage may vary in the literature according to the sample characteristics, and some authors verified a progressively decreased percentage of positive DSE findings.[26]

Typical pain was more frequently present in positive cases and was unquestionably related to the ischemic contractile abnormality. However, in cases in which the contractile abnormality was less expressed, bias for the positive diagnosis of ischemia may have been created. The occurrence of typical angina in positive cases may have been favored by the CAD itself as well as by suspending the use of beta-blockers, a condition that may also have caused, in this group, a higher incidence of hypertensive peak, which occurred in a low percentage of patients than that reported in previous studies.[27,28]

The paradoxical deceleration of the sinus rhythm may be secondary to the ischemic or mechanical process; however, in the population studied here, it did not occur in a case with positive DSE findings for ischemia. This information suggests that these episodes must have resulted from mechanical stimulation of the left ventricular posterior wall and/or from an arterial baroreceptor compatible with Bezold-Jarisch syndrome.[29-31]

Ventricular ectopias not presenting to be paired are common during DSE but are not relevant in this condition. A positive DSE for ischemia and the presence of associated comorbidities would infer the greater occurrence of SVTA, AF, and NSVT. However, the incidence of adverse effects was within the range of results published in other studies. This study detected a 1.89% incidence of SVTA, while the studies by Mathias et al.[22] and Elhendy et al.[3] reported rates of 1% and 4%, respectively. The 0.76% incidence of AF during DSE in this present study was lower than the 0.86% incidence of AF observed in the meta-analysis by Mansecal et al.[32] NSVT occurred in 0.6% of the DSE procedures performed in this present study, whereas De Sutter et al.[14], evaluating 1,685 patients, reported the occurrence of 3.3% NSVT but did not provide information on the dose or percentage of patients using atropine, a condition that could have influenced this result.

The most severe adverse effects occurred only in patients with a positive DSE result for ischemia. The two cases of VF were resolved and later revascularized, subsequently progressing without sequelae. There was a case of acute coronary syndrome characterized by strong typical angina, contractile abnormality, and inferior wall ST-segment elevation without arrhythmia or hemodynamic disorders. After the ischemia improved with beta-blockers and coronary vasodilators, the patient was referred for a hemodynamic study. Coronary angiography showed significant right coronary stenosis, and full reperfusion was promptly achieved after angioplasty without complications. There were no serious complications such as SVT, Takotsubo cardiomyopathy, asystole, ventricular rupture, or death.

The comparison of the DSE results by distribution of clinical, hemodynamic, and sex variables showed that a lower percentage of women needed atropine in addition to concluding the test with a lower cumulative dose regardless of positive and negative DSE results for ischemia, which could be explained by the fact that women have a higher HR at rest. Another justification would be the lower body surface area of women, but this variable was not analyzed in this study. These characteristics in female patients have been reported previously.[17,19]

Systolic BP at rest and under stress conditions was higher in cases of positive DSE results for ischemia, a finding that is compatible with the higher incidence of hypertension in this group. As for sex, males presented higher systolic BP both at rest and under stress. Diastolic BP differed between the sexes only in cases of negative DSE results for ischemia and was also higher in males. The other hemodynamic comparisons showed no difference between the sexes regardless of positive or negative DSE results for ischemia.

When associated with dobutamine, atropine causes cardiovascular response changes due to increased inotropic and chronotropic effects and cardiac work.[33,34] Abram et al.[35] analyzed 2,968 cases of negative DSE results for ischemia to verify the typical pressure response in patients without known cardiovascular disease. During dobutamine administration, systolic BP increased, and diastolic BP decreased according to sex and age, that is, in males and in younger patients. These pressure changes became even more significant when atropine was administered during DSE. This atropine effect occurred in both men and women and was more evident in younger people. These data show how complex it is to analyze the simultaneous effects of dobutamine and atropine on cardiovascular dynamics.

The occurrence of 4.78% inconclusive examinations in this study was low compared to those of other publications, with neither age nor a positive result for myocardial ischemia

being causal factors. A lower proportion of inconclusive tests reached the fourth stage of the protocol concomitantly to the low use of atropine, with greater occurrence of adverse effects such as hypertensive peak and NSVT. Better BP control before the test using adequate beta-blocker replacement may reduce the most frequent limiting adverse effects to achieve more complete DSE procedures. NSVT is a more difficult problem to solve, but fortunately, it presents low risk when not progressing to SVT.

The present study did not aim to register minor manifestations such as a feeling of palpitations, heart acceleration, or nausea, for example, as these are tolerable and present no risk, which was explained to the patient before the test to assure them of the immediate reversibility of discomfort should it occur. No specific statistical analysis was performed of patients referred to verify the viability due to the absence of a relevant adverse effect in this group.

The use of atropine during DSE as proposed by McNeil et al.[20] showed increased sensitivity without losing specificity in the diagnosis of myocardial ischemia. Ling et al.[16] analyzed a large sample and confirmed these findings, particularly for vessel damage and in patients treated with beta-blockers, making the association with atropine after the fourth stage routine in this diagnostic methodology without increasing the adverse effects. However, Santiago et al.[36] showed no difference in sensitivity, specificity, or positive predictive value with a mean dobutamine infusion of 30 and 40 μcg·kg^{-1}·min^{-1}. In this context, Dyle et al.[37] evaluated dobutamine pharmacokinetics and reported sufficient serum levels of the drug at the dose of 30 μcg·kg^{-1}·min^{-1} and concluded that atropine could be started in inadequate inotropic responses with dobutamine at doses of up to 20 μcg·kg^{-1}·min^{-1}.

The study by Tsutsui et al.[28] demonstrated the advantages of starting atropine after the second stage since it maintained its accuracy using less dobutamine and with shorter test duration, a decreased occurrence of minor adverse effects, and more diagnostic tests than the conventional protocol. However, consensus on a definitive protocol is still lacking since recent guidelines recommend the use of atropine in the third and fourth stages but with different total cumulative doses of 2 mg and 1.2 mg, respectively.[7,8]

One of the important objectives of stress echocardiography is to reduce the occurrence of adverse effects, especially severe complications. Varga et al.[15] conducted the largest review in the echocardiographic context that included 85,997 patients. However, it is important to note that the authors received data even from centers with experience performing only 20 tests, which would increase the possibility of severe complications. On the other hand, the authors found that no severe adverse effect was verified in 25 of the 75 participating centers. The largest study evaluating cardiovascular complications during exercise, published by Stuart and Ellestad[38], included 518,448 stress tests with exercise. These authors reported 8.86 complications considered severe per 10,000 tests. This evaluation included 0.5 deaths, 3.58 acute myocardial infarctions, and 4.78 arrhythmias, considered severe by the authors (requiring venous therapy or cardioversion), per 10,000 tests.

Severe complications can be unpredictable in physical or pharmacological stress conditions; however, with the more frequent and early use of atropine in DSE, the patient's exposure to the adverse effects of dobutamine decreases, favoring the use of DSE.

Limitations

Although this study was a retrospective analysis, the data were prospectively collected. The exact transition period for the DSE protocols was not determined. Hemodynamic studies were not analyzed to assess DSE accuracy at diagnosing significant CAD; however, this was not the objective of this study. Another limitation of our study is its single-center design. As suggested by Armstrong et al.,[39] multicentric publications or meta-analyses would be more compatible and representative of the real world. However, this study was rigorous regarding its safety aspects and the progression of protocols essential for this excellent methodology.

Conclusion

When properly performed, DSE is safe and has high feasibility.

Acknowledgment

The authors thank Dr. José Nogueira Paes Júnior for his valuable support for this research project and Secretary Juliana Moura Rocha, who organized and updated our database since its inception.

Authors' contributions

Research creation and design: Abreu JS. Data acquisition: Abreu JS, Pinheiro TCD, Farias AGLP. Data analysis and interpretation: Abreu JS, Pinheiro TCD, Abreu MEB. Statist ical an a lysis: Abreu JS. Manuscript writing: Abreu JS, Abreu MEB, Carneiro MM. Critical revision of the manuscript for important intellectual content: Abreu JS, Farias AGLP, Carneiro MM.

Conflict of interest

The authors have declared that they have no conflict of interest.

References

1. Poldermans D, Fioretti PM, Boersma E, Forster T, van Urk H, Cornel JH, et al. Safety of dobutamine-atropine stress echocardiography in patients with suspected or proven coronary artery disease. Arch Intern Med. 1994;73(7):456-9. doi: 10.1001/archinte.1994.00420230066008

2. Geleijnse ML, Fioretti PM, Roelandt JR. Methodology, feasibility, safety and diagnostic accuracy of dobutamine stress echocardiography. J Am Coll Cardiol. 1997;30(3):595-606. doi: 10.1016/s0735-1097(97)00206-4

3. Elhendy A, Van Domburg RT, Poldermans D, Bax JJ, Nierop P, Geleijnse M, et al. Safety and feasibility of dobutamine-atropine stress echocardiography for the diagnosis of coronary artery disease in diabetic patients unable to

perform an exercise stress test. Diabetes Care. 1998;21(11):1797-802. doi: 10.2337/diacare.21.11.1797

4. Cortigiani L, Picano E, Coletta C, Chiarella F, Mathias W, Gandolfo N, De Alcantara M, Mazzoni V, Gensini GF, Landi P; Echo Persantine International Cooperative (EPIC) Study Group; Echo Dobutamine International Cooperative (EDIC) Study Group. Safety, feasibility, and prognostic implications of pharmacologic stress echocardiography in 1482 patients evaluated in an ambulatory setting. Am Heart J. 2001;141(4):621-9. doi: 10.1067/mhj.2001.113997

5. Pellikka PA, Nagueh SF, Elhendy AA, Kuehl CA, Sawada SG; American Society of Echocardiography. American Society of Echocardiography recommendations for performance, interpretation, and application of stress echocardiography. J Am Soc Echocardiogr. 2007;20(9):1021-41. doi: 10.1016/j.echo.2007.07.003

6. Pellikka PA, Nagueh SF, Elhendy AA, Kuehl CA, Sawada SG. Recomendações da Sociedade Americana de Ecocardiografia para a realização, interpretação e aplicação da Ecocardiografia de Estresse. Tradução: Marcelo Luiz Campos Vieira, Ana Camarozano, Arnaldo Rabischoffsky, Vera Maria L. Gimenes. Revista Brasileira de Ecocardiografia e Imagem Cardiovascular [Internet]. 2013 [citado 2020 Set 28];26(4):242-26. Disponível em: https://www.asecho.org/wp-content/uploads/2013/05/stress_portuguese1.pdf

7. Steeds RP, Wheeler R, Bhattacharyya S, Reiken J, Nihoyannopoulos P, Senior R, et al. Stress echocardiography in coronary artery disease: a practical guideline from the British Society of Echocardiography. Echo Res Pract. 2019;6(2):G17-33.

8. Pellikka PA, Arruda-Olson A, Chaudhry FA, Chen MH, Marshall JE, Porter TR, et al. Guidelines for Performance, Interpretation, and Application of Stress Echocardiography in Ischemic Heart Disease: From the American Society of Echocardiography. J Am Soc Echocardiogr. 2020;33(1):1-41. e8. doi: 10.1016/j.echo.2019.07.001

9. Mertes H, Sawada SG, Ryan T, Segar DS, Kovacs R, Foltz J, et al. Symptoms, adverse effects, and complications associated with dobutamine stress echocardiography. Experience in 1118 patients. Circulation. 1993;88(1):15-9. doi: 10.1161/01.cir.88.1.15

10. Lanzarini L, Previtali M, Diotallevi P. Syncope caused by cardiac asystole during dobutamine stress echocardiography. Heart. 1996;75(3):320-1. doi: 10.1136/hrt.75.3.320

11. Lewis W, Arena F, Galloway M, Bommer W. Acute myocardial infarction associated with dobutamine stress echocardiography. J Am Soc Echocardiogr. 1997;10(5):576-8. doi: 10.1016/s0894-7317(97)70014-2

12. Orlandini AD, Tuero EI, Diaz R, Vilamajó OA, Paolasso EA. Acute cardiac rupture during dobutamine-atropine echocardiography stress test. J Am Soc Echocardiogr. 2000;13(2):152-3. doi: 10.1016/s0894-7317(00)90028-2

13. João I, Cotrim C, Duarte J, Rosário L, Freire G, Pereira H, et al. Cardiac rupture during exercise stress echocardiography: A case report. J Am Soc Echocardiogra. 2000;13(8):785-7. doi: 10.1067/mje.2000.104960

14. De Sutter J, Poldermans D, Vourvouri E, Van Donburg R, Elhendy A, Bax J, et al. Long-term prognostic significance of complex ventricular arrhythmias induced during dobutamine stress echocardiography. Ame J Cardiol. 2003;91(2):242-4. doi: https://doi.org/10.1016/S0002-9149(02)03118-1

15. Varga A, Garcia MAR, Picano E, Registry ISEC. Safety of stress echocardiography (from the international stress echo complication registry). The American Journal of Cardiology. 2006;98(4):541-3.

16. Ling LH, Pellikka PA, Mahoney DW, Oh JK, McCully RB, Roger VL, et al. Atropine augmentation in dobutamine stress echocardiography: role and incremental value in a clinical practice setting. J Am Coll Cardiol. 1996;28(3):551-7. doi: 10.1016/0735-1097(96)00195-7

17. Secknus MA, Marwick TH. Influence of gender on physiologic response and accuracy of dobutamine echocardiography. Am J Cardiol. 1997;80(6):721-4. doi: 10.1016/s0002-9149(97)00502-x

18. Lessick J, Mutlak D, Rinkevich D, Markiewicz W, Reisner S. Prospective study of early atropine use in dobutamine stress echocardiography. Eur J Echocardiogr. 2000;1(4):257-62. doi: 10.1053/euje.2000.0063

19. Abreu JS, Diógenes TC, Farias AG, Morais JM, Paes Júnior JN. [Safety and feasibility of dobutamine-atropine stress echocardiography in octogenarian patients]. Arq Bras Cardiol. 2005;85(3):198-204. Portuguese. doi: 10.1590/s0066-782x2005001600009

20. McNeill AJ, Fioretti PM, el-Said SM, Salustri A, Forster T, Roelandt JR. Enhanced sensitivity for detection of coronary artery disease by addition of atropine to dobutamine stress echocardiography. Am J Cardiol. 1992 Jul 1;70(1):41-6. doi: 10.1016/0002-9149(92)91387-j

21. Picano E, Mathias WJ, Pingitore A, Bigi R, Previtali M. Safety and tolerability of dobutamine-atropine stress echocardiography: a prospective, multicentre study. Echo Dobutamine International Cooperative Study Group. Lancet. 1994;344(8931):1190-2. doi: 10.1016/s0140-6736(94)90508-8

22. Mathias W, Arruda A, Santos FC, Arruda AL, Mattos E, Osório A, et al. Safety of dobutamine-atropine stress echocardiography: a prospective experience of 4033 consecutive studies. J Am Soc Echocardiogr. 1999;12(10):785-91. doi: 10.1016/s0894-7317(99)70182-3

23. Poldermans D, Fioretti PM, Boersma E, Bax JJ, Thomson IR, Roelandt JR, et al. Long-term prognostic value of dobutamine-atropine stress echocardiography in 1737 patients with known or suspected coronary artery disease: a single-center experience. Circulation. 1999;99(6):757-62. doi: 10.1161/01.cir.99.6.757

24. Sozzi FB, Poldermans D, Bax JJ, Boersma E, Vletter WB, Elhendy A, et al. Second harmonic imaging improves sensitivity of dobutamine stress echocardiography for the diagnosis of coronary artery disease. Am Heart J. 2001;142(1):153-9. doi: 10.1067/mhj.2001.116075

25. Shaikh K, Chang SM, Peterson L, Rosendahl-Garcia K, Quinones MA, Nagueh SF, et al. Safety of contrast administration for endocardial enhancement during stress echocardiography compared with noncontrast stress. Am Heart J. 2008;102(11):1444-50. doi: 10.1016/j.amjcard.2008.07.032

26. Carpeggiani C, Landi P, Michelassi C, Sicari R, Picano E. The declining frequency of inducible myocardial ischemia during stress echocardiography over 27 consecutive years (1983–2009). Int J Cardiol. 2016;224:57-61. doi: 10.1016/j.ijcard.2016.08.313

27. Lee CY, Pellikka PA, Shub C, Sinak L, Seward JB. Hypertensive response during dobutamine stress echocardiography. Am J Cardiol. 1997;80(7):970-1. doi: 10.1016/s0002-9149(97)00561-4

28. Tsutsui JM, Osório AF, Fernandes DR, Sodre G, Andrade JL, Ramires JA, et al. Comparison of safety and efficacy of the early injection of atropine during dobutamine stress echocardiography with the conventional protocol. Am J Cardiol. 2004;94(11):1367-72. doi: 10.1016/j.amjcard.2004.07.141

29. Mark AL. The Bezold-Jarisch reflex revisited: clinical implications of inhibitory reflexes originating in the heart. J Am Coll Cardiol. 1983;1(1):90-102. doi: 10.1016/s0735-1097(83)80014-x

30. Attenhofer CH, Pellikka PA, McCully RB, Roger VL, Seward JB. Paradoxical sinus deceleration during dobutamine stress echocardiography: description and angiographic correlation. J Am Coll Cardiol. 1997;29(5):994-9. doi: 10.1016/s0735-1097(97)00030-2

31. Hung KC, Lin FC, Chern MS, Chang HJ, Hsieh IC, Wu D. Mechanisms and clinical significance of transient atrioventricular block during dobutamine stress echocardiography. J Am Coll Cardiol. 1999;34(4):998-1004. doi: 10.1016/s0735-1097(99)00306-x

32. Mansencal N, Mustafic H, Hauguel-Moreau M, Lannou S, Szymanski C,

Dubourg O. Occurrence of Atrial Fibrillation During Dobutamine Stress Echocardiography. Am J Cardiol. 2019;123(8):1277-82. doi: 10.1016/j.amjcard.2019.01.022

33. Landzberg JS, Parker JD, Gauthier DF, Colucci WS. Effects of intracoronary acetylcholine and atropine on basal and dobutamine-stimulated left ventricular contractility. Circulation. 1994;89(1):164-8. doi: 10.1161/01.cir.89.1.164

34. Camarozano AC, Weitzel LH, Turano MM, Nascimento C, Savedra MM. Avaliação do inotropismo cardíaco ao ecocardiograma de estresse e contraste: comparação do protocolo precoce X protocolo padrão dobutamina-atropina. Rev Bras Ecocardiogr [Internet]. 2004 [citado 2020 Set 28];17:31-46. Disponível em: http://departamentos.cardiol.br/dic/publicacoes/revistadic/revista/2006/Revista03/06-artigoanalise.pdf

35. Abram S, Arruda-Olson AM, Scott CG, Pellikka PA, Nkomo VT, Oh JK, et al. Typical blood pressure response during dobutamine stress echocardiography of patients without known cardiovascular disease who have normal stress echocardiograms. Eur Heart J Cardiovasc Imaging. 2016;17(5):557-63. doi: 10.1093/ehjci/jev165

36. Santiago P, Vacek JL, Rosamond TL. Dobutamine stress echocardiography: clinical utility and predictive value at various infusion rates. Am Heart J. 1994;128(4):804-8. doi: 10.1016/0002-8703(94)90279-8

37. Daly AL, Linares OA, Smith MJ, Starling MR, Supiano MA. Dobutamine pharmacokinetics during dobutamine stress echocardiography. Am J Cardiol. 1997;79(10):1381-6. doi: 10.1016/s0002-9149(97)00144-6

38. Stuart R, Ellestad M. National survey of exercise stress testing facilities. CHEST Journal. 1980;77(1):94-7. doi: 10.1378/chest.77.1.94

39. Armstrong WF. Dobutamine stress echocardiography: single center studies vs. meta-analysis vs. the real world. J Am Soc Echocardiogr. 2009;22(11):1209-11. doi: 10.1016/j.echo.2009.09.018

Inverted Takotsubo Versus Acute Myocarditis: the Importance of Cardiac Resonance for Differential Diagnosis

Takotsubo Invertido Versus Miocardite Aguda: a Importância da Ressonância Cardíaca para Diagnóstico Diferencial

Carina Massariol Belinassi[1,2], Stella de Souza Carneiro[1,2], Débora Pereira Galvêas Negri[1,2], Davi Muzi Rios[2], Murilo Jardim de Carvalho[2], José Augusto Murad[2]

[1]Cassiano Antônio de Moraes University Hospital, Federal University of Espírito Santo, Vitória, ES; [2]Unimed Hospital of Vitória, Vitória, ES, Brazil.

Introduction

Takotsubo syndrome (TS) is a differential diagnosis of chest pain in the emergency similar to acute myocarditis. This is the case report of a patient who presented in the emergency department with chest pain and acute heart failure. Echocardiography findings were suggestive of inverted TS, a variant of TS, and it was impossible to exclude acute myocarditis. Cardiac magnetic resonance (CMR) was essential for the differential diagnosis.

Case report

A 32-year-old female patient born in the state of Espírito Santo was admitted to the emergency room with tight chest pain associated with dyspnea, dizziness, nausea, and vomiting. The patient developed acute pulmonary edema responsive to diuretic therapy and vasoactive drugs and was referred to the coronary intensive care unit. She denied any recent history of fever, respiratory symptoms, diarrhea, stress episodes, smoking, or use of illicit drugs, anorectics, or teas. The patient was vaccinated against influenza. An examination revealed a severe general condition consisting of pale skin, no changed on cardiac auscultation, no jugular turgescence, normotensive status with the use of dobutamine, and tachydyspnea at minimal effort using a 10 L/min reservoir mask. Electrocardiography revealed sinus tachycardia, with T wave inversion in DI and aVL. Laboratory tests presented changed myocardial necrosis markers (troponin at 5.13; reference value, <0.04). Transthoracic echocardiography showed an ejection fraction of 26%, severe global left ventricular (LV) systolic dysfunction with hypercontractility of apical segments, and akinesia of the middle and basal segments of all walls (Video 1). Coronary cineangiography showed no coronary lesions. CMR showed a delayed enhancement sequence with mesocardial distribution in the LV anteroseptal and middle segment compatible with myocarditis (Figure 1). The patient's cardiovascular condition progressed well; however, during the hospitalization, she presented with low back pain, the investigation of which revealed a retroperitoneal mass. Findings of resection of the mass followed by a frozen tissue examination were suggestive of an undifferentiated neoplasia awaiting histopathological and immunohistochemical analyses.

Keywords

Diagnosis; Magnetic Resonance Imaging; Takotsubo Cardiomyopathy.

Mailing Address: Carina Massariol Belinassi •
Hospital Universitário Cassiano Antônio de Moraes. Avenida Marechal Campos, 1.355 – Santa Cecília. CEP: 29043-260. Vitória, ES, Brazil.
E-mail: cahmassariol@gmail.com
Manuscript received 2/12/2020; revised 4/29/2020; accepted 5/4/2020

DOI: 10.47593/2675-312X/20203304eabc93

Discussion

Stress-induced cardiomyopathy, also known as TS, was initially described by Sato et al. in 1990. It is characterized by a transient change in LV contractility with ventricular apical akinesia and compensatory basal hypercontractility in the absence of obstructive coronary disease.[1,2]

Its pathophysiology remains to be elucidated. The possible mechanisms of its development include spasm in multiple coronary arteries, microcirculatory dysfunction, and injury caused by excessive endogenous catecholamines that causes myocardial stunning and microinfarction. This is a reversible cardiopathy related to physical or psychological stress that is predominant in postmenopausal women and often mimics an acute coronary syndrome. However, there is no correspondence between the affected myocardial region and the territory of a single coronary artery, and coronary angiography findings are typically normal or show mild lesions.[1,2]

A TS variant called inverted TS (ITS) has been described with an incidence of 2.2%, with coronary cineangiography findings evidencing the inversion of the contractile pattern.[1-3]

The patient can clinically present with chest pain and changed myocardial necrosis markers. Electrocardiography findings can range from nonspecific changes in ventricular repolarization to ST-segment elevation. Echocardiography shows characteristic changes as already described that can be confirmed on coronary cineangiography. Both TS and ITS have a favorable prognosis, with treatment consisting of supportive measures.

Acute myocarditis, which has an estimated incidence of 0.2–12%, is characterized by the presence of an inflammatory response of the myocardium, often as a result of a primary infectious aggression elsewhere.[4,5] The most frequent aggressor is the infectious agent, which can be secondary to immune system attacks, as in cases of peripartum myocarditis. Some of the most common infectious agents are viruses, especially enteroviruses.[6] The clinical presentation varies from oligosymptomatic cases without ventricular dysfunction to severe cases of fulminant myocarditis with significant impairment of ventricular function and sudden death in young patients with no previous history of coronary disease.[4] The disease in approximately 70% of patients with asymptomatic

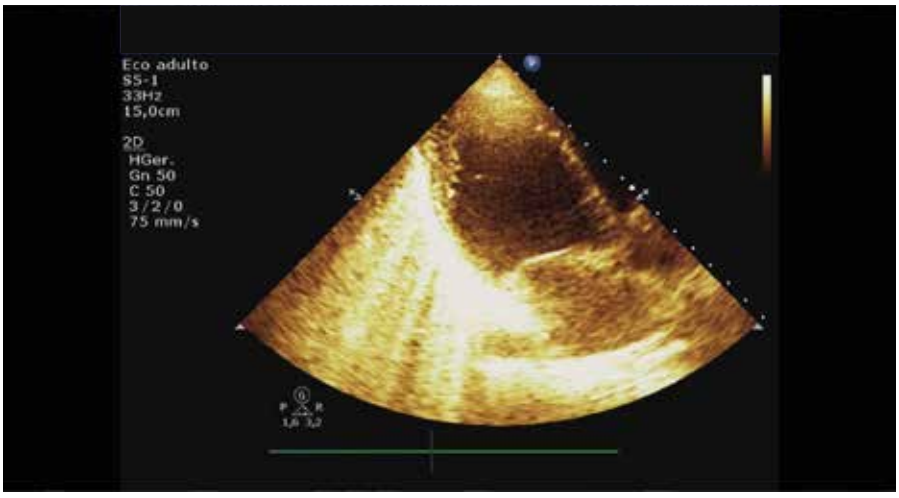

Video 1 – *Echocardiogram showing hypercontractility of apical segments and akinesia of the middle and basal segments of all LV walls.*

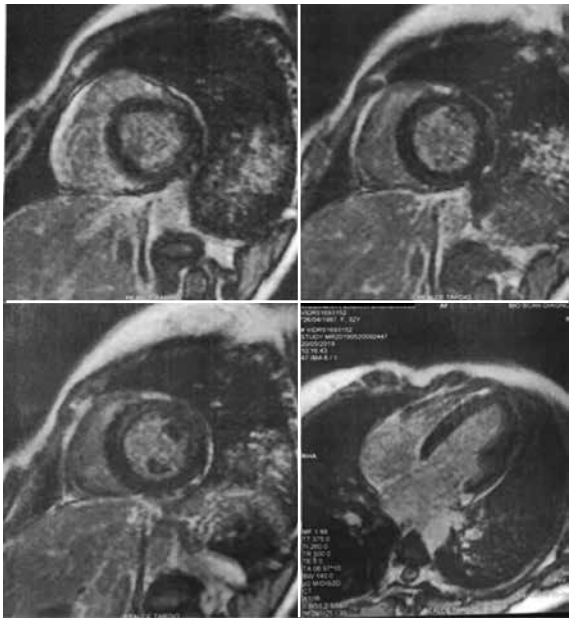

Figure 1 – *Cardiac resonance in the sequence of late enhancement with mesocardial distribution, demonstrated in the middle anter septal segment of the LV.*

ventricular dysfunction progresses with ventricular function recovery. In symptomatic patients, about 25% regress, 50% stabilize, and 25% progressively present with ventricular function worsening.[6]

Myocarditis is initially diagnostically evaluated via clinical suspicion using noninvasive methods. Diagnostic confirmation is only possible by histological analysis through endomyocardial biopsy of the right ventricle.[5] Echocardiography shows contractility changes and plays an important role in the differential diagnosis of myocarditis with other pathologies that have the same clinical presentation such as acute valve diseases, Takotsubo cardiomyopathy, and acute myocardial infarction in addition to being a guide during endomyocardial biopsy.[5] Considering the diverse clinical presentations and non-specificity of laboratory markers, the diagnosis is fundamentally based on a high degree of clinical suspicion and, more recently, on confirmation by CMR,[4,5] a greatly important noninvasive tool for the diagnosis of acute non-ischemic myocardial disorders such as myocarditis and TS.[7-9]

CMR can identify both inflammatory myocardial injuries in the acute and subacute phases and scarring injuries that frequently present in the chronic phase of the disease.[5] In acute myocarditis, T2-weighed images show hyperintense areas in the myocardium as myocyte lesions lead to extracellular and

interstitial edema. There is an overall increase in the rate of early enhancement by gadolinium between the myocardium and skeletal muscle in T1-weighted images and evidence of at least one focal lesion with non-ischemic regional distribution in the inversion recovery (IR) of the signal using the late enhancement technique. The presence of two of these three findings infers the presence of myocarditis. These findings are grouped in the Lake Louise criteria.[8,10]

In TS, CMR is useful both to diagnose and identify possible complications such as LV outflow pathway obstruction, valve disease, pericardial effusion, and LV thrombus.[9] In TS patients, CMR normally shows no IR, suggesting the absence of myocardial ischemic necrosis in addition to the presence of basal segment hyperkinesia suggestive of this syndrome. However, during the acute phase, there may be other contraction patterns such as middle ventricular akinesia and apical preservation as well as baseline akinesia with mid-ventricular and apical preservation.[9]

In short, TS and acute myocarditis are differential diagnoses of chest pain. Laboratory tests, electrocardiography, and echocardiography are nonspecific. Therefore, CMR is extremely important for the differential diagnosis, treatment, and prognosis. This report presented a case of acute myocarditis in which the initial echocardiographic examination suggested a pattern of ITS but CMR showed a myocarditis pattern.

Authors' contributions

Research conception and design: Belinassi CM, Carneiro SS, Negri DPG, Rios DM, Carvalho MJ, and Murad JA.

Conflict of interest

The authors have declared that they have no conflict of interest.

References

1. Macedo LA, Silva FB, Martins AB, Jorge JK, Medeiros P, Barbirato GB, et al. Takotsubo invertido: uma nova forma de apresentação de cardiopatia adrenérgica. Revista SOCERJ. 2008;21(2):114-7.
2. Rodrigues AC, Lira Filho EB, Guimarães LA, Mônaco CG, Cordovil A, Ponchirolli AP, et al. Disfunção ventricular esquerda induzida pelo estresse (Takotsubo-Invertido) em pós-operatório de cirurgia abdominal. Rev Bras Ecocardiogr Imagem Cardiovasc. 2011;24(1):103-16.
3. Nóbrega S, Brito D. The "broken heart syndrome": State of the art. Revista Portuguesa de Cardiologia. 2012;31(9):545-628.
4. Schettino CD, Martelo S, Deus F, Vargas A, Paschoal M, Tassi E, et al. [Clinical and radiological diagnosis of acute myocarditis with an unusual complication]. Revista SOCERJ. 2008;21(5):338-44.
5. Montera MW, Mesquita ET, Colafranceschi AS, Oliveira Junior AM, Rabischoffsky A, Ianni BM, et al. I Diretriz Brasileira de Miocardites e Pericardites. Arq Bras Cardiol. 2013;100(4 supl. 1):1-36.
6. Montera MW. Atualização diagnóstica e terapêutica da miocardite. Revista da Sociedade de Cardiologia do Rio Grande do Sul [Internet]. 2005 [citado 2020 Ago 14];XIII(4). Disponível em: http://sociedades.cardiol.br/sbc-rs/revista/2005/04/artigo12.pdf
7. Friedrich MG, Marcotte F. Cardiac Magnetic Ressonance Assessment of Myocarditis. Circ Cardiovasc Imaging. 2013;6:833-9.
8. Reis RC, Nobeschi L, Shito IT, Fragalle V, Goto RE, Munhoz BN, et al. Diagnóstico de miocardite por ressonância magnética cardíaca: revisão de literatura. Atas de Ciências da Saúde. 2016;4(4):20-30.
9. Bratis K. Cardiac magnetic resonance in Takotsubo Syndrome. ERC Journal [Internet]. 2017 [cited 2020 Aug 14];58-62. Available from: https://www.ncbi.nlm.nih.gov/pmc/articles/PMC6206452/pdf/ecr-12-1-58.pdf
10. Friedrich MG, Sechtem U, Schulz-Menger J, Holmvang G, Alakija P, Cooper LT, et al. Cardiovascular magnetic resonance in myocarditis: A JACC White Paper. J Am Coll Cardiol. 2009;53(17):1475-87.

Giant Coronary Fistula Between Circumflex Artery and Coronary Sinus: Initial Diagnosis by Echocardiography

Fístula Coronária Gigante da Artéria Circunflexa para o Seio Coronariano: Diagnóstico Inicial por Ecocardiografia

Israel Nilton de Almeida Feitosa[1], Maria Rafaela Viana de Sá[2], Jonas Silva Andrade[2], Ana Raquel Avelino Diniz Gonzaga[2]
[1]Department of Echocardiography, Federal University of Campina Grande, Campina Grande, PB; [2]School of Medical Sciences of Campina Grande, Campina Grande, PB, Brazil.

Introduction

Coronary fistula is defined as communication between the termination of a coronary artery (or its branches) and a cardiac chamber, a large vessel, or other vascular structure.[1] The term coronary-cameral fistula refers to communication between a coronary artery and a cardiac chamber.

This entity is responsible for 0.2–0.4% of cardiac anomalies, with a prevalence of approximately 0.7% based on coronary computed tomography angiography. About 20% of patients with coronary fistula have associated congenital heart disease (septal defects, bicuspid aortic valve, aortic coarctation, tetralogy of Fallot, transposition of the great arteries and, more commonly, pulmonary atresia with an intact ventricular septum). It was postulated that the embryological basis for congenital coronary fistulas is the persistence of portions of the embryonic coronary sinusoids that connect the primitive coronary arteries to the cardiac chambers.[2]

Case report

A 34-year-old woman undergoing a perioperative evaluation of the surgical correction of an umbilical hernia reported dyspnea on moderate effort, orthopnea, and tachycardic palpitations occurring at least weekly. She also affirmed that, during her first pregnancy at 16 years of age, she experienced severe dyspnea and that episodes of convulsive crises began in this period.

The patient's blood pressure was normal, and cardiac auscultation revealed a regular heart rhythm in two stages, with evidence of a systolic murmur (+3/+6) that was more clearly audible in the lower left sternal border. General and cardiovascular physical examinations revealed no other findings. Electrocardiography showed an unchanged sinus rhythm.

Two-dimensional transthoracic echocardiography showed dilation of the left chambers, right atrium, and coronary sinus. The trunk of the left coronary artery was dilated (Figure 1) and originated a dilated circumflex artery (Figure 2), with continuous and turbulent flow at the color Doppler, and a fistulous path, which drained into the coronary sinus and, sequentially, into the right atrium (Figures 2 and 3). Her biventricular systolic function was normal.

The patient was sent to a referral cardiology center and underwent coronary computed tomography angiography, which showed a long and dilated left coronary artery trunk and a circumflex artery with a fistulous and dilated path (Figure 4A) draining into the coronary sinus.

Coronary cineangiography showed a long coronary-cameral fistula with large caliber and tortuosity (Figure 4B) and the impression of a path that followed to the coronary sinus and, sequentially, the right atrium.

After a period of clinical follow-up, the patient underwent surgical correction of the fistula. The intraoperative description was of an aneurysmatic circumflex artery (approximately 2 cm in diameter) from its origin with a markedly tortuous path draining into the coronary sinus (referred to as a "great lake"). The intervention was successful and consisted of dissection and triple ligation of the circumflex coronary artery close to its origin. The patient's postoperative clinical progression was satisfactory, and she was discharged 6 days after the procedure.

Discussion

Coronary fistulas are mainly congenital. Acquired causes can be infectious, traumatic, or iatrogenic (percutaneous balloon coronary angioplasty, myocardial revascularization surgery, heart transplantation, permanent pacemaker placement, accessory anomalous bundle ablation, and endomyocardial biopsy). There are also reports of coronary fistulas being associated with myocardial infarction, hypertrophic cardiomyopathy, dilated cardiomyopathy, and tumors.[3]

Coronary fistulas can remain silent for years and be discovered incidentally during noninvasive or invasive procedures. However, patients can become symptomatic with age and/or increasing shunts. Symptoms include dyspnea on effort, fatigue, and angina pectoris; occasional complications can arise such as congestive heart failure, myocardial infarction, pericardial or pleural effusion, cardiac arrhythmias, and rupture of dilated aneurysmatic coronary arteries.[4]

Most statistics show greater involvement of the right coronary artery (60% of cases).[2] Fistulas rarely appear in the circumflex artery. The most common drainage area is the right ventricle, followed by the right atrium, pulmonary artery, and coronary sinus.[5]

Keywords

Diagnosis; Echocardiography; Fistula.

Mailing Address: Israel Nilton de Almeida Feitosa •
Rua José Bonifácio, 67 – Apartamento 1202 - Centro – Campina Grande/PB. CEP 58400-250
E-mail: inafeitosa@hotmail.com
Manuscript received 3/26/2020; revised 3/31/2020; accepted 4/29/2020

DOI: 10.47593/2675-312X/20203304eabc102

Case Report

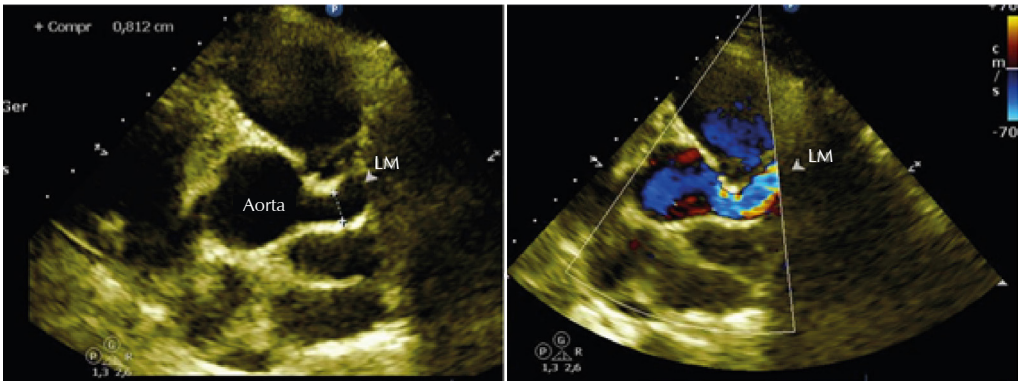

Figure 1 – *Transthoracic echocardiography (short-axis imaging plane at the level of the base vessels). Left coronary artery trunk dilated to two-dimensional and demonstration of turbulent flow on color Doppler.*

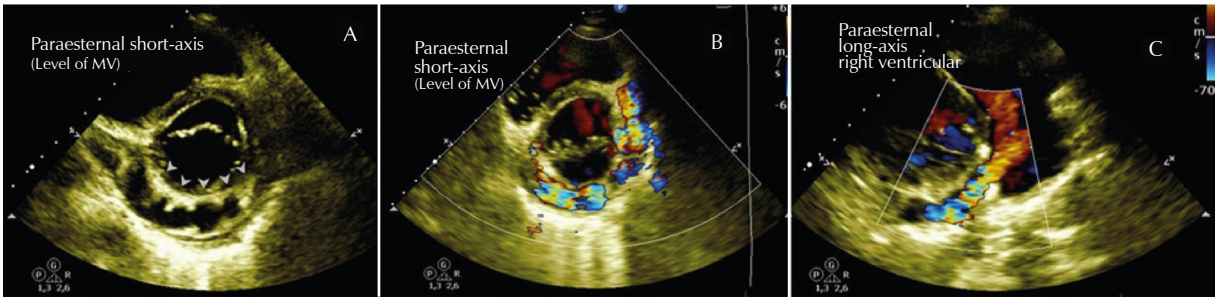

Figure 2 – *(A) and (B) Transthoracic echocardiography (short-axis imaging plane at the level of the mitral valve). Circumflex artery dilated and tortuous to two-dimensional with turbulent flow to color mapping. (C) Parasternal view, longitudinal plane of the right ventricular entry path. Color flow mapping shows drainage of the fistula in the coronary sinus and, sequentially, in the right atrium.*

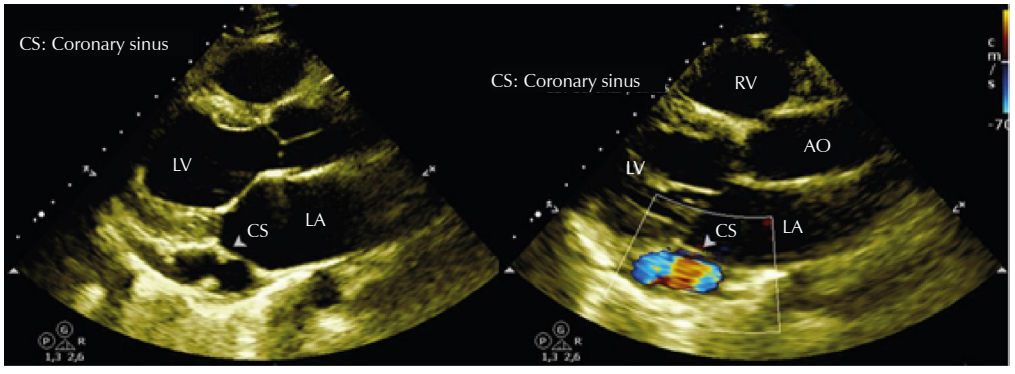

AO, aorta; CS, coronary sinus; LA, left atrium; LV, left ventricle; RV, right ventricle.

Figure 3 – *Transthoracic echocardiography (longitudinal plane of the left ventricle). Two-dimensional image and color flow mapping revealing an enlarged coronary sinus with turbulent flow inside.*

Transthoracic echocardiography, the initial method of investigation for most cardiovascular conditions, is useful in the evaluation and diagnosis of coronary fistula. It is possible to identify a coronary artery or dilated chamber and a variety of congenital or acquired cardiac defects.[6] Drainage can be verified through color flow mapping. The use of microbubbles to increase color Doppler signals can help define fistula location and extent.[7]

Conventional angiography is traditionally the reference exam for making the diagnosis of coronary fistulas and can assist the choice of intervention that may be necessary.

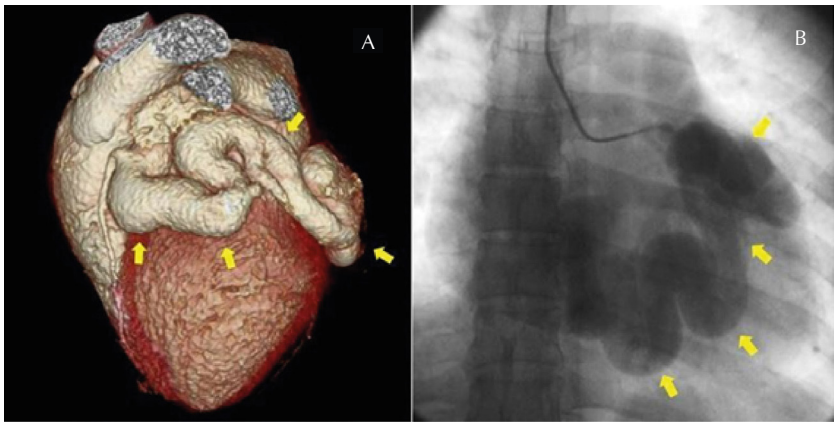

Figure 4 – *Dilated circumflex artery with a tortuous path demonstrated by coronary angiotomography (left) and coronary angiography (right).*

However, it is not the ideal method for documenting the artery's exact three-dimensional course. Also, drainage sites and aneurysms may not be well visualized using conventional angiography due to the significantly diluted contrast medium. Finally, the invasive nature of conventional angiography has a mortality rate of 0.1%.[8]

Despite the use of ionizing radiation, computed tomography coronary angiography is the reference noninvasive exam for viewing the coronary tree. High spatial resolution facilitates the demonstration of coronary anomalies and the presence of coronary artery disease. The procedure can show the origin of the coronary fistula, the drainage site (chamber or vessel), and the proximal and distal coronary anatomy. Coronary arteries as small as fifth-order branches can be visualized. Three-dimensional imaging establishes fistula size and location in any projection without repeated exposure to radiation or an additional contrast load for the patient.

Magnetic resonance imaging has limited ability to analyze coronary fistulas (trigger and movement artifacts, time consumption) and represents a research field that is not widespread in clinical practice. The coronary display is limited to the proximal course, mainly due to its lower spatial resolution and contrast/noise ratio compared with that of angiotomography.[9]

The management of coronary fistulas is based on the presence or absence of cardiovascular symptoms, degree of cardiac volume overload, and presence or absence of myocardial ischemia or ventricular dysfunction. Current recommendations include closing large fistulas regardless of symptoms.

Subsequent adverse events occur more commonly in patients with fistula draining into the coronary sinus regardless of surgical or percutaneous intervention. Even under open surgical inspection, this coronary anomaly can be particularly difficult to close completely due to multiple connections from the distal coronary artery to the coronary sinus and the location of the connection at the posterior base of the heart.[10]

Surgery can be indicated in cases in which percutaneous treatment cannot be performed (high-risk procedure due to the proximity of an adjacent coronary artery, multiple fistula connections, and difficulty accessing the abnormal coronary artery or its branches). It can also be used when there is a coexisting condition that justifies surgical treatment. Options include external ligation of the coronary fistula, an internal patch, or suture closure of the fistulous communication orifice.

Conclusion

Several diagnostic modalities are currently available to visualize coronary artery fistulas, including noninvasive exams that can provide essential information to guide the most appropriate clinical management and surgical planning.

Considering their clinical variables and anatomical and physiological characteristics, the therapeutic approach to coronary fistulas must be individualized.

Authors' contributions

Research conception and design: Feitosa INA; data collection: Feitosa INA; data analysis and interpretation: Feitosa INA; manuscript writing: Feitosa INA, Gonzaga ARAD, Andrade JS, and Sá MRV; critical review of the manuscript for important intellectual content: Feitosa INA; and collection of echocardiographic images: Feitosa INA.

Conflict of interest

The authors have declared that they have no conflict of interest.

References

1. Villa AD, Sammut E, Nair A, Rajani R, Bonamini R, Chiribiri A. Coronary artery anomalies overview: The normal and the abnormal. World J Radiol. 2016;8(6):537-55. doi: 10.4329/wjr.v8.i6.537

2. Lai WW, Mertens LL, Geva T, Cohen MS. Echocardiogrpahy in pediatric and congenital heart disease: from fetus to adult. 2. ed. Wiley, 2016.

3. Mendonça RM, Bandeira RL, Fonseca FJ, Macedo-Filho R. Fístula coronariana para ventrículo esquerdo: diagnóstico por tomografia computadorizada. Arq Bras Cardiol. 2011;97(4):e82-e85.

4. Ata Y, Turk T, Bicer M, Yalcin M, Ata F, Yavuz S. Coronary arteriovenous fistulas in the adults: natural history and management strategies. J Cardiothorac Surg. 2009;4:62. doi: 10.1186/1749-8090-4-62

5. Yeon MH, Choi YR, Lee SY, BAE JW, Hwang KK, Kim DW, et al. A rare combination of the left circumflex coronary artery fistula connecting a dilated coronary sinus with persistent left superior vena cava and multiple arteriovenous fistulae. Korean Circ J. 2013;43(5):356–359. doi: 10.4070/kcj.2013.43.5.356

6. Said SA. Current characteristics of congenital coronary artery fistulas in adults: A decade of global experience. World J Cardiol. 2011;3(8):267-77. doi: 10.4330/wjc.v3.i8.267

7. Zenooz NA, Habibi R, Mammen L, Finn JP, Gilkeson RC. Coronary artery fistulas: CT findings. Radiographics. 2009;29(3):781-9. doi: 10.1148/rg.293085120

8. Zhou K, Kong L, Wang Y, Li S, Song L, Wang Z, et al. Coronary artery fistula in adults: evaluation with dual-source CT coronary angiography. Br J Radiol. 2015;88(1049):20140754. doi: 10.1259/bjr.20140754

9. Forte E, Infante T, Baldi D, Salvatore M, Cademartiri F, Cavaliere C. A case of coronary arterio-venous fistula: the role of cardiac computed tomography. J Thorac Dis. 2018;10(9):E699-E703. doi: 10.21037/jtd.2018.08.69

10. Kiefer TL, Crowley AL, Jaggers J, Harrison JK. Coronary arteriovenous fistulae: the complexity of coronary artery-to-coronary sinus connections. Tex Heart Inst J. 2012;39(2):218-22.

A Young Patient with Chest Pain: Going Beyond the Obvious

Paciente Jovem com Dor Torácica: Além do Óbvio

Sebastian Gallo Bernal[1], Azucena Martínez [1], Juan F Vasquez-Rodriguez [1], Nicolás Isaza[2], Daniel Isaza[1], Camilo A Calixto [1], Claudia Jaimes[1]

[1]Division of Cardiology, Fundacion Cardioinfantil - Instituto de Cardiologia, Bogotá, Colombia. [2]Department of Medicine, Beth Israel Deaconess Medical Center, Harvard Medical School, Boston, MA, USA

Abstract

We describe the case of a young patient with a history of pulmonary embolism and a first-trimester spontaneous abortion, who presented with sudden-onset chest pain and dyspnea. After a systematic retrospective review of the patient's clinical history and work-up, she was diagnosed with myocardial infarction with nonobstructive coronary arteries secondary to coronary thrombosis. Background: Myocardial infarction with nonobstructive coronary arteries (MINOCA) is diagnostically and therapeutically challenging for clinicians, as a large spectrum of causes may result in this clinical condition, multiple entities can mimic it, and there are relatively few evidence-based recommendations for its assessment. Discussion: Accurate diagnosis of the underlying etiology of MINOCA requires a systematic and dynamic evaluation of the clinical history and work-up of each patient, as well as the use of additional diagnostic tools that allow more in-depth characterization of the cardiac anatomy and coronary function, such as cardiac magnetic resonance imaging, coronary vascular imaging (intravascular ultrasound, optical coherence tomography), and coronary functional assessments. The prognosis of MINOCA highly depends on its underlying cause, and therefore, an accurate diagnosis of its etiology is necessary.

Introduction

Myocardial infarction with nonobstructive coronary arteries (MINOCA) is diagnostically and therapeutically challenging for clinicians, as a large spectrum of causes may result in this clinical condition, multiple entities can mimic it, and there are relatively few evidence-based recommendations for its assessment.[1,2] Current evidence suggests that a diagnosis of MINOCA should only be considered after confirming the presence of acute coronary syndrome (ACS), as defined by the "Fourth Universal Definition of Myocardial Infarction,"[3] and after ruling out the coexistence of any other etiology that may cause myocardial injury (such as sepsis, pulmonary embolism [PE], trauma, etc.) and the presence of obstructive coronary arteries on coronary angiography.[1] Once the diagnosis of MINOCA is established, further investigations are necessary to clarify the underlying mechanism, so that appropriate therapeutic actions can be implemented.[4]

In order to achieve an accurate diagnosis of the underlying etiology, a systematic and dynamic evaluation of the patients' clinical history, as well as the use of additional diagnostic tools to better characterize the cardiac anatomy and coronary function, such as cardiac magnetic resonance imaging (cMRI), coronary vascular imaging (intravascular ultrasound, optical coherence tomography), and coronary functional assessments. Herein, we present the case of a young female patient with a previous history of PE who presented with chest pain, in whom, an underlying hypercoagulability syndrome led to a subsequent thrombotic event leading to a MINOCA. In all studies, a high degree of clinical suspicion and a thorough interpretation were necessary in order to reach an accurate diagnosis.

Case presentation

A 19-year-old woman presented to the emergency department with sudden-onset of intense oppressive substernal chest pain that radiated to the back and neck, and was accompanied by diffuse epigastric discomfort and severe shortness of breath. Physical examination revealed blood pressure of 132/89 mmHg, heart rate of 107 beats/min, respiratory rate of 30 breaths/minute, and oxygen saturation of 93% at room air. Her heart sounds were tachycardic but regular. Cardiac examination was otherwise unremarkable, without murmurs, gallops, or rubs. No other abnormal findings on examination were observed. Three months earlier, after a spontaneous first-trimester abortion, she presented with dyspnea and severe chest pain, accompanied by intense dizziness and palpitations. On that occasion, she was found to have multiple PE. She was discharged with enoxaparin therapy, but her compliance was suboptimal.

The initial differential diagnosis of this young patient with previous history of PE and poor adherence to anticoagulation therapy, who presented with new-onset chest pain, dyspnea, and tachycardia, was directed toward a possible recurrence or worsening of the recent PE. However, the signs and symptoms in the current presentation were different from those in the prior episode, leading the team to pursue work-up of other differential diagnoses; these included ACS, in the context of coronary artery dissection or coronary vasospasm (due to her young age, coronary atherosclerotic disease was unlikely), aortic dissection, and an inflammatory condition, such as pericarditis or myocarditis.

Keywords

Chest pain, Pulmonary embolism, Antiphospholipid syndrome.

Mailing Address: Sebastian Gallo Bernal •
Divisão de Cardiologia, Fundacion Cardioinfantil - Instituto de Cardiologia, Bogotá, Colômbia. Endereço para correspondência: Calle 163 A No. 13B-60, Bogotá, Colômbia. Código postal: 110131
E-mail: sebgal1230@gmail.com
Manuscript received 6/4/2020; revised 6/10/2020; accepted 6/29/2020

DOI: 10.47593/2675-312X/20203304eabc113

Baseline laboratory tests revealed normal renal and hepatic function, normal complete blood count, and normal electrolytes. Computed tomography angiography showed no evidence of aortic dissection. Pulmonary circulation evaluation revealed partial resolution of the previous PE, with no new acute findings.

Electrocardiogram showed sinus rhythm, with ST-segment depression in the anterolateral wall leads and ST-segment elevation in aVR (Figure 1). Her high-sensitivity troponin I concentrations were 4.2 ng/mL on presentation, and 3.4 ng/mL 4 hours later (normal < 0.026 ng/mL). A bedside transthoracic echocardiogram (TTE) revealed mildly reduced systolic function with a left ventricular ejection fraction (LVEF) of 45% (Video 1). Anterior wall hypokinesia with mild pericardial effusion was observed. The right ventricle had normal morphology and function. Despite her young age, ACS was considered to be the most likely diagnosis.

Initial coronary angiography showed no angiographic stenosis (normal coronary arteries). A working diagnosis of MINOCA was established. Considering the current recommendations for work-up of MINOCA, further investigation to exclude clinically elusive nonischemic mechanisms of myocardial injury was considered.[1] cMRI showed hypokinesia in the mid-segment of the anterolateral wall (Video 2), as well as a perfusion defect at the anterolateral papillary muscle and in the mid-segment of the anterolateral wall (Figures 2A and B; Video 3). Subendocardial late gadolinium enhancement (LGE) was observed at the basal

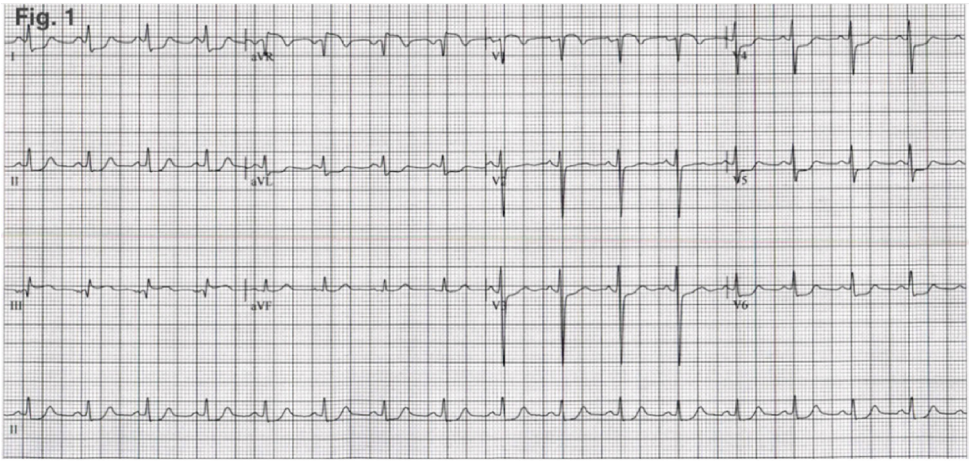

Figure 1 – *A 12-lead electrocardiogram showing ST -segment depression in the anterolateral wall leads and ST-segment elevation in aVR .*

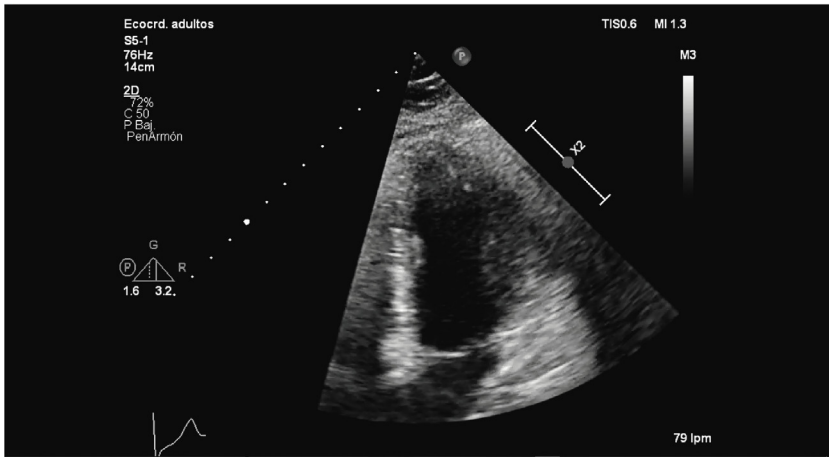

Video 1 – *Transthoracic echocardiogram (TTE): apical four-chamber view. TTE showing mildly reduced systolic function (left ventricular ejection fraction of 45%), with anterolateral wall hypokinesia and mild pericardial effusion. The right ventricle had normal morphology and function, with a preserved ejection fraction.*

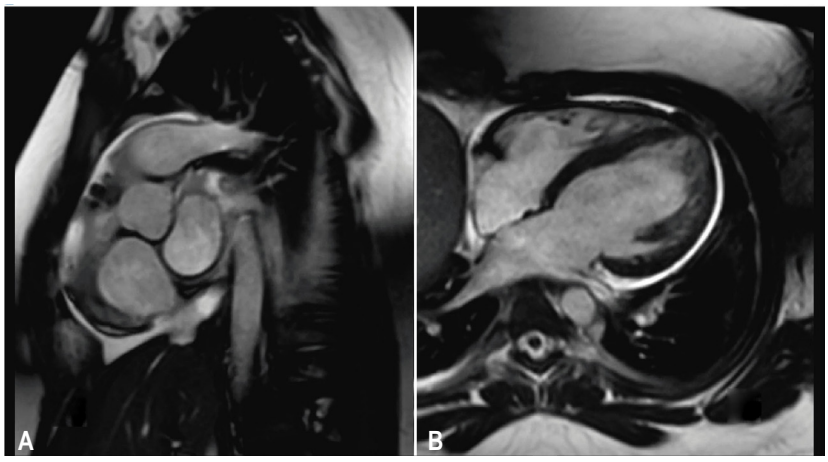

Video 2 – *Cardiac magnetic resonance: cine sequences. Short-axis (A) and horizontal long axis view (B) showing hypokinesia of the anterolateral mid-segment.*

segment of the anterior wall (Figure 2C), as well as edema in the T2-STIR sequence (Figure 2D). Together, these results confirmed the presence of myocardial infarction.

An exhaustive review of coronary angiography images suggested that the cause of the MINOCA was a possible re-canalized thrombus with microvascular obstruction of the small diagonal branch in the left anterior descending artery. Initial anticoagulation with intravenous unfractionated heparin was decided, and she was subsequently transitioned and discharged with enoxaparin. Considering her past medical history (spontaneous abortion and family history of autoimmune disease), thrombophilia work-up was performed, which confirmed the diagnosis of antiphospholipid syndrome.

A TTE 4 weeks after the initial presentation showed normalization of the previously depressed LVEF and resolution of the regional wall motion abnormalities. No long-term clinical sequelae were evident during her last visit to our outpatient clinic. Compliance with anticoagulation therapy was emphatically addressed. Due to the diagnosis of antiphospholipid syndrome, permanent anticoagulation was decided, with follow-up plans at her local anticoagulation clinic.

Discussion

We present the case of a young female patient with previous history of PE who presented with chest pain, in whom, an underlying pathophysiology of hypercoagulability led to a subsequent thrombotic event and MINOCA. Careful work-up for hypercoagulability led to the final diagnosis of antiphospholipid syndrome. A high degree of clinical suspicion and a thorough interpretation of all studies were necessary to reach an accurate diagnosis. Her past medical history of PE and first-trimester spontaneous abortion, in addition to the thrombotic obstruction of a coronary artery were just the manifestations of the hypercoagulable state caused by antiphospholipid syndrome.

MINOCA is diagnostically and therapeutically challenging for clinicians.[1,2] The optimal evaluation for patients with an established diagnosis of MINOCA should be focused on exploring and determining its specific cause. A systematic evaluation of the individual's clinical history and a dynamic work-up is necessary to determine the underlying etiology of MINOCA, in order to provide the most appropriate management for each causal mechanism.

As illustrated in this case report, cMRI is a key diagnostic tool for the assessment of patients presenting with MINOCA, owing to its safety and ability to characterize the myocardium with high definition and low inter-observer variability.[2] In this way, cMRI is useful to confirm the diagnosis of ACS, and to rule out entities such as myocarditis, takotsubo cardiomyopathy, and other cardiomyopathies.

The causes of MINOCA can be divided into atherosclerotic and non-atherosclerotic. Non-atherosclerotic causes of MINOCA include epicardial coronary vasospasm, coronary dissection, coronary microvascular dysfunction, supply/demand mismatch, and coronary thrombosis/embolism. As illustrated by the current case, coronary thrombosis may result in MINOCA if transient complete thrombosis with spontaneous thrombolysis results in nonobstructive angiographic disease, or if the thrombus involves the downstream microcirculation[1]. Hypercoagulable states, such as antiphospholipid syndrome, significantly increase the risk of venous and arterial thrombosis and embolisms. However, coronary thrombosis is not a common initial presentation. Venous thromboembolisms are more common, and within arterial thrombosis, strokes are significantly more prevalent than ACS.[5] Nonetheless, in patients with coronary embolism, approximately 7.5% were later found to have antiphospholipid syndrome.[5]

Funding

This research received no specific grant from any funding agency, commercial, or not-for-profit sectors.

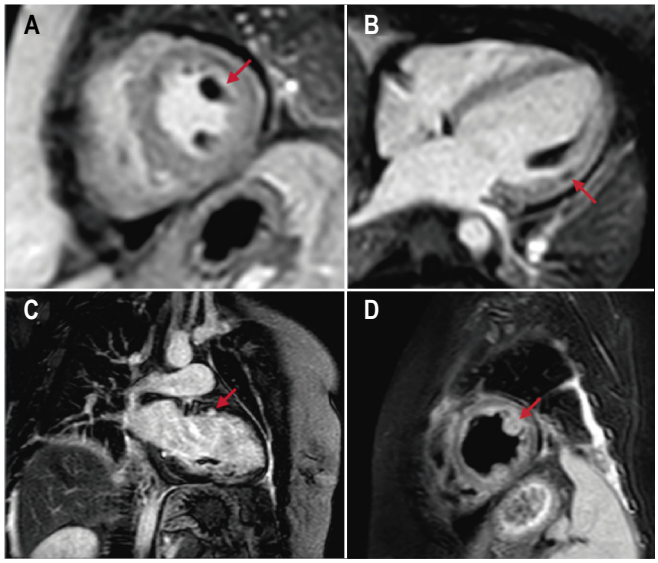

Figure 2 – *Cardiac magnetic resonance imaging. Perfusion sequences showing a perfusion defect of the anterolateral (red-arrow) and posteromedial (blue-arrow) papillary muscles (A), as well as in the mid-segment of the anterolateral wall (red-arrow on B). Subendocardial Late Gadolinium Enhancement (LGE) at the basal segment of the anterior wall (red-arrow on C). STIR-T2 sequence showing myocardial edema in the anterolateral papillary muscle (red-arrow on D).*

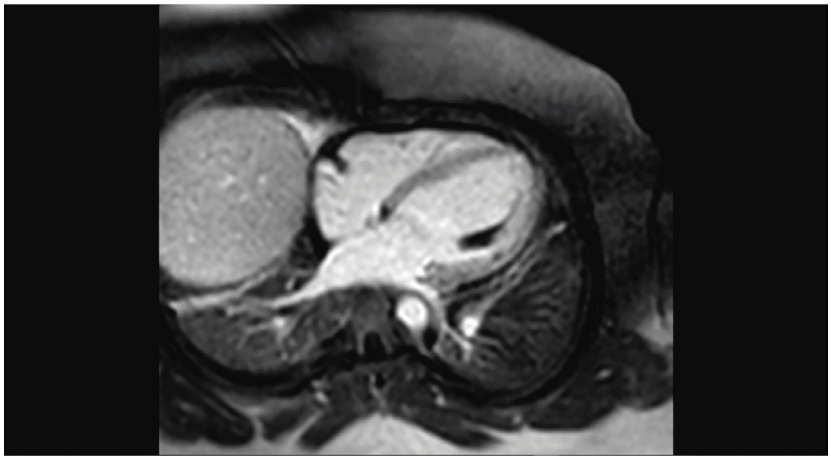

Video 3 – *Cardiac magnetic resonance imaging: perfusion sequence. Perfusion defect of the anterolateral and posteromedial papillary muscles, as well as in the mid-segment of the anterolateral wall.*

Consent

The author/s confirm that written consent for submission and publication of this case report including image(s) and associated text has been obtained from the patient in line with COPE guidance.

Acknowledgment

We would like to thank the Fundación Cardioinfantil for the support during the development of this project.

Authors' contributions

Research creation and design: Bernal SG; Vasquez-Rodriguez JF; Isaza D; Calixto CA; Jaimes C.: Data acquisition: Bernal SG; Martínez A; Vasquez-Rodriguez JF; Isaza D; Calixto CA; Jaimes C.: Data analysis and interpretation: Bernal SG; Martínez A; Isaza D; Calixto CA; Jaimes C.: Writing: Bernal SG; Isaza N; Isaza D; Jaimes C.: Critical revision for important intellectual content: Bernal SG; Martínez A; Vasquez-Rodriguez JF; Isaza N; Isaza D; Jaimes C

Conflict of interest

The authors have declared that they have no conflict of interest.

References

1. Tamis-Holland JE, Jneid H, Reynolds HR, Agewall S, Brilakis ES, Brown TM, et al; American Heart Association Interventional Cardiovascular Care Committee of the Council on Clinical Cardiology; Council on Cardiovascular and Stroke Nursing; Council on Epidemiology and Prevention; and Council on Quality of Care and Outcomes Research. Contemporary Diagnosis and Management of Patients With Myocardial Infarction in the Absence of Obstructive Coronary Artery Disease: A Scientific Statement From the American Heart Association. Circulation. 2019;139(18):e891-e908. doi: 10.1161/CIR.0000000000000670.

2. Niccoli G, Scalone G, Crea F. Acute myocardial infarction with no obstructive coronary atherosclerosis: mechanisms and management. Eur Heart J. 2015;36:475–81. doi: 10.1093/eurheartj/ehu469.

3. Thygesen K, Alpert JS, Jaffe AS, Chaitman BR, Bax JJ, Morrow DA, White HD; Executive Group on behalf of the Joint European Society of Cardiology (ESC)/American College of Cardiology (ACC)/American Heart Association (AHA)/World Heart Federation (WHF) Task Force for the Universal Definition of Myocardial Infarction. Fourth Universal Definition of Myocardial Infarction (2018). Circulation. 2018 Nov 13;138(20):e618-e651. doi: 10.1161/CIR.0000000000000617. Erratum in: Circulation. 2018;138(20):e652.

4. Beltrame JF. Assessing patients with myocardial infarction and nonobstructed coronary arteries (MINOCA). J Intern Med. 2013 Feb;273(2):182-5. doi: 10.1111/j.1365-2796.2012.02591.

5. Garcia D, Erkan D. Diagnosis and Management of the Antiphospholipid Syndrome. N Engl J Med. 2018;378:2010–21. doi: 10.1056/NEJMra1705454.

Left Atrial Myxoma Involving Multisystemic Manifestations in an Eldery Female Patient

Mixoma Atrial Esquerdo Envolvendo Manifestações Multissistêmicas em Paciente Idosa

Vanessa de Assis Reis[1], Bruno Oliveira Isabella[1], Marcelo Loula Novais de Paula[1], Ana Terra Fonseca Barreto[1]
Ana Nery Hospital, Federal University of Bahia,[1] Salvador, BA, Brazil.

Abstract

Atrial myxomas may progress asymptomatically or present systemic manifestations. Echocardiography is an effective complementary exam to diagnose such pathology. Cardiac surgery represents the definitive treatment; particularly when performed early, it can avoid tumor growth–related complications. This article reports the case of an elderly high-risk cardiovascular patient admitted with acute ST elevation myocardial infarction in a cardiac unit progressing with cardiogenic shock, which contributed to the low suspicion of cardiac tumor as the initial diagnosis.

Introduction

Atrial myxomas correspond to 50% of benign cardiac tumors. Generally, they have nonspecific symptoms, which contributes to their late or incidental diagnosis, and can affect any age group, predominantly women aged 30–50 years.[1]

In most cases, clinical manifestations depend on tumor size, location, and architecture.[2] Symptomatic patients may present with cardiac (atrioventricular, coronary, and conduction disorders), embolic, and constitutional (fever, shivering, weight loss, and hematological changes) symptoms.[1-3] The objective of this case report was to illustrate the diagnostic process and the multisystemic manifestations of left atrial myxoma in an elderly patient.

Case Report

The patient was a 73-year-old woman who was presented to the emergency room with typical chest pain associated with respiratory distress. Electrocardiography (ECG) performed upon emergency room admission showed elevation of the lower ST segment, Killip II (Figure 1A). The patient underwent thrombolysis within approximately 4 hours, and showed pain improvements as well as ST elevation on ECG. Six hours after the event, the patient was transferred to a cardiology referral hospital for invasive stratification, which revealed 25% stenosis in the proximal anterior descending artery, 25% in the middle third of the right coronary, 75–90% ostial obstruction lesion in the first diagonal, and moderately important fine-caliber occlusion in the distal third of the posterior descending branch (Figures 1B and 1C). Left ventriculography showed inferomedial hypocontractility. Thus, the patient underwent conservative treatment for acute coronary disease due to distal obstructive lesion.

Transthoracic Doppler echocardiography (ECO) performed 3 days after the infarction showed preserved left ventricular (LV) systolic function (70% ejection fraction) without segmental dysfunction and a heterogeneous echogenic 6 × 3.5 cm mass adherent to the interatrial septum causing discrete obstruction of the anterograde transmitral flow (mean gradient, 4 mmHg) (Figure 2).

After underwent complementary exams, while walking, she presented symptomatic hypotension with spontaneous improvement. The following day, her symptoms recurred but were more pronounced, with low cardiac output and the need for volume and vasoactive drugs. A physical examination performed at that time showed a grade 4/6 diastolic murmur in the mitral focus, mild crepitus in one third of the lower lung regions, and warm extremities. The patient showed no tolerance to vasoactive drug withdrawal in the subsequent 3 days, maintaining hypotension even at rest.

Considering the hemodynamic repercussions, emergency cardiac surgery was indicated for excision of the left atrial mass. The surgery revealed a large tumor with a gelatinous aspect in the left atrium (4 × 5 cm) that was easily shattered (Figure 2D). Histopathological analysis confirmed its identity as a myxoma.

On the second postoperative day, the patient presented with right hemiplegia and bradypsychia. Cranial computed tomography revealed left cerebellar hemisphere hypodensity with a mass effect obliterating the mesencephalic cistern and fourth ventricle, with the acute chronology of the event confirmed on brain resonance. Doppler ultrasonography of the carotid and vertebral arteries showed only carotid intima-medial thickening. In the following days, she presented with improvements in the neurological deficits, was discharged in good clinical condition, and remained asymptomatic at 1-month outpatient after hospital discharge follow-up.

Discussion

Myxomas can have diverse clinical manifestations that can include obstructive, constitutional, and embolic symptoms. However, this diagnosis is suspected in only 5.7% of cases, as myxomas often progress asymptomatically and, when the symptoms described above manifest, they are often confused with several other conditions.[4-6] The initial misdiagnosis occurred in the present case: the conjunction of cardiovascular risk factors, the typical clinical presentation, and the anatomical

Keywords

Diagnosis; Echocardiography; Myxoma.

Mailing Address: Ana Terra Fonseca Barreto •
Saldanha Marinho, s/n - Caixa D'agua, Salvador - BA, 40301-155
E-mail: anaterrafbarreto@yahoo.com.br
Manuscript received 2/14/2020; revised 3/2/2020; accepted 3/31/2020

DOI: 10.47593/2675-312X/20203304eabc86

<< SUMÁRIO

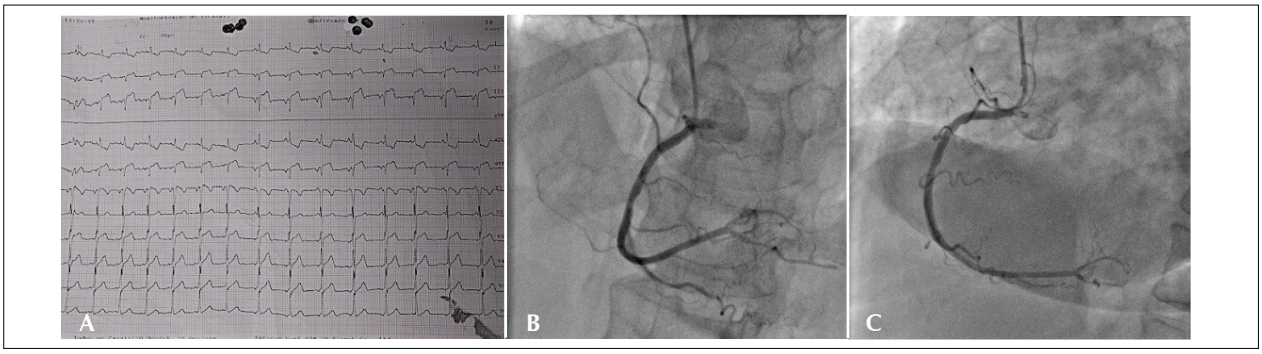

Figure 1 – *(A) A 12-lead electrocardiogram showing ST elevation of inferior wall. (B) A projection showing a 25% lesion in the middle third of the right coronary and posterior descending artery. (C) A left oblique projection showing a 25% lesion in the middle third of the right coronary and distal occlusion of the posterior descending artery.*

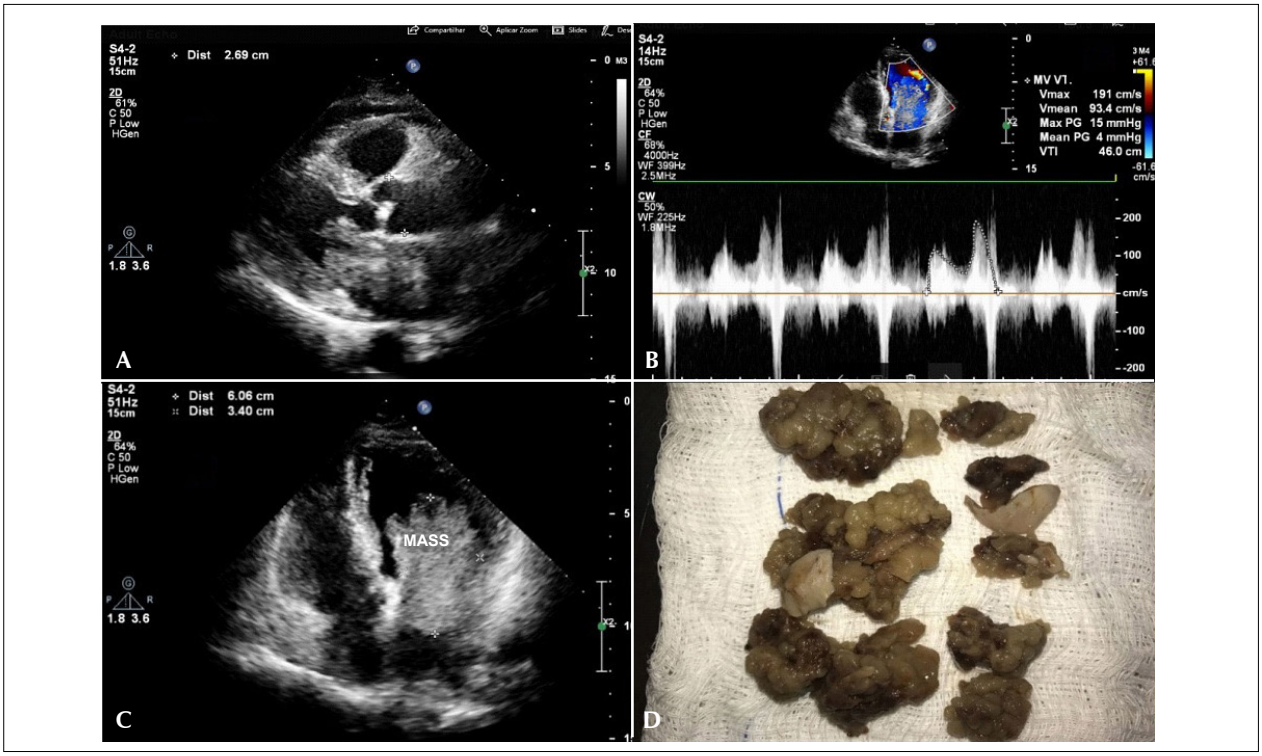

Figure 2 – *(A) A transthoracic echocardiogram taken in the parasternal long-axis view showing a mass adherent to the oval fossa. (B) A transthoracic echocardiogram showing obstruction of the left ventricular entry path. (C) A four-chamber apical transthoracic echocardiogram showing a left atrial mass with diastolic extension to the left ventricle suggestive of a myxoma. (D) A view of the cardiac myxoma after excision.*

diagnosis of acute coronary obstruction caused the myxoma to mimic coronary artery disease as the etiology of infarction.

The diagnosis was favored by the performance of the ECO 3 days after the infarction, showing the relevance of this low cost and easy-to-access method, which is often not performed immediately after acute coronary syndrome, even in a cardiology reference center. ECO is usually the initial examination used to assess a cardiac mass since it provides relevant information to define surgical strategy such as intracavitary flow mobility and repercussion in addition to the mass's origin and extension.[7]

In a retrospective analysis, the coronary lesions of the analyzed patient would not satisfactorily justify the presentation of a Killip II infarction with a probable contribution of the LV filling obstruction as a cause of congestion at the time of infarction diagnosis of the infarction. The first diagonal lesions and the distal occlusion of the posterior descending branch were possibly due to a tumor-related coronary embolism. Coronary embolic manifestations are very rare, and the right coronary artery is described as the most commonly affected due to the orientation of its ostium in relation to the aortic flow.[8]

The acute neurological event in more than one territory was probably secondary to a myxoma embolism during surgical manipulation as since it was extremely friable. It is noteworthy

that clinical signs of cerebral ischemia are found in 30–50% of symptomatic cardiac myxomas[9] and may present with acute deficits as in the present case. However, they can also have a later presentation due to cerebral aneurysm induced by myxoma and myxomatous metastasis.[6] Also, globular myxomas present with symptoms of heart failure due to reduced ventricular filling, whereas papillary tumors present with thromboembolism syndrome, primarily cerebral.[10]

In the present report, prompt surgical indication reduced the risk of repeated obstructive and embolic complications. The surgical removal of myxomas is the treatment of choice and usually performed on an elective basis. In the presence of embolic complications or heart failure, emergency surgery is indicated.[2]

Conclusion

Atrial myxomas may present with obstructive and embolic manifestations, which worsen the prognosis. The ECO is an accessible and low-cost complementary exam that is essential in the investigation of this pathology. In the present case, multisystemic manifestations denoted its seriousness. The early identification and prompt excision of the tumor are related to decreased complications.

Ethical responsibilities

Protection of people and animals

The authors declare that no experiments were performed on humans and/or animals during this investigation.

Data confidentiality

The authors declare that they followed the protocols of their work center regarding the publication of patient data and that all patients included in the study received sufficient information and provided written informed consent to participate.

Right to privacy and written consent

The authors declare that they received written consent from the patients and/or subjects mentioned in the article. The corresponding author holds this document.

Conflict of interest

The authors have declared that they have no conflict of interest.

References

1. El Sabbagh A, Al-Hijji MA, Thaden JJ, Pislaru SV, Pislaru C, Pellikka PA, et al. Cardiac Myxoma: The Great Mimicker. JACC Cardiovasc Imaging. 2017;10(2):203-206. doi: 10.1016/j.jcmg.2016.06.018
2. Spartalis M, TzatzakiE, Spartalis E, et al. Atrial Myxoma Mimicking Mitral Stenosis. Cardiol Res. 2017; 8(3): 128-130. doi: 10.14740/cr558w
3. Zhang RD, Zeng ZH, Zheng JY, Li TD, Zhao YQ, Liu YH, et al. Left atrial myxoma complicated with multi-system embolization. J Cardiothorac Surg. 2017;12(1):76. doi: 10.1186/s13019-017-0640-2
4. Pinede L, Duhaut P, Loire R. Clinical presentation of left atrial cardiac myxoma. A series of 112 consecutive cases. Medicine (Baltimore). 2001;80(3):159-72. doi: 10.1097/00005792-200105000-00002
5. Kalçık M, Bayam E, Güner A, Küp A, Kalkan S, Yesin M, et al. Evaluation of the potential predictors of embolism in patients with left atrial myxoma. Echocardiography. 2019;36(5):837-843. doi: 10.1111/echo.14331
6. Yuan SM, Humuruola G. Stroke of a cardiac myxoma origin. Rev Bras Cir Cardiovasc. 2015;30(2):225-34. doi: 10.5935/1678-9741.20150022
7. Poterucha TJ, Kochav J, O'Connor DS, Rosner GF. Cardiac Tumors: Clinical Presentation, Diagnosis, and Management. Curr Treat Options Oncol. 2019;20(8):66. doi: 10.1007/s11864-019-0662-1
8. Bartolomucci F, Tito A, Navarese EP, Iacovelli F, Mele M, Larosa C, et al. STEMI and NSTEMI ACS in a 30-Year-Old Patient: An Extremely Rare Complication of a Left Atrial Myxoma. Heart Surg Forum. 2017 Jun 30;20(3):E116-E118. doi: 10.1532/hsf.1607.
9. Wen XY, Chen YM, Yu LL, Wang SR, Zheng HB, Chen ZB, et al. Neurological manifestations of atrial myxoma: A retrospective analysis. Oncol Lett. 2018 Oct;16(4):4635-4639. doi: 10.3892/ol.2018.9218
10. Ferreira MC, Pott JH. Mixoma Cardíaco: Patologia e Correlação Clínica em Material de Ressecção Cirúrgica. Arq Med. 2009;23(5):177-80.

Non-Hodgkin's Lymphoma with Heart Disease as a Rare Cause of Acute Heart Failure: A Case Report

Linfoma Não Hodgkin com Acometimento Cardíaco: Uma Causa Rara de Insuficiência Cardíaca Aguda – Relato de Caso

Edielle de Sant'Anna Melo[1], Fernanda Sayuri Oshiro[1], Patrícia Maquinêz Veloso[1], Andréia Sevestrin Terêncio[1], Gilberto Szarf[1], Maria Eduarda Menezes de Siqueira[1]

[1] Department of Cardiology, Federal University of São Paulo, São Paulo, SP, Brazil.

Introduction

Lymphoma is the third most common cause of cardiac metastases, following only lung and breast cancers. Cardiac involvement represents 13.6% of metastatic tumors of the heart.[1] Diffuse large B-cell lymphoma (DLBCL) is the most common non-Hodgkin's lymphoma (31%) and rapidly fatal when left untreated.[2] Cardiac involvement can occur through three paths: continuity from intrathoracic lesions, retrograde lymphatic dissemination, or the blood.[3] It is most commonly found in the interatrial septum of the right chambers extending to the pericardium, with a lower prevalence in the left atrium and ventricle.[4-6]

The spectrum of cardiac manifestations is wide and ranges from an absence of symptoms to heart failure (HF), pericardial effusion, or arrhythmias.[4,5] Cardiac involvement is rarely the initial manifestation of lymphoma.[5] However, it generally presents a poor prognosis due to delayed clinical diagnosis and high invasive potential. Thus, an early identification of the tumor allows for timely treatment in an attempt to improve prognosis.

This article presents a rare clinical case of lymphoproliferative disease with cardiac involvement of the pericardium extending to the left atrium and ventricle.

Case report

A 67-year-old female patient born in Pernambuco and living in São Paulo was admitted to a tertiary hospital with a dry cough, progressive dyspnea, orthopnea, and paroxysmal nocturnal dyspnea for 2 weeks that had worsened in the previous 3 days. The patient was hypertensive, a 20 pack-years ex-smoker, and used acetylsalicylic acid, losartan, spironolactone, and carvedilol.

A physical examination showed tachypnea, tachycardia, slight jugular stasis, and palpable bilateral cervical lymph nodes with a hardened consistency. No murmurs were found on cardiac auscultation, and the cardiac rhythm was regular. Pulmonary auscultation identified diffuse wheezing and bibasilar crackling rales. Palpation of the abdomen revealed painful hepatomegaly up to 4 cm from the right costal margin with peripheral edema (2+/4+). Chest radiography showed an enlarged cardiac area, slight pulmonary congestion, and mediastinal enlargement.

Transthoracic echocardiography showed an intracardiac lobulated heterogeneous mass approximately 5 cm in its longest axis adherent to the lateral and inferior walls of the left ventricle with a movable component at the extremity.

Chest computed tomography (CT) was performed to assess the intracardiac mass and its relationship with the surrounding structures and determine its limits. Chest CT showed contact with the adjacent pericardium and a central area of necrotic aspect measuring approximately 11.0 × 3.2 cm. Lymph node enlargement was also identified in the right upper and lower paratracheal, subcarinal, left pre-vascular, right supraclavicular, and left internal thoracic chains (Figure 1). Staging was performed using CT scans of the skull, abdomen, and pelvis, but no extracardiac tumors were identified.

Cardiac magnetic resonance imaging (CMR) for the morphological and functional evaluation of the heart and better characterization of the intracardiac mass showed the presence of a large pericardial mass located predominantly in the lower and lateral portions of the left atrium and basal inferolateral segment of the left ventricle. The mass infiltrated the myocardium and the interatrial septum, was hyperintense in T2-weighted images, and demonstrated perfusion after contrast injection with areas of heterogeneous impregnation (Figure 2).

Considering the morphological and hemodynamic characteristics of this intracardiac mass of undetermined nature and the presence of lymph node enlargement in the right upper and lower paratracheal chains, a right cervical lymph node biopsy was performed. The immunohistochemical study was positive for CD20, MUM1, BCL2, BCL6, c-myc, Ki-67 (90% of neoplastic cells), CD3, and CD5 (positive in small mature lymphocytes), negative for the other markers, and Epstein-Barr virus–negative. The association with histopathological findings led to the diagnosis of DLBCL, activated B-cell immunophenotype (Hans algorithm), with the double immunohistochemical expression of myc and bcl-2.

The patient underwent pulse therapy with prednisone, followed by a rituximab regimen of chemotherapy associated with miniCHOP (cyclophosphamide, adriamycin, vincristine,

Keywords

Heart Failure; Lymphoma, Non-Hodgkin; Neoplasm Metastasis.

Mailing Address: Edielle de Sant'Anna Melo •
Rua Napoleão de Barros, 715, térreo, Departamento de Cardiologia – Vila Clementino, CEP: 04024-002 – São Paulo, SP, Brasil
E-mail: ediellesm@yahoo.com.br
Manuscript received 6/6/2020; revised 6/10/2020; accepted 6/17/2020

DOI: 10.47593/2675-312X/20203304eabc114

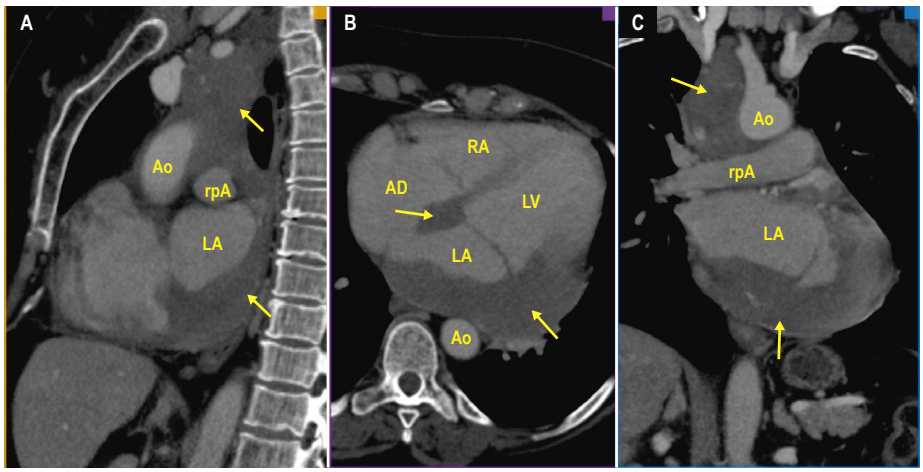

Ao, aorta; LA, left atrium; LV, left ventricle; RA, right atrium; rpA, right pulmonary artery; RV, right ventricle.

Figure 1 – *Computed tomography. (A) Sagittal section. (B) Axial section. (C) Coronal section. Mediastinal lymph node enlargement and expansive formation with heterogeneous content located in the lower and lateral regions of the left atrium. Infiltration is noted in the interatrial septum and the basal segment of the lower and lateral left ventricle walls.*

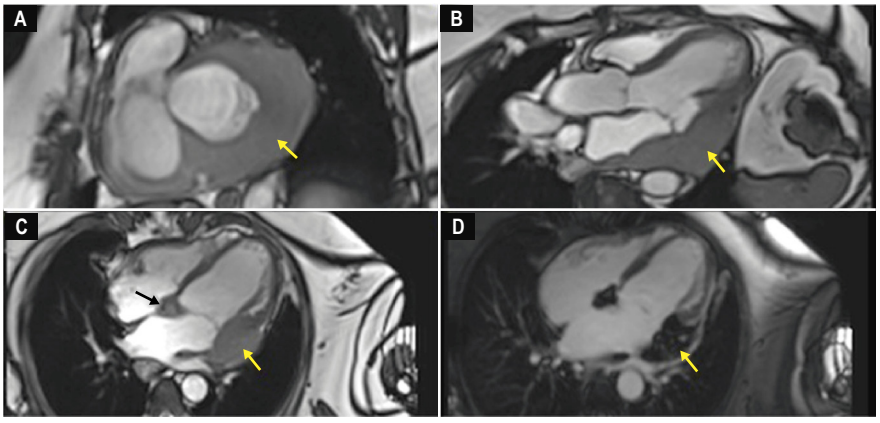

Figure 2 – *Cardiac magnetic resonance. (A) Short axis. (B) Three chambers. (C) Four chambers. (D) Late enhancement after administration of the contrast medium with heterogeneous impregnation suggestive of neoplasia. A mass is visible in the inferior and lateral regions of the left atrium. It also infiltrates the interatrial septum (black arrow) and the basal segment of the lower and lateral left ventricle walls.*

and prednisolone associated with rituximab), methotrexate, and intrathecal dexamethasone. The patient's clinical status improved, and she was discharged from the hospital while continuing the chemotherapy regimen. After 4 months of treatment, positron emission tomography–CT (PET-CT) showed total remission of the pericardial mass.

Discussion

This article presented a case of DLBCL involving the pericardium and extending to the posterior wall of the left cardiac chambers associated with cervical and mediastinal lymph node enlargement.

Lymphomas affecting the heart occur more commonly in the right chambers, with more than 80% located on the left ventricle wall. Of these, about half are associated with pericardial involvement causing a pericardial effusion. They can also occupy the right atrium, extending to the interatrial septum and left atrium.[8] Symptoms depend on tumor position and appear mostly in the final stage of the disease. The presence of HF is relatively common, as reported here.

Imaging exams can assist with the diagnosis. Chest radiography, despite its low sensitivity and specificity, can show changes such as mediastinal structure deviation or widening, cardiomegaly, cardiac silhouette changes, and HF signs. Transthoracic echocardiography is a sensitive method for identifying cardiac involvement by tumors.[7] Chest CT characterized the cardiac mass's morphology, location, and extension as well as the involvement of extracardiac structures, including lymph node enlargement. Magnetic resonance imaging enabled differentiation between the tumor mass and the myocardium due to better tissue characterization.

The diagnosis is usually confirmed by histopathological analysis of the pericardial or pleural fluid, when affected, or by endomyocardial biopsy. Adjuvant treatment includes several chemotherapy regimens such as CHOP, either alone or associated with radiotherapy. In this case, the patient underwent a cervical ganglion biopsy due to the risks inherent to myocardial biopsy as well as isolated chemotherapy due to her clinical conditions and tumor characteristics. The prognosis of these cases is generally poor, with a survival of less than 1 month without treatment. However, with an early diagnosis followed by appropriate treatment, survival can reach approximately 5 years.[8]

Conclusion

This case shows the early diagnosis of cardiac involvement by a lymphoproliferative malignant tumor in an elderly patient. Imaging examinations provided information about its location and involvement of the pericardium, left cardiac chambers, and lymph nodes. An early diagnosis and treatment change the natural history of the disease, improving the patient's prognosis and survival.

Authors' contributions

Research conception and design: Melo ESA, Oshiro FS, Veloso PM, and Terêncio AS; data collection: Melo ESA, Oshiro FS, Veloso PM, and Terêncio AS; data analysis and interpretation: Melo ESA, Oshiro FS, and Siqueira MEM; manuscript writing: Melo ESA, Oshiro FS, and Siqueira MEM; and critical review of the manuscript for important intellectual content: Siqueira MEM and Szarf G. Funding: This study received no funding.

Conflict of interest

The authors have declared that they have no conflict of interest.

References

1. Chinen K, Izumo T. Cardiac involvement by malignant lymphoma: a clinicopathologic study of 25 autopsy cases based on the WHO classification. Ann Hematol. 2005;84(8):498-505. doi: 10.1007/s00277-005-1009-5

2. Zuppiroli A, Cecchi F, Ciaccheri M, Dolara A, Bellesi G, Cecchin A, et al. Two-dimensional findings in a case of massive cardiac involvement by malignant lymphoma. Acta Cardiol. 1985;40(5):485-92 PMID: 3878648.

3. Anghel G, Zoli V, Petti N, Remotti D, Feccia M, Pino P, et al. Primary cardiac lymphoma: report of two cases occurring in immunocompetent subjects. Leuk Lymphoma. 2004;45(4):781-8. doi: 10.1080/10428190310001617259

4. Chalabreysse L, Berger F, Loire R, Devouassoux G, Cordier JF, Thivolet-Bejui F. Primary cardiac lymphoma in immunocompetent patients: a report of three cases and review of the literature. Virchows Arch. 2002;441(5):456-61. doi: 10.1007/s00428-002-0711-0

5. Ceresoli GL, Ferreri AJ, Bucci E, Ripa C, Ponzoni M, Villa E. Primary cardiac lymphoma in immunocompetent patients: diagnostic and therapeutic management. Cancer. 1997;80(8):1497-506. doi: 10.1002/(sici)1097-0142(19971015)80:8<1497::aid-cncr18>3.0.co;2-0

6. Gaspar A, Salomé N, Nabais S, Brandão A, Simões A, Portela C, et al. Echocardiographic assessment of a cardiac lymphoma: beyond two-dimensional imaging. Eur J Echocardiogr. 2009;10(8):975-8. doi: 10.1093/ejechocard/jep092

7. Ban-Hoefen M, Zeglin MA, Bisognano JD. Diffuse large B cell lymphoma presenting as a cardiac mass and odynophagia. Cardiol J. 2008;15(5):471-4. PMID: 18810725.

8. Temes R, Chavez T, Mapel D, Ketai L, Crowell R, Key C, et al. Primary mediastinal malignancies: findings in 219 patients. West J Med. 1999 Mar;170(3):161-6. PMID: 10214103.

Giant Left Atrial Myxoma and Mitral Valve Obstruction: a Case Report

Mixoma Atrial Esquerdo Gigante e Obstrução da Valva Mitral: Relato de Caso

Lucas F. Cardoso[1], Elinthon T. Veronese[1], Carlos Manuel de Almeida Brandão[1], Pablo Maria Alberto Pomerantzeff[1], Carlos E. Rochitte, Fabio B. Jatene[1]

Heart Institute (InCor), University of São Paulo Medical School,[1] São Paulo, Brazil.

Abstract

Myxomas are rare entities that represent the majority of benign cardiac tumors in adults. Their clinical presentation may vary by dimension and location, and they can occur in asymptomatic individuals as an incidental finding of cardiac mass from imaging exams. This article reports the case of a female patient with no known comorbidities who was admitted to the emergency department with acute heart failure. Transthoracic echocardiography revealed a mass in left atrium corresponding to a giant myxoma partially occluding the mitral valve, which required urgent surgical intervention.

Introduction

Primary cardiac tumors are a rare entity. Autopsy series found an incidence of 0.001 to 0.03%, and 75% of these cases are benign tumors. Myxomas are the most frequent tumors in adults, they account for 50–80% in clinical series and 70% in surgical cases.[1,2]

Myxomas mostly comprise single tumors located in the left atrium (LA; 75–80%), followed by the right atrium (RA;15–20%) and are more rarely related to other structures such as the ventricles and the valves.[3] They commonly present in female adults between 30 and 60 years, with an average age of diagnosis of 50 years. Grossly, myxomas have a globular aspect, with a smooth or slightly lobulated surface and soft gelatinous consistency, with a mean size of 3-4 cm. These tumors are usually attached to the endocardial surface close to the margin of the fossa ovalis by a fibrovascular stalk, with mobility related to the stalk size. Multiple cardiac myxomas are observed in patients with Carney complex.[4,5]

Clinical manifestations may vary and are related to intracardiac obstruction, systemic embolization, and systemic or constitutional symptoms. Dyspnea and orthopnea resulting from pulmonary venous hypertension are common, as are lipothymia and syncope due to transient obstruction of the left ventricular (LV) filling. Embolic events such as stroke, central retinal artery occlusion, and acute ischemia of the limbs can also occur. Systemic manifestations include fever, arthralgia, weight loss, fatigue, anemia, and increased inflammatory test levels.[2,3]

The following is a report of a young female patient with a large mass inside the LA diagnosed as a giant myxoma causing obstruction of the left ventricular inflow tract, mitral valve regurgitation, pulmonary hypertension, and significant left chamber dilatation.

Case report

A 48-year-old woman with no underlying diseases was admitted to the emergency department with progressive dyspnea for 30 days associated with orthopnea, paroxysmal nocturnal dyspnea, and lower limb edema. It was also reported episodes of lipothymia and syncope without neurological deficits. On physical examination she had irregular heart rhythm and presented with a systolic murmur in mitral area (3+/6+) radiated to the left axilla, and crepitant rales in both pulmonary bases. Electrocardiogram showed atrial fibrillation with a heart rate of 90 bpm. Chest radiography revealed an increased cardiothoracic ratio, double density sign, third mogul sign, and pulmonary vascular redistribution ("butterfly pattern").

Transthoracic echocardiography (TTE) showed severe enlargement of the left chambers (LA diameter, 78 mm; LV systolic and diastolic diameter, 67 and 44 mm, respectively), LV ejection fraction of 62%, moderate mitral regurgitation (+3), and a hyperechoic LA mass measuring 97 × 68 mm, attached to the interatrial septum, filling the entire left atrial chamber, with partial occlusion of the mitral annulus, and acceleration of left ventricle flow toward the mitral valve on color Doppler flow examination. Signs of pulmonary hypertension were also seen with a systolic pulmonary artery pressure (sPAP) of 85 mmHg. Cardiac magnetic resonance (CMR) imaging findings confirmed the presence of a large intracavitary mass of 80 x 60 x 90 mm in the LA (Figure 1), isointense in cine–steady-state free precession (SSFP) sequences, discretely hyperintense in double inversion recovery (IR) T1-weighted sequences, hyperintense in triple-IR T2-weighted sequences, with a discrete heterogeneous perfusion during first pass, indicating a solid lesion without hypervascularization, suggestive of LA myxoma (Video 1).

The patient was admitted to the intensive care unit for hemodynamic compensation, and then scheduled for urgent surgery. Surgical procedure was performed through median sternotomy, with cardiopulmonary bypass (CPB) under moderate hypothermia of 28ºC. After opening the left atrium, it was visualized a mass filling the left atrial chamber, with an infiltrative aspect over the posterior wall, attached to the interatrial septum. The tumor was resected carefully, followed by a posterior segmental annuloplasty of the mitral valve for

Keywords

Echocardiography; Magnetic Resonance Imaging; Myxoma.

Mailing Address: Lucas Figueredo Cardoso •
Instituto do Coração, Faculdade de Medicina, da Universidade de São Paulo
Avenida Dr. Enéas de Carvalho Aguiar, 44 - Pinheiros
E-mail: lucas.figueredo@gmail.com
Manuscript received 2/1/2020; revised 2/14/2020; accepted 4/17/2020

DOI: 10.47593/2675-312X/20203304eabc91

annular dilatation repair. Irrigation with saline solution was then performed to remove any debris.

Surgical specimen of 172 g was sent for anatomopathological examination, showing myxoid aspect and gelatinous consistency, without calcification or necrosis. Histological analysis concluded that it was a cardiac myxoma without signs of malignancy. The patient was discharged from hospital uneventfully after 10 days of postoperative and remained asymptomatic at late follow-up, with an 1-year TTE showing signs of reverse cardiac remodeling (LA diameter, 45 mm; LV end-diastolic diameter, 53 mm; and LV end-systolic diameter, 34 mm), trivial mitral regurgitation (+1), sPAP of 30 mmHg), and no evidence of tumor recurrence.

Discussion

Cardiac myxomas are usually found in young female adults and originate predominantly in the LA. Signs and symptoms of pulmonary venous hypertension must be differentiated from those resulting from heart valve diseases, congestive heart failure, and arrhythmias.[6]

Doppler echocardiography is the most common method used for diagnosis, since it can assess the myxoma size, form, and mobility, as well the location where it is attached.[5,7] CMR can be used additionally to provide valuable information, regarding the differential diagnosis of cardiac tumors. The most common presentation is a mass isointense at T1-weighted and hyperintense at T2-weighted imaging, with foci of hypointensity at one or two of these sequences.[8] Contrast echocardiography can also be used to allow mass differentiation by vascularization analysis.[9,10]

Surgical treatment is normally indicated and should be considered urgent in cases with potential risk of systemic embolization or valve orifice occlusion, a situation seen in atrial myxomas of great dimensions.[2] In present case, the patient underwent surgery before 24 hours since admission, due to clinical deterioration caused by the large myxoma and its hemodynamic consequences. If available, the use of intraoperative transesophageal echocardiography is recommended to optimize the surgical results.

Gajjar et al. suggested some strategies to prevent tumor recurrence, which include minimizing cardiac manipulation to

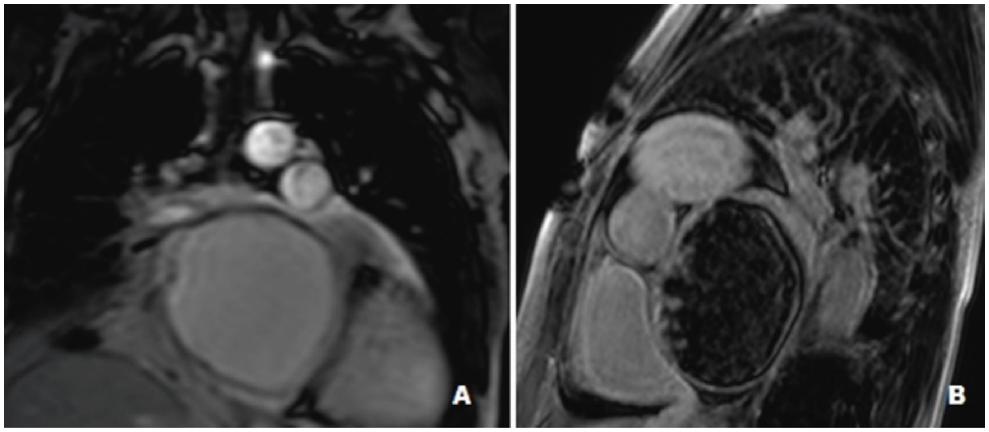

Figure 1 – *(A) Large intracavitary mass in the left atrium measuring 80 × 60 × 90 mm, isointense in cine–steady-state free precession sequences and discretely hyperintense in T1-weighted double inversion recovery sequences. (B) Hyperintense T2-weighted triple inversion recovery sequences with discrete heterogeneous first-pass perfusion indicative of a solid lesion without hypervascularization and suggestive of a left atrial myxoma.*

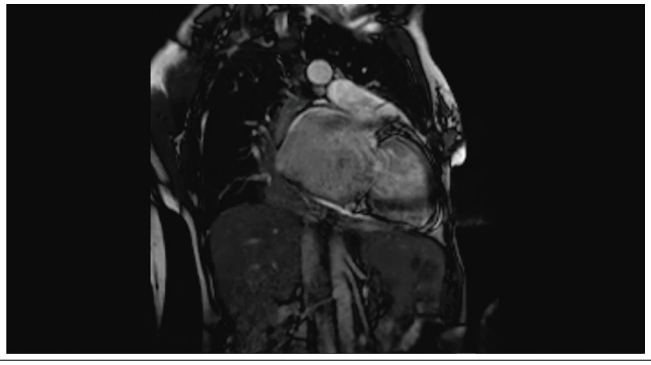

Video 1 – *Real-time cine cardiac magnetic resonance (CMR). Long-axis two-chamber view showing a giant mass in left atrium partially occluding the mitral valve.*

avoid embolization until aortic clamping; resecting completely the myxoma and the adjacent cardiac tissue and the septum, if necessary; removing carefully tumor debris with massive irrigation and suction; and resecting the myxoma intact whenever possible.[3] In our case, it was not feasible to resect the tumor intact due to the extensive infiltration into the atrial wall; however, precautions were taken to remove all debris.

Prognosis after surgery is excellent. Local recurrence is unusual, which is probably related to inadequate tumor resection.[2] The authors believe that the surgical approach should be performed urgently when there are signs of severe hemodynamic impairment.

Authors' contributions

Research conception and design: Lucas FC and Veronese ET; data collection: Lucas FC; data analysis and interpretation: Lucas FC, Veronese ET, and Brandão CMA; manuscript writing: Lucas FC, Veronese ET, and Brandão CMA; and critical review of the manuscript for important intellectual content: Brandão CMA, Pomerantzeff PMA, Rochitte CE, and Jatene FB.

Conflict of interest

The authors have declared that they have no conflict of interest.

References

1. Silverman NA. Primary cardiac tumors. Ann Surg. 1980;191(2):127-38. doi: 10.1097/00000658-198002000-00001

2. Butany J, Nair V, Naseemuddin A, Nair GM, Catton C, Yau T. Cardiac tumours: diagnosis and management. Lancet Oncol. 2005;6(4):219-28. doi: 10.1016/S1470-2045(05)70093-0

3. Neragi-Miandoab S, Kim J, Vlahakes GJ. Malignant tumours of the heart: a review of tumour type, diagnosis and therapy. Clin Oncol. 2007;19(10):748-56. doi: 10.1016/j.clon.2007.06.009

4. Silva RP, Pinheiro A, Costa I, Eloy J, Roberto C, Régis E, et al. Cardiac tumours: clinical , echocardiographic and pathological features. Rev Bras Cir Cardiovasc. 2003;18(1):60-4. doi: https://doi.org/10.1590/S0102-76382003000100012

5. Gajjar TP, Shah GB, Desai NB. Giant ventricular myxoma obstructing right ventricular outflow tract. Brazilian J Cardiovasc Surg. 2011;26(4):663-6. doi: https://doi.org/10.5935/1678-9741.20110060

6. Shah IK, Dearani JA, Daly RC, Suri RM, Park SJ, Joyce LD, et al. Cardiac Myxomas: A 50-Year Experience With Resection and Analysis of Risk Factors for Recurrence. Ann Thorac Surg. 2015;100(2):495-500. doi: 10.1016/j.athoracsur.2015.03.007

7. Pujol-López M, San Antonio R, Flores-Umanzor EJ, Guasch E, Azqueta M. A rare cause of severe mitral stenosis and reversible pulmonary hypertension. Echocardiography. 2017;34(10):1544-5. doi: 10.1111/echo.13586

8. Colin GC, Gerber BL, Amzulescu M, Bogaert J. Cardiac myxoma : a contemporary multimodality imaging review. Int J Cardiovasc Imaging. 2018;34(11):1789-808. doi: 10.1007/s10554-018-1396-z

9. Hari P, Mohamad T, Kondur A, Jahania SM, Afonso L. Incremental value of contrast echocardiography in the diagnosis of atrial myxoma. Echocardiography. 2010;27(5):46-9. 10.1111/j.1540-8175.2009.01128.x

10. Uenishi EK, Caldas MA, Saroute ANR, Tsutsui JM, Piotto GHM, Falcão SNRS, et al. Contrast echocardiography for the evaluation of tumors and thrombi. Arq Bras Cardiol. 2008;91(5):56-60. doi: 10.1590/s0066-782x2008001700015

Association among Subaortic Membrane, Interventricular Membranous Septal Aneurysm, and Septal Defect

Membrana Subaórtica, Aneurisma do Septo Membranoso Interventricular e Defeito Septal Associados

Israel Nilton de Almeida Feitosa[1]

[1]*Federal University of Campina Grande, Campina Grande, PB, Brazil*

An asymptomatic 32-year-old man with a history of a heart murmur since childhood presented with a systolic ejection murmur at the left sternal border that was audible during a physical examination. Transthoracic echocardiography showed a fibromuscular crest–type subaortic membrane with a slight gradient elevation in the left ventricular outflow tract. Perimembranous interventricular communication partially occluded by accessory tricuspid valve tissue forming a ventricular septal aneurysm was also evident. The cardiac chambers had normal dimensions and geometry (indexed diastolic diameter and left ventricular mass of 28.6 mm/m² and 96 g/m², respectively). The interventricular pressure gradient was high (126 mmHg), and the patient's systolic blood pressure during the examination was 140 mmHg, allowing estimation of the right ventricle pressure and, consequently, the pulmonary artery of approximately 14 mmHg. The subaortic membrane and the septal defect can change the aortic valve architecture, which creating aortic reflux (in this case, of a mild degree).

Conflict of interest

The authors have declared that they have no conflict of interest.

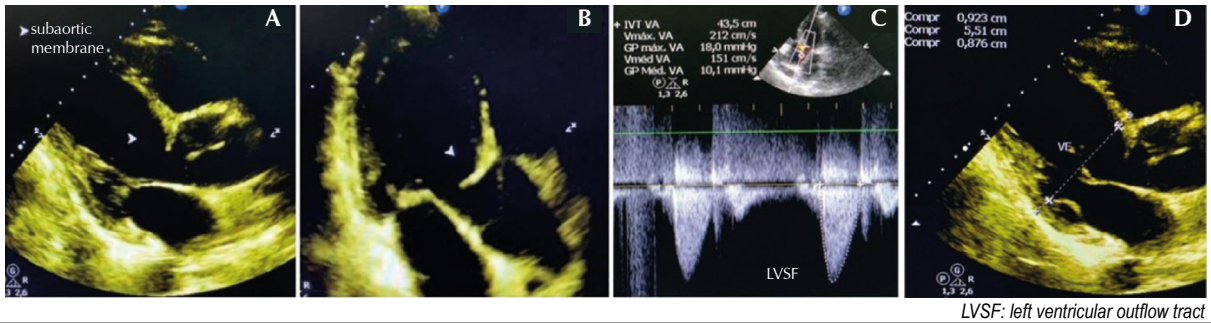

LVSF: left ventricular outflow tract

Figure 1 – *Subaortic membrane (arrow) viewed on transthoracic echocardiogram in long axis view (A) and apical 3-chamber view (B); (C) Discrete increase in systolic gradients in the left ventricular outflow tract (maximum and medium aortic transvalvular gradient were 18 and 10mmHg, respectively); (D) Diastolic diameter of the left ventricle (normal value after indexing to the body surface area).*

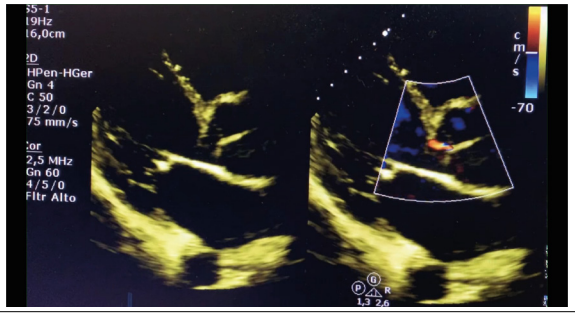

Video 1 – *Subaortic membrane (fibromuscular crest) and mild aortic regurgitation.*

Keywords

Aneurysm; Echocardiography; Septal Defect, Ventricular.

Mailing Address: Israel Nilton de Almeida Feitosa •
E-mail: inafeitosa@hotmail.com
Manuscript received 6/16/2020; revised 7/12/2020; accepted 7/16/2020

DOI: 10.47593/2675-312X/20203304eabc117

Images

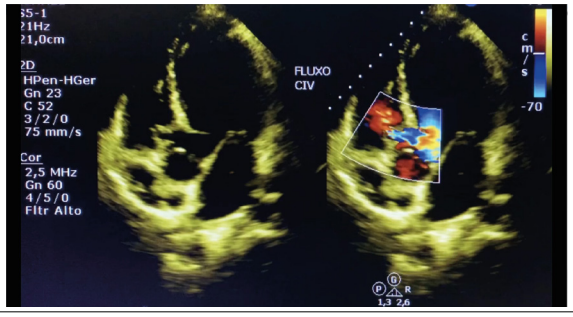

Video 2 – *Aneurysm of the membranous interventricular septum and color Doppler systolic flow showing septal defect at the apex of the aneurysm.*

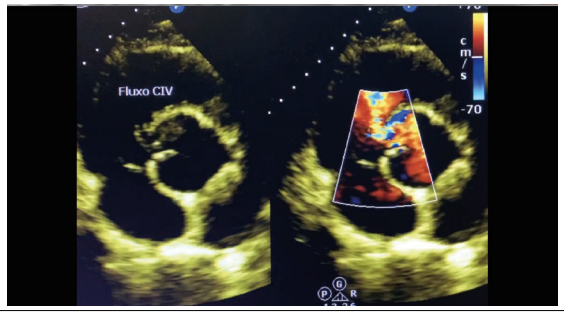

Video 3 – *Aneurysm of the membranous interventricular septum and color Doppler systolic flow (small septal defect at the apex of the aneurysm). Mild aortic regurgitation.*

Position Statement on Indications for Echocardiography in Fetal and Pediatric Cardiology and Congenital Heart Disease of the Adult – 2020

Development: Cardiovascular Imaging Department (Departamento de Imagem Cardiovascular – DIC) of the Brazilian Society of Cardiology (Sociedade Brasileira de Cardiologia – SBC) and the Cardiovascular Imaging Society of the Interamerican Society of Cardiology (Sociedad de Imágenes Cardiovasculares de Sociedad Interamericana de Cardiología – Sisiac, Siac)

Norms and Guidelines Council: Brivaldo Markman Filho, Antonio Carlos Sobral Sousa, Aurora Felice Castro Issa, Bruno Ramos Nascimento, Harry Correa Filho, Marcelo Luiz Campos Vieira

Norms and Guidelines Coordinator: Brivaldo Markman Filho

Coordinating Editor: Samira Saady Morhy

Co-editors: Silvio Henrique Barberato, Carlos Eduardo Rochitte, Marcelo Luiz Campos Vieira

Autores do Posicionamento: *Samira Saady Morhy,[1] Silvio Henrique Barberato,[2,3] Alessandro Cavalcanti Lianza,[1,4,5] Andressa Mussi Soares,[6] Gabriela Nunes Leal,[1,4,5,7] Ivan Romero Rivera,[8] Marcia Ferreira Alves Barberato,[2] Vitor Guerra,[9] Zilma Verçosa de Sá Ribeiro,[10,11] Ricardo Pignatelli,[12] Carlos Eduardo Rochitte,[13] Marcelo Luiz Campos Vieira[1,13]*

Hospital Israelita Albert Einstein,[1] São Paulo, SP – Brazil
Cardioeco – Centro de Diagnóstico Cardiovascular,[2] Curitiba, PR – Brazil
Quanta Diagnóstico e Terapia,[3] Curitiba, PR – Brazil
Instituto da Criança e do Adolescente do Hospital das Clínicas da Faculdade de Medicina da Universidade de São Paulo (HC-FMUSP),[4] São Paulo, SP – Brazil
Hospital do Coração,[5] São Paulo, SP – Brazil
Hospital Evangélico de Cachoeiro de Itapemirim e Clínica CORImagem,[6] Cachoeiro de Itapemirim, ES – Brazil
Hospital e Maternidade São Luiz Itaim,[7] São Paulo, SP – Brazil
Santa Casa de Misericórdia de Maceió,[8] AL – Brazil
The Hospital for Sick Children,[9] Toronto – Canada
Hospital Português,[10] Salvador, BA – Brazil
Hospital Aliança,[11] Salvador, BA – Brazil
Texas Children's Hospital, Baylor College of Medicine,[12] Houston, Texas – USA
Instituto do Coração da Faculdade de Medicina da Universidade de São Paulo (InCor, FMUSP),[13] São Paulo, SP – Brazil

How to cite this Statement:
Morhy SS, Barberato SH, Lianza AC, Soares AM, Leal GN, Rivera IR, et al. Position Statement on Indications for Echocardiography in Fetal and Pediatric Cardiology and Congenital Heart Disease of the Adult – 2020. Arq Bras Cardiol. 2020; 115(5):987-1005

Note: These statements are for information purposes and should not replace the clinical judgment of a physician, who must ultimately determine the appropriate treatment for each patient.

Correspondence: Sociedade Brasileira de Cardiologia – Av. Marechal Câmara, 360/330 – Centro – Rio de Janeiro – Postal Code: 20020-907. E-mail: diretrizes@cardiol.br

DOI: 10.47593/2675-312X/20203304epos

Declaration of potential conflict of interests of authors/collaborators of the Position Statement on Indications for Echocardiography in Fetal and Pediatric Cardiology and Congenital Heart Disease of the Adult – 2020

	If, within the last 3 years, the author/collaborator of the statement:						
Names of statement collaborators	**Participated in clinical and/or experimental studies sponsored by pharmaceutical or equipment companies related to this statement**	**Spoke at events or activities sponsored by industry related to this statement**	**Was (is) a member of a board of advisors or a board of directors of a pharmaceutical or equipment industry**	**Participated in normative committees of scientific research sponsored by industry**	**Received personal or institutional funding from industry**	**Wrote scientific papers in journals sponsored by industry**	**Owns stocks in industry**
Alessandro Cavalcanti Lianza	No	No	No	No	No	No	No
Andressa Mussi Soares	No	No	No	No	No	No	No
Carlos Eduardo Rochitte	No	No	No	No	No	No	No
Gabriela Nunes Leal	No	No	No	No	No	No	No
Ivan Romero Rivera	No	No	No	No	No	No	No
Marcelo Luiz Campos Vieira	No	No	No	No	No	No	No
Marcia Ferreira Alves Barberato	No	No	No	No	No	No	No
Ricardo Pignatelli	No	No	No	No	No	No	No
Samira Saady Morhy	No	No	No	No	No	No	No
Silvio Henrique Barberato	No	No	No	No	No	No	No
Vitor C. Guerra	No	No	No	No	No	No	No
Zilma Verçosa de Sá Ribeiro	No	No	No	No	No	No	No

Statement

Content

1. Introduction

In accordance with the "Standards for Production of Guidelines, Position Statements, and Standardizations" sanctioned by the Brazilian Society of Cardiology, this document was written to update indications for echocardiography in fetal and pediatric cardiology and congenital heart disease of the adult, and to supplement the recently-published position paper on indications for echocardiography in adults.[1] The position statement is not intended to be an in-depth review of echocardiography in congenital heart disease, but an indispensable basic guide to support rational clinical decision-making by physicians when ordering examinations. While it takes into consideration the significant technological advances achieved recently in echocardiography, its purpose is not to describe echocardiography methods in detail, but to clearly and concisely summarize the most important situations in which echocardiography is of benefit for diagnosis and/or treatment planning in these groups of patients. In this document, recommendation classes will be presented in accordance with the following definitions:

- Class I: conditions for which there is conclusive evidence or, in the absence thereof, general agreement that the examination procedure is useful and safe.
- Class II: conditions for which there is conflicting evidence and/or divergence of opinion on the utility and/or safety of the examination.
- Class IIa: evidence or opinions favorable to the examination. Most experts approve.
- Class IIb: utility and/or safety less well established, with divergent opinions.
- Class III: conditions for which there is evidence or consensus that the examination is not useful and, in some cases, may even be harmful.

Evidence levels are also presented, defined as follows:

- A: agreement between multiple randomized clinical trials or robust meta-analyses;
- B: less robust meta-analysis data or single randomized clinical study or observational studies;
- C: expert opinion.

All of the tables summarizing recommendations for use of echocardiography in different clinical scenarios will therefore include columns showing recommendation classes and evidence levels

2. Fetal Echocardiography

The incidence of congenital heart disease is estimated at 6-12/1,000 live births;[2,3] however, it is estimated that fetal prevalence is higher. There are several factors associated with increased risk of congenital heart disease in the fetus, including familial factors and maternal and fetal conditions. Fetal echocardiography is the most important tool for diagnosis of these cardiac pathologies, from the end of the first trimester up to term. The best timing for conducting fetal echocardiography is determined by multiple factors, including the reason for using it and the gestational age at which a cardiac and/or extracardiac abnormality is detected. Echocardiography for screening high-risk pregnancies can be conducted at 18 to 22 weeks' gestation. Considering that initial screening may not detect developing lesions[4] or arrhythmia,[5,6] abnormal findings at routine obstetric consultations should be promptly referred for additional fetal echocardiography examinations.

Fetal echocardiography can be performed at younger gestational ages, including at the end of the first and start of the second trimesters, generally in pregnancies at high risk of congenital heart disease, particularly when elevated nuchal translucency is present on morphological ultrasound in the first trimester.[7,8] In the majority of gestations, transabdominal fetal echocardiography provides images of adequate resolution to detect anomalies at between 13 and 14 weeks. However, if the examination is conducted before 13 weeks, transvaginal echocardiography is needed, because of the small size of the cardiac structures and the distance between the fetus and the maternal abdominal wall.[7,8] When fetal echocardiography is conducted before 18 weeks, it should be repeated between 18 and 22 weeks' gestation, because the limited image resolution may not be sufficient for diagnosis of certain cardiac abnormalities and also because of potential progression of lesions not detected at earlier gestational ages.[7-9]

The timing and frequency of echocardiography should be guided by: severity of lesions, signs of heart failure, mechanisms of progression, and perinatal management assessment.

Fetal echocardiography recommendations are listed in Tables 1 and 2.

Table 1 – Recommendations for fetal echocardiography in high-risk pregnancies[5-9]

Recommendations	Recommendation class	Evidence level
Pre-gestational DM	I	A
GDM diagnosed in first trimester	II	B
Maternal phenylketonuria	I	A
Maternal SSA/SSB antibodies	IIa	B
Maternal medications: ACE inhibitors Retinoic acid NSAID in third trimester	 IIa I I	 B B A
Maternal rubella infection in first trimester	I	C
Maternal infection with suspicion of myocarditis/pericarditis	I	C
Assisted reproduction	IIa	A
Congenital heart disease in first-degree relative	I	B
Heart disease with Mendelian inheritance in first or second-degree relative	I	C
Suspicion of heart disease on obstetric ultrasound	I	B
Extracardiac fetal anomaly	I	B
Fetus with chromosome abnormality	I	C
Fetus with tachycardia or bradycardia or frequent irregular heartbeats	I	C
NT > 95%	I	A
Monochorionic twinning	I	A
Fetus with hydrops or effusions	I	B

ACE: angiotensin-converting enzyme; DM: diabetes mellitus; GDM: gestational diabetes mellitus; NSAID: nonsteroidal anti-inflammatory drugs; NT: nuchal translucency. Adapted from Donafrio et al.[7]

Table 2 – Recommendations for fetal echocardiography in low-risk pregnancies[5-9]

Recommendations	Recommendation class	Evidence level
Maternal medication: Anticonvulsant Lithium Vitamin A Selective serotonin reuptake inhibitors NSAID during first and second trimesters	IIb	B
Heart diseases in second-degree relatives	IIb	B
Abnormalities of the umbilical cord and placenta	IIb	C
Fetal intra-abdominal venous abnormality	IIb	C

NSAID: nonsteroidal anti-inflammatories. Adapted from Donafrio et al.[7]

3. Echocardiography in the Newborn

Newborn infants transition from a state in which circulation is in parallel, with low systemic vascular resistance and high pulmonary vascular resistance, during fetal life, to a state in which circulation is in series and the cardiac output of both ventricles must be equal in the presence of high systemic vascular resistance. These circulatory changes that take place with birth may take days or weeks to be completed, particularly in preterms, because the communications present during fetal life cannot close promptly. Thus, persistent ductus arteriosus (PDA), persistent high pulmonary pressures, and the incapacity of the immature myocardium to pump blood against systemic vascular resistance that has suddenly increased can cause a transitory reduction in systemic blood flow, changing these patients' hemodynamics.[9] Moreover, structural cardiac anomalies or extracardiac conditions such as sepsis or diaphragmatic hernia are tolerated differently in this age group.[10]

The transitional physiology of the cardiovascular circulation during the neonatal period means that these patients must be evaluated as a distinct group.

The most common reasons for conducting an echocardiogram during the neonatal period are to detect or rule out congenital structural cardiac diseases in patients who have heart murmur, abnormal neonatal oximetry screening results,[11] are in shock, are hypoxemic, develop respiratory failure, or have multiple malformations. The next most common group of indications are to screen for functional anomalies, such as persistent ductus arteriosus, and to test pulmonary hemodynamics and cardiac function (see Table 2).

Echocardiographic assessment of patients in neonatal intensive care units is justified, including in an evolving manner, as a factor in specific changes to clinical management of the neonate.

The recommendations for echocardiography in newborn infants are listed in Table 3.

4. Echocardiography in Infants, Children and Adolescents

Since echocardiography is a noninvasive method for obtaining anatomic, hemodynamic, and physiological information on the pediatric heart, it is the first-choice diagnostic method for initial assessment of congenital or acquired heart disease in infants, children, and adolescents.

Children with cardiac diseases are a varied group of patients who often have complex anatomic malformations and require lifelong follow-up. Repeated studies may therefore be indicated to monitor heart valve function, growth of cardiovascular structures, and ventricular function and for follow-up of drug-based or surgical interventions.[9,16-18]

Signs and symptoms such as cyanosis, growth deficits, exercise-induced anginas, syncope, respiratory distress, murmurs, heart failure, pulse abnormalities, and cardiomegaly may suggest structural heart disease.

Echocardiography may also be indicated even in the absence of specific clinical status in patients with family history of hereditary heart disease, genetic syndromes associated with structural heart disease, or abnormal examination findings (fetal echocardiography, chest X-ray, and electrocardiogram).

Table 3 – Recommendations for echocardiography in newborn infants[9,11-15]

Recommendations	Recommendation class	Evidence level
Pathological heart murmur or other abnormal cardiac auscultation findings	I	C
Central cyanosis, heart failure, cardiogenic shock, respiratory distress	I	A
Asymmetry of pulses and/or arterial blood pressure gradient between upper and lower extremities	I	A
Cardiomegaly on radiological chest examination or abnormal findings suggestive of heart disease	I	A
Syndromes associated with cardiovascular disease	I	B
Extracardiac anomalies	I	B
Anomaly of heart position or site	I	B
Fetal and/or obstetric echocardiography findings showing or suggesting heart malformation	I	C
Corrective or palliative heart surgery	I	B
History of hydrops fetalis	I	B
Clinical suspicion of patent ductus arteriosus	I	A
Evaluation of the hemodynamic significance of PDA, monitoring effects of treatment	I	A
Assessment of progress of neonate after surgery for closure of ductus arteriosus with hemodynamic instability	I	A
Perinatal asphyxia with abnormal hemodynamics and/or biomarkers	I	A
Suspected pulmonary hypertension	I	A
Assessment of progress of neonate with pulmonary hypertension on drug treatment	I	A
Hypotension	I	A
Assessment of extracorporeal life support cannulae, maintenance and weaning from ECMO	I	A
Systemic maternal disease associated with known neonatal anomaly	IIa	B
Maternal infection during gestation or delivery with potential for fetal or neonatal cardiac sequelae	IIa	B
Maternal diabetes without fetal echocardiography or with normal fetal echocardiography	IIb	B
Maternal phenylketonuria	I	A
Maternal autoimmune dysfunction	IIa	B
Maternal exposure to teratogens	IIa	B
Failure to thrive in the absence of definite clinical abnormalities	IIa	C
History of nonsustained fetal ectopic heart rhythm, in the absence of postpartum arrhythmia	III	C
Acrocyanosis with normal pulse oximeter saturation in upper and lower extremities	III	C
Morphological and functional assessment during the postoperative period after heart surgery	I	B
To assess pericardial hemorrhage and evaluate hemodynamic impact and guide interventional procedures	I	A
To determine central venous catheter position and identify related complications (thrombosis and infection)	I	A

ECMO: extracorporeal membrane oxygenation; PDA: persistent ductus arteriosus.

Patients with arrhythmia may have structural heart disease, such as corrected transposition of the great arteries and Ebstein's anomaly, cardiac tumors, or cardiomyopathies. Sustained arrhythmia and use of antiarrhythmic medications can cause changes to myocardial function and echocardiography plays an important role in clinical management of these patients.

The recommendations for echocardiography in infants, children and adolescents are listed in Table 4.

5. Pediatric Echocardiography in Acquired Heart Diseases

Acquired heart diseases primarily occur in the context of systemic diseases linked to inflammatory processes, renal diseases, use of cardiotoxic chemotherapy, or parenchymatous pulmonary disease, and after heart transplantation.

Myocardial involvement can occur in several conditions, such as systemic inflammatory diseases (particularly those with a more aggressive course, such as juvenile systemic lupus erythematosus, juvenile idiopathic arthritis, and rheumatic fever).[19-22] During treatment with cardiotoxic chemotherapy (particularly with anthracyclines) and radiotherapy in the mediastinal region, echocardiography is indicated before, during, and after treatment, with the objective of indicating the need for cardioprotective measures and even for changing the treatment in some cases.[23]

In patients with chronic liver disease or hypertension and/or on dialysis, echocardiography provides clinicians with valuable information on ventricular geometry, systolic/diastolic function, and blood volume. This can very often guide changes in the dialysis regimen and introduction of (or changes to) antihypertensive and vasoactive drugs.[24]

In patients with pulmonary disease, echocardiography can be used to estimate pulmonary pressures and also to evaluate right ventricle performance, which has an important correlation with clinical prognosis.[25-27]

In children and adolescents with AIDS, echocardiography is used to investigate right cardiac involvement caused by the virus, which can result in dilated cardiomyopathy, pulmonary hypertension, and even ventricular hypertrophy, in addition to effects caused by opportunistic diseases and/or drug side effects.[28]

The growing number of children with end-stage heart failure must be evaluated before and after heart and/or cardiopulmonary transplantation[29] and echocardiography is also an aid to decision-making on introduction/withdrawal of cardiovascular support.[30]

The recommendations for echocardiography in newborn infants, infants, children, and adolescents with acquired heart disease are listed in Table 5.

6. Echocardiography in Adults with Congenital Heart Disease

Over the last 30 years, considerable advances were made in pediatric cardiology, both in the sphere of diagnosis with the advent of echocardiography and in the realm of treatment to correct heart diseases, initially surgically and more recently using percutaneous techniques in the catheterization laboratory. Recent data show that the estimated size of the population of adults with congenital heart disease in United States in 2010 was 1.4 million patients.[30] This population has problems related to residual defects, new acquired defects (such as pulmonary reflux after definitive correction of tetralogy of Fallot or obstructions after a Jatene procedure), arrhythmia, heart failure, acquired disease of the adult, infectious endocarditis, or indications for heart transplantation. Many survive with palliative surgery that may or may not require definitive correction (such as the Senning, Mustard, Rastelli, Glenn, or Fontan procedures, which induce new complications that are implicit in the surgical method employed) and many patients present with heart conditions for the first time, with no prior diagnosis of heart disease.[32-35]

There is no doubt that two-dimensional transthoracic echocardiography has an important role to play in diagnosis and follow-up of these malformations.[36] Recent advances such as 3D echocardiography have proved superior for determination of volumes and even ventricular function, particularly in complex malformations such as those with univentricular physiology, or for evaluation of the right ventricle, and these systems should be used whenever they are available and there are trained professionals to operated them.[37] Additionally, using 3D images to guide surgery gives surgeons better understanding of the case, enabling better surgical planning. Along the same lines, new techniques for assessment of diastolic function and segmental function, such as tissue Doppler, strain, and strain rate can be very useful, particularly in conditions with univentricular physiology or cardiac chamber deformities, primarily when involving the right ventricle[38] (see sections 9 and 10 below).

The primary limitation of echocardiography for assessment of adults with congenital heart disease is a poor transthoracic acoustic window in patients with previous heart surgery or deformities of the chest wall, and echocardiography is also inappropriate for assessing the aortic arch, the coronary arteries, the pulmonary arteries, and the collateral vessels. In these situations, transesophageal echocardiography, angiotomography, and magnetic resonance (MR) are extremely useful.

The recommendations for echocardiography in adults with congenital heart disease are listed in Table 6.

7. Transesophageal Echocardiography in Pediatric Cardiology

Transesophageal echocardiography (TEE) uses special transducers and a different access route, offering better definition of cardiac structures, increasing the method's diagnostic applications.

It is particularly important for definition of complex anatomic structures and functional abnormalities, which cannot always be evaluated using transthoracic echocardiography alone.

Technological advances and miniaturization of probes has led to increasing adoption of TEE in the field of pediatric cardiology and it can provide important information about patients from the neonatal age group up to adolescents and adults, for diagnosis, intraoperative assessment, in the immediate and late postoperative periods, and in the intensive care unit, and also in the catheterization laboratory, aiding in interventional procedures.

Table 4 – Recommendations for echocardiography in infants, children and adolescents[9,12,16-18]

Recommendations	Recommendation class	Evidence level
Pathological heart murmur or other evidence of cardiac abnormality	I	C
Anomaly of heart position or site	I	B
Cardiomegaly on radiological chest examination or abnormal findings suggestive of heart disease	I	B
Abnormal electrocardiogram	I	B
Immediate preoperative assessment for heart surgery	I	C
Change in clinical status of patient with known heart disease	I	B
Morphological and functional assessment during the postoperative period after heart surgery	I	C
Family history of heart disease transmitted genetically	I	B
Neuromuscular disease with myocardial involvement	I	B
Signs and symptoms of infectious endocarditis	I	A
Signs and symptoms of heart failure	I	A
Palpitations without other symptoms, benign family history, and normal electrocardiogram	IIb	C
Palpitations with family history of arrhythmia, sudden death, or cardiomyopathy.	I	B
Palpitations in patient with known cardiomyopathy	I	B
Palpitations with abnormal electrocardiogram or known ion channel defects	IIa	C
Asymmetry of peripheral pulses	I	A
Syndrome associated with cardiovascular disease; genotype positive for cardiomyopathy; chromosome anomaly associated with cardiovascular disease	I	B
To determine the appropriate timing of clinical or surgical treatment in patients with known heart disease	I	B
Selection, placement, patency, and monitoring of endovascular devices	I	A
Identification of intracardiac and intravascular shunts before, during, and after interventional percutaneous cardiac catheterization	I	A
Prolonged fever, without apparent cause, in a patient with congenital heart disease	I	A
Functional murmur in an asymptomatic patient	IIb	C
Retarded growth in the absence of specific clinical abnormality	IIb	C
Atypical angina, identified as of musculoskeletal origin in an asymptomatic patient	III	
Syncope with abnormal electrocardiogram, exercise-related syncope	I	A
Syncope with family history of cardiomyopathy or sudden death	I	A
Neurocardiogenic (vasovagal) syncope	IIa	C
Effort angina or angina at rest with abnormal electrocardiogram	I	B
Angina associated with fever or use of illicit drugs	IIa	B
Presumably innocent murmur with signs and symptoms of heart disease	I	C
Central cyanosis	I	A
Chest wall deformity and preoperative scoliosis	IIb	C
Extracorporeal life support: initiation, maintenance, and weaning	I	B
Previous normal echocardiography with change in cardiovascular status and/or new family history suggestive of hereditary heart disease	IIa	C
Abnormal cardiac biomarkers	I	B
Hemoglobinopathies	I	B
Connective tissue diseases (Marfan, Loeys, Dietz, and others)	I	B
Muscular dystrophy	I	B
Autoimmune diseases	I	B
Arterial hypertension	I	A
Stroke	I	B
Metabolic, mitochondrial, or storage disease	I	B
Family history of cardiovascular disease: sudden death before 50 years of age, connective tissue diseases (Marfan or Loeys Dietz syndromes), idiopathic arterial hypertension	IIa	C
Family history of cardiovascular disease: hypertrophic cardiomyopathy, nonischemic dilated cardiomyopathy, hereditary pulmonary arterial hypertension	IIa	B

Table 5 – Recommendations for echocardiography in newborn infants, infants, children, and adolescents with acquired heart disease[9,16-31]

Recommendations	Recommendation class	Evidence level
Initial assessment and reassessments in patients with suspected or confirmed diagnosis of Kawasaki syndrome, Takayasu's Arteritis, myopericarditis, AIDS, and rheumatic fever	I	B
After heart or cardiopulmonary transplantation	I	B
Initial assessment and reassessments in patients treated with cardiotoxic chemotherapy and mediastinal radiotherapy	I	B
Initial assessment and reassessments in patients with myocardial disease	I	C
Assessment of cardiac involvement in severe kidney disease and/or systemic arterial hypertension	I	B
Assessment of donors for heart transplantation	I	C
Pulmonary arterial hypertension	I	A
Assessment of progression of pulmonary arterial hypertension treated with drugs or surgery	I	B
Initiation or withdrawal of extracorporeal cardiopulmonary support	I	C
Thromboembolic event	I	C
Sepsis, right heart failure, or cyanosis in a patient with venous catheter	I	B
Systemic or pulmonary embolization in a patient with right-left flow and venous catheter	I	C
Superior vena cava syndrome in a patient with venous catheter	I	C
Liver disease	IIa	C
Obesity with other cardiovascular risk factors or obstructive sleep apnea	IIa	C
Sepsis	IIa	B
Cystic fibrosis without evidence of cor pulmonale	IIa	C
Follow-up of patients after rheumatic fever without evidence of cardiac involvement	IIb	C
Cardiac assessment after pericarditis without evidence of recurrent pericarditis or chronic pericarditis	IIb	C
Fever in a patient with venous catheter without evidence of systemic or pulmonary embolization	IIb	C
Routine assessment for participation in competitive sports in patients with normal cardiovascular examination	IIb	C
Late follow-up of Kawasaki syndrome without evidence of coronary abnormalities in the acute phase	III	C
Routine assessment in an asymptomatic patient with venous catheter	III	C

7.1. Transesophageal Echocardiography as a Diagnostic Tool

Transesophageal echocardiography should be adopted to improve diagnostic definition of heart disease in situations in which better anatomic evaluation is needed in certain specific congenital heart diseases, in the majority of cases in adults, since in children the image quality of transthoracic echocardiography is generally good (Table 7).

7.2. Intraoperative Transesophageal Echocardiography

The most important impact of transesophageal echocardiography in the operating room is detection of significant residual defects that are very often unsuspected. Several authors have reported putting patients back on extracorporeal circulation to review surgery after intraoperative TEE, with rates that vary from 6 to 11.4% of cases, in the different series analyzed.[46]

The indications for intraoperative TEE for congenital heart disease are listed in Table 8.

7.3. Transesophageal Echocardiography in the Intensive Care Unit (ICU)

In the immediate postoperative period, the definition of TEE images may be compromised by drains, dressings, meshes, and mechanical ventilation, making it necessary to use TEE, which can provide anatomic (residual lesions) and hemodynamic information that is important for clinical and therapeutic management of patients (Table 9).

7.4. Transesophageal Echocardiography in the Catheterization Laboratory

Transesophageal echocardiography is helpful during hemodynamic interventions, providing diagnostic details in a range of heart diseases and for monitoring procedures, in addition to providing anatomic information on the results and on possible residual lesions[47] (Table 10).

Table 6 – Recommendations for echocardiography in adults with congenital heart disease[9,29,36,38-44]

Recommendations	Recommendation class	Evidence level
Initial structural and functional assessment in suspected congenital heart disease because of murmur, cyanosis, poor arterial saturation, or abnormal electrocardiogram or chest X-ray findings	I	C
Changes in the clinical status of a patient with known congenital heart disease, whether operated or not	I	C
Doubts with regard to original diagnosis or unexplained structural or hemodynamic abnormalities in a patient with known congenital heart disease	I	C
Follow-up of patients with intraventricular communication for assessment of evolving morphological changes	I	C
Periodic follow-up of patients with congenital heart disease, operated or not, in whom assessment of contraction, valve, and conduction function is needed	I	C
Postoperative annual follow-up after total, partial, or palliative repair in patients with residual defects and sequelae that could compromise clinical progress	I	C
Identification of the origin and initial course of the coronary arteries	I	C
Assessment of unexplained post-exercise syncope for initial diagnostic definition	I	C
Evaluation of aortic injury in patients with suspected or confirmed Marfan Syndrome for serial assessment of the aorta and/or mitral valve	I	C
Periodic examinations in patients operated for PDA, ASD, VSD aortic coarction or bicuspid aortic valve, without residual defect and without changes in clinical condition	III	C
Follow-up of patients with heart diseases without hemodynamic significance and without changes in clinical condition	III	C
Assessment of lesions in the aortic arch, pulmonary arteries and collateral arteries, the anatomy of which is better defined using other diagnostic methods	III	C
Periodic assessment of cardiac malformations without changes in physical examination findings, in the clinical condition of the patient, or in other examinations such as electrocardiogram and chest X-ray	III	C

ASD: atrial septal defect; PDA: patent ductus arteriosus; VSD: ventricular septal defect.

Table 7 – Recommendations for transesophageal echocardiography as a diagnostic tool[9,45]

Recommendations	Recommendation class	Evidence level
Confirmation or exclusion of a relevant clinical diagnostic suspicion not observable using TTE	I	A
Insufficient anatomic and hemodynamic information using TEE, primarily in children with chest deformities or obesity and in adults with congenital heart disease	I	A
Assessment of PFO as a possible etiology of central or peripheral embolic events in young patients (< 60 years), with agitated saline contrast to determine the possibility of right-left flow. To assess PFO risk factors for stroke/TIA: interatrial septum aneurysm, passage of > 30 microbubbles from right atrium to left atrium, PFO tunnel > 10 mm, and prominent Eustachian valve	I	A
Assessment of PFO before placement of a transvenous pacemaker	I	A
Classification, dimensions, and location of atrial septal defect, primarily in adult patients and those with poor transthoracic definition for selection of possible candidates for percutaneous occlusion and choice of occlusion device.	I	A
Assessment of aortic dissection in Marfan, Ehlers-Danlos, and Turner syndromes and in aortic coarctation	I	A
Assessment of the aorta in the Takayasu's Arteritis	I	A
Assessment of the intra or extra-cardiac tubes during the postoperative period after Senning, Mustard, or Fontan procedures	I	A
Assessment of thrombi, masses, vegetations, abscesses, and prostheses	I	A
For determination of the degree and mechanisms of mitral valve reflux to aid in surgical or percutaneous repair (Mitraclip)	I	B

PFO: patent foramen ovale; TEE: transesophageal echocardiogram; TIA: transient ischemic attack; TTE: transthoracic echocardiogram.

Table 8 – Recommendations for intraoperative transesophageal echocardiography[9,45-46]

Recommendation	Recommendation class	Evidence level
Perioperative assessment of cardiac anatomy and function	I	A
Monitoring of surgical procedures involving risk of abnormal flows, valve reflux, residual obstructions, or myocardial ventricular dysfunction	I	A
Minimally invasive surgery, video-guided surgery, and hybrid procedures	I	A

Table 9 – Recommendations for transesophageal echocardiography in the ICU[9,45]

Recommendation	Recommendation class	Evidence level
Assessment of residual defects, pericardial hemorrhage, and ventricular function in patients with a poor transthoracic acoustic window	I	A
Postoperative monitoring in a patient with an open sternum	I	A

Table 10 – Recommendations for Transesophageal Echocardiography in the Catheterization Laboratory[9,45,47]

Recommendation	Recommendation class	Evidence level
In percutaneous closure of patent foramen ovale, interatrial and interventricular communications	I	A
Postoperative closure of fenestrations after Fontan procedures	I	A
During dilatation of Senning and Mustard procedure tunneling	I	A
During stenting of stenosis of pulmonary arteries and tubes	IIb	B
For guidance in mitral valvoplasty and percutaneous mitral valve repair (Mitraclip)	I	A
For guidance in pulmonary and aortic valvoplasties	IIa	A
Placement of aortic endoprostheses to treat aneurysms, dissections, hematoma, or parietal ulcers of the thoracic aorta	I	A
Catheter guidance for perforation and percutaneous dilatation of atretic valves	I	A
During therapeutic interventional catheterization for radio frequency ablation	I	A

8. Stress Echocardiography in Pediatric Cardiology

Echocardiography under stress (physical or pharmacological) is a well-established technique in adults.[48,49] There are not yet specific guidelines or recommendations for the pediatric age group. However, as in the adult population, applications in children and adolescents have been concentrated on investigation of ischemic disease,[50-56] but are being extended to other areas that are not necessarily ischemic[55-63] (Table 7).

Both types of stress, pharmacological and exercise, can be administered to children, with certain peculiarities.[64-66] Dobutamine is the most common pharmacological agent and is used in the same protocols as with adult patients. In general, sedation or even anesthesia is recommended for children under the age of 8. Physical exercise can be used with children over the age of 8 who are cooperative and able to exercise on a treadmill or bicycle.[67]

9. Three-dimensional Echocardiography

Three-dimensional (3D) echocardiography has been incorporated into clinical practice, providing additional information in comparison to two-dimensional (2D) echocardiography, and is primarily used for congenital defects in which the three-dimensional view offers images very close to the anatomic and surgical planes.[68] The same concept is applicable to procedures undertaken in the catheterization laboratory, in which the three-dimensional view can be used not only to guide the procedures, but also to better evaluate the anatomy when choosing which devices to employ. Assessment of ventricular volumes and function has also been performed using the 3D technology, primarily to evaluate ventricular geometry in the most diverse forms of congenital defects, including univentricular hearts.[69,70] Atrioventricular valves can be assessed not only from the point of view of anatomic details, including the subvalvular apparatus, but also in terms of functional assessment of valve ring movement, and interactions between movement of valve leaflets and chords.[71]

When dealing with pediatric patients, the larger transthoracic acoustic window is a great advantage. More recently, more advanced transducers have been developed with a smaller footprint and higher frequency (2 to 8 MHz). However, the image

quality is still not the same when a 2D-3D combination is used with the same transducer, particularly in small patients. Another significant challenge that remains to be overcome is development of a pediatric transesophageal transducer, which limits 3D TEE to use in patients weighing more than 30 kg, according to manufacturers' recommendations. In small children, use of a pediatric transducer with higher frequency is recommended, as well as the epicardial echocardiogram, for intraoperative scenarios. Three-dimensional transesophageal echocardiography should always by considered in larger patients (generally weighing more than 30 kg) if transthoracic 3D imaging does not yield sufficient information to plan surgery or other interventions.

In a variety of different congenital defects, 3D echocardiography can provide additional information on a wide range of anatomic structures, including atrial and ventricular septa, the semilunar and atrioventricular valves, and also the outflow tracts. Applications are expanding as technological progress advances and adaptations are made to suit the pediatric population. Currently, use is based more on clinical need for additional information than on randomized studies showing the advantage of 3D over 2D. Use is therefore individualized and depends on the profile of the imaging laboratory or hospital adopting the technology for specific lesions.

Valve lesions and isolated septal defects are the principal indications. However, in situations in which there are concomitant anomalies of the ventriculoarterial connection, as in double-outlet right ventricle, the position and size of the intraventricular communication can be better visualized and demonstrated with 3D echocardiography.

Depending on the area or structure assessed by transthoracic and/or transesophageal 3D echocardiography, it may provide relevant information that complements the findings of 2D echocardiography.[72-83] Little additional information is yielded by using 3D echocardiography to assess the pulmonary arteries, the pulmonary valve, and even the right ventricle outflow tract and the aortic arch (Table 12).

Three-dimensional echocardiography can provide additional information in the context of certain specific congenital heart disease in which there are connection anomalies (atrioventricular or ventriculoarterial)[76,84-86] (Table 13).

Application of 3D echocardiography in the catheterization laboratory for closure of atrial and ventricular septal defects complements 2D images for delimiting the margins of defects and related structures,[87,88] specifically in atrial communications of the type ostium secundum, which are very well demonstrated by real-time imaging with 3D transesophageal echocardiography. Closure of interventricular communications using percutaneous or transmural devices can also be guided and, primarily, assess nearby structures, such as, for example, leaflets and/or tricuspid valve chords. There are other applications in the catheterization laboratory in which 3D echocardiography can be used to guide procedures: closure of fenestrations in the Fontan procedure, coronary fistulae, ruptures of the sinus of Valsalva, paravalvular regurgitation, septal perforation, and location of electrodes for cardiac resynchronization.[89-94]

A major challenge in congenital heart disease is evaluation of ventricular volumes and function, because of reasons that are intrinsic to the congenital defects involved (position of the heart, connection anomalies, non-contractile material, and differences in ventricular preload, among others). The software packages available were developed on the basis of the left ventricular geometry of normal hearts, which can often invalidate the information obtained using 3D systems. Although measurements of volumes and ejection fractions are replicable, 3D echocardiography has shown smaller volumes than MR when quantifying volumes, which prevents one from being substituted for the other. As a result, clinical application is still complicated by the absense of values for normality in the pediatric population. It is not recommended that software developed for the normal left or right ventricle be used with congenitally malformed ventricles until new software or models have been validated.[70,95-97]

The general recommendation for use of 3D transthoracic echocardiography in pediatrics is that the decision should be taken in accordance with the type of patient and the profile of the echocardiography laboratory and/or hospital.

Table 11 – Recommendations for stress echocardiography in pediatric cardiology

Recommendation	Recommendation class	Evidence level
To investigate coronary failure in children after late heart transplantation	IIa	B
Late assessment in Kawasaki disease with coronary abnormalities in the acute phase	IIa	B
During the postoperative period after Jatene procedure and the postoperative periods of abnormal origin and course of coronary arteries, and coronary-cameral fistulae	IIa	B
Ventricular function in myocardiopathy and mitral and aortic valve failure	IIa	B
Screening for ventricular dysfunction in patients treated with chemotherapy regimens including anthracyclines and after transplant, to test myocardial function during exercise	IIa	B
To investigate coronary failure in children with pulmonary atresia with intact ventricular septum, dyslipidemia, insulin-dependent diabetes mellitus, or supravalvular aortic stenosis	IIb	B
Evaluation of pressure gradient behavior in hypertrophic cardiomyopathy and pulmonary and aortic valve stenosis	IIb	B
Evaluation of myocardial reserve in the late postoperative period after atrial switch surgery for great vessel transposition, right ventricle assessment in late postoperative period of tetralogy of Fallot surgery	IIb	B

Table 12 – Additional information yielded by 3D echocardiography on specific anatomic structures and recommendations[72-78,80-82,87,88,91]

Anatomic structure of interest	Modality	Additional information	Recommendation class	Evidence level
Interatrial septum	TTE/TEE	Dimension, format, and location of defect(s)	I – Complex or residual defects II – Central and single defects	B B
Tricuspid valve	TTE/TEE	Morphology of leaflets, subvalvular apparatus (chords), location of regurgitation jets	I	B
Mitral valve	TTE/TEE	Morphology of leaflets, subvalvular apparatus (chords), location of regurgitation jets	I	B
Interventricular septum	TTE/TEE	Dimension, format, and location of complex defect(s)	I	B
LV outflow tract	TTE/TEE	Morphology of subaortic obstruction	I	B
Aortic valve	TTE/TEE	Aortic valve measurements, morphology of leaflets, regurgitation mechanism	I	B
RV outflow tract	TTE/TEE	Morphology and visualization of site of obstruction	III	C
Pulmonary valve	TTE	Morphology	IIa	C

LV: left ventricle; RV: right ventricle; TEE: transesophageal echocardiogram; TTE: transthoracic echocardiogram.

Table 13 – Additional information yielded by 3D echocardiography on congenital defects and recommendations71,79,83-86

Congenital heart disease	Modality	Additional information	Recommendation class	Evidence level
AVSD	TTE/TEE	Dimension of atrial and/or ventricular defect; morphology of leaflets and subvalvular apparatus; assessment of regurgitation jets; dimensions of orifices and ventricles in unbalanced defects	I	B
Discordant AV connection	TTE/TEE	Morphology and function of tricuspid and mitral valves, location and dimensions of related VSD morphology of outflow tracts of the RV and LV	I	B
Complex TGA	TTE/TEE	Morphology and function of tricuspid and mitral valves, location and dimensions of the VSD, anatomy of RV and LV outflow tracts in cases of obstruction	I	B
Tetralogy of Fallot	TTE	Dimension and location of CIV and anatomy of RV outflow tract	III	C
Truncus Arteriosus	TTE/TEE	Morphology of truncal valve*	III	C
Double-outlet RV	TTE	Relationship of atrioventricular valves, position and size of the VSD with the great arteries	III	C

*AV: atrioventricular; AVSD: atrioventricular septal defect; TEE: transesophageal echocardiogram; TGA: transposition of the great arteries; TTE: transthoracic echocardiogram; VSD: ventricular septal defect. *Specifically for assessment of the truncal valve in older patients.*

There is consensus that 3D is a modality that complements rather than substitutes 2D echocardiography, irrespective of the type of disorder.

10. Myocardial Deformation Imaging in Pediatric Patients

Myocardial deformation (strain) is proving to be a useful tool for evaluation of diastolic and systolic function, in both adults and the pediatric population.[98] Myocardial strain analysis by speckle tracking imaging is a method that is independent of the angle of insonation and has low intraobserver and interobserver variability, enabling global and regional ventricular function to be quantified more accurately than with more traditional methods, such as tissue Doppler, fractional shortening, or ejection fraction.[99] Some studies have shown that strain obtained by speckle tracking has high prognostic value, underscoring its utility for both congenital and acquired pathologies.[100]

Notwithstanding, myocardial strain is subject to physiological variations caused by age, sex, heart rate, preload, arterial blood pressure, and body surface area, in addition to the type of software used for the analysis.[101] Efforts are ongoing to establish normal values for strain that can be used as a universal reference in pediatrics, so that myocardial deformation analysis can be incorporated into guidelines and start to be adopted in clinical routines.[102-104] Meanwhile, myocardial deformation imaging has recommendation class II and evidence level B for use in the many different pediatric diseases.

10.1. Ventricular Strain in Acquired Heart Diseases in Childhood

Analysis of right and left ventricular strain is particularly useful in situations in which the intention is to identify systolic and/or diastolic dysfunction while in the subclinical phase. The information obtained from strain analysis makes opportune

therapeutic intervention possible in a range of systemic diseases with myocardial involvement.

Early detection of myocardial damage secondary to use of anthracyclines is one of the most important contributions of myocardial deformation imaging to date and has been incorporated into protocols for monitoring patients in oncology.[105-108]

A correlation has been demonstrated between the degree of inflammatory activity and the values of LV strain and systolic and diastolic LV strain rate in patients with rheumatic diseases, such as childhood-onset systemic lupus erythematosus.[20]

Other studies have confirmed the efficacy of strain obtained using the speckle tracking technique for detection of myocarditis of both autoimmune and viral etiology.[109,110] In cases of dilated cardiomyopathy in children, the pattern of regional compromise of LV strain influenced the outcome of death or transplantation, as demonstrated by Forsha et al.[111] Another use for strain in cases of dilated cardiomyopathy is to detect dyssynchrony, identifying cases that could benefit from resynchronization.[111]

After orthotopic heart transplantation in children, strain analysis has reasonable sensitivity and specificity for identifying which individuals will manifest vascular graft disease in later years.[112] Some reports, including small numbers of transplanted children, suggest there is an association between reduced segmental strain and rejection in endomyocardial biopsies, suggesting the technique could become a less invasive diagnostic instrument in the near future.[113-115]

In young patients with Duchenne muscular dystrophy, studies have demonstrated a significant reduction in longitudinal and radial strain of the inferolateral and anterolateral walls of the LV, even before ejection fraction is compromised or symptoms of heart failure emerge.[116] Several studies have demonstrated improved cardiovascular performance and 10-year survival in patients with Duchenne muscular dystrophy who were put on angiotensin-converting enzyme inhibitors and beta blockers as soon as the first echocardiographic signs of myocardial deterioration were detected, while still asymptomatic from a cardiovascular point of view.[117]

Myocardial strain imaging can also contribute to detection of myocardial compromise in storage disorders such as the mucopolysaccharidoses (MPS)[118] and Pompe disease.[119] Studies have focused attention on myocardial strain as a parameter for assessment of the impact of long-term enzyme replacement on the ventricular function of patients with these diseases.[120]

Myocardial strain analysis has also emerged as a possible method for early diagnosis of myocardial inflammation and ventricular dysfunction in Kawasaki disease.[51] McCandless et al.[121] found evidence that longitudinal LV strain was reduced on initial echocardiograms of patients with Kawasaki who later developed coronary dilation or exhibited resistance to treatment with immunoglobulin. These findings suggest that LV strain could soon come to be used as a tool for risk stratification in Kawasaki patients.[121]

In cases of myocardial dysfunction induced by pediatric sepsis, LV longitudinal and circumferential strain appear to already be reduced in the initial phases, even though ejection fraction is still unimpaired.[122]

In adult patients with chronic renal failure (CRF), reduction of LV longitudinal strain has been confirmed even in initial stages of the disease and with unimpaired ejection fraction. This early compromise of myocardial deformation has been attributed to fibrosis induced by chronic inflammation and uremic toxins. Additionally, the endothelial dysfunction that occurs in CRF may cause an inappropriate vasodilator response, leading to ischemia in an already hypertrophic ventricle. Similar findings have also been documented in pediatric populations, although it remains to be established whether this reduction in longitudinal LV strain can be used as a specific predictor of morbidity and mortality in children with CRF.[123]

Cardiovascular disorders are common among people with HIV infection, but are frequently underdiagnosed and left untreated, which impacts on patients' quality of life and on long-term mortality. They have been attributed both to the direct effects of the virus and to the effects of antiretroviral medications on the myocardium and vasculature. Symptomatic systolic dysfunction is normally only observed in more advanced cases of the acquired immunodeficiency syndrome.[124] More recent studies with children and young adults confirm compromised longitudinal RV and LV strain, in patients who are still asymptomatic and have normal LV ejection fraction. In 2016, these results prompted Naami et al. to suggest that myocardial deformation imaging should be included in echocardiographic examinations of pediatric patients with HIV, with the objective of identifying patients with subclinical dysfunction and increased cardiovascular risk.[125]

In a study that enrolled adolescents and young adults with thalassemia who underwent multiple transfusions, Chen et al.[126] identified a negative correlation between serum ferritin and longitudinal LV strain. Additionally, even after correction for sex, age, serum ferritin, and ventricular mass index, longitudinal LV strain remained an independent predictor of adverse events in thalassemic patients, such as heart failure, arrhythmia, and death (HR: 6.05; $p = 0.033$).[127]

Okumura et al. investigated children and adolescents with idiopathic pulmonary hypertension (IPH), confirming the prognostic value of serial assessment of longitudinal RV strain in the pediatric population. A strain value lower than -14% on the initial echocardiogram identified patients who progressed to lung transplant or death with 100% sensitivity and 54.5% specificity. They concluded that myocardial deformation in pediatric IPH is a more sensitive tool than conventional parameters for evaluation of RV function (TAPSE – tricuspid annular plane systolic excursion, FAC – fractional area change, tricuspid S wave velocity) to detect patients with worse prognosis.[127] In a recent publication, Hooper et al.[128] confirmed the utility of longitudinal RV strain in clinical follow-up of IPH in children, demonstrating that strain values had an excellent correlation with BNP – B-type natriuretic peptide values, in the course of treatment with prostacyclin analogues.[13] Table 14 lists recommendation classes and evidence levels.

10.2. Ventricular Strain in Congenital Heart Disease

Analysis of longitudinal RV strain in a subpulmonary position proved feasible and reproducible for perioperative assessment of several congenital heart disorders.[129] However, in the presence of significant residual obstruction during the postoperative period (PO), parameters for evaluation of the longitudinal RV systolic function, such as TAPSE, S wave velocity, and longitudinal peak systolic strain, did not exhibit adequate correlations with ejection fraction according to MR. In situations with residual pulmonary stenosis or a combination of stenosis and pulmonary failure, RV hypertrophy causes a predominance of circumferential fibers, changing the deformation pattern of this chamber, which is habitually more dependent on longitudinal fibers.[130] Hayabuchi et al.[131] evaluated RV free wall circumferential peak systolic strain in the subcostal view, specifically in children with congenital heart disease with RV pressure overload. Using this method, they found a better correlation between strain values and ejection fraction in the RV.[131] Studies with asymptomatic children in the late postoperative period after surgery for tetralogy of Fallot (T4F) identified compromised biventricular longitudinal systolic peak strain. Some authors found a negative correlation between RV longitudinal systolic peak strain and RV ejection fraction and the pulmonary regurgitation fraction, both estimated by MR.[132] Other studies have documented a negative correlation between LV longitudinal strain and the degree of pulmonary regurgitation, emphasizing the importance of ventricle interdependence.[133] Although myocardial deformation imaging can detect subclinical systolic dysfunction in postoperative T4F patients who progress to pulmonary regurgitation, unfortunately there is not yet any consensus on a strain cutoff value that can indicate the best timing for pulmonary valve replacement.

Patients with the RV in the systemic position also exhibit abnormal myocardial deformation patterns, with predominance of contraction of circumferential fibers. In this condition, the discrete reduction of longitudinal strain is indicative of changes to right ventricular geometry, and not of true systolic dysfunction. This is an adaptive mechanism, which makes contractility of the systemic RV similar to LV contractility. Recent publications therefore suggest a normal range of longitudinal systolic peak strain values in systemic RV that are below those expected for subpulmonary RV (–10% to –14.5%).[130] Longitudinal RV strain values below –10% have been associated with occurrence of adverse events, in the late PO after Senning procedures.[134]

Selection of patients with a single ventricle (SV) for Fontan procedure surgery takes into consideration pulmonary vascular resistance and end-diastolic ventricular pressure. However, current indication criteria have proved fallible for a considerable proportion of these patients, who are subject to complications and extended hospital stays. When associated with pulmonary vascular resistance and end-diastolic ventricular pressure, the preoperative circumferential strain rate improves risk stratification for patients with SV who are candidates for Fontan surgery, irrespective of whether the ventricle has right or left morphology.[135]

In the case of Ebstein's anomaly, myocardial deformation imaging has little to contribute to right ventricular function assessment, since strain has a weak correlation with ejection fraction measured with MR.[136]

Castaldi et al.[137] have demonstrated the utility of left ventricle longitudinal strain to diagnosis of patients with coronary obstruction in late PO after correction of anomalous origin of the left coronary artery. A strain value < –14.8% on echocardiography identified myocardial segments with fibrosis on MR, with sensitivity of 92.5% and specificity of 93.7%.[137]

Table 14 – Recommendations for ventricular strain analysis in acquired heart diseases of childhood[20,51,105-128]

Indication	Recommendation class	Evidence level
Cardiotoxicity in pediatric oncology	IIa	B
Autoimmune and viral myocarditis	IIa	B
Dilated cardiomyopathy: selection for resynchronization therapy	IIa	B
Vascular graft disease after heart transplantation	IIb	B
Rejection after heart transplantation	IIb	B
Muscular dystrophies (e.g. Duchenne)	IIa	B
Storage diseases (e.g. Pompe and MPS)	IIa	B
Kawasaki disease	IIa	C
Sepsis	IIb	B
Chronic renal failure	IIb	B
HIV/AIDS infection	IIa	B
Chronic anemias (e.g. thalassemia)	IIa	B
Pulmonary hypertension	IIa	B

AIDS: acquired immunodeficiency syndrome; HIV: human immunodeficiency virus; MPS: mucopolysaccharidoses.

10.3. Right and Left Atrial Strain in Pediatrics

Analysis of right atrial mechanics using speckle tracking was recently introduced in pediatrics, emerging as a promising tool for detection of right ventricular dysfunction. Hope et al.[139] found a significant reduction in right atrium longitudinal strain in children with IPH. Atrial strain proved more sensitive and specific than conventional right ventricular function assessment parameters for identifying patients with IPH who would later develop unfavorable outcomes (death, pulmonary and/or cardiac transplant).[139]

Several studies have described the clinical implications of left atrial strain measurements using the speckle tracking technique. Left atrium strain in the reservoir phase proved more accurate for estimation of end-diastolic pressure of the LV than classical echocardiographic parameters such as left atrial volume and the E/E' ratio and was also inversely correlated with plasma NT-ProBNP levels.[140]

10.4. Prospects for Utilization of Ventricular Strain in the Fetus

Recent studies have suggested that analysis of myocardial deformation can also contribute to evaluation of biventricular systolic and diastolic function in fetuses. For example, Miranda et al. documented reduced early and late diastolic strain rate in the longitudinal axes of RV and LV in fetuses with diabetic mothers. Additionally, they also observed reductions in right ventricle longitudinal systolic peak strain in comparison with normal fetuses of the same gestational age. These authors pointed out that diastolic deformation compromise was irrespective of the presence of septal hypertrophy. They concluded that myocardial deformation analysis could detect subclinical changes in the fetuses of diabetic mothers before classical echocardiographic parameters are able to do so.[141]

Dusenbery et al.[138] confirmed the association between reduced LV longitudinal strain and presence of myocardial fibrosis, assessing children and young adults with aortic valve stenosis and preserved LV ejection fraction.[138] It is known that adults with aortic stenosis who have late enhancement on MR with gadolinium and reduced LV longitudinal strain values have higher mortality rates after valve interventions.[138] See Table 15 for recommendation classes and evidence levels.

Table 15 – Recommendations for ventricular strain in congenital heart disease[129-135,137]

Indication	Recommendation class	Evidence level
Functional evaluation of subpulmonary RV (e.g. T4F)	IIb	B
Functional evaluation of systemic RV (e.g. PO of Senning procedure, CCTGA)	IIb	B
Evaluation of SV before Fontan procedure	IIb	B
Evaluation of SV after Fontan procedure	IIb	B
Assessment of LV after ALCAPA surgical repair	IIa	B
Evaluation of LV function in aortic stenosis	IIb	B

ALCAPA: anomalous left main coronary artery from the pulmonary artery; CCTGA: congenitally corrected transposition of the great arteries; LV: left ventricle; PO: postoperative; RV: right ventricle; SV: single ventricle; T4F: tetralogy of Fallot.

References

1. Barberato SH, Romano MMD, Beck ALS, Rodrigues ACT, Almeida ALC, Assunção BMBL, et al. Posicionamento sobre Indicações da Ecocardiografia em Adultos – 2019. Arq Bras Cardiol. 2019; 113(1):135-181.
2. Ferencz C, Rubin JD, McCarter RJ, Brenner JI, Neil CA, Perry LW. Congenital heart disease: prevalence at livebirth. The Baltimore-Washington Infant Study. Am J Epidemiol.1985; 121(1):31-6.
3. Wren C, Richmond S, Donaldson L. Temporal variability in birth prevalence of cardiovascular malformations. Heart. 2000; 83(4):414-9.
4. Yagel S, Weissman A, Rotstein Z, 2 Manor M, Hegesh J, Stoutenbeek P. Congenital heart defects: natural course and in utero development. Circulation. 1997; 96(2):550-5.
5. van Engelen AD, Weijtens O, Brenner JI, Kleinman CS, Copel JA, Stoutenbeek P. et al. Management outcome and follow-up of fetal tachycardia. J Am Coll Cardiol. 1994; 24(5):1371-5.
6. Simpson JM, Sharland GK. Fetal tachycardias: management and outcome of 127 consecutive cases. Heart.1998; 79(6):576-81.
7. Donofrio MT, Moon-Grady AJ, Hornberger LK, Copel JA, Slonsky MS, Abuhamed A, et al. Diagnosis and treatment of fetal cardiac disease: a scientific statement from the American Heart Association. Circulation. 2014; 129(21):2183-242.
8. Pedra SRF, Zielinnsky P, Binotto CN, Martins CN, Fonseca ES, Guimarães IC, et al., Sociedade Brasileira de Cardiologia. Diretriz Brasileira de Cardiologia Fetal - 2019. Arq Bras Cardiol. 2019; 112 (5):600-48.
9. Barbosa MM, Nunes MCP, Campos Filho O,Camarozano A, Rabischoffsky A, Maciel BC. , et al., Sociedade Brasileira de Cardiologia. Diretrizes das Indicações da Ecocardiografia. Arq Bras Cardiol. 2009; 936(Supl 3):e265-e302.
10. Noori SS, Seri I. Principles of Developmental Cardiovascular Physiology and Pathophysiology. In: Polin RA.ed. Hemodynamics and Cardiology: Neonatology Questions. 2nd ed. Philadelphia, PA: Elsevier Saunders; 2012.p.3-27.
11. Mertens L, Seri I, Marek J, Arlett0z R, Barker P, McNamara P, et al. Targeted Neonatal Echocardiography in the Neonatal Intensive Care Unit: practice guidelines and recommendations for training. Writing Group of the American Society of Echocardiography (ASE) in collaboration with the European Association of Echocardiography (EAE) and the Association for European Pediatric Cardiologists (AEPC). J Am Soc Echocardiogr. 2011; 24(10):1057-78.
12. Kemper AR, Mahle WT, Martin GR, Cooley WC, Kumar P, Morrow WP. Strategies for implementing screening for critical congenital heart disease. Pediatrics 2011; 128(5):e1259-67.
13. Afiune JY, Leal SMB, Andrade JL. Avaliação ecocardiográfica das alterações cardiovasculares funcionais do recém-nascido. Rev Bras Ecocardiogr. 2002; 15(2):41-67.
14. Adatia I, Beghetti M. Immediate postoperative care. Cardiol Young . 2009; 19 (Suppl 1):23-7.
15. Badesch DB, Champion HC, Sanchez MA, Hoeper MM, Loyd JE, Manes A. et al. Diagnosis and assessment of pulmonary arterial hypertension. J Am Coll Cardiol. 2009; 54(1 Suppl): S55-66.
16. Cheitlin MD, Armstrong WF, Aurigemma GP. ACC/AHA/ASE 2003 Guideline Update for the Clinical Application of Echocardiography: summary article. A report of the American College of Cardiology/American Heart Association Task Force on Practice Guidelines (ACC/AHA/ASE Committee to Update the 1997 Guidelines for the Clinical Application of Echocardiography). J Am Soc Echocardiogr.2003; 16:1091-110.
17. Lai WW, Geva T, Shirali GS, Frommelt PC, Humes RA, Brook MM, et al. Guidelines and standards for performance of a pediatric echocardiogram: a report from the Task Force of the Pediatric Council of the American Society of Echocardiography. J Am Soc Echocardiogr. 2006; 19(12):1413-30.
18. Campbell RM, Douglas PS, Eidem BW, Lai WW, Lopez L, Sachdeva R. ACC/AAP/AHA/ASE/HRS/SCAI/SCCT/SCMR/SOPE 2014 appropriate use criteria for initial transthoracic echocardiography in outpatient pediatric cardiology: a report of the American College of Cardiology Appropriate Use Criteria Task Force, American Academy of Pediatrics, American Heart Association,

American Society of Echocardiography, Heart Rhythm Society, Society for Cardiovascular Angiography and Interventions, Society of Cardiovascular Computed Tomography, Society for Cardiovascular Magnetic Resonance, and Society of Pediatric Echocardiography. J Am Coll Cardiol. 2014; 64(19):2039-60.

19. Leal GN, Silva KF, França CM, Lianza AC, Andrade JL, Kozu K. Subclinical right ventricle systolic dysfunction in chlidhood-onset systemic lupus erythematosus: insights from two-dimensional speckle-tracking echocardiography. Lupus .2015; 24(6):613-20.

20. Leal GN, Silva KF, Lianza AC, Giacomin MF, Andrade JL, Campos LM. Subclinical left ventricular dysfunction in childhood-onset systemic lupus erythematosus: a two-dimensional speckle-tracking echocardiography study. Scand J Rheumatol. 2016 ; 45(3):202-9.

21. Lianza AC, Aikawa NE, Morae JC, Leal GN, Morhy SS, Andrade JL. Long-term evaluation of cardiac function in juvenile idiopathic arthritis under anti-TNF therapy. Clin Exp Rheumatol.2014; 32(5):754-9.

22. Gewitz MH, Baltimore RS, Tani LY, Sable CA, Shulman ST, Carapetis J. Revision of the Jones Criteria for the diagnosis of acute rheumatic fever in the era of Doppler echocardiography: a scientific statement from the American Heart Association. Circulation. 2015; 131(20):1806-18.

23. Ryan TD, Nagarajan R, Godown J. Pediatric cardio-oncology: development of cancer treatment-related cardiotoxicity and the therapeutic approach to affected patients. Curr Treat. Options Oncol. 2019; 20(7):56.

24. Flynn JT, Kaelber DC, Baker-Smith CM, Blowey D, Carroll AE, Daniels SR. Clinical practice guideline for screening and management of high blood pressure in children and adolescents. Pediatrics. 2017; 140(3):1-72.

25. Anuardo P, Verdier M, Gormezano NW, Ferreira GR, Leal GN, Lianza A. Subclinical pulmonary hypertension in childhood systemic lupus erythematosus associated with minor disease manifestations. Pediatr Cardiol. 2007; 38(2):234-9.

26. Patel MD, Breatnach CR, James AT, Choudhry S, McNamara PJ, Jain A, et al. Echocardiographic assessment of right ventricular afterload in preterm infants: maturational patterns of pulmonary artery acceleratio time over the first year of age and implications for pulmonary hypertension. J Am Soc Echocardiogr. 2019; 32(7):884-894.

27. Koestenberger M, Apitz C, Abdul-Khaliq H, Hansmann G. Transthoracic echocardiography for the evaluation of children and adolescents with suspected or confirmed pulmonary hypertension. Expert consensus statement on the diagnosis and treatment of paediatric pulmonary hypertension. The European Paediatric Pulmonary Vascular Disease Network, endorsed by ISHLT and D6PK. Heart 2016; 102 (Suppl 2):ii14-22.

28. Lipshultz SE, Wilkinson JD, Thompson B, Cheng I,Briston DA, Shearer WT. Cardiac effects of highly active antiretorviral therapy in perinatally HIV-infected children: The CHAART-@ Study. J Am Coll Cardiol. 2017; 70(18):2240-7.

29. Kindel SJ, Hsu HH, Hussain T, Johnson JN, McMahon Cj, Kutty S, et al. Multimodality noninvasive imaging in the monitoring of pediatric heart transplantation. J Am Soc Echocardiogr. 2017; 30(9):859-70.

30. Platts DG, Sedgwick JF, Burstow DJ, Mullany DV, Fraser JF. The role of echocardiography in the management of patients supported by extracorporeal membrane oxygenation. J Am Soc Echocardiogr. 2012; 25:131-41.

31. Newburger JW, Takahashi M, Gerver MA. Diagnosis, treatment, and long-term management of Kawasaki disease: a statement for health professionals from the Committee on Rheumatic Fever, Endocarditis and Kawasaki Disease, Council on Cardiovascular Disease in the Young, American Heart Association. Circulation.2004; 110(17):2747–71.

32. Gilboa SM, Devine OJ, Kucik JE, et al. Congenital Heart Defects in the United States: Estimating the Magnitude of the Affected Population in 2010. Circulation 2016; 134(2):101-9.

33. Di Nardo JA. Grown-up congenital heart (GUCH) disease: an evolving global challenge. Ann Card Anaesth. 2008; 11(1):3-5.

34. Van der Bom T, Bouma BJ, Meijboom FJ,Zwinderman AH, Mulder BJ, et al. The prevalence of adult congenital heart disease, results froma asystematic review and evidence based calculation. Am Heart J. 2012; 164(4):568-75.

35. Thakkar AN, Chinnadurai P, Lin CH. Adult congenital heart disease: magnitude of the problem. Curr Opin Cardiology 2017; 32(5):467-74.

36. Baumgartner H, Bonhoeffer P, De Groot NM et al. ESC Guidelines for the management of grown-up congenital heart disease (new version 2010). Eur Heart J.2010; 31(23):2915-57.

37. Simpson J, Lopez L, Acar P, et al. Three-dimensional Echocardiography in Congenital Heart Disease: An Expert Consensus Document from the European Association of Cardiovascular Imaging and the American Society of Echocardiography. J Am Soc Echocardiogr. 2017; 30:1-27.

38. Graziani F, Delogu AB. Evaluation of Adults With Congenital Heart Disease. World J Pediatr Congenit Heart Surg. 2016; 7(2):185-91.

39. Bhatt AB, Foster E, Kuehl K, Alpert J, Brabeck S, Crumb S, et al. Congenital heart disease in the older adult: a scientific statement from the American Heart Association. Circulation. 2015; 131(21):1884-931.

40. Group TTACW, Douglas PS, Khandheria B et al. ACCF/ASE/ACEP/ASNC/SCAI/SCCT/SCMR 2007 appropriateness criteria for transthoracic and transesophageal echocardiography: a report of the American College of Cardiology Foundation Quality Strategic Directions Committee Appropriateness Criteria Working Group, American Society of Echocardiography, American College of Emergency Physicians, American Society of Nuclear Cardiology, Society for Cardiovascular Angiography and Interventions, Society of Cardiovascular Computed Tomography, and the Society for Cardiovascular Magnetic Resonance. Endorsed by the American College of Chest Physicians and the Society of Critical Care Medicine. J Am Soc Echocardiogr. 2007; 20:787-805.

41. Stout KK, Daniels CJ, Aboulhosn JA, Bozkurt B, Broberg CS, Colman JM, et al. 2018 AHA/ACC Guideline for the management of adults with congenital heart disease. A report of the American College of Cardiology/American Heart Association Task Force on Clinical Practice Guidelines. Circulation 2019; 139(14):e698-e800.

42. Silversides CK, Kiess M, Beauchesne L, Bradley T, Broberg CS, Colman JM. et al. Canadian Cardiovascular Society 2009 Consensus Conference on the management of adults with congenital heart disease: outflow tract obstruction, coarctation of the aorta, tetralogy of Fallot, Ebstein anomaly and Marfan's syndrome. Canad J Cardiol. 2010; 26(3):e80-97.

43. Silversides CK, Salehian O, Oechslin E, Schwerzmann M, Muhll IV, Klairy P, et al. Canadian Cardiovascular Society 2009 Consensus Conference on the management of adults with congenital heart disease: complex congenital cardiac lesions. Can J Cardiol.2010; 26(3):e98-117.

44. Hiratzka LF, Bakris GL, Beckman JA, et al. 2010 ACCF/AHA/AATS/ACR/ASA/SCA/SCAI/SIR/STS/SVM Guidelines for the diagnosis and management of patients with thoracic aortic disease. A Report of the American College of Cardiology Foundation/American Heart Association Task Force on Practice Guidelines, American Association for Thoracic Surgery, American College of Radiology,American Stroke Association, Society of Cardiovascular Anesthesiologists, Society for Cardiovascular Angiography and Interventions, Society of Interventional Radiology, Society of Thoracic Surgeons,and Society for Vascular Medicine. J Am Coll Cardiol.2010; 55:e27-e129.

45. Puchalski MD, Lui GK, Miller-Hance WC,Brook MM, Young LT, Bhat A. Guidelines for Performing a Comprehensive Transesophageal Echocardiographic Examination in Children and All Patients with Congenital Heart Disease: Recommendations from the American Society of Echocardiography. J Am Soc Echocardiogr. 2019; 32(2):173-215.

46. Bettex DA, Pretre R, Jenni R, Schmid ER. Cost-effectiveness of routine intraoperative transesophageal echocardiography in pediatric cardiac surgery: a 10-year experience. Anesthes Analg. 2005; 100(5):1271-5.

47. Rigby ML. Transoesophageal echocardiography during interventional cardiac catheterisation in congenital heart disease. Heart. 2001; 86(Suppl 2):II23-9.

48. Pellikka PA, Nagueh SF, Elhendy AA, Kuehl CA, Sawada SG, American Society of E. American Society of Echocardiography recommendations for performance, interpretation, and application of stress echocardiography. J Am Soc Echocariogr. 2007; 20(9):1021-41.

49. Sicari R, Nihoyannopoulos P, Evangelista A, Kasprzak J, Lancellotti P, Poldermans D. Stress Echocardiography Expert Consensus Statement--Executive Summary: European Association of Echocardiography (EAE) (a registered branch of the ESC). Eur Heart J. 2009; 30(3):278-89.

50. Noto N, Kamiyama H, Karasawa K,Ayusawa M, Sumitomo N, Okada T, et al. Long-term prognostic impact of dobutamine stress echocardiography in patients with Kawasaki disease and coronary artery lesions: a 15-year follow-up study. J Am Coll Cardiol.2014; 63(4):337-44.

51. McCrindle BW, Rowley AH, Newburger JW et al. Diagnosis, Treatment, and Long-Term Management of Kawasaki Disease: A Scientific Statement for Health Professionals From the American Heart Association. Circulation. 2017; 135(17):e927-e999.

52. Dipchand AI, Bharat W, Manlhiot C, Safi M, Lobach NE, McCrindle BW. A prospective study of dobutamine stress echocardiography for the assessment of cardiac allograft vasculopathy in pediatric heart transplant recipients. Pediat Transplant. 2008; 129(5):570-6.

53. Ou P, Khraiche D, Celermajer DS,Agnoletti G, Sang KH, Thalabard JC, et al. Mechanisms of coronary complications after the arterial switch for transposition of the great arteries. The Journal of thoracic and cardiovascular surgery 2013; 145(5):1263-9.

54. Hui L, Chau AK, Leung MP, Chiu CS, Cheung YF. Assessment of left ventricular function long term after arterial switch operation for transposition of the great arteries by dobutamine stress echocardiography. Heart. 2005; 91(1):68-72.

55. Brothers JA, Frommelt MA, Jaquiss RDB, Myerburg RJ, Fraser CD Jr., Tweddell JS. Expert consensus guidelines: Anomalous aortic origin of a coronary artery. J Thorac Cardiovasc Surg. 2017; 153(6):1440-57.

56. Lancellotti P, Pellikka PA, Budts W, et al. The Clinical Use of Stress Echocardiography in Non-Ischaemic Heart Disease: Recommendations from the European Association of Cardiovascular Imaging and the American Society of Echocardiography. J Am Soc Echocardiogr. 2017; 30:101-38.

57. Cifra B, Dragulescu A, Brun H,McCrindle BW, Dipchand A, MertensL, et al. Left ventricular myocardial response to exercise in children after heart transplant. The J Heart Lung Transplant. 2014; 33(2):1241-7.

58. De Meester P, Buys R, Van De Bruaene A, Gabroels C, Voigt JU, Vanhees L, et al. Functional and haemodynamic assessment of mild-to-moderate pulmonary valve stenosis at rest and during exercise. Heart. 2014; 100(17):1354-9.

59. Hasan BS, Lunze FI, McElhinney DB, Stantchevo E, Bron DW, Rhodes J. et al. Exercise stress echocardiographic assessment of outflow tract and ventricular function in patients with an obstructed right ventricular-to-pulmonary artery conduit after repair of conotruncal heart defects. Am J Cardiol. 2012; 110(10):1527-33.

60. Chen CK, Cifra B, Morgan GJ, Sarcola T, Slorach C, Wei H. Left Ventricular Myocardial and Hemodynamic Response to Exercise in Young Patients after Endovascular Stenting for Aortic Coarctation. J Am Soc Echocardiogr. 2016; 29(3):237-46.

61. Ait-Ali L, Siciliano V, Passino C, Molinoro S, Pasanisi E, Sicari R, et al. Role of stress echocardiography in operated fallot: feasibility and detection of right ventricular response. J Am Soc Echocardiogr.2014; 27(12): 1319-28.

62. Oosterhof T, Tulevski, II, Roest AA,Steendijk P, Vliegen HW, Wall E, et al. Disparity between dobutamine stress and physical exercise magnetic resonance imaging in patients with an intra-atrial correction for transposition of the great arteries. J Cardiovasc Magn Reson. 2005; 7(2):383-9.

63. Vogt M, Kuhn A, Wiese J, Eicken A, Hess J, Vogel M. Reduced contractile reserve of the systemic right ventricle under Dobutamine stress is associated with increased brain natriuretic peptide levels in patients with complete transposition after atrial repair. Eur J Echocardiogr.2009; 10(5):691-4.

64. Klewer SE, Goldberg SJ, Donnerstein RL, Berg RA, Hutter JJ Jr. Dobutamine stress echocardiography: a sensitive indicator of diminished myocardial function in asymptomatic doxorubicin-treated long-term survivors of childhood cancer. J Am Coll Cardiol. 1992; 19(2):394-401.

65. Ryerson AB, Border WL, Wasilewski-Masker K, Goodman M, Meachman L, Austin H. Assessing anthracycline-treated childhood cancer survivors with advanced stress echocardiography. Pediatr Blood Cancer. 2015; 62(3):502-8.

66. Cifra B, Dragulescu A, Border WL, Mertens L. Stress echocardiography in paediatric cardiology. Eur Heart J Cardiovasc Imag.2015; 16(10):1051-9.

67. Hecht HS, DeBord L, Sotomayor N, Shaw R, Dunlap R, Ryan C. Supine bicycle stress echocardiography: peak exercise imaging is superior to postexercise imaging. J Am Soc Echocardiogr.1993; 6(3 pt 1):265-71.

68. Simpson JM. Real-time three-dimensional echocardiography of congenital heart disease using a high frequency paediatric matrix transducer. Eur J Echocardiogr. 2008; 9(2):222-4.

69. van der Zwaan HB, Helbing WA, McGhie JS, Geleijnse ML, Luijnenburg SE, Hesselink JW. Clinical value of real-time three-dimensional echocardiography for right ventricular quantification in congenital heart disease: validation with cardiac magnetic resonance imaging. J Am Soc Echocardiogr; 2010; 23(2):134-40.

70. Friedberg MK, Su X, Tworetzky W, Soriano BD, Powell AJ, Marx GR. Validation of 3D echocardiographic assessment of left ventricular volumes, mass, and ejection fraction in neonates and infants with congenital heart disease: a comparison study with cardiac MRI. Circ Cardiovasc Imaging 2010; 3(6):735-42.

71. Takahashi K, Mackie AS, Thompson R,Naami G, Inage A, Rebyka IM. Quantitative real-time three-dimensional echocardiography provides new insight into the mechanisms of mitral valve regurgitation post-repair of atrioventricular septal defect. J Am Soc Echocardiogr 2012; 25(11):1231-44.

72. Simpson J, Lopez L, Acar P, Friedberg MK, Khoo NS, Ko HH, et al. Three-dimensional Echocardiography in Congenital Heart Disease: An Expert ConsensusDocument from the European Association of Cardiovascular Imaging and the American Society of Echocardiography J Am Soc Echocardiogr. 2017; 30(1):1-27.

73. McGhie JS, van den Bosch AE, HaarmanMG, Ren B, Roos-Hesselink JW, Witsenburg M, et al. Characterization of atrial septal defect by simultaneous multiplane two-dimensional echocardiography. Eur Heart J Cardiovasc Imaging 2014; 15(10):1145-51.

74. Pushparajah K, MillerOI, Simpson JM. 3Dechocardiography of the atrial septum: anatomical features and landmarks for the echocardiographer. JACC Cardiovasc Imaging 2010; 3(9):981-4.

75. Bharucha T, Anderson RH, Lim ZS, Vettukattil JJ. Multiplanar review of three-dimensional echocardiography gives new insights into the morphology of Ebstein's malformation. Cardiol Young. 2010; 20(1):49-53.

76. van Noord PT, Scohy TV, McGhie J, Bogers AJJC. Three-dimensional transesophageal echocardiography in Ebstein's anomaly. Interact Cardiovasc Thorac Surg. 2010; 10(5):836-7.

77. Roberson DA, Cui W, Patel D, Tsang W, Sugeng L, Weinert L, et al. Three-dimensional transesophageal echocardiography of atrial septal defect: a qualitative and quantitative anatomic study. J Am Soc Echocardiogr. 2011; 24(6):600-10.

78. Sivakumar K, Singhi A, Pavithran S. Enface reconstruction of VSD on RV septal surface using real-time 3D echocardiography. JACC Cardiovasc Imaging. 2012; 5(11):1176-80.

79. Kutty S, Smallhorn JF. Evaluation of atrioventricular septal defects by three-dimensional echocardiography: benefits of navigating the third dimension. J Am Soc Echocardiogr. 2012; 25(9):932-44.

80. Marechaux S, Juthier F, Banfi C, Vincentelli A, Prat A, Ennezat P-V. Illustration of the echocardiographic diagnosis of subaortic membrane tenosis in adults: surgical and live three-dimensional transoesophageal findings. Eur J Echocardiogr. 2011; 12(1):E2.

81. Noel CV, Choy RM, Lester JR, Soriano BD. Accuracy of matrix-array three-dimensional echocardiographic measurements of aortic root dilation and comparison with two-dimensional echocardiography in pediatric patients. J Am Soc Echocardiogr. 2012; 25(3):287-93.

82. Hlavacek A, Lucas J, Baker H, Chessa K, Shirali G. Feasibility and utility of three-dimensional color flow echocardiography of the aortic arch: The ''echocardiographic angiogram''. Echocardiography. 2006; 23:860-4.

83. Valente AM, Cook S, Festa P, Ko HH, Krishnamurthy R, Taylor AM, et al. Multimodality imaging guidelines for patients with repaired tetralogy of fallot: a report from the American Society of Echocardiography: developed in collaboration with the Society for Cardiovascular Magnetic Resonance and the Society for Pediatric Radiology. J Am Soc Echocardiogr. 2014; 27(5):111-41.

84. Abadir S, Leobon B, Acar P. Assessment of tricuspid regurgitation mechanism by three-dimensional echocardiography in an adult patient with congenitally corrected transposition of the great arteries. Arch Cardiovasc Dis. 2009; 102(5):459-60.

85. Del Pasqua A, Sanders SP, De Zorzi A, Toscano A, Iacobelli R, Pierli C, et al. Impact of three-dimensional echocardiography in complex congenital heart defect cases: the surgical view. Pediatr Cardiol. 2009; 30(3):293-300.

86. Pushparajah K, Barlow A, Tran V-H, Miller OI, Zidere V, Vaidyanathan B, et al. A systematic three-dimensional echocardiographic approach to assist surgical planning in double outlet right ventricle. Echocardiography. 2013; 30(2):234-8.

87. Saric M, Perk G, Purgess JR, Kronzon I. Imaging atrial septal defects by real-time three-dimensional transesophageal echocardiography: stepby-step approach. J Am Soc Echocardiogr.(11):1128-35.

88. Charakida M, Qureshi S, Simpson JM. 3D echocardiography for planning and guidance of interventional closure of VSD. JACC Cardiovasc Imaging. 2013; 6(1):120-3.

89. Giannakoulas G, Thanopoulos V. Three-dimensional transesophageal echocardiography for guiding percutaneous fontan fenestration closure. Echocardiography. 2014; 31(7):e230-1.

90. Raslan S, Nanda NC, Lloyd L, Khairnar P, Reilly SD, Holman WL. Incremental value of live/real time three-dimensional transesophageal echocardiography over the two-dimensional technique in the assessment of sinus of valsalva aneurysm rupture. Echocardiography. 2011; 28(8):918-20.

91. Cavalcante JL, Rodriguez LL, Kapadia S, Tuzcu EM, Stewart WJ. Role of echocardiography in percutaneous mitral valve interventions. JACC Cardiovasc Imaging. 2012; 5(7):733-46.

92. Cua CL, Kollins K, Roble S, Holzer RJ. Three-dimensional image of a baffle leak in a patient with a mustard operation. Echocardiography. 2014; 31(10):e315-6.

93. Deoring M, Braunschweig F, Eitel C, Gaspar T, Wetzel U, Nitsche B, et al. Individually tailored left ventricular lead placement: lessons from multimodality integration between three-dimensional echocardiography and coronary sinus angiogram. Europace. 2013; 15(5):718-27.

94. Mishra J, Puri HP, Hsiung MC, Misra S, Khairnar P, Laxmi Gollamudi B, et al. Incremental value of live/real time three-dimensional over two dimensional transesophageal echocardiography in the evaluation of right coronary artery fistula. Echocardiography. 2011; 28(7):805-8.

95. Renella P, Marx GR, Zhou J, Gauvreau K, Geva T. Feasibility and reproducibility of three-dimensional echocardiographic assessment of right ventricular size and function in pediatric patients. J Am Soc Echocardiogr. 2014; 27(8):903-10.

96. Maffessanti F, Muraru D, Esposito R, Gripari P, Ermacora D, Santoro C, et al. Age-, body size-, and sex-specific reference values for right ventricular volumes and ejection fraction by three-dimensional echocardiography: a multicenter echocardiographic study in 507 healthy volunteers. Circ Cardiovasc Imaging. 2013; 6(5):700-10.

97. Leibundgut G, Rohner A, Grize L, Bernheim A, Kessel-Schaefer A, Bremerich J, et al. Dynamic assessment of right ventricular volumes and function by real-time three-dimensional echocardiography: a comparison study with magnetic resonance imaging in 100 adult patients. J Am Soc Echocardiogr. 2010; 23(2):116-26.

98. Dragulescu A, Mertens LL. Developments in echocardiographic techniques for the evaluation of ventricular function in children. Arch Cardiovasc Dis. 2010; 103(11-12):603 -14.

99. Mor-Avi V, Lang RM, Badano LP, Belohlavek M, Cardim NM, Derumeaux G, et al. Current and evolving echocardiographic techniques for the quantitative evaluation of cardiac mechanics: ASE/EAE consensus statement on methodology and indications endorsed by the Japanese Society of Echocardiography. Eur J Echocardiogr. 2011; 12(3):167-205.

100. Collier P, Phelan D, Klein A. Test in Context: Myocardial Strain Measured by Speckle-Tracking Echocardiography. J Am Coll Cardiol. 2017; 69(8):1043-56.

101. Forsey J, Friedberg MK, Mertens L. Speckle tracking echocardiography in pediatric and congenital heart disease. Echocardiography. 2013; 30(4):447-59.

102. Levy PT, Sanchez Mejia AA, Machefsky A, Fowler S, Holland MR, Singh GK. Normal ranges of right ventricular systolic and diastolic strain measures in children: a systematic review and meta-analysis. J Am Soc Echocardiogr. 2014; 27(5):549-60.

103. Levy PT, Machefsky A, Sanchez AA, Patel MD, Rogal S, Fowler S, et al. Reference Ranges of Left Ventricular Strain Measures by Two-Dimensional Speckle-TrackingEchocardiography in Children: A Systematic Review and Meta-Analysis. J Am Soc Echocardiogr. 2016; 29(3):209-25.

104. Kutty S, Padiyath A, Li L, Peng Q, Rangamani S, Schuster A, et al.

105. Larsen CM, Mulvagh SL. Cardio-oncology: what you need to know now for clinical practice and echocardiography. Echo Res Pract. 2017; 4(1): R33-R41.

106. Plana JC, Galderisi M, Barac A, Ewer MS, Ky B, Scherrer-Crosbie M, et al.Expert consensus for multimodality imaging evaluation of adult patients during and after cancer therapy: a report from the American Society of Echocardiography and the European Association of Cardiovascular Imaging. Eur Heart J Cardiovasc Imaging. 2014; 15(10):1063-93.

107. Negishi T, Thavendiranathan P, Negishi K, Marwick TH; SUCCOUR investigators. Rationale and Design of the Strain Surveillance of Chemotherapy for Improving Cardiovascular Outcomes (SUCCOUR) Trial. JACC Cardiovasc Imaging. 2018. pii: S1936-878X (18)30302-4.

108. Agha H, Shalaby L, Attia W, Abdelmohsen G, Aziz OA, Rahman MY. Early Ventricular Dysfunction After Anthracycline Chemotherapy in Children. Pediatr Cardiol. 2016; 37(3):537-44.

109. Leal GN, Diniz MF, Brunelli J, Lianza AC, Sallum AM, Silva CA. What are the benefits of two-dimensional speckle tracking echocardiography for diagnosis and treatment follow-up of childhood-onset systemic lupus erythematosus myocarditis? Rev Assoc Med Bras. 2016; 62(6):490-3.

110. Caspar T, Germain P, El Ghannudi S, Morel O, Samet H, Trinh A, et al. Acute Myocarditis Diagnosed by Layer-Specific 2D Longitudinal Speckle Tracking Analysis. Echocardiography. 2016; 33(1):157-8.

111. Forsha D, Slorach C, Chen CK, Sherman A, Mertens L, Barker P, et al. Patterns of Mechanical Inefficiency in Pediatric Dilated Cardiomyopathy and Their Relation to LeftVentricular Function and Clinical Outcomes. J Am Soc Echocardiogr. 2016; 29(3):226-36.

112. Boruta RJ, Miyamoto SD, Younoszai AK, Patel SS, Landeck BF 2nd. Worsening in Longitudinal Strain and Strain Rate Anticipates Development of pediatric transplant coronary artery vasculopathy as soon as one year following transplant. Pediatr Cardiol. 2018; 39(1):129-39.

113. Badano LP, Miglioranza MH, Edvardsen T, Colafranceschi AS, Muraru D, Bacal F, Nieman K, et al. European Association of Cardiovascular Imaging/Cardiovascular Imaging Department of the Brazilian Society of Cardiology recommendations for the use of cardiac imaging to assess and follow patients after heart transplantation. Eur Heart J Cardiovasc Imaging. 2015; 16(9):919-48.

114. Gursu HA, Varan B, Sade E, Erdogan I, Sezgin A, Aslamaci S. Evaluation of Acute Rejection by Measuring Strain and Strain Rate in Children with Heart Transplant: A Preliminary Report. Exp Clin Transplant. 2017; 15(5):561-6.

115. Dandel M, Hetzer R. Post-transplant surveillance for acute rejection and allograft vasculopathy by echocardiography: Usefulness of myocardial velocity and deformation imaging. J Heart Lung Transplant. 2017; 36(2):117-31.

116. Jo WH, Eun LY, Jung JW, Choi JY, Gang SW. Early marker of myocardial deformation in children with Duchenne Muscular Dystrophy assessed using echocardiographic myocardial strain analysis. Yonsei Med J. 2016 ; 57(4):900-4.

117. Duboc D, Meune C, Pierre B, Wahbi K, Eymard B, Toutain A, et al. Perindopril preventive treatment on mortality in Duchenne muscular dystrophy: 10 years' follow-up. Am Heart J. 2007; 154(3):596-602.

118. Borgia F, Pezzullo E, Schiano Lomoriello V, Sorrentino R, Lo Iudice F, Cocozza S, et al. Myocardial deformation in pediatric patients with mucopolysaccharidoses: A two-dimensional speckle tracking echocardiography study. Echocardiography. 2017; 34(2):240-9.

119. Chen CA, Chien YH, Hwu WL, et al. Left ventricular geometry, global function, and dyssynchrony in infants and children with Pompe cardiomyopathy undergoing enzyme replacement therapy. J Cardiac Fail. 2011; 17(11):930–6.

120. Avula S, Nguyen TM, Marble M, Lilje C. Cardiac response to enzyme replacement therapy in infantile Pompe disease with severe hypertrophic cardiomyopathy. Echocardiography. 2017; 34(4):621-4.

121. McCandless RT, Minich LL, Wilkinson SE, McFadden ML, Tani LY, Menon SC. Myocardial strain and strain rate in Kawasaki disease. Eur Heart J Cardiovasc Imaging. 2013 Nov; 14(11):1061-8.

122. Haileselassie B, Su E, Pozios I, Fiskum T, Thompson R, Abraham T. Strain echocardiography parameters correlate with disease severity in children and infants with sepsis. Pediatr Crit Care Med. 2016 May; 17(5):383-90.

123. van Huis M, Schoenmaker NJ, Groothoff JW, van der Lee JH, van Dyk M Gewillig M, et al. Impaired longitudinal deformation measured by speckle-tracking echocardiography in children with end-stage renal disease. Pediatr Nephrol. 2016; 31(9):1499-508.

124. Starc TJ, Lipshultz SE, Easley KA, Kaplan S, Bricker JT, Colan SD, et al. Incidence of cardiac abnormalities in children with human immunodeficiency virus infection: The prospective P2C2 HIV study. J Pediatr. 2002 ; 141(3):327-34.

125. Al-Naami G, Kiblawi F, Kest H, Hamdan A, Myridakis D. Cardiac mechanics in patients with human immunodeficiency virus: a study of systolic myocardial deformation in children and young adults. Pediatr Cardiol. 2014; 35(6):1046-51.

126. Chen MR, Ko HS, Chao TF, Liu HC, Kuo JY, Bulwer BE, et al. Relation of myocardial systolic mechanics to serum ferritin level as a prognosticator in thalassemia patients undergoing repeated transfusion. Echocardiography. 2015; 32(1):79-88.

127. Okumura K, Humpl T, Dragulescu A, Mertens L, Friedberg MK. Longitudinal assessment of right ventricular myocardial strain in relation to transplant-free survival in children with idiopathic pulmonary hypertension. *J Am Soc Echocardiogr*. 2014; 27(12):1344-51.

128. Hopper RK, Wang Y, DeMatteo V, Santo A, Kawut SM, Elci OU, *et al*. Right ventricular function mirrors clinical improvement with use of prostacyclin analogues in pediatric pulmonary hypertension. *Pulm Circ*. 2018; 8(2):2045894018759247.

129. Forsey J, Friedberg MK, Mertens L. Speckle tracking echocardiography in pediatric and congenital heart disease. Echocardiography. 2013; 30(4):447-59.

130. Karsenty C, Hadeed K, Dulac Y, Semet F, Alacoque X, Breinig S, et al. Two-dimensional right ventricular strain by speckle tracking for assessment of longitudinal right ventricular function after pediatric congenital heart disease surgery. Arch Cardiovasc Dis. 2017; 110(3):157-66.

131. Hayabuchi Y, Sakata M, Kagami S. Right ventricular myocardial deformation patterns in children with congenital heart diseaseassociated with right ventricular pressure overload. Eur Heart J Cardiovasc Imaging. 2015; 16(8):890-9.

132. Yim D, Mertens L, Morgan CT, Friedberg MK, Grosse-Wortmann L, Dragulescu A. Impact of surgical pulmonary valve replacement on ventricular mechanics in children with repaired tetralogy of Fallot. Int J Cardiovasc Imaging. 2017; 33(5):711-20.

133. Sabate Rotes A, Bonnichsen CR, Reece CL, Connolly HM, Burkhart HM, Dearani JA, et al. Long-term follow-up in repaired tetralogy of Fallot: can deformation imaging help identify optimal timing of pulmonary valve replacement? J Am Soc Echocardiogr. 2014; 27(12):1305-10.

134. Iriart X, Roubertie F, Jalal Z, Thambo JB. Quantification of systemic right ventricle by echocardiography. *Arch Cardiovasc Dis*. 2016; 109(2):120-7.

135. Park PW, Atz AM, Taylor CL, Chowdhury SM. Speckle-Tracking Echocardiography Improves Pre-Operative Risk Stratification Before the Total Cavopulmonary Connection. *J Am Soc Echocardiogr*. 2017; 30(5):478-84.

136. Kühn A, Meierhofer C, Rutz T, Rondak IC, Röhlig C, Schreiber C, et al. Non - volumetric echocardiographic indices and qualitative assessment of right ventricular systolic function in Ebstein's anomaly: comparison with CMR-derived ejection fraction in 49 patients. Eur Heart J Cardiovasc Imaging. 2016; 17(8):930-5.

137. Castaldi B, Vida V, Reffo E, Padalino M, Daniels Q, Stellin G, *et al*. Speckle Tracking in ALCAPA Patients After Surgical Repair as Predictorof Residual Coronary Disease. *Pediatr Cardiol*. 2017; 38(4):794-800.

138. Dusenbery SM, Lunze FI, Jerosch-Herold M, Geva T, Newburger JW, Colan SD, et al. Left Ventricular Strain and Myocardial Fibrosis in Congenital Aortic Stenosis. *Am J Cardiol*. 2015; 116(8):1257-62.

139. Hope KD, Calderón Anyosa RJC, Wang Y, Montero AE, Sato T, Hanna BD, *et al*. Right atrial mechanics provide useful insight in pediatric pulmonary hypertension. *Pulm Circ*. 2018; 8(1):2045893218754852

140. Cameli M, Mandoli GE, Loiacono F, Dini FL, Henein M, Mondillo S. Left atrial strain: a new parameter for assessment of left ventricular filling pressure. *Heart Fail Rev*. 2016; 21(1):65-76.

141. Miranda JO, Cerqueira RJ, Ramalho C, Areias JC, Henriques-Coelho T. Fetal Cardiac Function in Maternal Diabetes: A Conventional and Speckle-Tracking Echocardiographic Study. J Am Soc Echocardiogr. 2018; 31(3):333-41.